Patrik Krieger · Alexander Groh *Editors*

Sensorimotor Integration in the Whisker System

Springer

Sensorimotor Integration in the Whisker System

Patrik Krieger • Alexander Groh
Editors

Sensorimotor Integration in the Whisker System

Springer

Editors
Patrik Krieger
Department of Systems Neuroscience
Ruhr University Bochum
Bochum
Germany

Alexander Groh
Institute of Neuroscience
Technische Universitaet Muenchen
Munich
Germany

ISBN 978-1-4939-2974-0 ISBN 978-1-4939-2975-7 (eBook)
DOI 10.1007/978-1-4939-2975-7

Library of Congress Control Number: 2015947147

Springer New York Heidelberg Dordrecht London

Printed on acid-free paper

Springer Science+Business Media LLC New York is part of Springer Science+Business Media (www.springer.com)

Contents

Contributors

Ehud Ahissar Department of Neurobiology, Weizmann Institute of Science, Rehovot, Israel

Sean R. Anderson Automatic Control and Systems Engineering, University of Sheffield, Sheffield, UK

Eldad Assa Department of Neurobiology, Weizmann Institute of Science, Rehovot, Israel

Manuel A. Castro-Alamancos Neurobiology and Anatomy, Drexel University College of Medicine, Philadelphia, PA, USA

Elizabeth H Catania Department of Biological Science, Vanderbilt University, Nashville, TN, USA

Kenneth C Catania Department of Biological Science, Vanderbilt University, Nashville, TN, USA

Tansu Celikel Neurophysiology, Donders Institute for Brain, Cognition, and Behaviour, Radboud University Nijmegen, The Netherlands

Shubhodeep Chakrabarti Systems Neurophysiology Group, Department of Cognitive Neurology, Werner Reichardt Center for Integrative Neuroscience, University of Tübingen, Hertie Institute for Clinical Brain Research, Bernstein Center for Computational Neuroscience, Tübingen, Germany

Jerry L. Chen Laboratory of Neural Circuit Dynamics, Brain Research Institute, University of Zurich, Zurich, Switzerland

Paul Dean Department of Psychology, The University of Sheffield, Sheffield, UK

Martin Deschênes Department of Psychiatry and Neuroscience, Laval University, Quebec City, QC, Canada

Mathew E. Diamond Tactile Perception and Learning Lab, International School for Advanced Studies-SISSA, Trieste, Italy

Dirk Feldmeyer Institute of Neuroscience and Medicine, INM-2, Research Centre Jülich, Jülich, Leo-Brandt-Strasse, Germany

Department of Psychiatry, Psychotherapy and Psychosomatics, Function of Cortical Microcircuits Group, RWTH Aachen University, Aachen, Germany

JARA Brain—Translational Brain Medicine, Aachen, Germany

Charles W. Fox Institute for Transport Studies, University of Leeds, Leeds, UK

Alexander Groh Institute of Neuroscience, Technische Universität München, Munich, Germany

Fritjof Helmchen Laboratory of Neural Circuit Dynamics, Brain Research Institute, University of Zurich, Zurich, Switzerland

Judith Homberg Department of Cognitive Neuroscience, Donders Institute for Brain, Cognition, and Behaviour, Radboud University Medical Center, Nijmegen, The Netherlands

David Kleinfeld Department of Physics and Section on Neurobiology, University of California San Diego, La Jolla, CA, USA

Per Magne Knutsen Department of Physics, University of California at San Diego, La Jolla, CA, USA

Patrik Krieger Department of Systems Neuroscience, Medical Faculty, Ruhr University Bochum, Bochum, Germany

Nathan F. Lepora Department of Engineering Mathematics, University of Bristol, Bristol, UK

Miguel Maravall School of Life Sciences, University of Sussex, Brighton, BN1 9QG, United Kingdom

Ben Mitchinson Department of Psychology, The University of Sheffield, Sheffield, UK

Jeffrey D. Moore Graduate Program in Neuroscience, University of California San Diego, La Jolla, CA, USA

Nael Nadif Kasri Department of Cognitive Neuroscience, Donders Institute for Brain, Cognition, and Behaviour, Radboud Radboud University Medical Center, Nijmegen, The Netherlands

Tess Baker Oram Department of Neurobiology, Weizmann Institute of Science, Rehovot, Israel

Martin J. Pearson Bristol Robotics Laboratory, University of the West of England, Bristol, UK

Anthony G. Pipe Bristol Robotics Laboratory, University of the West of England, Bristol, UK

John Porrill Department of Psychology, The University of Sheffield, Sheffield, UK

Tony J. Prescott Department of Psychology, The University of Sheffield, Sheffield, UK

Guanxiao Qi Institute of Neuroscience and Medicine, INM-2, Research Centre Jülich, Jülich, Leo-Brandt-Strasse, Germany

Department of Psychiatry, Psychotherapy and Psychosomatics, Function of Cortical Microcircuits Group, RWTH Aachen University, Aachen, Germany

JARA Brain—Translational Brain Medicine, Aachen, Germany

Gabriele Radnikow Institute of Neuroscience and Medicine, INM-2, Research Centre Jülich, Jülich, Leo-Brandt-Strasse, Germany

Department of Psychiatry, Psychotherapy and Psychosomatics, Function of Cortical Microcircuits Group, RWTH Aachen University, Aachen, Germany

JARA Brain—Translational Brain Medicine, Aachen, Germany

Dirk Schubert Department of Cognitive Neuroscience, Donders Institute for Brain, Cognition and Behaviour, Radboud University Medical Center, Nijmegen, The Netherlands

Cornelius Schwarz Systems Neurophysiology Group, Department of Cognitive Neurology, Werner Reichardt Center for Integrative Neuroscience, University of Tübingen, Hertie Institute for Clinical Brain Research, Bernstein Center for Computational Neuroscience, Tübingen, Germany

J. Charles Sullivan Bristol Robotics Laboratory, University of the West of England, Bristol, UK

Stuart P. Wilson Bristol Robotics Laboratory, University of the West of England, Bristol, UK

Chapter 1
Introduction

Alexander Groh and Patrik Krieger

Abstract Sensation in animals and humans is often an active process that involves motion, e.g., moving fingers on a textured surface and eye movements. In this dynamic process, motion and sensation are strongly interdependent: internal motor information is needed to interpret external sensory signals, and sensory information is used to shape appropriate behavior. This book explores the neural mechanisms underlying sensorimotor integration that allow the sensory and motor systems to communicate and coordinate their activity. Studying the rodent whisker system has tremendously advanced our understanding of sensorimotor integration in mammals and is the focus of this book. In ten chapters, written by leading scientists, we present important findings and exciting current directions in the field.

Keywords Sensorimotor integration · Whisker system · Somatosensory barrel cortex · Shrew · Thalamus · Central pattern generator · Whiskered robot · Neuromodulator · Connectivity

Analyzing the neural mechanisms underlying sensorimotor integration requires a model system that allows well-defined sensory stimulation and simple readouts of motor output. The rodent whisker system fulfills these criteria and in addition offers transgenic approaches that can be used, in particular in mice to dissect functional units underlying touch perception. The facial whiskers are tactile organs used to identify and locate objects, similarly to how humans use fingers to explore texture and shape of objects. The chapters in this book describe how animals use tactile sensory organs—whiskers in rodents and shrews—in behavioral tasks and describe how data on whisker kinematics can be used to understand the nature of the sensory data that is collected in order to initiate a motor program. Furthermore, data on the

A. Groh (✉)
Institute of Neuroscience, Technische Universität München, Biedersteiner Str. 29, 80802 Munich, Germany
e-mail: alexander.groh@lrz.tum.de

P. Krieger (✉)
Department of Systems Neuroscience, Medical Faculty, Ruhr University Bochum, Germany
e-mail: sysnw@rub.de

P. Krieger, A. Groh (eds.), *Sensorimotor Integration in the Whisker System,*
DOI 10.1007/978-1-4939-2975-7_1

role of cortical and sub-cortical brain areas in linking sensory perception and motor control are discussed.

One feature of the whisker system which is often highlighted is the striking one-to-one correspondence between the peripheral whisker pad and corresponding brain areas in the brainstem, thalamus and the somatosensory barrel cortex. The fact that there is a strong link between structural and functional properties—you can "see" the circuit—is experimentally advantageous. However, it is noteworthy that cortical barrel column are not always present in animals with whiskers, e.g., shrews. Understanding tactile information processing should thus be done using a combination of species, each with its peculiar specialization. One such comparison is made in Chap. 2 where tactile exploration is studied in water shrews, star-nosed moles and the eastern mole. Accompanied by outstanding photography the authors take us on a journey into the world of water shrews, which use their whisker to detect prey, and the star-nosed mole, which uses a different type of tactile sensory organ. Like rats and mice, water shrews have an exquisitely specialized whisker system used to explore their environment, but the central representation of whisker input is different in the neocortex. Moles on the other hand don't have whiskers but rely on specialized skin surfaces. Similar to the barrel system, there is a somatotopic map connecting the sensory skin receptors with brain modules. The chapter also touches on a behaviorally relevant integration of touch and smell (further explored in Chap. 7), used by the eastern moles for food localization. Comparing tactile information processing in different species provides different examples of modular brain maps. Furthermore, incorporating the concept of a "sensory fovea" the authors show parallels between somatosensory, visual, and auditory systems. A structure-function subdivision of the whisker system includes the mechanoreceptors in the hair follicles that transmit sensory information to the brainstem, and from the brainstem information is transmitted to the thalamus. Chapter 3 describes the physiological properties of the whisker thalamus, in particular the ventral posterior medial thalamus (VPM). The chapter discusses in detail how thalamic responses are influenced by sensory, cortical, inhibitory (from reticular nucleus of the thalamus) and modulatory (brainstem) afferents. Furthermore, the chapter discusses how low- and high-frequency sensory inputs are differentially processed depending on the operational mode of the thalamic cells, and it is shown how these operating modes are affected by neuromodulators (see also Chap. 11), in particular cholinergic and noradrenergic modulation. The chapter furthermore raises many interesting questions regarding similarities and differences in brainstem versus cortical modulation of thalamic activity.

The somatosensory barrel cortex is the first cortical station for the whisker input. The barrel cortex is a prototypic neocortical area with its vertical columnar organization and its six layers, each layer thought to make different contributions to information processing. The barrel columns are defined based on the visible "barrel" pattern in layer four. The intricate circuitry of the somatosensory barrel cortex has been mapped in great detail using paired/multiple whole cell recordings in the brain slice. This wealth of data is reviewed in Chap. 4, with data on anatomical and functional properties of monosynaptic connections. Although the authors structure their

review on the concept of an easily defined cortical column, they also give evidence that emerging data challenges a too simplified model of how information is transmitted within and between columns. In particular there is a lack of data on inhibitory connections and how the translaminar connectivity fits with the columnar module. The previous chapters presented the thalamocortical circuitry that is underlying the sensory "aspects" of the whisker system. Chapter 5 focuses on mechanisms behind cortical processing of touch and its relation to long-range projections to motor cortex. A further emphasis is on imaging techniques that have tremendously advanced our knowledge about sensory processing in the cortex. The authors also show how the use of genetic tools, including genetically encoded calcium or voltage indicators, can be used to answer key questions in neuroscience. For example, using these methods, in particular using in vivo two-photon calcium imaging, the authors show how somatosensory and motor areas interact. Furthermore, with a focus on studies using two-photon calcium imaging it is shown how the spatial-temporal dynamics of cortical representation whisker information processing. Chapter 6 explores the transformation of tactile information into behaviour via activation of the whisker motor cortex. Evidence is presented showing that the whisker motor cortex can be sub-divided, both structurally and functionally, into modules each having different functions. In addition the authors discuss how whisker movements occur as a result of interactions between cortical command signals with sub-cortical central pattern generators (CPG). Whereas the whisker representation in the somatosensory cortex shows the characteristic barrel pattern, the equivalent topographic representation in the vibrissal motor cortex has not been found. The motor cortex is suggested to contain a motor map rather than a map of the whisker pad, such that more or less complex motion programs are elicited by activity in different areas of the motor cortex. The encoding of whisker deflections is thus rather "diffusely" represented in the motor cortex such that different sensory experiences activate a behaviourally appropriate whisker movement pattern. Chapter 7 summarizes recent evidence for a brainstem central pattern generator (CPG) for rhythmic whisking. Importantly, whisking, breathing, sniffing and possibly locomotion are controlled by this CPG, suggesting a common "master clock" for rhythmic behaviors. From a functional perspective it appears that a coordination of whisking and sniffing, in addition to being advantageous in regard to activating common facial musculatures, can provide a mechanism by which spatial information from the whisker movements can serve as a spatial map. This mechanism in addition to binding the sensory events to one object, can provide information on where in space the odor is coming from.

In previous chapters "Information processing" is discussed in terms of the evoked spike trains analyzed either directly using electrophysiology or indirectly using imaging techniques to visualize changes in voltage or calcium as readout of cortical spiking activity. In Chap. 8 a more theoretical approach is outlined where the computations underlying the encoding of physical parameters by the mechanoreceptors, the further transmission of this information along the sensory system to cortex, and ultimately the transformation of the tactile information into behavior. An emphasis is on the importance of studying whisker movements and the forces exerted on the whisker follicle when the animal uses the whiskers to touch objects

and explore textured surfaces. The chapter furthermore explores how sensory processing can be understood in terms of concepts such as “adaptive representations”, and “population coding”. In Chap. 9 the whisking system is considered as a “closed-loop” which cannot be strictly divided into exclusive “sensory” or “motor” areas. Building on this concept the authors present a model of object localization that describes the process as an interaction of phase-locked loops. As a complement to the previous chapter, the authors also discuss in more general terms the different coding schemes that are likely employed by the whisker system. Modelling tactile information processing using a robotics’ approach the authors of Chap. 10 show how a biologically inspired robot can mimic relevant aspects of active touch behavior. The authors model several features of tactile information processing, including how interactions between cortex and sub-cortical structures are import for decision-making based on tactile input. The whiskered robot is not only designed to replicate touch behavior, but rather also made such that experimental observations of how the robot behaves, and the constraints put on behavior by the brain architecture, can provide understandings into the biology. Based on such observations the authors discuss, e.g., the hypothesis for how cerebellum is involved in tactile information processing. The chapter thus tries to answer the question: Does our current knowledge about sensorimotor integration suffice to engineer a robot that is capable of tactile based behavior?

Chapter 11 summarizes how the sensorimotor circuitry is modulated by monoaminergic neuromodulators: serotonin, dopamine and norepinephrine. The release of these neuromodulators during embryonic development and early post-natal development are shown to be important for neural circuit development. An abnormal neuromodulation early in development is shown to have long-lasting consequences that can underlie individual differences in the development of the somatosensory circuitry. The projection pathways from brainstem areas to cortex are described and data presented how alterations in specific projection pathways affect the cortical circuitry and ultimately behavior. In an outlook chapter the authors discuss how these differences in neuromodulation could be linked neurodevelopmental disorders.

Acknowledgements The authors’ work has been supported by the Deutsche Forschungsgemeinschaft (GR 3757/1-1) and SFB 874/A9.

Part I
Whisker System in Mammals

Chapter 2
Comparative Studies of Somatosensory Systems and Active Sensing

Kenneth C Catania and Elizabeth H Catania

Abstract Comparative studies of diverse species provide a wealth of information about active touch and corresponding brain specializations in the somatosensory system. Here the results of numerous studies of brain and behavior in shrews and moles are reviewed and discussed. Water shrews have elaborate whiskers and can detect prey based on both texture and movement. In contrast to rodents, shrew whiskers are not reflected by barrels in the cortex, but are reflected in the brainstem by prominent barrelettes. Although shrews have a simpler cortical anatomy than rodents, star-nosed mole's cortices are more complex, with three histologically visible and interconnected cortical maps that reflect the nasal rays on the contralateral star. One ray of the star is used as the tactile fovea, and is greatly over-represented in the neocortex. This finding highlights similarities between specialized somatosensory, visual, and auditory systems—each of which may have a sensory fovea for high resolution sensory processing. Both water shrews and star-nosed moles exhibit the remarkable ability to sniff underwater by exhaling and reinhaling air bubbles as they forage. This allows visualization of sniffing during natural behaviors and provides a unique window into the behavioral integration of touch and smell. Finally, eastern moles have the least specialized set of mechanoreceptors but exhibit remarkable olfactory abilities using stereo nasal cues—in conjunction with touch—to efficiently locate prey. These results highlight the many insights that may be derived from specialized model animals.

Supported by NSF grant 1456472 to KCC

Keywords Tactile · Touch · Olfaction · Smell · Stereo · Mechanosensory · Barrel · Barrelette · Whisker · Brain Evolution · Shrew · Mole · Neocortex · Trigeminal · Behavior

K. C. Catania (✉) · E. H. Catania
Department of Biological Science, Vanderbilt University,
U7224 MRB III, 465 21st Ave. S, Nashville, TN 37232, USA
e-mail: ken.catania@vanderbilt.edu

E. H. Catania
e-mail: Elizabeth.catania@vanderbilt.edu

P. Krieger, A. Groh (eds.), *Sensorimotor Integration in the Whisker System,*
DOI 10.1007/978-1-4939-2975-7_2

Introduction

Investigations of sensory and motor specialists have provided many key insights into brain organization, function, and evolution. Perhaps the best-known example of this strategy is Hodgkin and Huxley's landmark studies of the giant axon that mediates escape responses in squid, which revealed the ionic basis of action potential conduction [1, 2]. Some other well know examples include studies of barn owls for understanding the neural basis of auditory localization based on coincidence detection [3–5], the use of electric fish for determining the neural basis of rhythmic signaling, jamming avoidance, and animal communication [6, 7], and the study of songbirds for determining the plasticity of networks mediating social learning [8–10]. In a similar way, the specialized whisker-barrel system of rodents has been particularly useful for understanding the neural basis of touch because rodents have an elaborate somatosensory system and at the same time they share many features in common with other mammals. Most importantly, they have a neocortex with somatosensory areas that are homologous to the somatosensory areas found in nearly all other mammals including humans [11]. This homology from mouse to man allows inferences about basic cortical circuitry to be more confidently extended to a wide range of other mammal species. But the key technical advantage of the rodent system was the discovery of histologically visible units, or barrels, in the primary somatosensory system of mice [12] and subsequently rats [13]. The later discovery of similar barrel-like subdivisions at the thalamic [14] and brainstem [15] level (barreloids and barrelettes, respectively) added another dimension to the system, providing the advantages of "visible" whisker maps in the entire pathway from mechanoreceptors to primary somatosensory cortex. These findings greatly facilitated subsequent investigations of neuronal electrophysiology, connectivity, development, and plasticity. More recently these studies have been integrated with detailed behavioral and biomechanical studies, providing one of the most comprehensive views of brain and behavior for any mammalian species.

At the same time that our understanding of rodents' somatosensory systems have been expanding, advances in the technique of flattening cortex by carefully removing underlying white matter before compressing the cortical hemispheres have provided ever more clear views of the histological patterns in layer 4 cortex in diverse species. This includes the discovery of whisker related barrels in numerous rodents, marsupials, and insectivores. Modules representing alternating electrosensory and mechanosensory inputs have been described in the cortex of the duck-billed platypus [16] and stripes corresponding to nasal appendages have been identified in both S1 and S2 of the star-nosed mole [17, 18]. In the case of primates, myelin-dark modules representing individual fingers have been described in the hand area of area 3B [19, 20]. The latter finding suggests that similar mechanisms may segregate cortical (and subcortical) inputs from discontinuous sensory surfaces into modules during development in diverse species, ranging from rodents to primates.

Clearly there is a rich source of diversity for revealing general principles of brain organization and development by examining a range of different mammalian somatosensory systems. In this chapter we will provide an overview of the brains

and behavior of the water shrew, the star-nosed mole, and the eastern mole. Each of these species is differently specialized in a manner that illuminates a particular facet of sensory biology. Like rats and mice, water shrews have an exquisitely specialized whisker system used to explore their environment. Yet, despite sharing similar mechanoreceptors (whiskers) the central representation of those receptors is strikingly different in the neocortex. Moles on the other hand are also touch specialists, but instead of whiskers they rely on specialized skin surfaces to explore their environment. As in the barrel system, the nasal appendages of star-nosed moles are reflected at cortical and subcortical levels by modules isomorphic with the sensory surface. But in this case, they appear as stripes rather than traditional columns and their sizes reflect the differential behavioral importance of different sensory appendages. This species provides an additional example of modular, visible brain maps and illustrates parallels between high-resolution somatosensory systems, visual systems, and auditory systems. Finally, eastern moles have recently been shown to integrate their somatosensory exploration with the use of bilateral comparisons of olfactory cues (stereo smell) for food localization. Together these insectivores demonstrate a wide range of peripheral mechanoreceptors, diverse cortical representations, and interesting behaviors.

Water Shrews—Variations on a Theme

Figure 2.1 shows a predatory grasshopper mouse (*Onychimys leucogaster*) alongside of a water shrew (*Sorex palustris*). These two species nicely illustrate some of the commonalities and differences in anatomy and brain organization found among mammals. First, we should point out that water shrews are not rodents, they are part of the historical order Insectivora that includes moles, shrews, hedgehogs, and solenodons. Thus, despite appearances, shrews are only very distantly related to rodents. Like all other shrew species, the water shrew is a predator. The grasshopper mouse, on the other hand, is a rodent, albeit it has the distinction of being one of the few predatory rodent species. Both species use their elaborate whiskers in active touch as they identify prey and guide attacks on fast moving and sometimes dangerous invertebrates (grasshopper mice feed on scorpions). Yet despite this similarity in form and function, the cortical representation of the whiskers is very different between these two small mammals.

The flattened juvenile neocortex of the grasshopper mouse (Fig. 2.1c), labeled in this case with the serotonin transporter antibody, appears much like that of other rodent species similarly prepared. It has a patently visible primary somatosensory cortex (S1) containing subdivisions that can be very easily recognized as representing the same body parts that are visible in cortex of laboratory rats and mice. This includes a barrel pattern that clearly reflects the prominent facial whiskers. In contrast, the juvenile water shrew neocortex (in this case processed for the metabolic enzyme cytochrome oxidase (CO)) contains a prominent whisker representation (see [21] for physiological recording data), but no obvious barrels representing the

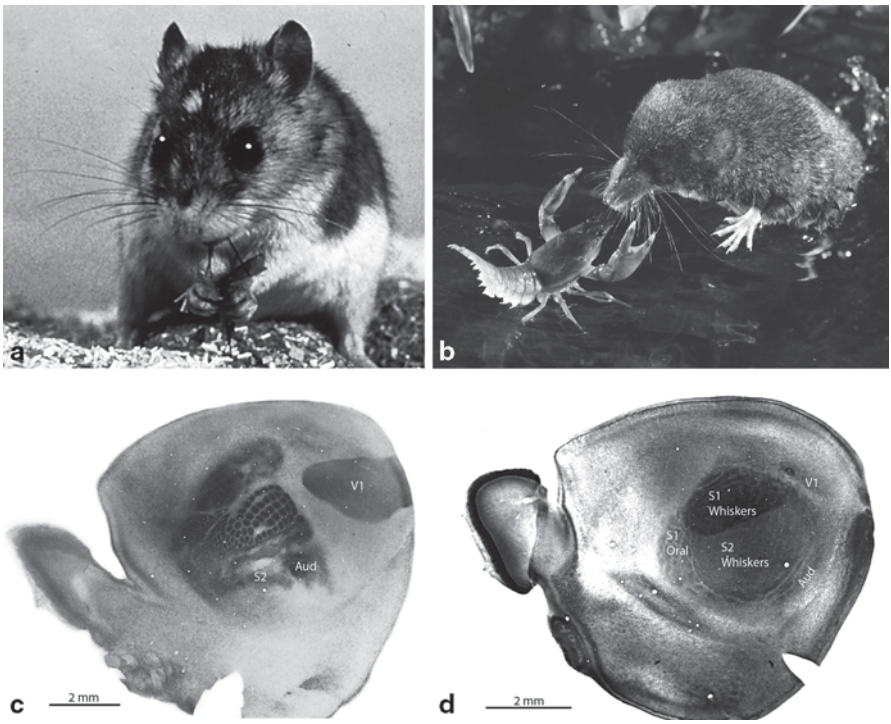

Fig. 2.1 Comparison of a rodent and an insectivore. Although the grasshopper mouse (**a**) and the water shrew (**b**) are both predatory and locate prey using whiskers, they have very different sensory cortices. (**c**) The flattened cortex of the grasshopper mouse shows very prominent cortical barrels (*dark circles* labeled with the serotonin transporter antibody) and large primary visual and auditory areas. (**d**) The flattened cortex of the water shrew shows a large somatosensory cortex with two large whisker representations, but there are no visible barrels. Note also the very small areas of sensory cortex devoted to vision and olfaction in (V1 and Aud, respectively). Data in (**b**) from [61]. Data in (**d**) from [26]. Photo in (**a**) by Jan Decher. (Abbreviations: *Aud* auditory, *V1* primary visual cortex, *Oral* oral). (Published with kind permission of © Kenneth Catania and Jan Dreher 2014)

large facial whiskers (Fig. 2.1d). Why this striking difference in brain organization between physically similar animals with otherwise similar peripheral anatomical features? The answer is not clear, but additional aspects of water shrew behavior may provide some clues.

Water Shrew Senses

Water shrews are adept predators that forage primarily at night along the sides of streams and ponds in North America. It seems remarkable that these animals, the world's smallest mammalian divers, can make a living and avoid predators using

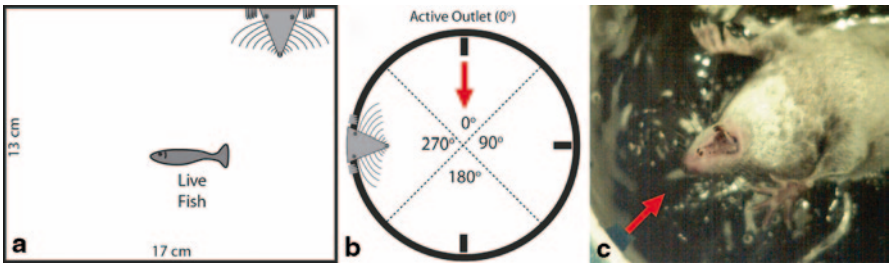

Fig. 2.2 Water shrews detect motion and can capture prey in water without the use of vision. **a** Schematic illustration of the chamber used to examine the foraging efficiency of water shrews capturing live fish under either full spectrum lighting or infrared lighting. Shrews were filmed with a high-speed camera. Shrews were equally efficient under both lighting conditions. **b** Schematic illustration of the chamber used to test responses to brief water pulses simulating escaping fish. Shrews attacked the water motion with a short latency. **c** Frame captured from high-speed video showing a shrew attacking the water motion in the absence of prey. (Published with kind permission of © Kenneth Catania 2014

this foraging strategy, and it is natural to wonder about the relative contribution of their different senses to this activity. Figure 2.1 (c and d) provides an important and obvious clue to the sensory priorities of this species. In contrast to the grasshopper mouse, water shrews have tiny eyes. This anatomical feature is in turn reflected in their neocortex. Water shrews have a very small primary visual area (V1) compressed to the far caudal and dorsal aspect of the hemisphere. Somatosensory cortex appears to have "taken over" much of the cortical territory. Though this last interpretation is almost certainly backwards. Because shrews resemble ancestral mammals in many respects [22], it is more likely that visual cortex in rodents has "taken over" territory that was once somatosensory during the course of evolution. In any case, visual cortex is very small in water shrews, and the same is true for auditory cortex at the more caudal and lateral extreme of the hemisphere (see [21] for shrew electrophysiology). The latter observation is of interest because it has been suggested that some shrews may echolocate [23, 24]. This would be surprising in the case of water shrews, as auditory cortex is very small. Indeed, experiments show water shrews do not use echolocation [25]. In concordance with these observations, counts of cranial nerve number in water shrews reveal a tiny optic nerve (6000 fibers) and an equally small auditory nerve (7000 fibers). In contrast, the trigeminal nerve carrying information from the whiskers contains 27,500 fibers—similar in size to that of laboratory mice [26].

To investigate water shrew behavior and the possible contribution of vision in foraging, shrews were offered live fish in a small chamber under either full spectrum lighting or infrared lighting (Fig. 2.2a). Shrews were very efficient and equally fast at capturing fish under both conditions, demonstrating that vision was not required for this behavior. Many fish were captured in less than one second from the time the shrew entered the water [25]. Slow motion analysis of water shrews capturing fish suggested that water motion generated by fish escape responses might be an important cue used to identify the location of prey. To further investigate this possibility,

water shrews were presented with very brief, periodic pulses of water in the absence of prey and filmed with high speed video. This paradigm was designed to simulate the brief water disturbance caused by an escaping fish. The results clearly showed that water shrew attacks were triggered by brief water movements (Fig. 2.2b, c). In addition to illustrating that water shrews may use prey escape responses for localization, the experiments further highlight their reliance on somatosensation, rather than vision, as the water movements were not visible [25]. Finally, water shrews were incredibly fast, attacking the stimulus with a latency of only 20 milliseconds (from stimulus to initiation of attack).

The experiments described above highlight the strategy shrews use to locate active prey, but shrews also feed on many immobile invertebrates. To investigate their responses to shapes and textures, rather than just movement, water shrews were presented with simulated, highly detailed caste silicone fish, along with a series of rectangular and spherical shapes as distractors (Fig. 2.3a). Even in the absence of visual or olfactory information the shrews were dramatically successful at choos-

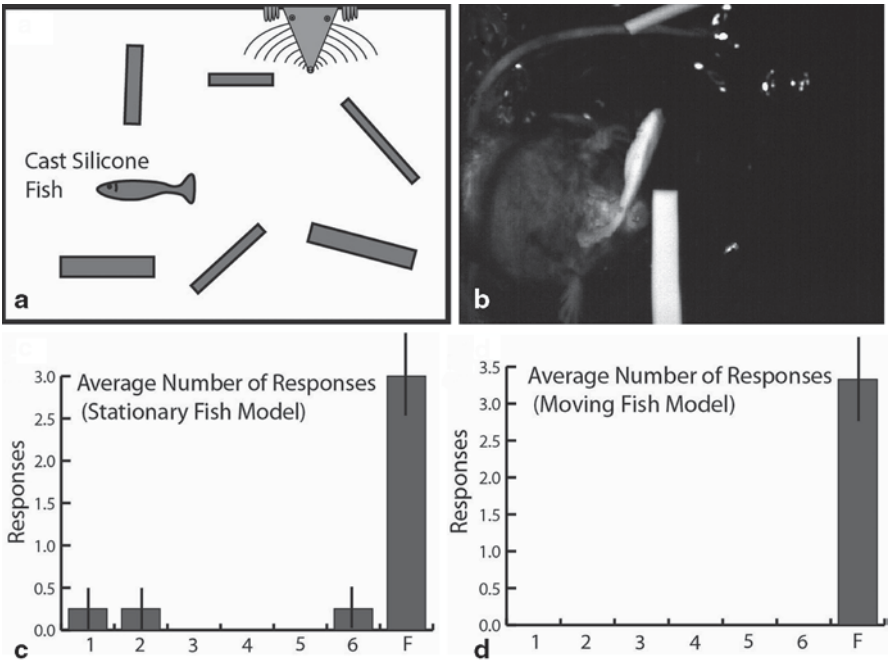

Fig. 2.3 Water shrews use their whiskers to detect texture/shape of objects. **a** Schematic illustration of the chamber used to test water shrews' ability to detect an object without olfactory or visual cues. Three silicone rectangles and three silicone cylinders were placed in the chamber, along with a silicone model fish. **b** A water shrew attacks and grabs a silicone fish under infrared lighting. Shrews often took the model fish back to their home cages. **c** Graph showing the average number of times over 4 trials that each of 4 shrews bit either a distractor object (1–6) or the model fish "F". **d** Graph showing the average number of attacks (retrieving, biting or lunging with open mouth) for each moving object for 3 shrews over 4 trials. Objects were moved with a magnet under the chamber. (Published with kind permission of © Kenneth Catania 2014)

ing the silicone fish over the similarly sized silicone shape models (Fig. 2.3c). This demonstrated that water shrews cannot only detect movements, but they can also use their whiskers to identify objects via shape and texture. As might be expected, with no reward for retrieving inedible silicone fish, the shrews soon stopped capturing these imposters. But if caste fish were made to move (by placing a small piece of metal in them and moving them with a magnet) the water shrews' responses were resurrected and they again attacked the silicone fish in preference to the other objects. Together these results show the value of both movement and shape in eliciting attacks (Fig. 2.3d). This seems appropriate, given that small prey hidden in the shallow water along streams and ponds would be expected to exhibit distinctive shapes and textures and some would also be likely to move (e.g. escape responses of fish and crayfish, for example). Other shrews have also been shown to use prey shape as an important criterion for predatory attack [27].

Underwater Sniffing

As suggested by their anatomy, behavioral experiments indicate that water shrews depend heavily on their whiskers to locate prey while foraging. Yet their speed and efficiency raise the possibility that other senses might be involved. As described previously, there was no evidence for the use of echolocation or sonar. In addition, we tested for the ability to detect electric fields, both in terms of behavioral responses and by surveying the skin surface of the head to detect potential electroreceptive organs. There was no evidence for electroreception in terms of behavior or peripheral anatomy. However, water shrews were able to use olfaction in a very unique way. When searching for prey while submerged, they emitted air bubbles from their nostrils that spread over objects they were exploring and then re-inhaled the same air (Fig. 2.4).

This behavior was remarkable, because it had all the characteristics of sniffing, but occurred underwater (the behavior was first observed in semi-aquatic star-nosed moles, see later section). To investigate this further, shrews were trained to follow a scent trail underwater in a two choice test. They were very proficient at following the trail as long as the emitted air bubbles could make direct contact with the scent trail they were following [28]. When the air bubbles were blocked with a stainless steel grid, the shrews' performances dropped to chance, despite the close proximity of the scent trail. This form of underwater sniffing seems to require direct contact of the air with odorants to provide relevant information.

Water Shrew Brainstem—Barrelettes without Barrels

When first investigating the neocortex of shrews [21] one of our interests was determining whether this lineage of mammals exhibited cortical barrels. Five different shrew species (including water shrews) were examined using eletrophysiological

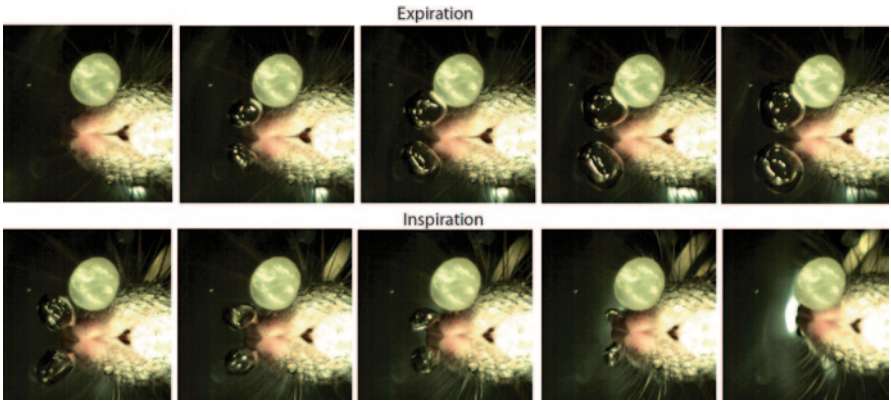

Fig. 2.4 Ten frames taken from high-speed video showing a single underwater sniff by a water shrew. In this case the shrew is sniffing a small piece of wax. The animal has paused during its movements and expires air (*upper row*) that comes in direct contact with the object. This air is then re-inhaled (*lower row*). Using this strategy, water shrews can follow a submerged scent trail. (Published with kind permission of © Kenneth Catania 2014)

mapping with dense microelectrode penetrations combined with subsequent analysis of flattened cortical sections processed for CO. The primary (S1) and secondary (S2) somatosensory areas were both identified. S2 was larger in shrews compared to most other mammal species that have been investigated, taking up roughly the same amount of neocortex as S1 and being characterized by neurons with relatively small receptive fields. As expected from shrew behavior and the cranial nerve counts described above, both S1 and S2 were dominated by large representations of the whiskers from the contralateral side of the face. The S1 representation of the whiskers was visible by a CO dark wedge of tissue in most species. The S1 whisker representation was most obvious in the smallest shrew species (the masked shrew, Sorex cinereus) [21]. But in no case, for any species, were cortical barrels apparent.

As is familiar to most investigators of small mammal cortical histology, cyto- and chemoarchitectural borders and modules such as barrels are usually more apparent in juvenile animals than in adults. When water shrews fortuitously gave birth in the lab, we once again examined somatosensory cortex, this time in juveniles [26]. The goal was to specify borders between areas in greater detail for these unique species and to search once more for cortical barrels that might be evident at early stages of development but later obscured. We were successful at more clearly delineating borders of sensory areas and even numerous subdivisions representing body parts, especially the large, S1 whisker representation marked by the wedge of CO dark tissue. But, once again, we concluded there were no cortical barrels apparent even at juvenile stages of cortical development [26].

With these previous investigations in mind, we were surprised to later discover in the juvenile water shrew brainstem [29] perhaps the clearest and most prominent barrelettes yet observed in a mammal (Fig. 2.5b, c, d). Barrelettes were apparent in the principle nucleus (PrV), the interpolar spinal trigeminal nucleus (SpI), and the

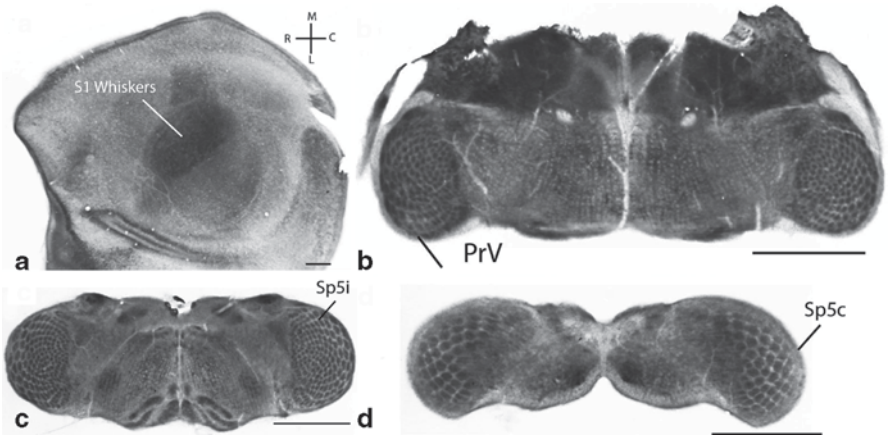

Fig. 2.5 Water shrews have barrelettes without barrels. (**a**) Flattened juvenile water shrew cortex processed for cytochrome oxidase and showing the large whisker representation devoid of barrels. (**b**–**d**) Prominent barrelettes are visible in trigeminal sensory nuclei: (**b**) the principle trigeminal nuclei (PrV), (**c**) the interpolar spinal trigeminal nucleus (SpI) and (**c**) the caudal spinal trigeminal nucleus (SpC) of juvenile water shrews. Scale = 0.5 mm. (Published with kind permission of © Kenneth Catania 2014)

caudal spinal trigeminal nucleus (SpC). Barrelettes were apparent in adult water shrew brainstem as well, though (as is the case for rodents) they were slightly less clear than in juveniles. Injection of anatomical tracers into the adult water shrew whisker pad indicated that barrelettes in shrews, as in rodents, reflect the selective aggregation of afferent terminals from the whiskerpad [29].

These findings highlight the different ways that whiskers can be represented in diverse mammals. In rodents, cortical barrels representing the whiskers are the most obvious, whereas trigeminal barrelettes and thalamic barreloids are much less clear. In contrast, trigeminal barrelettes in water shrews are strikingly clear despite the absence of barrels at the cortical level.

Star-Nosed Moles

Olfaction might be the first thing that comes to mind when one considers a star-nosed mole (*Condylura cristata*). In fact, recent studies show that star-nosed moles and their relatives have impressive olfactory abilities, but the star is a tactile organ, not a chemoreceptor. It consists of 22 epidermal appendages that ring the nostrils in 11 symmetric pairs (Fig. 2.6a). Each appendage, or "ray" is covered with many hundreds of small epidermal domes called Eimer's organs (Fig. 2.6b). Together they are innervated by over 100,000 myelinated nerve fibers, giving this skin surface, which is only about a centimeter across, the highest innervation density of any known skin surface. Eimer's organs are a characteristic feature of mole nasal epidermis

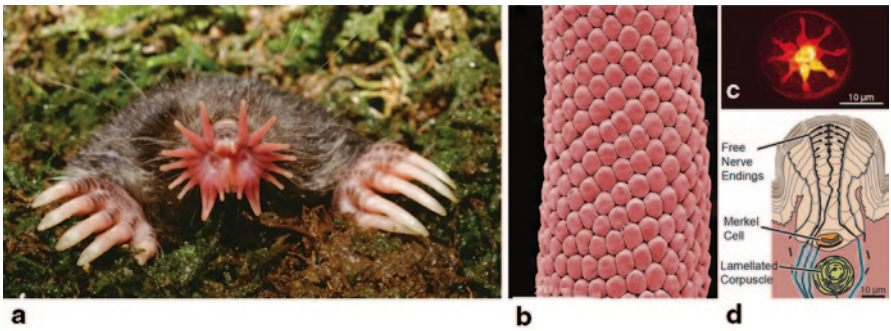

Fig. 2.6 Anatomy of the star. **a** Star-nosed moles have an impressive epidermal specialization on their nose consisting of 22 appendages (rays) that surround their nostrils. **b** Each ray is covered with small domes called Eimer's organs that are densely innervated. **c** Top view of nerve endings in a single Eimer's organ visualized with DiI. The star has the highest innervation density of any known skin surface. **d** Each Eimer's organ contains a Merkel cell-neurite complex, a lamellated corpuscle, and free nerve endings. (Published with kind permission of © Kenneth Catania 2014)

and are found on the skin of almost all of the nearly 30 different mole species [30]. But only the star-nosed mole has evolved nasal rays that increase the surface area of the sensory epithelium providing room for 25,000 Eimer's organs. Evolution of this delicate structure could probably only occur in the star-nosed mole's wetland environment, a unique habitat for moles, and this at least partially explains why no other mole has such an elaborate and fragile snout. Because the star is essentially made of Eimer's organs, knowing the function of these structures is fundamental for understanding the star.

Function of Eimer's Organs

Eimer's organs were first described in the 1800s by Theodor Eimer in the European mole [31] and they were subsequently found on each mole species that was investigated with the exception of the eastern mole (*Scalopus aquaticus*) [32]. Most investigators concluded that Eimer's organs must have a mechanoreceptive function based on their anatomy and mole behavior. Each organ is associated with Merkel cell-neurite complexes, lamellated corpuscles, and free nerve endings (Fig. 2.6c, d) [33–35]. In addition, moles repeatedly touch the skin surface containing Eimer's organs to objects or prey as they explore their environment and search for food. More direct evidence for a mechanosensory function comes from electrophysiological recordings from the somatosensory cortex [17, 18], from afferents supplying Eimer's organs [36], and from findings in the principle trigeminal sensory nucleus (PrV) [37].

The first direct evidence of Eimer's organ responses came from electrophysiology recordings in the somatosensory cortex of star-nosed moles [17, 38]. Multi-unit

receptive fields were extremely small and often had to be defined with the aid of a microscope. Even so, the lower limit of receptive field size was probably not determined given the limitations of manual stimulation of the skin surface. Nevertheless receptive fields on the star were well under a millimeter in diameter in some areas. Even at this early stage of investigations, there was an evident trend in relative receptive field size with the smallest receptive fields located on the midline and ventral parts of the star and larger receptive fields found for the more lateral parts of the star (see next section for correlations with behavior). Single unit analysis revealed that roughly half of cortical neurons were inhibited when areas just outside their excitatory receptive fields were stimulated—i.e. they demonstrated surround inhibition.

Later recordings from primary afferents in both star-nosed moles and coast moles provide additional evidence for Eimer's organ function [36]. Three different response classes were evident in both species using either a dedicated Chubbuck mechanosensory stimulator [39] or a piezo bending element stimulator. These responses consisted of a Merkel-like response with sustained volleys of action potentials having variable interspike intervals, a Pacinian like response that was evident only at the onset and offset of skin depression (stimulation), and a rapidly adapting response that was directionally sensitive to a sweeping motion across the skin surface [36]. These responses were consistent with the three receptor classes associated with each Eimer's organ. The most interesting response was the directionally sensitive afferents that suggest a roll for Eimer's organs in detecting minute surface features on objects and prey items in the moles' environments [36].

Stars and Stripes in the Brain

When considered in light of the whisker-barrel system of rodents, the anatomy of the star -with its separate appendages, dense innervation, and high concentration of mechanoreceptors—raised the possibility of corresponding cortical modules that separately represent each appendage. To investigate this possibility, star-nosed mole neocortex was mapped using dense microelectrode penetrations followed by anatomical analysis of layer 4 cortex processed for CO [18]. In addition to providing the initial evidence for Eimer's organ function described above, the results of electrophysiological recordings revealed the layout of the star appendages and other body parts in neocortical maps. Three separate representations of the star were identified in lateral cortex, corresponding to the expected location of the face representation in mammals generally (Fig. 2.7a). When the neocortex was flattened and sectioned tangentially, in the same manner that reveals barrels in rodents, each of the three maps of the star was visible as a pinwheel of CO dark stripes (Fig. 2.7c). Not only did this result represent an additional example of distinctive modules in primary somatosensory cortex reflecting the distribution of mechanoreceptors on the face, but it was also the first (and only) demonstration of multiple visible maps representing the same sensory surface. Subsequent investigation of these areas us-

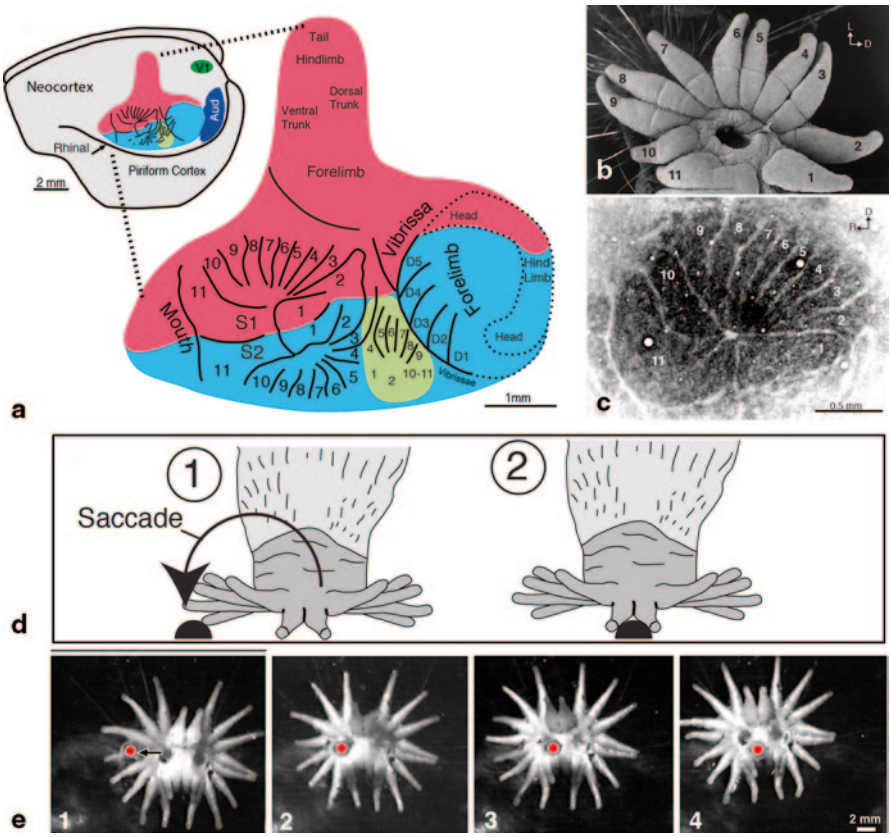

Fig. 2.7 Cortical organization and behavior in the star-nosed mole. **a** Three maps of the contralateral star exist in somatosensory cortex (S1, S2, and S3). The S2 map of the star-nosed mole is comparatively large compared to most other mammals. The S3 representation is not found in other moles or shrews, and thus arose independently. **b** Half of the star under a scanning electron microscope with the 11 rays labeled. **c** The star representation can be seen in flattened cortex processed for cytochrome oxidase. Although ray 11 is small compared to the other rays (b) it has the largest representation in S1. This reflects its use as the somatosensory fovea. **d** Schematic of a star-nosed mole saccade used to move the 11th appendage over an object being explored. **e** Frames from high-speed video showing a star saccade relative to a small prey item (*red circle*). (Published with kind permission of © Kenneth Catania 2014)

ing neuroanatomical tracers [40] revealed that the maps are topographically interconnected to form a cortical processing network.

Several features of this processing network differ substantially from the condition in rodents. For example, in addition to containing modules representing the individual rays, the secondary somatosensory cortex is much larger than would be predicted based on studies in rodents and most other mammals. S2 is usually much smaller than S1 and is characterized by large receptive fields. In contrast star-nosed mole S2 has proportions similar to S1 and is characterized by small receptive fields

on both the star and other body parts. Interestingly, a large S2 is found in shrews as well (see previous section on water shrews) and may be a general feature of shrews and moles rather than a specialization in star-nosed moles.

Despite sharing some features in common with other moles and shrews (a large S2) comparisons across species indicate that the extra, third map of the nose in lateral and caudal cortex is unique to star-nosed moles. This means that it arose independently in star-nosed moles and was most likely not in the common ancestor to shrews and moles. This is a very interesting finding because the addition of cortical areas is often hypothesized to be one of the substrates for more complex sensory processing and behavioral abilities. In most cases, such comparisons involve distantly related species that differ substantially in brain size. But moles are closely related species of similar brain and body size. The obvious difference between star-nosed moles and other mole species is the elaboration of the sensory surface and corresponding behaviors (see next section). This suggests that star-nosed moles added a cortical area to handle large amounts of complex sensory information from the star, perhaps depending on parallel processing of some aspects of touch.

An additional interesting and obvious characteristic of the star-nosed mole's somatosensory cortex is the overrepresentation of the 11th appendage. Despite the small size of this nasal ray and the relatively few Eimer's organs on its surface, its representation takes up 25% of the S1 star map (Fig. 2.7b, c). In addition, although the 11th appendage is more densely innervated then the rest of the star, only approximately 10% of the afferents supplying the star serve this appendage. Its greater innervation density stems from its small size and few sensory organs compared to the number of innervating afferents, rather than the number of afferents in total. Put another way, the innervation density of ray 11 is high as a ratio of nerve fibers to sensory organs (or skin surface).

When afferent numbers supplying the star are compared to their representations in primary somatosensory cortex, the sizes of the ray representations are not proportional to the number of nerve fibers supplying each ray [41, 42]. This can be contrasted to the situation in rodents, where the size of each cortical barrel has been found to be proportional to the number of nerve fibers supplying each whisker on the face [43]. Investigation of star-nosed mole behavior provides an explanation for the dramatic mismatch between the anatomy of the star and its representation in cortex.

Somatosensory Fovea

Star-nosed moles use the star to explore their environment with a series of high-speed touches. They may touch 10–13 different places every second as they search for food and navigate their tunnels. As was the case for water shrews, detailed investigations required the use of high-speed video recordings [44]. These revealed the explanation for the differential magnification of nasal appendages in the cortical representation; star-nosed moles have a somatosensory fovea at the center of the

star. The 11th, midline pair of appendages is used for detailed investigations of objects of interest (usually food). Most objects encountered as the mole searches its environment are first contacted by the large array of Eimer's organs that cover rays 1–10, as these make up most of the surface area of the star. For detailed investigation, moles make sudden movements of the star to reposition the 11th rays on an object for multiple touches (Fig. 2.7d, e). These nose movements are remarkably similar in their form and time-course to saccadic eye movements in primates [44].

Underwater Sniffing

Star-nosed moles are semi-aquatic and occasionally dive for food, much like water shrews. This raised the question of whether tactile cues used for detecting prey with the star would be degraded in water as a result of its greater viscosity than air. It seemed possible, for example, that movements would be slower underwater. There was no obvious indication of different use of the star underwater for mechanosensory investigation, but a different and unanticipated behavior was observed. This was under-water sniffing—as already described for water shrews, but first discovered in star-nosed moles [28]. Star-nosed moles exhaled air bubbles over objects of interest and then re-inhaled the same air. As was the case for water shrews, they could follow a scent trail laid underwater. In the case of star-nosed moles, a stainless steel grid with large openings was placed over the scent trail at all times. This prevented contact of the star to the scent trail, but allowed for air to be exhaled through the grid and then re-inhaled with each sniff. When the coarse grid was replaced by a fine grid that did not admit air bubbles the moles' performances deteriorated to chance levels.

Measurement of the timing of sniffs and the volume of air expired and re-inhaled showed that underwater sniffing is very similar to sniffing behavior exhibited on land by other small mammals. It is important to keep in mind that small mammal sniffing consists of repeated cycles of small expirations of air paired with small inspirations of air. In contrast to human sniffing, which generally consists of repeated short inspirations, small mammal sniffing on land is essentially the same as underwater sniffing in star-nosed moles and water shrews. That is, expiring air as a part of the sniffing process is not an innovation restricted to the aquatic medium. It is worth noting in this regard, that the terrestrial small mammals (e.g. short-tailed shrews) tested did not exhibit underwater sniffing when trained to retrieve food from a shallow enclosure [45]. Despite the close similarity between terrestrial sniffing and underwater sniffing, this does not appear to be a general feature of small mammal behavior, but rather a specialization of semiaquatic mammals.

That underwater sniffing happens at all is perhaps the most surprising conclusion from these studies. But this behavior also provides an obvious and very informative window into sniffing behavior; you can see the sniffs. Because each sniff is visible as an air bubble that emerges from the nostrils and is then re-inhaled, it is possible to clearly note the timing of sniffs relative to other behaviors using high-speed video.

The conclusion from such observations is that sniffing is coordinated with touching. Underwater sniffs occur as the animal decelerates to make a touch and gather tactile information with the star (mole) or whiskers (water shrew). This in turn is consistent with classical [46] and more recent [47–49] studies of sensory integration in rodents that suggest sniffing and touching are coordinated. The other obvious conclusion from this somewhat esoteric behavior of semi-aquatic moles and shrews is that coordinated sniffing and touching likely also occur as these animals explore their terrestrial environment; we just can't see the sniffs. This possibility was confirmed by examining a related mole species (eastern moles, *Scalopus aquaticus*) that have a much less developed sense of touch compared to star-nosed moles.

Stereo Sniffing in Eastern Moles

The eastern mole (*Scalopus aquaticus*) does not have a star and is one of the only mole species that does not have Eimer's organs in the epidermis of its snout. This is likely the result of foraging in a drier and more abrasive environment compared to most other moles. The outer epidermal layer (stratum corneum) on the snout of eastern moles is very thick compared to other species and in this condition could not support functional Eimer's organs [32]. Because eastern moles are among the least specialized in this regard, they were chosen as subjects in preliminary studies of foraging efficiency in comparison to star-nosed moles. Star-nosed moles are among the fastest foragers [50] and it was suspected, based on their less elaborate somatosensory system, that eastern moles would be far less efficient.

The results were surprising and defied expectations. When presented with numerous small prey items (small earthworm segments), eastern moles moved almost directly from one to the next in rapid succession. This ability was so marked, that despite their tiny eyes hidden below the fur and an optic nerve so small that we have not been able to locate it upon dissection, experiments were repeated (with the same result) under infrared lighting to exclude all possibility that vision played a role [51].

High-speed video suggested that eastern moles were using a serial sniffing behavior to home in on earthworms. To test this possibility, an experimental chamber was designed that allowed for non-invasive sniff monitoring, using a pressure gauge. In this way, the sniff cycle could be correlated with video frames. These experiments showed that eastern moles sniff in coordination with nose movements (Fig. 2.8), as suggested by the behavior observed for star-nosed moles and water shrews foraging while submerged. However, the extremely accurate and rapid localization of olfactory stimuli by eastern moles (see [51] for movies) raised the possibility that bilateral (stereo) olfactory cues might be aiding in the localization process. Recent investigations in rats suggest that rodents also use this strategy [52].

To investigate this possibility in moles, a single nostril was blocked with a small silicone tube and moles were given the challenge of localizing a prey item under a number of different circumstances [51]. These experiments were inspired by similar

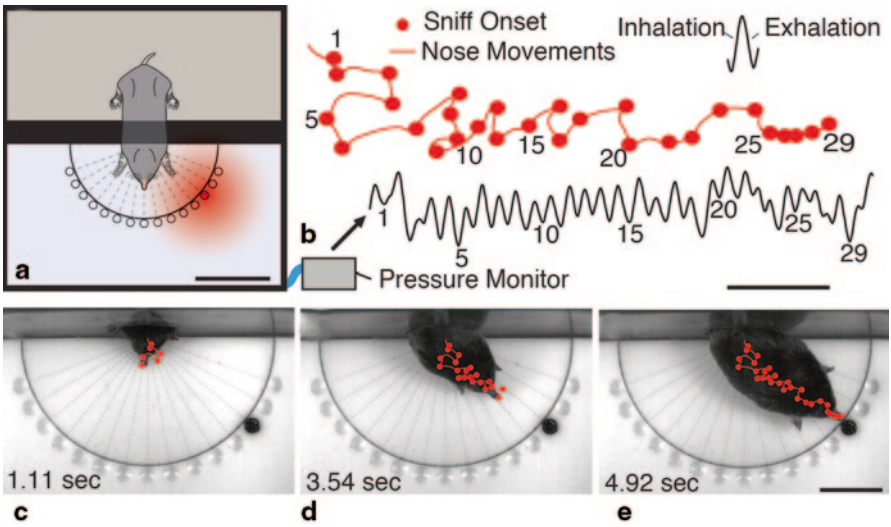

Fig. 2.8 Eastern moles coordinate sniffs with touches as they explore their environment. (**a**) A schematic of the experimental chamber used to measure sniffing. The chamber was sealed so that a pressure gauge could monitor each sniff and be compared to simultaneous high-speed video recordings. (**b**) Example of one mole's sniffing behavior in the chamber. The mole moved and then sniffed repeatedly. (**c**–**e**) Frames from high-speed video as a mole moves directly toward an olfactory stimulus (earthworm segment). Note that eastern moles are blind. From [51]. (Published with kind permission of © Kenneth Catania 2014)

investigations of auditory localization in barn owls, in which ear plugs were used to attenuate sound in one ear [3]. The presumption in moles was that use of stereo cues based on intensity differences between the two nostrils would be revealed by a search bias toward the side of the open nostril, as occurred for sound localization in barn owls based on intensity cues. For controls, moles were allowed to search with no tube or with an open tube that did not block the airflow through the nostril.

The results of these experiments were definitive (for example experiment see Fig. 2.9). In every paradigm, moles headed in the general direction of the food item but showed a bias in the search pattern away from the food and towards the open nostril as compared to moles that had no block or an open tube (Fig. 2.9a vs. b). This suggested an important influence of comparative intensity cues across the nostrils. It is perhaps not surprising that moles headed in the general direction of the food item, given that serial sampling cues were not disrupted by this manipulation and stereo cues from the nostrils would only be expected to provide information close to the stimulus where olfactory gradients are relatively steep. Despite their bias toward the open nostrils compared to controls when approaching the food item, (Fig. 2.9c, d) they were ultimately able to locate the food (earthworm segments). This suggests that serial sniffing cues, derived from the sequential nose movements and sniffs (typically considered to be the mechanism of olfactory localization) overcame the seemingly smaller effect of nostril block.

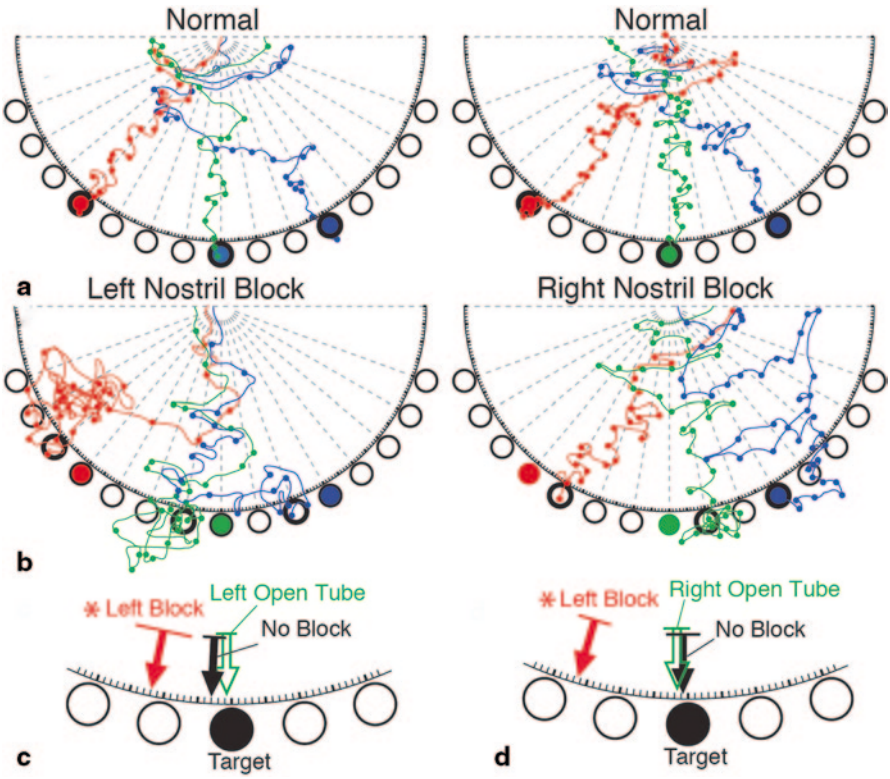

Fig. 2.9 Eastern moles used stereo sniffing to located food items. (**a**) Under normal conditions, with both nostrils open, moles take a relatively straight path to the food item and search the food well first. (**b**) When one nostril was blocked moles erred by moving in the direction of the open nostril as they searched. Moles with a left block searched to the right of the item and those with a right block searched to the left. (**c–d**) Summary data from multiple trials, left nostril blocks in both these examples. The arrows mark the average cross point relative to the food item for each condition. Adapted from: [51]. (Published with kind permission of © Kenneth Catania 2014)

In order to further test the use of bilateral olfactory cues by eastern moles, the nostrils were "flipped" by inserting longer, open tubes into each nostril and crossing them so that the left nostril received air from the right side and right nostril received air from the left side. In this condition the results were even more striking. Moles usually moved towards the food item until close (presumably using serial sniffing cues) but then moved back and forth in apparent confusion as they tried to localize the stimulus (earthworm segment). This greater disruption compared to the nostril block is consistent with a stereo sniffing strategy, because there is a continual mismatch between the intensity cues and the stimulus location as the animal moves back and forth in front of the stimulus. In the crossed nostril condition the moles had great difficulty locating the prey item and often missed it completely. These experiments suggest that eastern moles combine both serial sniffing cues, based on

sequential olfactory samples, with instantaneous comparisons across the nostrils during each sniff. At the same time, moles are making nose movements that provide somatosensory information for each location. The combined use of touch, serial olfactory sampling, and stereo nasal cues provides and impressive sensory armament and helps to explain the success of moles in exploiting diverse soil environments.

Conclusions

The results described above raise a number of interesting questions about the organization and evolution of mammalian brains and behavior related to active touch. Water shrews most certainly use active touch as they search—at high speed—for (often) elusive prey in the shallow waters of streams and ponds. They are primed to attack water movements that result from escaping prey and can respond in as little as 20 milliseconds. They can also use their whiskers to discriminate the details of immobile objects. These two abilities are impressive and in line with the expected characteristics of the water shrews' prey, which include stationary insect larvae but also mobile animals such as fish or crayfish. Given their heavy dependence on whiskers, it was somewhat surprising that water shrews do not exhibit the cortical barrels that characterize the whisker representation in rodents and a number of other small mammals. It is even more surprising that water shrew brainstem trigeminal nuclei exhibit what appear to be the most prominent barrelettes described in mammals. At the same time, there is to date no evidence of thalamic barreloids in water shrews. Together these results raise the possibility that water shrews emphasize sub-cortical processing of touch to a comparatively greater extent than do rodents. It is possible that such an emphasis allows for faster responses by not requiring the longer path lengths to and from the neocortex. The implications of this possibility are interesting in light of shrews' many similarities to ancestral, stem mammals, based on fossil evidence [22]. It is tempting to conjecture that the ancestral mammalian plan had a greater sub-cortical emphasis and that enhanced cortical processing was key to mammalian diversification. Of course an alternative possibility is that there are many ways to efficiently represent mechanoreceptors in cortex—as has been proposed for ocular dominance columns in primates [53]. Shrews and rodents might simply have different but equally efficient cortical circuitries for processing whisker inputs. In support of the latter possibility, many species with whiskers do not exhibit barrels (cats and dogs) and do not resemble ancestral mammals.

Star-nosed moles can be contrasted with water shrews by their complex set of interconnected somatosensory cortical modules. The star is represented in three different maps each characterized by a set of stripes that represent the nasal appendages. These results highlight the flexibility of module form in the mammalian neocortex. For example, it is often suggested that cortical barrels are a reflection of universal cortical subdivisions, the classical columns [54]. But, as Woolsey and Van der Loos

pointed out in their original paper, the shape of a barrel reflects the distribution of mechanoreceptors around a whisker [12]. Therefore, topographic mapping could explain the cylindrical form of a barrel, rather than a fundamental constraint of cortical circuitry. In support of this latter possibility, the receptors of the star are laid out in elongated strips of tissue on each appendage. The cortex representing the rays is not organized in circular columns but rather mirrors the topography of the sensory sheet. Findings in primate somatosensory cortex show a similar reflection of fingers in the form of myelin dense modules in the area 3b finger representation (3b is the homologue of S1—[11]).

Another significant finding from star-nosed moles is the existence of a somatosensory fovea [41, 55]. The central 11th pair of rays are used for detailed investigations and moles make constant saccadic nose movements to position this area on objects of interest. The parallels with visual systems are obvious and, in addition to the behavior, include the preferential expansion of the fovea representation in cortex. The expanded cortical territory representing the tactile fovea is greater than would be predicted from afferent number alone and this too parallels the organization of (primate) visual systems [56]. The result emphasizes that common solutions arise in mammals for processing high-resolution sensory systems. We are intimately familiar with primate visual systems not only from the impressive literature resulting from years of study but also from personal, daily experience scrutinizing visual scenes with our foveas. However, it may come as some surprise that some bats have an auditory fovea. The mustached bat analyzes the 60 kHz frequency range and devotes a large part of its cochlea and cortex to analyzing this behaviorally important frequency. Most surprising is the parallel to saccades that can be drawn from bats' Doppler shift compensation behavior. Bats constantly change outgoing call frequency to "move" the returning echoes into the range of the auditory fovea [57].

Finally, the discovery of underwater sniffing behavior in semi-aquatic water shrews and star-nosed moles stands as one of the more surprising findings in mammal sensory biology. It was thought impossible for mammals to use olfaction underwater [58–60] but moles and shrews have found a work-around. By exhaling and re-inhaling the same air as they sniff while submerged, these species can detect odorants. This behavior is fascinating by itself, but it also provided unexpected insights into the coordination of touch and smell in these species. This stems from the convenience of seeing sniffs, revealing that moles and shrews gather tactile and olfactory information in unison—supporting the generality of similar findings from laboratory rodents [47–49]. These revelations about olfactory abilities in semiaquatic moles and shrews suggested the solution to the impressive prey localization ability in terrestrial, eastern moles. This species coordinates its touches and sniffs in air, as is the case for underwater sniffing. But in addition to this serial sampling strategy, eastern moles add stereo olfactory cues to the analysis allowing for remarkably rapid and efficient movement toward olfactory stimuli.

References

1. Hodgkin AL, Huxley AF (1946) Potassium leakage from an active nerve fibre. Nature 158:376
2. Hodgkin AL, Huxley AF (1952) Movement of sodium and potassium ions during nervous activity. Cold Spring Harb Symp Quant Biol 17:43–52
3. Knudsen EI, Konishi M (1979) Mechanisms of sound localization in the Barn Owl (Tyto-Alba). J Comp Physiol 133(1):13–21
4. Knudsen EI, Konishi M (1980) Monaural occlusion shifts receptive-field locations of auditory midbrain units in the owl. J Neurophysiol 44(4):687–695
5. Carr CE, Boudreau RE (1991) Central projections of auditory nerve fibers in the barn owl. J Comp Neurol 314(2):306–318
6. Moller P (2002) Multimodal sensory integration in weakly electric fish: a behavioral account. J Physiol Paris 96(5–6):547–556
7. Heiligenberg W (1990) Electrosensory systems in fish. Synapse 6(2):196–206
8. Nottebohm F (2005) The neural basis of birdsong. PLoS Biol 3(5):e164
9. Nottebohm F, Liu WC (2010) The origins of vocal learning: new sounds, new circuits, new cells. Brain Lang 115(1):3–17
10. Doupe AJ (1993) A neural circuit specialized for vocal learning. Curr Opin Neurobiol 3(1):104–111
11. Kaas JH, What, If Anything (1983) Is Si - organization of 1st somatosensory area of cortex. Physiol Rev 63(1):206–231
12. Woolsey TA, Vanderlo H (1970) Structural organization of layer-Iv in somatosensory region (Si) of mouse cerebral cortex. Description of a cortical field composed of discrete cytoarchitectonic units. Brain Res 17(2):205
13. Feldman ML, Peters A (1974) A study of barrels and pyramidal dendritic clusters in the cerebral cortex. Brain Res 77(1):55–76
14. Van Der Loos H (1976) Barreloids in mouse somatosensory thalamus. Neurosci Lett 2(1):1–6
15. Ma PM, The barrelettes–architectonic vibrissal representations in the brainstem trigeminal complex of the mouse. I (1991) Normal structural organization. J Comp Neurol 309(2):161–199
16. Krubitzer L, Manger P, Pettigrew J, Calford M (1995) Organization of somatosensory cortex in monotremes: in search of the prototypical plan. J Comp Neurol 351(2):261–306
17. Catania KC, Northcutt RG, Kaas JH, Beck PD (1993) Nose stars and brain stripes. Nature 364(6437):493
18. Catania KC, Kaas JH (1995) Organization of the somatosensory cortex of the star-nosed mole. J Comp Neurol 351(4):549–567
19. Jain N, Catania KC, Kaas JH (1998) A histologically visible representation of the fingers and palm in primate area 3b and its immutability following long-term deafferentations. Cereb Cortex 8(3):227–236
20. Qi HX, Kaas JH (2004) Myelin stains reveal an anatomical framework for the representation of the digits in somatosensory area 3b of macaque monkeys. J Comp Neurol 477(2):172–187
21. Catania KC, Lyon DC, Mock OB, Kaas JH (1999) Cortical organization in shrews: evidence from five species. J Comp Neurol 410(1):55–72
22. Rowe TB, Macrini TE, Luo ZX (2011) Fossil evidence on origin of the mammalian brain. Science 332(6032):955–957
23. Gould E, Negus NC, Novick A (1964) Evidence for echolocation in shrews. J Exp Zool 156:19–37
24. Siemers BM, Schauermann G, Turni H, von Merten S (2009) Why do shrews twitter? Communication or simple echo-based orientation. Biol Lett 5(5):593–596
25. Catania KC, Hare JF, Campbell KL (2008) Water shrews detect movement, shape, and smell to find prey underwater. Proc Natl Acad Sci U S A 105(2):571–576

26. Leitch DB, Gauthier D, Sarko DK, Catania KC (2011) Chemoarchitecture of layer 4 isocortex in the american water shrew (sorex palustris). Brain Behav Evol 78(4):261–271
27. Anjum F, Turni H, Mulder PGH, van der Burg J, Brecht M (2006) Tactile guidance of prey capture in Etruscan shrews. Proc Natl Acad Sci U S A 103(44):16544–16549
28. Catania KC (2006) Olfaction: underwater 'sniffing' by semi-aquatic mammals. Nature 444(7122):1024–1025
29. Catania KC, Catania EH, Sawyer EK, Leitch DB (2013) Barrelettes without barrels in the American water shrew. PLoS One 8(6):e65975
30. Catania KC (2000) Epidermal sensory organs of moles, shrew moles, and desmans: a study of the family talpidae with comments on the function and evolution of Eimer's organ. Brain Behav Evol 56(3):146–174
31. Eimer T (1871) Die schnauze des maulwurfes als tastwerkzeug. Arch Mikr Anat 7:181–191
32. Catania KC (1995) A comparison of the Eimer's organs of three North American moles: the hairy-tailed mole (Parascalops breweri), the star-nosed mole (Condylura cristata), and the eastern mole (Scalopus aquaticus). J Comp Neurol 354(1):150–160
33. Halata Z (1972) Innervation of hairless skin of the nose of mole. I Intraepidermal nerve endings. Z Zellforsch Mikrosk Anat 125(1):108–120
34. Shibanai S (1988) Ultrastructure of the Eimer's organs of the Japanese shrew mole, Urotrichus talpoides (Insectivora, Mammalia) and their changes following infraorbital axotomy. Anat Anz 165(2–3):105–129
35. Catania KC (1996) Ultrastructure of the Eimer's organ of the star-nosed mole. J Comp Neurol 365(3):343–354
36. Marasco PD, Catania KC (2007) Response properties of primary afferents supplying Eimer's organ. J Exp Biol 210(Pt 5):765–780
37. Catania KC, Leitch DB, Gauthier D (2011) A star in the brainstem reveals the first step of cortical magnification. PLoS One 6(7):e22406
38. Catania KC, Kaas JH (1995) Organization of the Somatosensory Cortex of the Star-Nosed Mole. J Comp Neurol 351(4):549–567
39. Chubbuck JG (1966) Small motion biological stimulator. John Hopkins APL Tech Dig 5:18–23
40. Catania KC, Kaas JH (2001) Areal and callosal connections in the somatosensory cortex of the star-nosed mole. Somatosens Mot Res 18(4):303–311
41. Catania KC (1995) Magnified cortex in star-nosed moles. Nature 375(6531):453–454
42. Catania KC, Kaas JH (1997) Somatosensory fovea in the star-nosed mole: behavioral use of the star in relation to innervation patterns and cortical representation. J Comp Neurol 387(2):215–233
43. Lee KJ, Woolsey TA (1975) A proportional relationship between peripheral innervation density and cortical neuron number in the somatosensory system of the mouse. Brain Res 99(2):349–353
44. Catania KC, Remple FE (2004) Tactile foveation in the star-nosed mole. Brain Behav Evol 63(1):1–12
45. Catania KC (2009) Symposium overview: Underwater sniffing guides olfactory localization in semiaquatic mammals. Ann N Y Acad Sci 1170:407–412
46. Welker WI (1964) Analysis of sniffing of the albino rat. Behaviour 22(3/4):223–244
47. Deschenes M, Moore J, Kleinfeld D (2012) Sniffing and whisking in rodents. Curr Opin Neurobiol 22(2):243–250
48. Moore JD, Deschenes M, Furuta T, Huber D, Smear MC, Demers M et al (2013) Hierarchy of orofacial rhythms revealed through whisking and breathing. Nature 497(7448):205–210
49. Ranade S, Hangya B, Kepecs A (2013) Multiple modes of phase locking between sniffing and whisking during active exploration. J Neurosci 33(19):8250–8256
50. Catania KC, Remple FE (2005) Asymptotic prey profitability drives star-nosed moles to the foraging speed limit. Nature 433(7025):519–522
51. Catania KC (2013) Stereo and serial sniffing guide navigation to an odour source in a mammal. Nat Commun 4:1441

52. Rajan R, Clement JP, Bhalla US (2006) Rats smell in stereo. Science 311(5761):666–670
53. Horton JC, Adams DL (2005) The cortical column: a structure without a function. Philos Trans R Soc Lond B Biol Sci 360(1456):837–862
54. Mountcastle VB (1957) Modality and topographic properties of single neurons of cat's somatic sensory cortex. J Neurophysiol 20(4):408–434
55. Catania KC (2001) Early development of a somatosensory fovea: a head start in the cortical space race? Nat Neurosci 4(4):353–354
56. Azzopardi P, Cowey A (1993) Preferential representation of the fovea in the primary visual-cortex. Nature 361(6414):719–721
57. Schnitzler H-U (1968) Die Ultraschall-Ortungslaute der Hufeisen-Fledermäuse (Chiroptera-Rhinolophidae) in verschiedenen Orientierungssituationen. Z Vergl Physiol 57(4):376–408
58. Stephan H, Baron G, Fons R (1984) Brains of soricidae. 2. Volume comparison of brain components. Z Zool Syst Evol 22(4):328–342
59. Estes JA (1989) Adaptations for aquatic living by carnivores. Cornell University Press, Ithaca
60. Repenning CA (1976) Adaptive evolution of sea lions and walruses. Syst Zool 25(4):375–390
61. Sarko DK, Leitch DB, Girard I, Sikes RS, Catania KC (2011) Organization of somatosensory cortex in the Northern grasshopper mouse (Onychomys leucogaster), a predatory rodent. J Comp Neurol 519(1):64–74

Part II
Building Blocks of the Whisker System

Chapter 3
The Whisker Thalamus

Manuel A. Castro-Alamancos

Abstract Sensory information from the whiskers ascends through the trigeminal nuclei in the brainstem to the midbrain and forebrain where it reaches primarily the superior colliculus, the pretectal nuclei, the zona incerta, and the thalamus. The whisker thalamus is at the center of this network because it regulates passage to the barrel cortex as dictated by behavioral state. From barrel cortex, descending activity is fed back to the thalamus and to the other nuclei that process ascending information. Thalamocortical cells in the whisker thalamus receive sensory, cortical, inhibitory, and modulatory afferents. The physiological properties of this network and the functions that emerge from its activity are described here.

Keywords Whisker thalamus · Thalamocortical cells · Trigeminothalamic inputs · Inhibitory inputs · Corticothalamic inputs · Neuromodulator inputs · Operating modes · Thalamocortical modes · Neocortex modes

Components of the Whisker Thalamus

The whisker thalamus consists of two distinct nuclei, the ventroposterior medial thalamus (VPM) and the medial sector of the posterior complex (POm), that receive direct synaptic afferents from the whisker representations in the principal (Pr5)and/or spinal (Sp5) trigeminal nuclei (Fig. 3.1). Sp5 is comprised of subnucleus caudalis (Sp5c), interpolaris (Sp5i) and oralis (Sp5o). Neurons in the whisker thalamus generally project to the primary (S1) and/or secondary somatosensory cortex (S2) and, consequently, are called thalamocortical or relay cells.

Barreloids are a defining cytoarchitectonic feature of a part of the somatosensory thalamus. Barreloids are visible in VPM with cytochrome oxidase staining, but not in POm, and consist of clusters of thalamocortical cells that project to clusters of cells, called *barrels,* located in layer 4 of S1 [1, 2]. Barreloids in VPM receive afferents from Pr5 cells, which also form clusters of cells called *barreletes.* Pr5

M. A. Castro-Alamancos (✉)
Neurobiology and Anatomy, Drexel University College of Medicine,
2900 Queen Lane, Philadelphia, PA 19129, USA
e-mail: mcastro@drexelmed.edu

P. Krieger, A. Groh (eds.), *Sensorimotor Integration in the Whisker System,*
DOI 10.1007/978-1-4939-2975-7_3

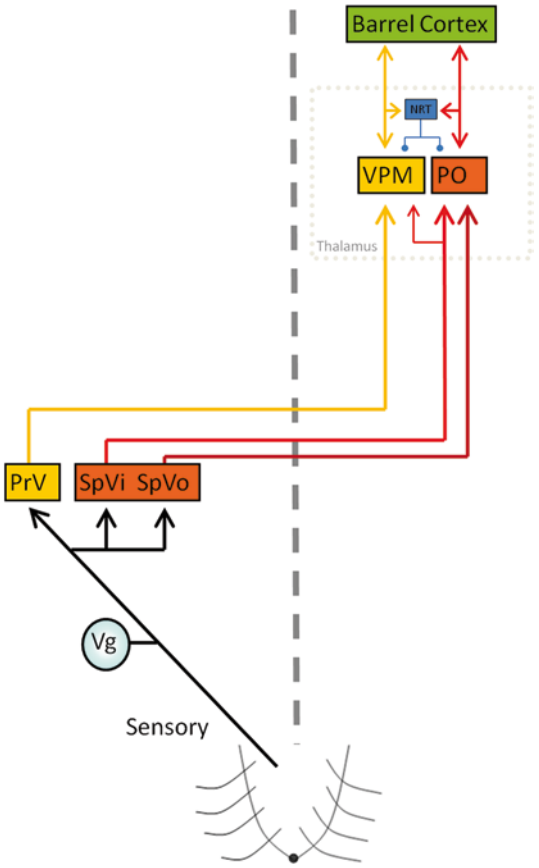

Fig. 3.1 Schematic diagram showing the main connections of the whisker thalamus

barreletes are important for imparting VPM barreloids during development [3]. Barreloids in rat VPM have a rod shape and consist of about 250 neurons [4]. Injecting a retrograde tracer in a single barrel of S1[5] reveals that barreloids consist of a core and a tail;the tails are not observed with cytochrome oxide staining. The cores are located in the dorsal portion of VPM while the tails extend into the ventrolateral portion of VPM. Thalamocortical cells in the dorsal (cores) and ventrolateral (tails) portions of VPM project to different areas of neocortex. The cores selectively innervate barrels in S1, while the tails project more broadly, including dysgranular zones in S1 (i.e. non barrel areas) and S2 [6].

Thalamocortical Cells

At the core of the whisker thalamus circuitry are thalamocortical cells that project to the cortex. The intrinsic excitability of thalamocortical cells has been extensively characterized (for reviews see [7]. Briefly, application of intracellular

current pulses during current clamp recordings produces stereotypical membrane potential (Vm) responses with two main features. First, negative current pulses from resting Vm drive a hyperpolarization that attenuates during a sustained pulse. This sag in the Vm is caused by the hyperpolarization-activated cation current (I_H). Second, upon elimination of the negative current pulse the Vm overshoots the resting Vm and drives a slow depolarization which can trigger a burst of action potentials. This rebound excitation is caused by the low threshold calcium current (I_T). Depending on the Vm of the cell, I_T can be available for activation or it can be inactivated. If the cell is sufficiently hyperpolarized, I_T is available and a positive current pulse will produce the slow depolarization and a burst of action potentials. If the cell is more depolarized, I_T is inactivated and a positive current pulse will drive tonic firing of action potentials, instead of bursts. Thus, depending on the Vm of thalamocortical cells, synaptic inputs can drive bursts of action potentials or single action potentials, in what are termed bursting and tonic firing modes, respectively.

Thalamocortical cells in VPM receive synaptic signals from four main sources and therefore are at the center of a neuronal network that involves trigeminothalamic (sensory), corticothalamic, inhibitory and modulatory inputs. Cells in the reticular nucleus of the thalamus (NRT) provide inhibitory inputs, while cells in the brainstem reticular formation (BRF) provide modulatory inputs. Thalamocortical cells in POm also receive signals from the same four sources as VPM but in different arrangements, and receive additional inputs.

Trigeminothalamic Inputs

Trigeminothalamic sensory fibers originating in different trigeminal nuclei innervate different parts of the whisker thalamus [6, 8–13]. Most of the axons originating in Pr5 (70–90 %) form bushy terminal fields that fill the barreloid cores in VPM, and arise from medium-sized cells with small dendritic trees that are circumscribed to barreletes. The remaining axons that originate in Pr5 (10–30 %) innervate POm and arise from larger-sized cells with expansive dendritic trees that span several barreletes. Slow conducting thin axons that originate in the caudal portion of Sp5i project to the tails of the barreloids in VPM, while fast conducting thick axons originating in the rostral portion of Sp5i project to POm. Only few axons from Sp5o project to the thalamus, and they innervate POm.

Therefore, there are at least five different types of trigeminothalamic synapses according to their target and origin: (1) from Pr5 to the VPM cores, (2) from Sp5i to the VPM tails, (3) from Pr5 to POm, (4) from Sp5i to POm, and (5) from Sp5o to POm. Typically, the response properties of trigeminothalamic synapses in VPM have been studied with intracellular recordings in slices [14, 15] and in vivo [16–18], but no distinction has been made so far between the synaptic responses of the five different trigeminothalamic pathways. Here we focus on trigeminothalamic synapses in VPM.

Trigeminothalamic Synapses in VPM Are Specialized for Driving Thalamocortical Cells

Trigeminothalamic terminals form glutamatergic synaptic contacts with the soma and proximal dendrites of VPM neurons [11, 19]. At the electron microscope level, trigeminothalamic synapses form complex connections called synaptic glomeruli in which axonal and dendritic components are ensheathed by glial cell processes [8]. Several elements are involved: (1) a postsynaptic dendrite which produces prominent excrescences or protrusions; (2) a large axon terminal deeply invaginated by the excrescences that contains spherical synaptic vesicles and makes multiple synaptic contacts or release sites on the dendritic excrescences but no synaptic contacts with the dendritic shaft; (3) a small number of synaptic terminals that contain flattened synaptic vesicles and make contacts with the dendritic shafts at the periphery and immediately adjacent to the glomerulus, which likely consist of inhibitory inputs from the NRT and modulatory inputs from the BRF; (4) the postsynaptic excrescences-presynaptic trigeminothalamic fiber complex is surrounded by glial processes, which may serve to limit the spread of glutamate and may also limit the influence of other neurotransmitters on trigeminothalamic synapses. A fully reconstructed glomerulus of the rat somatosensory thalamus was found to be 5 μm in diameter, in which two dendrites produced a total of 10 excrescences receiving a total of 44 synaptic contacts [8]. Thus, each trigeminothalamic synaptic glomerulus forms a large number of closely spaced synaptic contacts or release sites. This, in combination with the proximal location on the dendrite, combines to produce a very powerful synaptic input.

At the electrophysiological level, trigeminothalamic synapses of adult rodents studied in slices produce short latency, fast rising, large amplitude, highly secure all-or-none EPSPs, which depress in response to repetitive stimulation at frequencies above 2 Hz [14] (Fig. 3.2). The short latency of trigeminothalamic EPSPs is likely due to the fast conducting large-caliber myelinated trigeminothalamic axons and the optimization of the molecular steps responsible for fast synaptic transmission at these synapses. The rise time of the EPSP for synapses that are electrotonically close to the soma, such as trigeminothalamic synapses, is a function of the rate of rise of neurotransmitter concentration and the activation kinetics of the receptor channels. The fast rise time of trigeminothalamic EPSPs may be related to the fast kinetics of the AMPA receptor subunits expressed at these synapses, and the possibility that synaptic glomeruli favor a fast rise of neurotransmitter concentration. The large amplitude EPSPs evoked by a single trigeminothalamic fiber correlates well with the observation at the morphological level that trigeminothalamic synapses contain large size terminals with numerous closely spaced release sites. It also relates well with the fact that evoked trigeminothalamic EPSPs are highly secure, occurring invariantly on almost every stimulus trial at low frequencies, which indicates that this synapse has a high release probability [14].

Repetitive stimulation of trigeminothalamic fibers at frequencies above 2 Hz produces frequency-dependent depression of trigeminothalamic EPSPs [14]. As shown in Fig. 3.2c, the synaptic depression suppresses the efficacy of trigeminal inputs to drive thalamocortical cells unless they are sufficiently depolarized. The depression

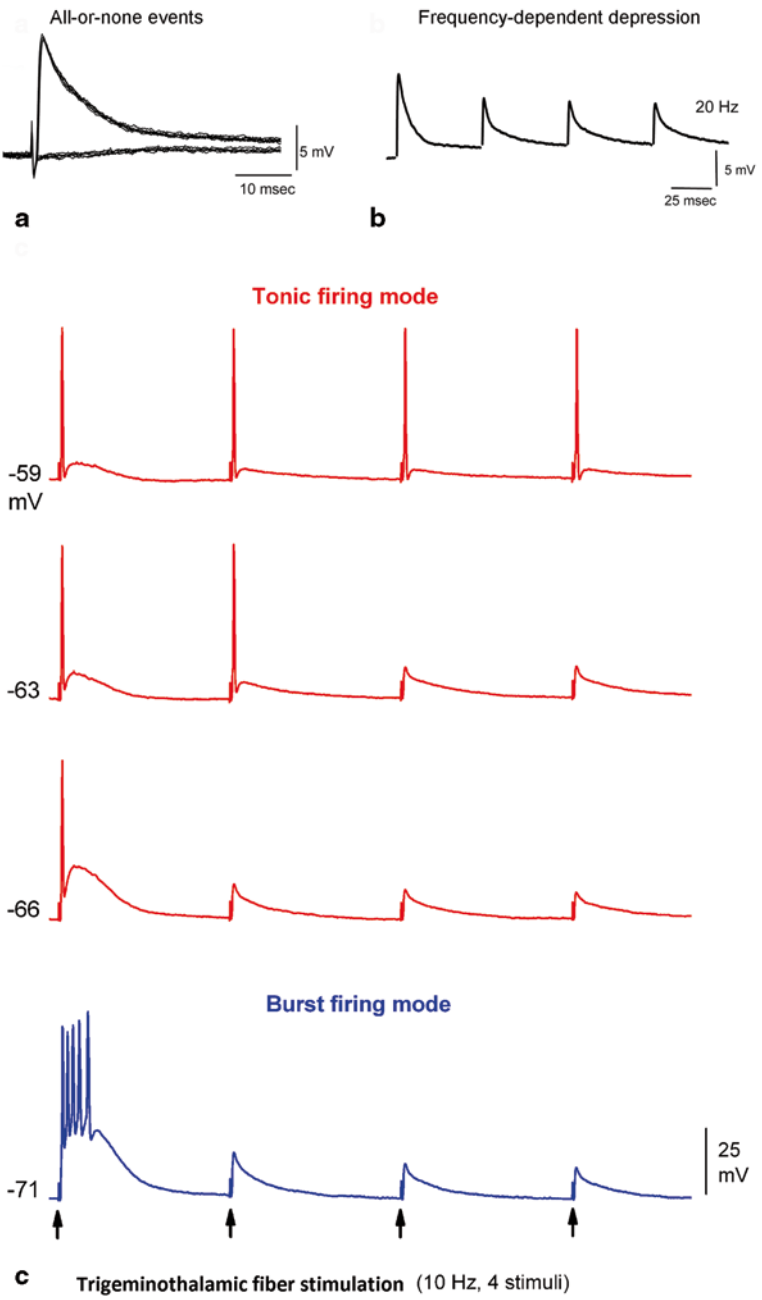

Fig. 3.2 Electrophysiological properties of trigeminothalamic synapses. **a** Large amplitude all or none events evoked in a thalamocortical VPM cell by stimulating the medial lemniscus in a slice preparation. **b** Trigeminothalamic synaptic responses depress with frequency. **c** Trigeminothalamic synaptic depression leads to the low-pass filtering of thalamocortical cells so that cells reach firing threshold only during low frequency trigeminothalamic stimuli (1st stimulus in the 10 Hz train). During high frequency trigeminothalamic stimuli, the thalamocortical cell does not reach firing threshold unless the cell is depolarized. (based on [14])

of trigeminothalamic synapses may be related to their high release probability. Indeed, synapses with high release probability tend to display synaptic depression. As discussed below, these specialized properties of trigeminothalamic synapses serve to endow the trigeminothalamic pathway with useful mechanisms for the regulation of sensory inputs traveling through the thalamus.

Trigeminothalamic synapses are insensitive to acetylcholine and norepinephrine [14]. Application of these neuromodulators, or their respective receptor agonists, does not significantly affect the amplitude of trigeminothalamic EPSPs evoked in thalamocortical cells that are recorded with intracellular solutions used to suppress the postsynaptic actions of these neuromodulators. Thus, thalamocortical cells are affected by these neuromodulators but trigeminothalamic synapses per se appear not to be. This may be related to the protection provided by the glomeruli, which can impede neuromodulators from reaching the presynaptic terminal.

Trigeminothalamic Synapses Dictate Whisker Responses in vivo

The properties displayed by trigeminothalamic EPSPs in slices [14] are also present in vivo [17]. Generally, whisker stimulation evokes few large amplitude unitary trigeminothalamic events (~2) on a given VPM neuron, suggesting that VPM neurons are contacted by few trigeminothalamic fibers [17, 18]. These events usually have a slight difference in latency and sum to produce a larger composite trigeminothalamic EPSP that very effectively drives a VPM neuron during low frequency stimulation. The characteristics of trigeminothalamic EPSPs endow the trigeminothalamic pathway with a powerful capacity to drive thalamocortical neurons. The best whisker stimulus to effectively drive thalamocortical cells is a high velocity/acceleration deflection; not the amplitude of the whisker deflection [20]. Thus, in anesthetized animals receiving low frequency (<2 Hz) and high velocity whisker deflections, the principal whisker (PW) is able to drive a VPM cell very reliably (~80 % of trials) at very short latencies (3–6 ms) [16, 17, 21–26].

However, as we will discuss later, thalamocortical neurons follow high frequency whisker stimulation with great difficulty in anesthetized rats. In other words, only low frequency inputs are effectively relayed to the neocortex in anesthetized rats. This means that the output of thalamocortical neurons to whisker inputs is low-pass filtered;a process also termed rapid sensory adaptation. The analogy with a low-pass filter refers to the fact that steady state responses of thalamocortical cells depress with increases in whisker stimulation frequency (see control in Fig. 3.3). Intracellular recordings in anesthetized rats revealed that the underlying cause of this low-pass filter is the synaptic depression of trigeminothalamic inputs [14, 17]. Like in slices, trigeminothalamic synapses in vivo present robust frequency-dependent depression. As a consequence, whisker stimulation at frequencies above 2 Hz depresses trigeminothalamic EPSPs driving the cell away from its discharge threshold and resulting in a low probability of thalamocortical firing to high frequency whisker stimulation [17]. Strong IPSPs driven by preceding whisker stimuli also drive cells away from their discharge threshold suppressing responses to subsequent

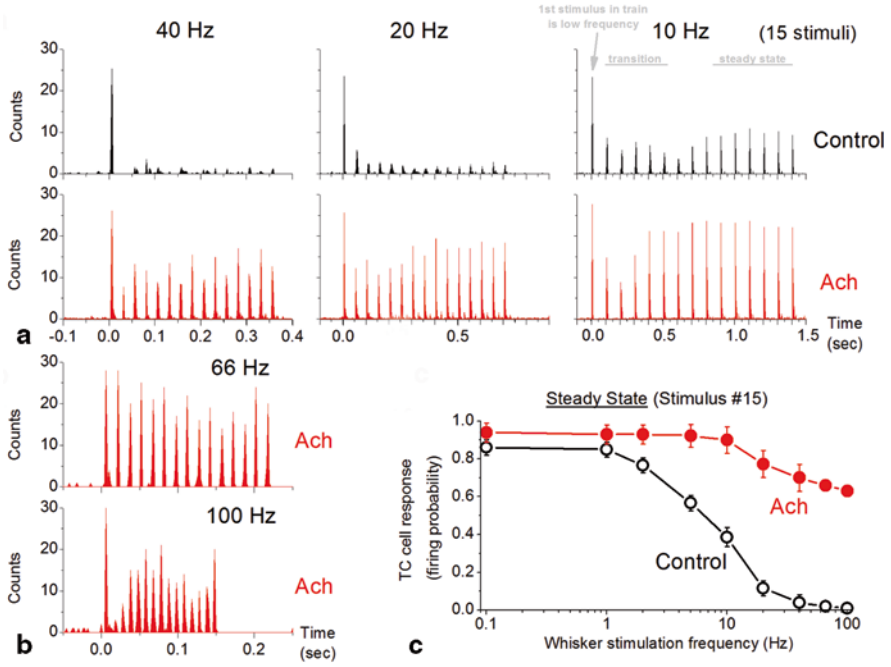

Fig. 3.3 Effect of cholinergic activation on thalamocortical cell responses to whisker stimulation. **a** Upper plots correspond to counts per 2-msec bins evoked by 15 whisker stimuli (30 trials) at different frequencies during quiescent states in a urethane-anesthetized rat (control). Lower plots correspond to the same stimuli during application of acetylcholine in VPM. Note the strong low-pass filtering of VPM responses at frequencies above 2 Hz, but not during application of acetylcholine. The upper right panel notes (in gray) that the first stimulus (#1) in each train is delivered at low frequency reflecting the inter-train interval (10 s). The following few stimuli are transition stimuli that reflect the change between the low frequency stimulus (stimulus #1) and the true effect of the frequency being tested, which is reflected in the steady state response of the later stimuli. **b** Example of whisker stimulation delivered at 66 and at 100 Hz during acetylcholine. Notice that the cell is able to follow these high frequencies during application of acetylcholine in VPM. **c** Population data showing a spectrum analysis of whisker evoked responses in VPM neurons before and during the application of acetylcholine. Note the low-pass filtering of steady state responses during the quiescent state (control) and the opening of this filter during the cholinergic activation state (Ach). Based on [17]

whisker stimulation. But this occurs mostly for transition stimuli, which are those at the beginning of a high frequency train, before IPSPs depress and steady state responses are obtained. Thus, the low-pass filtering of steady state responses seems to be independent of IPSPs [17, 27]. Moreover, this low-pass filtering occurs at the level of the thalamus since it is not apparent in trigeminal nuclei under the same conditions [26, 27]. Hence, the activity-dependent synaptic depression at trigeminothalamic synapses causes the low-pass filtering of sensory inputs through the thalamus. VPM responses driven by trigeminothalamic synapses are further affected by inhibitory inputs, corticothalamic inputs, and neuromodulatory inputs.

Inhibitory Inputs

The source of inhibition in VPM is the NRT. NRT cells have two intrinsic firing modes; burst and tonic firing [7]. NRT synapses are inhibitory, release GABA and trigger IPSPs in thalamocortical cells by activating $GABA_A$ and $GABA_B$ receptors. $GABA_A$ receptors are activated by the amount of GABA released by a single action potential in an NRT fiber, while $GABA_B$ receptor activation appears to require more GABA, usually released by bursts of action potentials, as shown in visual thalamus [28].

Intracellular recordings in vivo reveal that whisker stimulation produces a short latency, fast rising, large amplitude trigeminothalamic EPSP followed by a longer latency GABAergic IPSP in some VPM cells, and only an IPSP in other VPM cells [16, 17]. Trigeminothalamic-evoked IPSPs recorded in VPM cells originate in the NRT because there are apparently no inhibitory interneurons within the ventrobasal thalamus of rodents [8, 29–31]. In vivo, the EPSP-IPSP sequence occurs in cells that are contacted directly by trigeminothalamic fibers representing the stimulated whisker, while the IPSP-alone responses appears to correspond to cells that are not directly innervated by the trigeminothalamic fibers for the stimulated whisker but that receive recurrent inhibition from NRT (cross-inhibition) as a consequence of the whisker stimulation [17, 32].

NRT cells project to thalamocortical cells in VPM in a closed-loop pattern; they project back to the barreloid from where they receive excitation [33]. NRT axons entering adjacent barreloids do not seem to provide the source for cross-inhibition between barreloids. VPM cells extend their dendrites into adjacent barreloids where they can sample recurrent inhibition evoked by adjacent whiskers and this may well be a substrate for cross-inhibition [34, 35]. In addition, it is likely that the excitation received by a population of NRT cells from a barreloid spreads within NRT by means of intra-NRT synaptic collaterals and gap junctions [36–38] leading to the stimulation of NRT cells that project to other barreloids, which could also explain cross-inhibition between barreloids.

POm receives inhibitory inputs from NRT and two other sources; GABAergic inputs arrive from the anterior pretectal nucleus (APT) [39] and the zona incerta (ZI) [40]. In fact, whisker evoked responses are usually absent in POm unless activity in the ZI is suppressed [41, 42].

Corticothalamic Inputs

Corticothalamic fibersoriginate in cells located in layers 5 and 6, and produce distinct synapses in VPM and POm. Corticothalamic cells in the upper part of layer 6 of a barrel column leave a fiber collateral in NRT and project exclusively to VPM where they form rod-like terminal fields in a thalamic barreloid. Thus, thalamocortical cells in VPM and corticothalamic cells in layer 6 form closed-loops for the flow of information between a thalamic barreloid and a cortical barrel column [43],

with NRT inputs controlling this loop. In contrast, corticothalamic cells located in the lower part of layer 6 also leave fiber collaterals in NRT but innervate large sectors of POm and intralaminar thalamic nuclei [44]. Corticothalamic cells located in layer 5 leave fiber collaterals in POm as they continue to midbrain and brainstem. There are potentially at least three different types of corticothalamic synapses: layer 6(upper) to VPM, layer6 (lower) to POM, and layer 5 to POm. In fact, anterograde tracers injected in barrel cortex produce three distinct types of synapses in whisker thalamus. Small (0.5–0.8 μm in diameter) varicosities that correspond to small axon terminals form synapses with small dendritic arbors in VPM, and with dendritic shafts in POm. Giant terminals (3–5 μm in diameter), similar to trigeminothalamic synapses in VPM (see above), form synapses only in POm [45].

Corticothalamic synapses in VPM release glutamate and trigger EPSPs in thalamocortical and NRT cells by activating AMPA, NMDA and mGLUR receptors [46]. Corticothalamic EPSPs are different compared to trigeminothalamic EPSPs. They have long latencies, slow rise times, small amplitudes, and they are unreliable, but facilitate at frequencies above 2 Hz (for a review see [32]). The long latencies and slow rise times reflect the thinness and sparse myelination of corticothalamic fibers, and the fact that the synapses they form are located in distal dendrites;electrotonically far from the soma. The small amplitude and low security at low frequencies and the facilitation at high frequencies reflect a small number of release sites per synapse (estimated to be 1), and a low release probability at those sites during low frequency inputs that increases sharply during high frequency inputs. Corticothalamic synapses display robust forms of post-tetanic potentiation and long-term potentiation (LTP) when stimulated repetitively at relatively high frequencies (10 Hz and above) [47]. This contrasts with trigeminothalamic synapses which display no evidence of long-term synaptic plasticity, such as LTP (unpublished). Long-term depression (LTD) is also induced when repetitive stimulation occurs at low frequencies (1 Hz). Thereby, corticothalamic synapses have mechanisms for bidirectional changes in long-term synaptic efficacy [47].

Corticothalamic EPSPs mediated by metabotropic glutamate receptors (mGluR) are triggered by robust high-frequency stimulation and produce a long-lasting slow depolarization [48]. This observation has lead to the proposal that corticothalamic synapses are modulators of thalamocortical cells [49]. However, it seems more reasonable to consider corticothalamic synapses as *frequency-dependent drivers* of thalamocortical cells because high frequency (>2 Hz) corticothalamic activity can drive thalamocortical cells through ionotropic glutamate receptors as effectively as sensory inputs [32]. On the other hand, it is not clear when corticothalamic cells would display such a high-frequency firing rate synchronously in order to effectively trigger synaptic facilitation and drive thalamocortical cells; but this caveat also applies to the proposed modulatory role of corticothalamic synapses, which also require high frequency trains to trigger the mGluR depolarization.

In addition, the efficacy of corticothalamic synapses is suppressed by neuromodulators, such as acetylcholine and norepinephrine [50], which contrasts with the lack of sensitivity of trigeminothalamic synapses to these same neuromodulators [14]. The amplitude of EPSPs evoked in NRT neurons by stimulating single

corticothalamic fibers is several times larger than EPSPs evoked in thalamocortical neurons, and the number of GluR4-receptor subunits at these synapses may provide a basis for the differential synaptic strength [46]. The stronger corticothalamic EPSPs on NRT cells assures that low-frequency corticothalamic activity drives NRT cells and triggers robust feedforward inhibition in VPM thalamocortical cells.

Corticothalamic synapses in POm can produce two different types of responses, which have been ascribed to corticothalamic cells originating in layers 5 and 6. POm responses for cells originating in layer 6 are similar to the responses evoked in VPM by layer 6 cells, while POm responses originating in layer 5 are similar to trigeminothalamic synapses [51]. Consequently, corticothalamic synapses originating in layer 5 have been assigned the role of drivers of POm cells [45, 52].

Neuromodulator Inputs

The response properties of the whisker thalamus are modified on a moment to moment basis (i.e. rapidly and dynamically) by neuromodulators acting locally or in afferent structures [32]. Neurotransmitters often act through ionotropic receptors (ligand-gated channels), while neuromodulators typically act through metabotropic receptors (G-protein coupled). The effects of neurotransmitters acting on ionotropic receptors are usually phasic, lasting only 10's of milliseconds. The effects of neuromodulators acting on metabotropic receptors are usually slower and longer lasting, in the range of 100's of milliseconds to seconds or more. However, the distinction between a neurotransmitter and a neuromodulator can be rather arbitrary and most neuroactive substances can function as both. For instance, a substance acting as a neuromodulator can alter the properties of ion channels that are activated by the same substance acting as a neurotransmitter (e.g. by affecting channel opening probabilities, receptor desensitization, release probability). Substances acting on ionotropic receptors may also (appear to) act as neuromodulators if the presynaptic neuron fires continuously in a sustained manner. A number of substances are well-known neuromodulators and some of these have significant actions in the whisker thalamus:

- *Glutamate* acts on ionotropic receptors (AMPA, NMDA, kainate) and on metabotropic receptors (mGluR1-8). Glutamate is released by trigeminothalamic and corticothalamic synapses. It appears that metabotropic receptors are activated by corticothalamic synapses innervating NRT and thalamocortical cells [48].
- *Norepinephrine* is a catecholamine that acts on α and β type metabotropic receptors. Noradrenergic neurons are found in the locus coeruleus in the brainstem reticular formation, from where they projectthroughout the brain, including the thalamus. Noradrenergic neurons discharge robustly during high levels of vigilance and attention, reduce their firing during slow-wave sleep and stop firing during REM sleep [53–55]. As described below, norepinephrine has significant effects in the whisker thalamus.

- *Dopamine* is a catecholamine that acts on D1 and D2 type metabotropic receptors. So far, there is little evidence of any role of dopamine in the whisker thalamus.
- *Histamine* acts on $H_{1–4}$ type metabotropic receptors. Histamine neurons are found in the posterior hypothalamus, in thetuberomammillary complex, from where they project throughout the brain, including the thalamus. Histaminergic neurons discharge robustly during wakefulness [56].
- *Serotonin* acts on ionotropic (5-HT_3 and metabotropic (5-HT_1, 5-HT_2, 5-HT_4, 5-HT_5, 5-HT_6, 5-HT_7) receptors. Serotonin neurons are found in the raphe nuclei in the brainstem reticular formation, from where they project throughout the brain, including the thalamus. Similar to noradrenergic neurons, 5-HT neurons fire tonically during wakefulness, decrease their activity in slow-wave sleep, and are nearly quiet during REM sleep [57, 58].
- *Acetylcholine* acts on ionotropic (nicotinic) and metabotropic (muscarinic) receptors. Acetylcholine or cholinergic neurons projecting to the thalamus are found in the pedunculopontine nuclei (PPT) and in the dorsolateral tegmental nuclei (LDT) in the brainstem. Cholinergic neurons are also found in the basal forebrain from where they project to the neocortex. Cholinergic neurons in the LDT/PPT complex discharge vigorously during REM sleep and also during wakefulness [59], and the levels of acetylcholine increase in the thalamus during those states [60]. As described below, acetylcholine has significant effects in the whisker thalamus.
- *Neuropeptides* usually act at metabotropic receptors. Neurons very often make both a conventional neurotransmitter (glutamate, GABA) and one or more neuropeptides. Examples include opioids (endorphins, enkephalins, dynorphins), substance P, etc.
- *Hormones* are chemicals released by cells that affect cells in other parts of the organism generally through the bloodstream. For example, epinephrine (adrenaline) is a catecholamine that is released by the adrenal gland.
- Other *intrinsic neuroactive substances* released within the thalamus may include adenosine, cannabinoids, growth factors, cytokines, etc.
- *Extrinsic neuroactive substances* that reach the thalamus may also affect thalamic modes. For example, nicotine from tobacco, caffeine from coffee, etc.

Neuromodulators Set Different Modes in the Whisker Thalamus

A mode or state is a particular arrangement of the properties of the thalamic network components that gives rise to a distinct input-output function. The properties that are most commonly affected to determine a mode include the Vm, intrinsic firing mode, intrinsic excitability and the strength of synaptic inputs. Neuromodulators act directly on thalamocortical cells and on afferent synapses within the thalamus to change these properties. Neuromodulators may also indirectly influence thalamocortical cells by affecting the activity of the main excitatory and inhibitory afferents,

such as those from trigeminal complex, cortex and NRT. Activity in these afferents changes their strength via short-term synaptic plasticity but may also affect the Vm, firing mode, and intrinsic excitability of thalamocortical cells. Thus, thalamocortical modes are set in a complex way, through direct and indirect effects of neuromodulators affecting several variables. The main variables determining a thalamocortical mode are:

- *Vm of thalamocortical cells*: This critical variable is highly dynamic because it is affected by most, if not all, neurotransmitters and neuromodulators present in the thalamocortical network.
- *Intrinsic excitability*: Neurons express a number of voltage-dependent conductances that endow them with different response properties. For example, thalamocortical cells are characterized by strong I_H and I_T. These currents are not only affected by Vm but can be directly affected by many neuromodulators. Excitatory and inhibitory inputs can affect the intrinsic excitability of thalamocortical cells by changing the Vm and engaging voltage-dependent currents. In addition, when the resting Vm of thalamocortical cells is at the reversal of incoming synaptic inputs, the increased conductance produced by the synaptic inputs can affect the integrative properties of the cell, without changing the Vm, by shunting the membrane (e.g. shunting inhibition).
- *Thalamocortical firing mode and rate*: As already mentioned, thalamocortical cells are characterized by two distinct firing modes: bursting and tonic. These firing modes are set primarily by the Vm of thalamocortical cells. Thus, factors that influence Vm also determine firing mode. During bursting, thalamocortical cells produce a cluster of action potentials (usually between 3–6 action potentials) at very high frequencies (> 100 Hz) riding on the low-threshold calcium spike. However, thalamocortical cells are limited by how fast they can produce bursts because of the dependence of bursts on the low-threshold calcium current, which must be deinactivated by hyperpolarization; cells can usually burst at < 15 Hz. In contrast, during tonic firing, cells can produce action potentials at much higher constant firing rates.
- *Activity and strength of excitatory and inhibitory afferents:* As already mentioned, thalamocortical cells in VPM receive excitatory (glutamatergic) inputs from trigeminothalamic and corticothalamic synapses, and inhibitory (GABAergic) inputs from synapses originating in NRT. Activity in these afferents can change the Vm of thalamocortical cells, which can result in changes in intrinsic excitability and firing mode. In addition, some of these afferents can activate metabotropic receptors leading to a modulator action on thalamocortical cells. For example, glutamate released from corticothalamic synapses can activate mGLUR, and GABA released from inhibitory synapses can activate $GABA_B$ receptors. The frequency and pattern of activity in the afferents also sets the strength of these synapses by affecting short-term synaptic plasticity and temporal integration. For example, high-frequency activity in corticothalamic synapses will increase release probability at these synapses and enhance the strength of this pathway. In contrast, activity in Pr5 cells will depress trigeminothalamic synapses and

decrease the strength of this pathway. Finally, neuromodulators released in the thalamus can directly affect the efficacy of excitatory and inhibitory neurotransmission rather selectively. For example, acetylcholine and norepinephrine decreases corticothalamic but not trigeminothalamic synaptic strength [14, 50].

The Operating Modes (states) of the Whisker Thalamus

The Thalamus Displays Slow Oscillations During Quiescence

There are two obvious major operating modes of the whisker thalamus. The first mode is called slow oscillation, quiescent or deactivated. The second mode, discussed later, is called activated or arousal. The slow oscillation, quiescent or deactivated mode is considered here as a broad baseline state during which active sensory processing per se does not occur because animals are either sleeping, inattentive/drowsy, or anesthetized. While there may be different modes within these states, for simplicity, we encompass them here within a single mode. In this mode, slow synchronous oscillations are common, particularly when animals are in non-REM sleep. In addition, this mode is induced by surgical anesthesia, which is when most electrophysiological studies take place. During non-REM sleep, slow wave oscillations are most prevalent in the deeper stage(s) (typically referred as stage 3 or 3/4). In less deep stages of sleep, slow oscillations occur interposed with other rhythms, such as spindle oscillations. Similar to non-REM sleep stages, there are also stages of anesthesia. During the surgical anesthesia stage, the slow oscillation mode is evident but varies in frequency and amplitude depending on the level or plane of surgical anesthesia and the anesthetic used. Thus, the depth of anesthesia and the specific effects of the anesthetic used are critical at setting the particular characteristics of this mode. The main characteristics of the thalamic modes we will discuss are summarized in Table 3.1.

During slow-wave sleep and surgical anesthesia thalamocortical cells fire at low frequencies producing either bursts or single spikes. This slow activity in thalamocortical cells can be driven by cortical activity, such as cortical Up states during ongoing cortical slow oscillations (also known as Up and Down states) [7, 61]. Slow activity can also be driven by intrinsic currents in thalamocortical cells in the absence of corticothalamic activity [61, 62]. Full expression of slow oscillations in thalamocortical cells appears to require both thalamic and cortical oscillators [63]. During the slow oscillation mode, thalamocortical cells are usually fairly hyperpolarized close to the reversal potential of K^+ (Down states), and they may transition for short periods of time to more depolarized states due to synaptic bombardment, usually produced by spontaneous corticothalamic and NRT activity (Up states) [7]. In this situation, NRT cells can burst and drive strong IPSPs in thalamocortical cells. The hyperpolarization caused by the IPSPs deinactivates I_T and activates I_H

Table 3.1 Effects of thalamocortical modes on

		Spontaneous thalamocortical firing	Relay of sensory inputs	Sensory response receptive field	Corticothalamic feedback
Thalamocortical modes	*Slow oscillation*	Low tonic and bursts	Relay of low frequency inputs (low-pass filter)	Focused	Frequency-dependent facilitation (high-pass filter)
	Activated	Noisy tonic	Relay of low and high frequency inputs	Broader	Strong high-pass filter
	Cholinergic	Noisy tonic	Relay of low and high frequency inputs	Broader	Removal of high-pass filter by low frequency response enhancement
	Noradrenergic	Quiet tonic	Relay of Low and high frequency Inputs	Highly focused	Strong high-pass filter
	Epileptic ($GABA_A$ block)	Rhythmic ~ 3 Hz bursts	Relay of low frequency inputs; long-latency response enhancement	Broader (long-latency)	Removal of high-pass filter by low-frequency response enhancement

in thalamocortical cells. This sets up thalamocortical cells so that at the outset of the IPSP a rebound depolarization occurs caused by activation of I_T. The rebound triggers a burst of action potentials in thalamocortical cells that feedback to NRT and cortex. Such an interplay between NRT and thalamocortical cells repeated in a sequence at 5–12 Hz is responsible for the generation of spindle oscillations that recur every few seconds [64]. Spindles are waxing and waning rhythms with dominant frequencies of 7–14 Hz, grouped in sequences that last 1–3 s and recur periodically at 0.1–0.2 Hz. Spindle oscillations are common during the slow oscillation mode and are prominent at sleep onset, during loss of awareness, and are prevalent during barbiturate anesthesia, which enhances inhibitory efficacy. Apart from the occasional spindle oscillations, thalamocortical activity in VPM during this state is of low frequency (< 1 Hz) [17, 26, 65].

During Quiescence the Thalamus Suppresses High Frequency Sensory Inputs

Sensory responses driven by whisker stimulation during the slow oscillation mode are of high probability, as long as the stimulus is delivered at low frequencies. As soon as the frequency of the whisker stimulus augments, the thalamocortical response is strongly depressed [17]. Thalamocortical neurons follow high-frequency

whisker stimulation with great difficulty in the slow oscillation mode. In other words, steady state thalamocortical sensory responses are low-pass filtered or display rapid sensory adaptation. Intracellular recordings in urethane anesthetized rats during the slow oscillation mode show that whisker stimulation evokes EPSP–IPSP sequences in thalamocortical neurons, and both the EPSPs and IPSPs depress with repetitive whisker stimulation at frequencies above 2 Hz [17].

The underlying cause of the low-pass filter or rapid sensory adaptation is the frequency-dependent depression of trigeminothalamic synapses [14]. Sensory inputs at frequencies above 2 Hz reduce the efficacy of trigeminothalamic synapses, which drives the trigeminothalamic EPSP away from the discharge threshold of the cell and results in a low probability of firing for thalamocortical cells. Importantly, as described below, a major impact of activated (arousal) states is to change the amount of rapid sensory adaptation (i.e. to open the low-pass filter); in other words, to allow high frequency sensory inputs through the thalamus. In addition to the depression of trigeminothalamic synapses, thalamocortical IPSPs (returning from NRT) driven by sensory inputs may also contribute to the low-pass filtering of sensory inputs during the slow oscillation mode [17]. The suppression by IPSPs is most notable at the beginning of a high-frequency sensory stimulus train, when IPSPs are more robust and produce a stronger hyperpolarization. However, less effect of feedback inhibition is observed for steady state sensory responses that occur at the end of a long high-frequency train [17, 27]. Steady state responses are mostly depressed by trigeminothalamic synaptic depression with little contribution of synaptic inhibition from NRT.

Excitatory receptive fields of VPM cells consist of an excitatory center, the principal whisker (PW), and an excitatory surround, the adjacent whiskers (AWs) [21]. For low-frequency sensory inputs, during the slow oscillation mode, the response to the PW (receptive field excitatory center) is much stronger and faster than the response to AWs (receptive field excitatory surround) [26]. As mentioned above, for high-frequency sensory inputs, both PW and AW responses are depressed because of the low-pass filtering at the trigeminothalamic pathway. Simultaneous stimulation of the PW and several AWs (i.e. multiwhisker stimulation) produces a response in thalamocortical cells that matches the PW, as if the AWs had not been stimulated [26, 65]. This may reflect little convergence form different whiskers onto VPM cells and/or the fact that PW responses are already maximal due to the efficacy of trigeminothalamic synapses from the PW, so that converging synapses from AWs can ad little more. Interestingly, in the next stage of processing, the barrel cortex, simultaneous multiwhisker responses obtained with intracellular recordings are clearly distinguishable from PW responses starting in layer 4[66]. Multiwhisker responses are slightly faster and stronger than PW responses in layer 4, and even more clearly distinguishable in upper layers indicating slight convergence in layer 4 and stronger convergence from several whiskers in layers 2/3 [66]. Interestingly, in the superior colliculus, which is also a target of trigeminal synapses (like the whisker thalamus), simultaneous multiwhisker stimulation produces much stronger postsynaptic responses than stimulation of the PW or any of the AWs alone [67]. In contrast to VPM, most superior colliculus cells respond weakly to single whisker stimulation,

so there is room to express convergence during multiwhisker stimulation. Indeed, intracellular recordings demonstrate that the multiwhisker enhancement in superior colliculus reflects convergence of trigeminotectal synapses from several whiskers [67]. Thus, trigeminothalamic and trigeminotectal pathways are very distinct in their responses to whisker stimulation.

Arousal allows the Flow of High Frequency Sensory Inputs Through the Thalamus

The activated mode of the thalamus is typical when animals are awake during arousal, and it is most robust when animals are in a state of vigilance during attentive processing, such as during performance in a behavioral task [68]. A somewhat similar activated mode to that observed during waking occurs when animals enter REM sleep. The activated mode can be induced in anesthetized animals (e.g. urethane-anesthetized animals) that are in a slow oscillation mode by electrically stimulating the brainstem reticular formation (BRF), and this is a useful method to determine the impact of the activated mode on sensory thalamocortical responses because it allows to compare slow oscillation and activated sensory responses in the same neurons [17, 26, 69, 70]. In addition, animals that are sedated and slightly narcotized are usually also in this activated mode [21, 25]. In this narcotized state, VPM cells show response adaptation within a sustained ramp-and-hold (i.e. long-lasting and non repetitive) whisker deflection, some directional tuning (preference for a particular direction of whisker deflection), responses to both the PW and at least one AW, and significant spontaneous firing rates (~15 Hz) [25]. The VPM firing rate of narcotized animals is equivalent to the activated (arousal) mode induced in urethane anesthetized animals after BRF stimulation [17, 70].

A main effect of arousal on whisker evoked VPM responses is on rapid sensory adaptation to repetitive stimuli. During the activated mode, typical of arousal, low-frequency sensory responses are a bit stronger (increase slightly in probability) and become faster (evoked spikes display shorter latencies) [17, 26]. But the most robust change occurs at the level of high-frequency sensory processing. During the activated mode, thalamocortical cells robustly enhance their responses to high-frequency sensory signals, virtually eliminating the low-pass filtering(rapid sensory adaptation) typical of the slow oscillation mode [17] (Fig. 3.4).

Interestingly, early studies revealed significant differences regarding the cut-off frequency of the low-pass filter or rapid sensory adaptation in VPM. Some studies performed in urethane-anesthetized animals reported strong frequency-dependent depression at frequencies above ~2 Hz [23, 24], while others using narcotized rats reported the ability to follow frequencies of up to at least 12 Hz [21, 71, 72]. Our findings were able to explain these differences as a consequence of the level of activation imposed by the anesthesia employed. In urethane-anesthetized rats, the output of thalamic neurons to sensory inputs is very effectively low-pass filtered so that whisker stimulation above 2 Hz is not relayed to neocortex [17]. However,

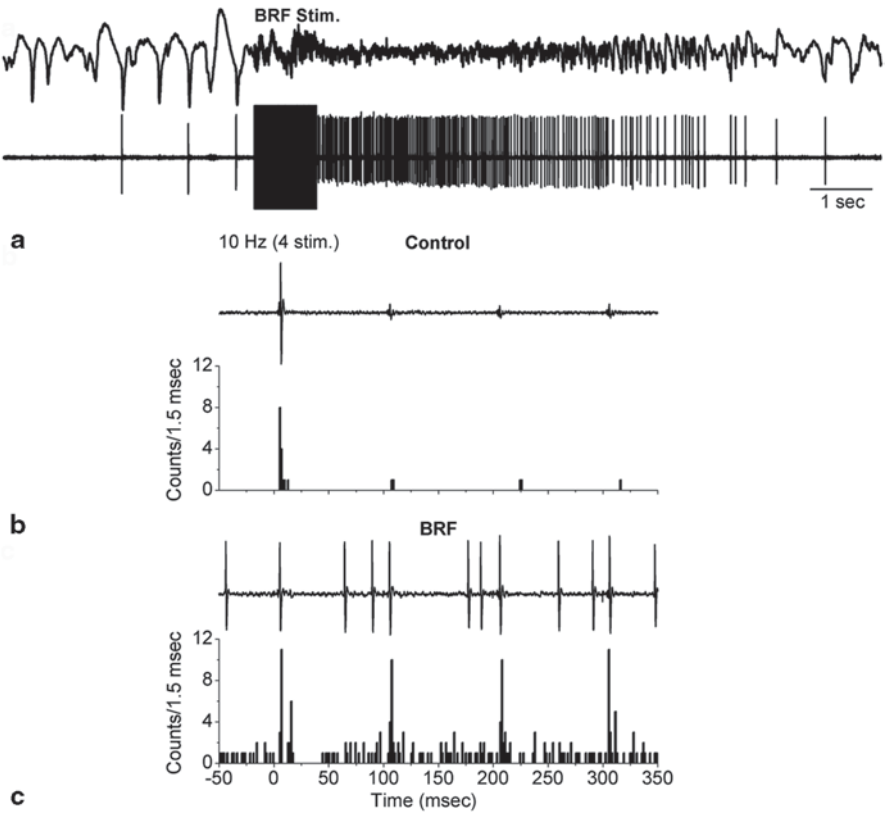

Fig. 3.4 Effect of activation (arousal) on thalamocortical cell responses to whisker stimulation. **a** Stimulation of the brainstem reticular formation (BRF) increases the spontaneous firing of thalamocortical cellsin VPM. Note also the abolishment of slow oscillations and the activation of the field potential recorded through the same electrode as the VPM single-unit. **b** Raw traces and PSTH of the responses evokedin a VPM single-unit by whisker deflections at 10 Hz (train of 4 stimuli) during the quiescence or slow oscillation state. Note that the cell only spikes in response to the 1st stimulus in the train, which is delivered at low frequency. **c** Activation or arousal caused by BRF stimulation enhances the spontaneous firing of the cell but also allows the cell to respond to each of the whisker deflections in the 10 Hz train, eliminating the low-pass filtering or adaptation. (based on [17])

when the thalamus of these anesthetized rats is aroused or activated by lessening the level of anesthesia, stimulating the brainstem reticular formation (BRF stimulation) (Fig. 3.4), or applying acetylcholine to the thalamus (Fig. 3.3), the trigeminothalamic low-pass filter is significantly opened allowing the relay of sensory inputs at much higher frequencies. Indeed, during activated states, VPM cells can follow whisker stimulation fairly efficiently at frequencies of up to 40 Hz, and even 100 Hz [17, 32]. Thus, during activated states the low-pass filtering of sensory inputs is largely eliminated; low frequency and high frequency sensory stimuli are able to effectively drive thalamocortical cells [17, 70].

Arousal Enlarges Thalamocortical Receptive Fields

The excitatory receptive fields of VPM cells consist of an excitatory center, the PW, and an excitatory surround, the AWs. Early studies that recorded from VPM neurons in anesthetized rats indicated that they respond solely to a single whisker [10]. However, subsequent work revealed that many VPM cells respond to deflections of multiple whiskers during light anesthesia [21–23, 25]. The receptive field size (i.e. the number of whiskers that stimulate a neuron) of thalamocortical cells in the whisker thalamus varies according to their location. VPM cells in the core of the barreloid have been characterized as having small (single whisker) receptive fields, while those in the ventrolateral portion of VPM have larger (multiwhisker) receptive fields [6].

The size of the receptive field can be rapidly modified by the thalamic mode. To demonstrate this requires the use of multiple whisker stimulators and recording the same cells during different thalamic modes. In anesthetized animals that are in the slow oscillation mode, thalamic or forebrain activation produced by BRF stimulation, neuromodulators, or lessening the level of anesthesia, enlarge the excitatory surround of VPM cells [26]. Thus, for low-frequency sensory inputs, during the slow oscillation mode, the response (spike probability) to the PW (receptive field excitatory center) is much stronger than the response to AWs (receptive field excitatory surround). However, during activation, there is an enhancement of the response to AWs, which typically still have longer latencies than the PW. For high-frequency sensory inputs, during the slow oscillation mode, both PW and AW responses are depressed because of the low-pass filtering at the trigeminothalamic pathway. However, during the activated mode, there is a significant increase in both PW and AW responses so that they become similar, but PW responses are generally stronger than AW responses during high frequency sensory inputs [26]. During the activated mode, the excitatory responses of VPM cells to the PW are identical to those of multiwhisker stimulation (simultaneous PW and AWs stimulation). Consequently, multiwhisker and PW responses in VPM are similar during either the slow oscillation and activated modes [26].

Arousal High-Pass Filters corticothalamic Responses

Corticothalamic responses display synaptic facilitation, which contrasts with the synaptic depression of trigeminothalamic responses. Thus, the amplitude of corticothalamic EPSPs is relatively small during low frequency corticothalamic activity because corticothalamic synapses have a low release probability and occur at distal portions of the dendritic tree. However, during high frequency corticothalamic activity (>5 Hz) the probability of release at corticothalamic synapses sharply increases due to synaptic facilitation, producing large amplitude EPSPs that can be as powerful as those produced by trigeminothalamic sensory afferents. Thus, the corticothalamic pathway is an activity dependent driver of thalamocortical activity,

an effect that can be demonstrated by using electrical stimulation to stimulate corticothalamic fibers [32]. However, it is not clear when corticothalamic cells discharge synchronously at high-frequencies to engage the activity dependent facilitation of corticothalamic synapses.

During thalamic activation, produced by BRF stimulation or specific neuromodulators applied into the thalamus (e.g. norepinephrine) in anesthetized animals, corticothalamic responses are further high-pass filtered [50]. This means that during arousal low frequency corticothalamic inputs are suppressed in the thalamus, while high frequency inputs are allowed. Such a mechanism may function to regulate the activity that can drive thalamocortical cells depending on behavioral state, so that only very salient activity from the cortex can drive thalamocortical cells during arousal.

Cholinergic Activation of the Thalamus Produces Effects similar to Arousal

Neuromodulators produce highly selective effects that set different modes of thalamocortical and corticothalamic information processing. Natural behavioral states are likely set by a combination of neuromodulators acting in synergy. The cholinergic mode is expected to occur during both REM sleep and during states of vigilance in awake animals. Cholinergic activation leads to a sharp increase of spontaneous thalamocortical tonic firing in VPM, which reduces signal to noise ratios [26, 65]. Typically, cells increase their spontaneous firing by more than 10-fold compared to the slow oscillation mode. The effect of cholinergic activation on spontaneous firing is explained by both a direct depolarization of VPM cells and a suppression of NRT cell firing. The depolarizing effect of acetylcholine on thalamocortical cells is mediated by muscarinic receptors, which block a resting K^+ conductance, and the hyperpolarizing effect of acetylcholine on NRT cells is produced by activation of a K^+ conductance [73].

During the cholinergic activated mode, low-frequency sensory responses are a bit stronger (increase slightly in probability) and become faster (evoked spikes display shorter latencies) compared to the slow oscillation mode but signal to noise ratios are sharply reduced because thalamocortical cells increase their spontaneous firing rates [17, 26, 65]. Another robust change occurs at the level of high-frequency sensory processing (Fig. 3.3). During cholinergic activation, thalamocortical cells robustly enhance their responses to high-frequency sensory signals, virtually eliminating the low-pass filtering of sensory signals in the sensory thalamus [17]. The post synaptic depolarization of thalamocortical neurons produced by cholinergic activation is sufficient to eliminate the effect of trigeminothalamic synaptic depression on the relay of high frequency inputs [14, 17]. Cholinergic activation also reduces the effects of inhibition from NRT by suppressing IPSPs in thalamocortical cells [14, 17]. Just like the effect of activation produced by BRF stimulation (see above), cholinergic activation enlarges the excitatory surround of VPM cells.

Isolated corticothalamic EPSPs studied in slices (inhibition blocked)are suppressed by acetylcholine, an effect that is independent of the postsynaptic depolarizing actions of acetylcholine [50]. However, cholinergic activation in vivo leads to an enhancement of low-frequency corticothalamic responses, which reduces the amount of facilitation in corticothalamic responses, making thalamocortical cells responsive to a wide frequency band of cortical signals [65]. This is likely explained because acetylcholine suppresses feedforward inhibition and depolarizes thalamocortical cells, making them more responsive to corticothalamic inputs [50]. Consequently, during cholinergic activation, the selectivity of VPM cells for high-frequency corticothalamic signals (high-pass filtering) is lost. This may cause a major problem for thalamocortical sensory processing, because it allows low-frequency cortical signals to become effective drivers of thalamocortical cells. Such an effect seems undesirable during sensory processing, because thalamocortical cells may not be able to distinguish sensory and cortical inputs. One possibility is that the enhanced responsiveness to low-frequency cortical signals during cholinergic activation is related to sensory experiences (dreams) that are driven by internal, top-down, representations during REM sleep (when cholinergic activation is strong). During REM sleep, cortical cells may be strong drivers of thalamocortical neurons, which could serve to feed top-down representations to upper layers of primary sensory cortex via the thalamus, perhaps related to sensory experiences during this phase of sleep.

Noradrenergic Activation Increases Signal-to-Noise Ratios of Thalamocortical Cells

The noradrenergic mode is expected to occur during states of vigilance in attentive animals. In VPM, noradrenergic activation leads to a reduction of thalamocortical cell firing so that they have basically nil spontaneous firing [65]. The effect of noradrenergic activation on spontaneous thalamocortical firing is completely mediated by the NRT because during thalamic disinhibition (block of GABA receptors) norepinephrine no longer suppresses thalamocortical cells. In fact, during disinhibition, thalamocortical cells in VPM are excited by norepinephrine. Noradrenergic activation strongly excites NRT cells, which inhibit thalamocortical cells in VPM [65].

The effects of norepinephrine on sensory responses are similar to those produced by cholinergic activation but without the increase in spontaneous firing [65]. For sensory signals, noradrenergic activation sets sensory processing to a focused and noise-free excitatory receptive field, which contrasts with the broad and noisy excitatory receptive field characteristic of cholinergic activation. Norepinephrine also facilitates the high-frequency responses to whisker stimulation, albeit less effectively than cholinergic activation.

Noradrenergic activation enhances AW responses but only for one whisker and for low-frequency responses. Whereas cholinergic activation enhances high-frequency responses for several AWs, norepinephrine only enhances high-frequency

responses for the PW. This indicates that high-frequency sensory inputs are highly focused to the center of the receptive field during noradrenergic activation. Consequently, VPM receptive fields are more focused during noradrenergic activation than during cholinergic activation.

Similar to the effects of acetylcholine in slices, isolated corticothalamic EPSPs are suppressed by norepinephrine [50]. In vivo, noradrenergic activation further high-pass filters corticothalamic responses [65]. The high-pass filtering ensures that thalamocortical cells are not driven by cortical signals unless those signals arrive at high frequencies. This effect is similar to that observed after BRF stimulation in anesthetized animals [50]. Thus, for corticothalamic signals, noradrenergic activation sets corticothalamic processing to a noise-free high-frequency signal detection mode.

Noradrenergic activation may provide a dynamic mechanism to focus thalamocortical receptive fields, high-pass filter corticothalamic signals, and enhance signal-to-noise ratios. Possibly, the more focused receptive fields and higher signal-to-noise ratios during noradrenergic activation reflect a more appropriate information processing mode for spatial discrimination of sensory inputs.

During Active Whisking Thalamocortical Activity Increases

Rodents use their whiskers to navigate the environment by performing fast rhythmic whisker movements. During active exploration, whisking consists in ellipsoid movements (which are characterized by whisker protractions) through the air and over objects at between 4 and 15 Hz. During active whisking in air, thalamocortical cell activity in VPM increases compared to non-whisking [74, 75]. VPM cell firing also increases during artificial whisking in air, which is induced by electrical stimulation of motor nerves in a pattern resembling active whisking [76].

Sensory responses evoked by stimuli delivered during active whisking are usually suppressed compared to non-whisking. For example, whisker follicle or infraorbital nerve stimulation evokes a smaller field potential and/or fewer spikes in VPM during active whisking periods than during non-whisking [74, 75]. Also, paired-pulse ratios (amplitude of the response to the second stimulus divided by the amplitude of the first) are significantly smaller during non-whisking, indicating stronger pairedpulse depression. Thus, just like during activated modes [17], thalamocortical cells appear to follow high-frequency stimuli much better during active whisking. During artificial whisking, most VPM cells enhance their response when the whiskers contact an object compared to the response during whisking in air, while other cells suppress their responses [76]; cells in the ventrolateral portion of VPM appear to convey a pure touch signal because they mostly fire when a whisker contacts an object but not during whisking in air, while cells in the dorsal portion of VPM may convey both touch and movement signals. However, it is worth noting that there may be significant differences between active whisking in behaving rats and artificial whisking in anesthetized rats.

The Whisker Thalamus is not Required for Detection of Salient Stimuli

We have employed an active avoidance task to study sensory detection. In this task, freely moving rats must detect a whisker conditioned stimulus (WCS) that signals an upcoming aversive event (footshock); if the animal detects the WCS, and moves (shuttles) to an adjacent compartment (within 7 s after stimulus onset), the aversive stimulus is completely avoided. The WCS consists of an electrical pulse (1 ms) delivered at 10 Hz to the whisker pad through a pair of implanted wires. The WCS produces responses in thalamus, neocortex and other brain areas that are similar to those evoked by deflecting a few whiskers simultaneously [68, 77]. Intriguingly, reversible or irreversible lesions of the whisker thalamus blocks detection of a low salience (low intensity)WCS but does not affect detection of a high salience (high intensity) WCS [78, 79]. In the absence of the thalamus, the animals are able to detect the high salience WCS with the superior colliculus. However, the whisker thalamus alone was not sufficient to detect the low salience WCS; both the thalamus and superior colliculus were required to detect low salience stimuli. Trigeminothalamic and trigeminotectal whisker pathways work synergistically to detect low salient (hard to detect) stimuli, but are redundant during detection of highly salient (easy to detect) stimuli.

Thalamic Disinhibition Leads to Epilepsy

Epilepsy has many different causes and there are a number of rodent genetic models that produce spontaneous seizures involving the thalamocortical network. Apart from genetic models, the simplest way to generate seizures in the brain is to impair the control that GABA-mediated inhibition has on excitation. This can be accomplished by blocking GABA receptors (disinhibition) using specific antagonists. Disinhibition may occur naturally in the brain due to a variety of mechanisms including withdrawal of inhibitory synapses or death of inhibitory cells caused by various insults, developmental disorders and/or activity-dependent mechanisms.

Block of thalamic $GABA_A$ receptors in vivo leads to ~3 Hz activity in thalamocortical cells that is translated into ~3 Hz spike-wave discharges in the neocortex, and these discharges are abolished by subsequent block of thalamic $GABA_B$ receptors [80]. Work in vitro has shown that when thalamic $GABA_A$ receptors are blocked, $GABA_B$-mediated responses are observed in thalamocortical cells due to longer and higher frequency bursts in NRT neurons caused by a reduction of intra-NRT inhibition [81]. The longer time constants of $GABA_B$-mediated hyperpolarization drive the slower ~3 Hz activity, which is then logically abolished by blocking $GABA_B$ receptors. This ~3 Hz activity resembles the activity observed during absence seizures, and has been proposed as a laboratory model of this disorder (for a review see [82]).

Block of thalamic GABA receptors has robust consequences on sensory responses in VPM indicating strong control of whisker responses by the NRT [27]. During

high-frequency (10 Hz) whisker stimulation, thalamic disinhibition enhances short-latency multiwhisker (PW and AWs) and PW responses but only of "transition stimuli", which are those stimuli in between the first stimulus and the last of a 10 Hz train [27], which are those stimuli that are most affected by whisker-evoked IPSPs [17]. Thalamic disinhibition also enhances long-latency multiwhisker and PW responses evoked by all stimuli in a train regardless of their frequency and position within a train. Thalamic disinhibition slightly enhances the short-latency response of the strongest whisker in the surround during low-frequency stimulation. In addition, thalamic disinhibition enhances the long-latency response of most of the whiskers in the surround during low-frequency stimulation.

During thalamic disinhibition, there are two major effects on corticothalamic responses. First, low-frequency responses are strongly enhanced [27]; similar to the effects of acetylcholine [65]. Responses to all 10 stimuli in a train at 2 and 5 Hz are significantly enhanced by thalamic disinhibition. Second, there are complex effects of thalamic disinhibition on frequency-dependent facilitation evoked by corticothalamic stimulation. Steady-state facilitated responses (i.e., last 5 stimuli in a 10 stimulus train), evoked at 5 and 10 Hz, are further enhanced by disinhibition. However, the last five stimuli in 20 and 40 Hz trains do not reach a steady facilitated state; instead these responses depress after reaching peak facilitation. This depression phenomenon appears to be related to the ability of high-frequency corticothalamic stimulation (facilitation) to trigger epileptic-like discharges (leading to post-discharge depression). These discharges are not evoked during thalamic disinhibition when high-frequency whisker stimulation is used. Thus, it appears that during thalamic disinhibition high-frequency corticothalamic activity can trigger seizures.

Thalamocortical Modes Set Neocortex Modes

Thalamocortical Firing controls Activation (Arousal) in the Barrelcortex

During quiescence the neocortex generates slow oscillations consisting of Up and Down states. The Up states resemble short periods of cortical activation (arousal). Sparse thalamocortical activity resulting in low synaptic cooperativity is the best trigger of cortical Up states in slices [61, 83]. Similarly, in vivo, the different spontaneous tonic firing of thalamocortical cells during different thalamic modes leads to different modes in the barrel cortex [84]. Cholinergic stimulation of the thalamus increases thalamocortical spontaneous tonic firing and leads to activation(arousal) of the barrel cortex. In contrast, noradrenergic stimulation of the thalamus abolishes thalamocortical spontaneous tonic firing and leads to deactivation or slow oscillations in the barrel cortex [84]. Thalamocortical activity per se can control barrel cortex activation and deactivation.

Thalamocortical Firing Suppresses Whisker Responses in Barrel Cortex

One of the main findings we have made in behaving animals is that arousal suppresses sensory (whisker-evoked) responses in barrel cortex [68, 70, 85]. The sensory suppression caused by arousal is mimicked in anesthetized animals by BRF stimulation, and the cause of the suppression has been shown to be the activity dependent depression of the thalamocortical pathway [68, 70]. Basically, increases in thalamocortical firing caused by arousal depress (or adapt) the thalamocortical pathway, so that when low-frequency sensory stimuli arrive in the neocortex they encounter an activated barrel cortex and a suppressed thalamocortical pathway. Consequently, rapid sensory adaptation mainly occurs during slow oscillation states because during arousal increased thalamocortical firing adapts the thalamocortical pathway, so that the thalamocortical pathways of alert animals is in the adapted (suppressed) state [68]. Cortical sensory responses evoked by whisker stimulation at low-frequency during the slow oscillation mode are very large, driving many action potentials in single cells, and spread widely in barrel cortex, driving many neurons. Sensory suppression during arousal appears to be useful to make cortical responses sharper and more selective [85, 86]. Thalamocortical activity per se can control sensory responsiveness in barrel cortex.

References

1. Woolsey TA, Van der Loos H (1970) The structural organization of layer IV in the somatosensory region (SI) of mouse cerebral cortex. The description of a cortical field composed of discrete cytoarchitectonic units. Brain Res 17:205–242
2. Van Der Loos H (1976) Barreloids in mouse somatosensory thalamus. NeurosciLett 2:1–6
3. Erzurumlu RS, Murakami Y, Rijli FM (2010) Mapping the face in the somatosensory brainstem. Nat Rev Neurosci 11:252–263
4. Land PW, Buffer SA Jr, Yaskosky JD (1995) Barreloids in adult rat thalamus: three-dimensional architecture and relationship to somatosensory cortical barrels. J Comp Neurol 355:573–588
5. Saporta S, Kruger L (1977) The organization of thalamocortical relay neurons in the rat ventrobasal complex studied by the retrograde transport of horseradish peroxidase. J Comp Neurol 174:187–208
6. Pierret T, Lavallee P, Deschenes M (2000) Parallel streams for the relay of vibrissal information through thalamic barreloids. J Neurosci 20:7455–7462
7. Steriade M, Jones EG, McCormick DA (1997) Thalamus. Elsevier, New York
8. Spacek J, Lieberman AR (1974) Ultrastructure and three-dimensional organization of synaptic glomeruli in rat somatosensory thalamus. J Anat 117:487–516
9. Feldman SG, Kruger L (1980) An axonal transport study of the ascending projection of medial lemniscal neurons in the rat. J Comp Neurol 192:427–454
10. Chiaia NL, Rhoades RW, Bennett-Clarke CA, Fish SE, Killackey HP (1991) Thalamic processing of vibrissal information in the rat. I. Afferent input to the medial ventral posterior and posterior nuclei. J Comp Neurol 314:201–216

11. Williams MN, Zahm DS, Jacquin MF (1994b) Differential foci and synaptic organization of the principal and spinal trigeminal projections to the thalamus in the rat. Eur J Neurosci 6:429–453
12. Veinante P, Deschenes M (1999) Single- and multi-whisker channels in the ascending projections from the principal trigeminal nucleus in the rat. J Neurosci 19:5085–5095
13. Veinante P, Jacquin MF, Deschenes M (2000) Thalamic projections from the whisker-sensitive regions of the spinal trigeminal complex in the rat. J Comp Neurol 420:233–243
14. Castro-Alamancos MA (2002c) Properties of primary sensory (lemniscal) synapses in the ventrobasal thalamus and the relay of high-frequency sensory inputs. J Neurophysiol 87:946–953
15. Miyata M, Imoto K (2006) Different composition of glutamate receptors in corticothalamic and lemniscal synaptic responses and their roles in the firing responses of ventrobasal thalamic neurons in juvenile mice. J Physiol 575:161–174
16. Brecht M, Sakmann B (2002) Whisker maps of neuronal subclasses of the rat ventral posterior medial thalamus, identified by whole-cell voltage recording and morphological reconstruction. J Physiol 538:495–515
17. Castro-Alamancos MA (2002b) Different temporal processing of sensory inputs in the rat thalamus during quiescent and information processing states in vivo. J Physiol 539:567–578
18. Deschenes M, Timofeeva E, Lavallee P (2003) The relay of high-frequency sensory signals in the Whisker-to-barreloid pathway. J Neurosci 23:6778–6787
19. De Biasi S, Amadeo A, Spreafico R, Rustioni A (1994) Enrichment of glutamate immunoreactivity in lemniscal terminals in the ventropostero lateral thalamic nucleus of the rat: an immunogold and WGA-HRP study. Anat Rec 240:131–140
20. Temereanca S, Simons DJ (2003) Local field potentials and the encoding of whisker deflections by population firing synchrony in thalamic barreloids. J Neurophysiol 89:2137–2145
21. Simons DJ, Carvell GE (1989) Thalamocortical response transformation in the rat vibrissa/barrel system. J Neurophysiol 61:311–330
22. Armstrong-James M, Callahan CA (1991) Thalamo-cortical processing of vibrissal information in the rat. II. spatiotemporal convergence in the thalamic ventroposterior medial nucleus (VPm) and its relevance to generation of receptive fields of S1 cortical “barrel” neurones. J Comp Neurol 303:211–224
23. Diamond ME, Armstrong-James M, Ebner FF (1992) Somatic sensory responses in the rostral sector of the posterior group (POm) and in the ventral posterior medial nucleus (VPM) of the rat thalamus. J Comp Neurol 318:462–476
24. Ahissar E, Sosnik R, Haidarliu S (2000) Transformation from temporal to rate coding in a somatosensory thalamocortical pathway [see comments]. Nature 406:302–306
25. Minnery BS, Bruno RM, Simons DJ (2003) Response transformation and receptive field synthesis in the lemniscaltrigeminothalamic circuit. J Neurophysiol 90:1556–1570
26. Aguilar JR, Castro-Alamancos MA (2005) Spatiotemporal gating of sensory inputs in thalamus during quiescent and activated states. J Neurosci 25:10990–11002
27. Hirata A, Aguilar J, Castro-Alamancos MA (2009) Influence of subcortical inhibition on barrel cortex receptive fields. J Neurophysiol 102:437–450
28. Kim U, McCormick DA (1998) The functional influence of burst and tonic firing mode on synaptic interactions in the thalamus. J Neurosci 18:9500–9516
29. Barbaresi P, Spreafico R, Frassoni C, Rustioni A (1986) GABAergic neurons are present in the dorsal column nuclei but not in the ventroposterior complex of rats. Brain Res 382:305–326
30. Harris RM, Hendrickson AE (1987) Local circuit neurons in the rat ventrobasal thalamus–a GABA immunocytochemical study. Neuroscience 21:229–236
31. Ohara PT, Lieberman AR (1993) Some aspects of the synaptic circuitry underlying inhibition in the ventrobasal thalamus. J Neurocytol 22:815–825
32. Castro-Alamancos MA (2004b) Dynamics of sensory thalamocortical synaptic networks during information processing states. Prog Neurobiol 74:213–247
33. Desilets-Roy B, Varga C, Lavallee P, Deschenes M (2002) Substrate for cross-talk inhibition between thalamic barreloids. J Neurosci 22:RC218

34. Varga C, Sik A, Lavallee P, Deschenes M (2002) Dendroarchitecture of relay cells in thalamic barreloids: a substrate for cross-whisker modulation. J Neurosci 22:6186–6194
35. Lavallee P, Deschenes M (2004) Dendroarchitecture and lateral inhibition in thalamic barreloids. J Neurosci 24:6098–6105
36. Landisman CE, Long MA, Beierlein M, Deans MR, Paul DL, Connors BW (2002) Electrical synapses in the thalamic reticular nucleus. J Neurosci 22:1002–1009
37. Shu Y, McCormick DA (2002) Inhibitory interactions between ferret thalamic reticular neurons. J Neurophysiol 87:2571–2576
38. Sohal VS, Huguenard JR (2003) Inhibitory interconnections control burst pattern and emergent network synchrony in reticular thalamus. J Neurosci 23:8978–8988
39. Bokor H, Frere SG, Eyre MD, Slezia A, Ulbert I, Luthi A, Acsady L (2005) Selective GABAergic control of higher-order thalamic relays. Neuron 45:929–940
40. Bartho P, Freund TF, Acsady L (2002) Selective GABAergic innervation of thalamic nuclei from zonaincerta. Eur J Neurosci 16:999–1014
41. Trageser JC, Keller A (2004) Reducing the uncertainty: gating of peripheral inputs by zonaincerta. J Neurosci 24:8911–8915
42. Lavallee P, Urbain N, Dufresne C, Bokor H, Acsady L, Deschenes M (2005) Feedforward inhibitory control of sensory information in higher-order thalamic nuclei. J Neurosci 25:7489–7498
43. Bourassa J, Pinault D, Deschenes M (1995) Corticothalamic projections from the cortical barrel field to the somatosensory thalamus in rats: a single-fibre study using biocytin as an anterograde tracer. Eur J Neurosci 7:19–30
44. Deschenes M, Veinante P, Zhang ZW (1998) The organization of corticothalamic projections: reciprocity versus parity. Brain Res Brain Res Rev 28:286–308
45. Hoogland PV, Wouterlood FG, Welker E, Van der Loos H (1991) Ultrastructure of giant and small thalamic terminals of cortical origin: a study of the projections from the barrel cortex in mice using Phaseolus vulgaris leuco-agglutinin (PHA-L). Exp Brain Res 87:159–172
46. Golshani P, Liu XB, Jones EG (2001) Differences in quantal amplitude reflect GluR4- subunit number at corticothalamic synapses on two populations of thalamic neurons. Proc Natl Acad Sci U S A 98:4172–4177
47. Castro-Alamancos MA, Calcagnotto ME (1999) Presynaptic long-term potentiation in corticothalamic synapses. J Neurosci 19:9090–9097
48. McCormick DA, von Krosigk M (1992) Corticothalamic activation modulates thalamic firing through glutamate "metabotropic" receptors. Proc Natl Acad Sci U S A 89:2774–2778
49. Sherman SM, Guillery RW (1998) On the actions that one nerve cell can have on another: distinguishing "drivers" from "modulators". Proc Natl Acad Sci U S A 95:7121–7126
50. Castro-Alamancos MA, Calcagnotto ME (2001) High-pass filtering of corticothalamic activity by neuromodulators released in the thalamus during arousal: in vitro and in vivo. J Neurophysiol 85:1489–1497
51. Reichova I, Sherman SM (2004) Somatosensorycorticothalamic projections: distinguishing drivers from modulators. J Neurophysiol 92:2185–2197
52. Sherman SM, Guillery RW (1996) Functional organization of thalamocortical relays. J Neurophysiol 76:1367–1395
53. Hobson JA, McCarley RW, Wyzinski PW (1975) Sleep cycle oscillation: reciprocal discharge by two brainstem neuronal groups. Science 189:55–58
54. Foote SL, Aston-Jones G, Bloom FE (1980) Impulse activity of locus coeruleus neurons in awake rats and monkeys is a function of sensory stimulation and arousal. Proc Natl Acad Sci U S A 77:3033–3037
55. Aston-Jones G, Bloom FE (1981) Nonrepinephrine-containing locus coeruleus neurons in behaving rats exhibit pronounced responses to non-noxious environmental stimuli. J Neurosci 1:887–900
56. Brown RE, Stevens DR, Haas HL (2001) The physiology of brain histamine. Prog Neurobiol 63:637–672

57. McGinty DJ, Harper RM (1976) Dorsal raphe neurons: depression of firing during sleep in cats. Brain Res 101:569–575
58. Trulson ME, Jacobs BL (1979) Raphe unit activity in freely moving cats: correlation with level of behavioral arousal. Brain Res 163:135–150
59. el Mansari M, Sakai K, Jouvet M (1989) Unitary characteristics of presumptive cholinergic tegmental neurons during the sleep-waking cycle in freely moving cats. Exp Brain Res 76:519–529
60. Williams JA, Comisarow J, Day J, Fibiger HC, Reiner PB (1994a) State-dependent release of acetylcholine in rat thalamus measured by in vivo microdialysis. J Neurosci 14:5236–5242
61. Rigas P, Castro-Alamancos MA (2007) Thalamocortical Up states: differential effects of intrinsic and extrinsic cortical inputs on persistent activity. J Neurosci 27:4261–4272
62. Hughes SW, Cope DW, Blethyn KL, Crunelli V (2002) Cellular mechanisms of the slow (< 1 Hz) oscillation in thalamocortical neurons in vitro. Neuron 33:947–958
63. Crunelli V, Hughes SW (2010) The slow (< 1 Hz) rhythm of non-REM sleep: a dialogue between three cardinal oscillators. Nat Neurosci 13:9–17
64. McCormick DA, Bal T (1997) Sleep and arousal: thalamocortical mechanisms. Annu Rev Neurosci 20:185–215
65. Hirata A, Aguilar J, Castro-Alamancos MA (2006) Noradrenergic activation amplifies bottom-up and top-down signal-to-noise ratios in sensory thalamus. J Neurosci 26:4426–4436
66. Hirata A, Castro-Alamancos MA (2008) Cortical transformation of wide-field (multiwhisker) sensory responses. J Neurophysiol 100:358–370
67. Cohen JD, Hirata A, Castro-Alamancos MA (2008) Vibrissa sensation in superior colliculus: wide-field sensitivity and state-dependent cortical feedback. J Neurosci 28:11205–11220
68. Castro-Alamancos MA (2004a) Absence of rapid sensory adaptation in neocortex during information processing states. Neuron 41:455–464
69. Moruzzi G, Magoun HW (1949) Brain stem reticular formation and activation of the EEG. Electroencephalogr Clin Neurophysiol 1:455–473
70. Castro-Alamancos MA, Oldford E (2002) Cortical sensory suppression during arousal is due to the activity- dependent depression of thalamocortical synapses. J Physiol 541:319–331
71. Simons DJ (1985) Temporal and spatial integration in the rat SI vibrissa cortex. J Neurophysiol 54:615–635
72. Hartings JA, Simons DJ (1998) Thalamic relay of afferent responses to 1- to 12-Hz whisker stimulation in the rat. J Neurophysiol 80:1016–1019
73. McCormick DA (1992) Neurotransmitter actions in the thalamus and cerebral cortex and their role in neuromodulation of thalamocortical activity. Prog Neurobiol 39:337–388
74. Fanselow EE, Nicolelis MA (1999) Behavioral modulation of tactile responses in the rat somatosensory system. J Neurosci 19:7603–7616
75. Lee S, Carvell GE, Simons DJ (2008) Motor modulation of afferent somatosensory circuits. Nat Neurosci 11:1430–1438
76. Yu C, Derdikman D, Haidarliu S, Ahissar E (2006) Parallel thalamic pathways for whisking and touch signals in the rat. PLoS Biol 4:e124
77. Cohen JD, Castro-Alamancos MA (2010b) Behavioral state dependency of neural activity and sensory (whisker) responses in superior colliculus. J Neurophysiol 104:1661–1672
78. Cohen JD, Castro-Alamancos MA (2007) Early sensory pathways for detection of fearful conditioned stimuli: tectal and thalamic relays. J Neurosci 27:7762–7776
79. Cohen JD, Castro-Alamancos MA (2010a) Detection of low salience whisker stimuli requires synergy of tectal and thalamic sensory relays. J Neurosci 30:2245–2256
80. Castro-Alamancos MA (1999) Neocortical synchronized oscillations induced by thalamic disinhibition in vivo. J Neurosci 19:RC27
81. Huntsman MM, Porcello DM, Homanics GE, DeLorey TM, Huguenard JR (1999) Reciprocal inhibitory connections and network synchrony in the mammalian thalamus. Science 283:541–543
82. Beenhakker MP, Huguenard JR (2009) Neurons that fire together also conspire together: is normal sleep circuitry hijacked to generate epilepsy? Neuron 62:612–632

83. Favero M, Castro-Alamancos MA (2013) Synaptic cooperativity regulates persistent network activity in neocortex. J Neurosci 33:3151–3163
84. Hirata A, Castro-Alamancos MA (2010) Neocortex network activation and deactivation states controlled by the thalamus. J Neurophysiol 103:1147–1157
85. Castro-Alamancos MA (2002a) Role of thalamocortical sensory suppression during arousal: focusing sensory inputs in neocortex. J Neurosci 22:9651–9655
86. Hirata A, Castro-Alamancos MA (2011) Effects of cortical activation on sensory responses in barrel cortex. J Neurophysiol 105:1495–1505

Chapter 4
Synaptic Microcircuits in the Barrel Cortex

Gabriele Radnikow, Guanxiao Qi and Dirk Feldmeyer

Abstract An elementary feature of sensory cortices is thought to be their organisation into functional signal-processing units called 'cortical columns'. These elementary units process sensory information arriving from peripheral receptors; they are vertically oriented throughout all cortical layers and contain several thousands of excitatory and inhibitory synaptic connections. To understand how sensory signals are transformed into electrical activity in the neocortex it is necessary to elucidate the spatial-temporal dynamics of cortical signal processing and the underlying neurons and synaptic 'microcircuits'.

In the somatosensory barrel cortex there appears to be a structural correlate for the 'functional' cortical column. Therefore, it has become an attractive model system to study the synaptic microcircuitry in the neocortex. Although many synaptic connections in whisker-related cortical 'columns' have been characterised over the past years our knowledge is far from complete, in particular with respect to inhibitory connections. In this chapter we will summarise recent data on different excitatory and inhibitory synaptic connections in a whisker-related 'column' of the somatosensory cortex and try to outline their function in the neuronal network. This requires an appreciation of the diverse types of excitatory and inhibitory neurons and their function within cortical columns and beyond. When necessary, we will also discuss the synaptic input from and to subcortical structures, in particular the thalamus. However, we will not provide a detailed description of the functional mechanisms of these connections; this is beyond the scope of this chapter.

D. Feldmeyer (✉) · G. Radnikow · G. Qi
Institute of Neuroscience and Medicine, INM-2, Research Centre Jülich,
Leo-Brandt-Strasse, Jülich 52425, Germany
e-mail: dfeldmeyer@ukaachen.de; d.feldmeyer@fz-juelich.de

Department of Psychiatry, Psychotherapy and Psychosomatics, Function of Cortical Microcircuits Group, RWTH Aachen University, Aachen 52074, Germany

JARA Brain—Translational Brain Medicine, Aachen, Germany

G. Radnikow
e-mail: g.radnikow@fz-juelich.de

G. Qi
e-mail: g.qi@fz-juelich.de

P. Krieger, A. Groh (eds.), *Sensorimotor Integration in the Whisker System,*
DOI 10.1007/978-1-4939-2975-7_4

Keywords Sensory cortices · Cortical columns · Cortical signal processing · Somatosensory barrel cortex · Excitatory and inhibitory synaptic connection · Thalamus

Abbreviations

5-$HT_{3a}R$	Serotonin 3a receptor
AP	Action potential
BC	Basket cell
BPC	Bipolar cell
BTC	Bitufted cell
CB	Calbindin
CC	Corticocortical
ChR2	Channelrhodopsin 2
CR	Calretinin
CT	Corticothalamic
c.v.	Coefficient of variation
DBC	Double bouquet cell
ENGC	Elongated neurogliaform cell
EPSP	Excitatory postsynaptic potential
FS	Fast spiking
IPSP	Inhibitory postsynaptic potential
KCC2	Potassium chloride co-transporter
LTS	Low threshold spiking
MB	Multipolar bursting
M1	The primary motor cortex
NGFC	Neurogliaform cell
NPY	Neuropeptide Y
POm	Posterior medial
PPR	Paired pulse ratio
PV	Parvalbumin
SBC	Single bouquet cell
SOM	Somatostatin
S1	The primary somatosensory
S2	The secondary somatosensory
TC	Thalamocortical
VIP	Vasoactive intestinal peptide
vM1	The primary vibrissal motor cortex
VPM	Ventroposterior medial

Introduction

The whisker-related portion of the primary somatosensory (S1) area (the ‘barrel cortex’) in rodents exhibits a topological organisation similar to the peripheral (contralateral) tactile receptors, the vibrissae on the rodent’s snout. Because of this the

barrel cortex has become a model system for investigating synaptic microcircuits and even long-range synaptic connectivity related to the structural representation of sensory receptors (for recent reviews see e.g. [1–3]).

In this chapter we will attempt to provide an overview of the neuronal composition of 'barrel columns' [4] and their local (in contrast to long-range) excitatory and inhibitory synaptic connections. In particular, we will concentrate on those synaptic connections for which the morphology and the functional properties for both pre- and postsynaptic neurons have been characterised; this was mostly done using paired or multiple recordings. Only when little or no information is available for the barrel cortex, we will also refer to synaptic connections and their functional roles in other cortical areas.

Our description of the synaptic network in the barrel cortex and its activation will start with the thalamocortical (TC) input to this cortical region. We will then proceed with the description of individual, mostly monosynaptic neuronal microcircuits. Neocortical microcircuits can be classified as excitatory or inhibitory, feed-forward, feedback and/or recurrent and synaptic connections to and within the barrel cortex are heavily interdigitated. Thus, drawing a sequential activation scheme is extremely complicated. Nevertheless, we have to use a starting point for the description of synaptic connections in the barrel 'column', *i.e*. neurons above and below a single barrel. We will therefore begin with the 'canonical microcircuit' (Fig. 4.1) [5–8] although this description is certainly oversimplified in the light of present-day knowledge about the neuronal microcircuitry in the neocortex. The

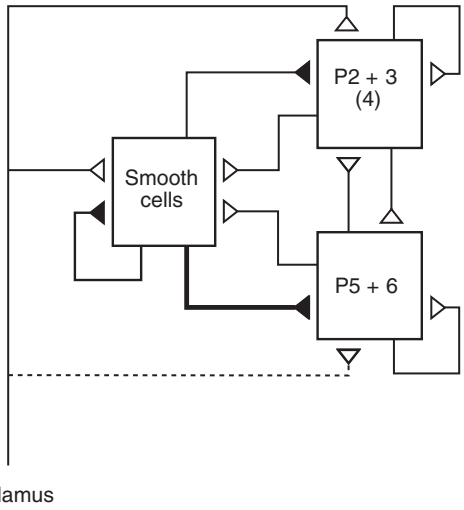

Fig. 4.1 The concept of canonical microcircuits. Schematic of the 'canonical microcircuit' of synaptic connections in a sensory cortical area as described by Douglas and Martin (1991) [5] for the visual cortex. Open triangles: excitatory synaptic contacts; closed triangles, inhibitory contacts. Note that layers 2/3 and 4 are treated as 'input layers' and layers 5 and 6 as 'output layers'. Inhibitory interneurons of all cortical layers are lumped together as 'smooth cells'. However, the 'canonical microcircuit' shown here suggests the thalamic input to all cortical layers and represents already the high degree of reciprocal and recurrent connectivity in the neocortex. Modified from Douglas and Martin 1991 [5]

'canonical microcircuit' describes cortical layer 4 as the main thalamocortical input station and we will begin from there and subsequently proceed with synaptic connections to and within layer 2/3, then layer 5 and finally layer 6. In this chapter, long-range projections of excitatory neurons in the barrel cortex from and to other cortical and subcortical areas are discussed only in passing and when needed. More detailed descriptions can be found elsewhere (for reviews see [9–11]).

Because of the high degree of recurrent synaptic connections both within and between cortical layers, the description of interneuron signalling in the framework of the 'canonical microcircuit' is fraught with problems. Nevertheless, for the sake of consistency we will use the same layer sequence as for excitatory neurons (with layer 1, the layer that contains predominantly GABAergic neurons, placed in layers 2/3, 4 and 5). Only recently, interneuron connectivity, their activation and synaptic properties are beginning to emerge, a fact that is mainly due to the large number of structurally and functionally different interneuron types. Interneurons are recruited via many different mechanisms which will be discussed in this chapter. Here, we will describe specific subsets of interneuron microcircuits in the different cortical layers. However, a comprehensive connectivity map for GABAergic interneurons in the barrel cortex has not been achieved to date. Therefore, further studies on the distribution, morphology and function of interneuron types in a 'barrel column' and the synaptic microcircuits they form are required.

Synaptic Microcircuits Between Excitatory Neurons in the 'Barrel Column'

Thalamic Input to the Barrel Cortex

The last 15 years have seen intensive research with respect to the synaptic connectivity of a barrel-related cortical column. However, the main focus of this research was on excitatory neurons and hence the excitatory signal flow in a 'barrel column' is much better known than the inhibitory synaptic connectivity. Here, we will outline the excitatory connections from the whisker thalamus to and within the neocortex (see also [3, 8, 10]).

Almost all layers of the barrel cortex receive synaptic input from either the ventroposterior medial (VPM; lemniscal pathway) or the posterior medial (POm; paralemniscal pathway) nucleus of the thalamus [12]. Axons from VPM neurons target mainly lower layer 3, 4, 5B and 6A (see Fig. 4.2, *red lines*; see also Fig. 4.3a; [13, 14]). Other cortical layers are almost devoid of VPM boutons; however, most of these layers receive TC synaptic input from POm. The majority of POm axons terminate in layers 5A and 1 with some boutons also being present in layers 2, 5B/6A and the septa betweens the barrels in layer 4 (see Fig. 4.3, *green lines*; [13–15]). Layer 2 receives very little TC input from either VPM or POm and apparently layer 6B none at all.

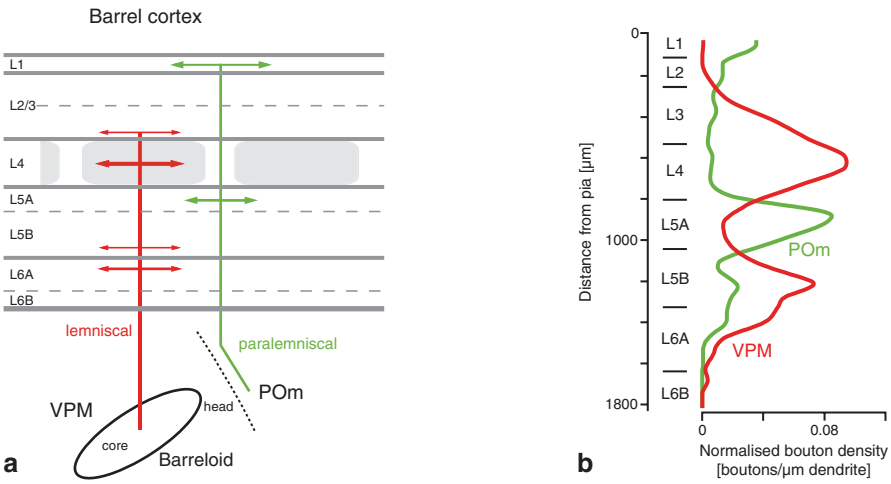

Fig. 4.2 Lemniscal (VPM) and paralemniscal (POm) thalamic target layers in the barrel cortex. **a** Thalamocortical sections of the lemniscal and paralemniscal pathways to the barrel cortex. Red, thalamic afferents from the VPM (lemniscal whisker-to-barrel cortex pathway); green, CC afferents arising from the POm (paralemniscal pathway). Modified from Feldmeyer 2012 [10]. **b** Relative bouton density of VPM and POm axons, respectively, per µm dendrite in a single 'barrel column' plotted against the cortical depth in a mature rat brain (pia = 0 µm). Note that the distribution of TC bouton density is almost complementary, i.e. where the VPM bouton density is high that of POm is low and *vice versa*. Modified from Meyer et al. 2010 [13]with permission from Oxford University Press

The highest density of TC afferents per dendritic length can be found in layer 4 [14, 16–19], which can therefore be considered to be the major thalamorecipient layer of the somatosensory barrel cortex. The axonal projection pattern of TC afferents is often barrel-related as can be seen in Fig. 4.3a. Similarly, excitatory L4 neurons and several different types of GABAergic L4 interneurons show a axonal projection pattern that is related to the 'barrel column'as do CT L6A pyramidal cells and a subtype of L6B pyramidal cells (Fig. 4.3b, 4.3c, 4.3d, 4.3e).

In layer 4, the lemniscal afferents from VPM neurons establish synaptic connections with both excitatory and inhibitory neurons located in one specific barrel as shown in electron microscopic studies by Ed White's group [20–23]. The majority of the VPM boutons synapse onto excitatory neurons because these outnumber L4 interneurons by far (inhibitory/excitatory neuron ratio in layer 4 ~ 8 % *vs.* 92 %; [24, 25]). Excitatory L4 neuron types contacted by VPM afferents are spiny stellate and star pyramidal neurons [14, 26, 27]. However, synaptic contacts formed by VPM axons comprise only about 10–20 % of the total number of synaptic contacts in layer 4 [20, 28] and are therefore considerably outnumbered by the intracortical synaptic connections.

The average amplitude of unitary EPSPs at the monosynaptic VPM-L4 spiny neuron connection is ~ 1 mV measured under *in vivo* conditions during anaesthesia and is reduced even further under mild sedation [27]. This suggests that this synapse is of very low efficacy. However, after stimulation of the whiskers, synaptic inputs from VPM neurons onto L4 spiny neurons are relatively frequent and often

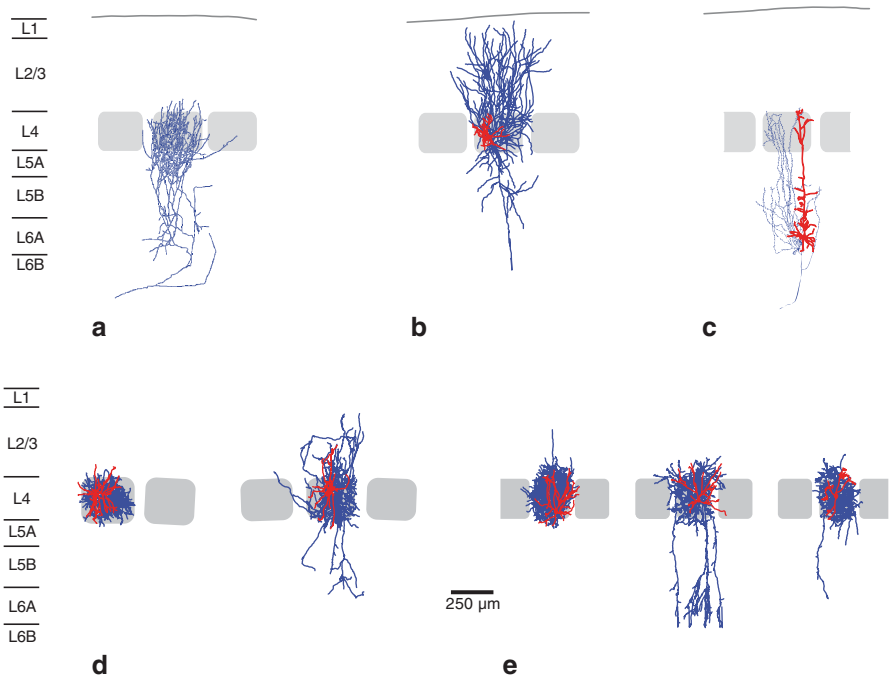

Fig. 4.3 Axonal projections in the barrel cortex neurons with a 'columnar' geometry. Barrel column-related axonal projection patterns. **a** tc afferents; **b** L4 spiny stellate neuron; **c** CT L6A pyramidal cell; **d** fast-spiking, PV+ L4 interneurons; **e** SOM^+ L4 interneurons with an adapting firing pattern. Note the dense axonal domain of L4 interneurons in d and e. Neurons in panels a-c were modified from Feldmeyer 2012 with permission from Frontiers Media SA with a creative commons license. Neurons in panel d were modified from Koelbl et al. 2013 [154] with permission from Oxford University Press. Neurons in panel E were modified from Xu et al. 2013 [155]

show synchronous activity. Therefore, amplification via intralaminar synaptic connections in layer 4 is not required to drive the intracortical signal flow [27, 29, 30]. Recently, synaptic contacts between VPM and L4 spiny neurons and corticocortical (CC) synapses have been shown to be similarly 'weak' (i.e. of low efficacy). They also show a largely overlapping distribution (with the TC synapses being slightly more proximal; [31, 32]). Therefore, the commonly held notion that individual TC L4 synapses must be stronger than intracortical L4 synapses is not correct. The observed 'strength' of the TC input is likely to result from coincident activation of VPM inputs [31, 32].

Intralaminar and Translaminar Excitatory-Excitatory Connections in the Barrel Cortex

The TC activation of neurons in different layers of the barrel cortex can be considered as the initiation of intracortical signal processing. Significant advances were made with respect to the study of intracortical excitatory neuronal connections and

their synaptic properties. The main focus of this section will be on correlated functional *and* structural approaches in the characterisation of intracortical connectivity mainly using paired recordings combined with biocytin fillings from synaptically coupled neurons (for an example see Fig. 4.4 which shows an excitatory L4-L2/3 connection).

Synaptic microcircuits have been proposed to exist either in the lemniscal or the paralemniscal streams [33–35]. These two streams of thalamocortical signalling may interact within the barrel cortex and result also in corticothalamic feedback to thalamic nuclei in both the lemniscal and paralemniscal pathway (Fig. 4.5a, b, c). Within the barrel cortex, neuronal connections can be subdivided into local intracolumnar, translaminar connections as well as lateral connections between cortical columns. We will use this terminology for both excitatory and inhibito-

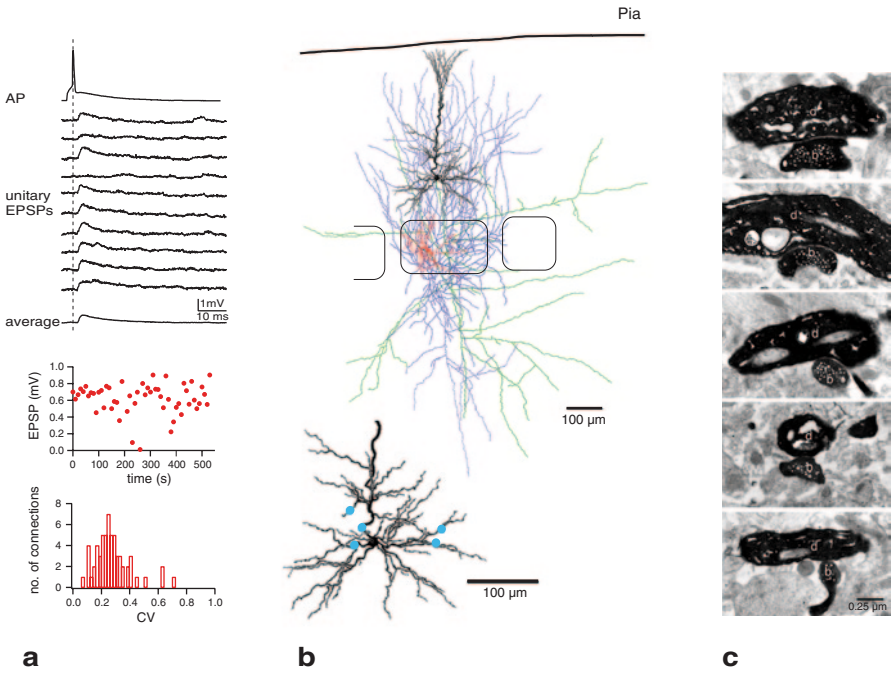

Fig. 4.4 Functional and structural characterisation of a synaptic connection using paired recordings. Recording from a pair of synaptically coupled neurons. Here, a translaminar synaptic connection between a L4 spiny neuron and a L2/3 pyramidal cell is shown. **a** top panel: the presynaptic AP elicits uEPSPs in the postsynaptic L2/3 pyramidal cell of various amplitudes. Occasionally, failures can also be observed. Middle panel, variation of the uEPSP amplitudes over time for this connection. Bottom panel, normalised variability (c.v.) of L4-L2/3 synaptic connections. Note that this connection type is very reliable, i.e. has a high release probability. **b** light microscopy reconstruction of a synaptically coupled L4 spiny neuron and a L2/3 pyramidal cell. The dendrite and axon of the presynaptic L4 spiny neuron are red and blue respectively, those of the postsynaptic L2/3 pyramidal cells black and green. Inset, dendritic domain of the L2/3 pyramidal cell with blue dots marking the location of light microscopically identified, putative synaptic contacts on basal and proximal apical oblique dendrites. **c** electron microscopic verification of the putative L4-L2/3 synaptic contacts. Modified from Feldmeyer et al. 2002 [45] (a) and Silver et al. 2003 [47] (b, c) with permission from John Wiley and Sons Publisher and AAAS

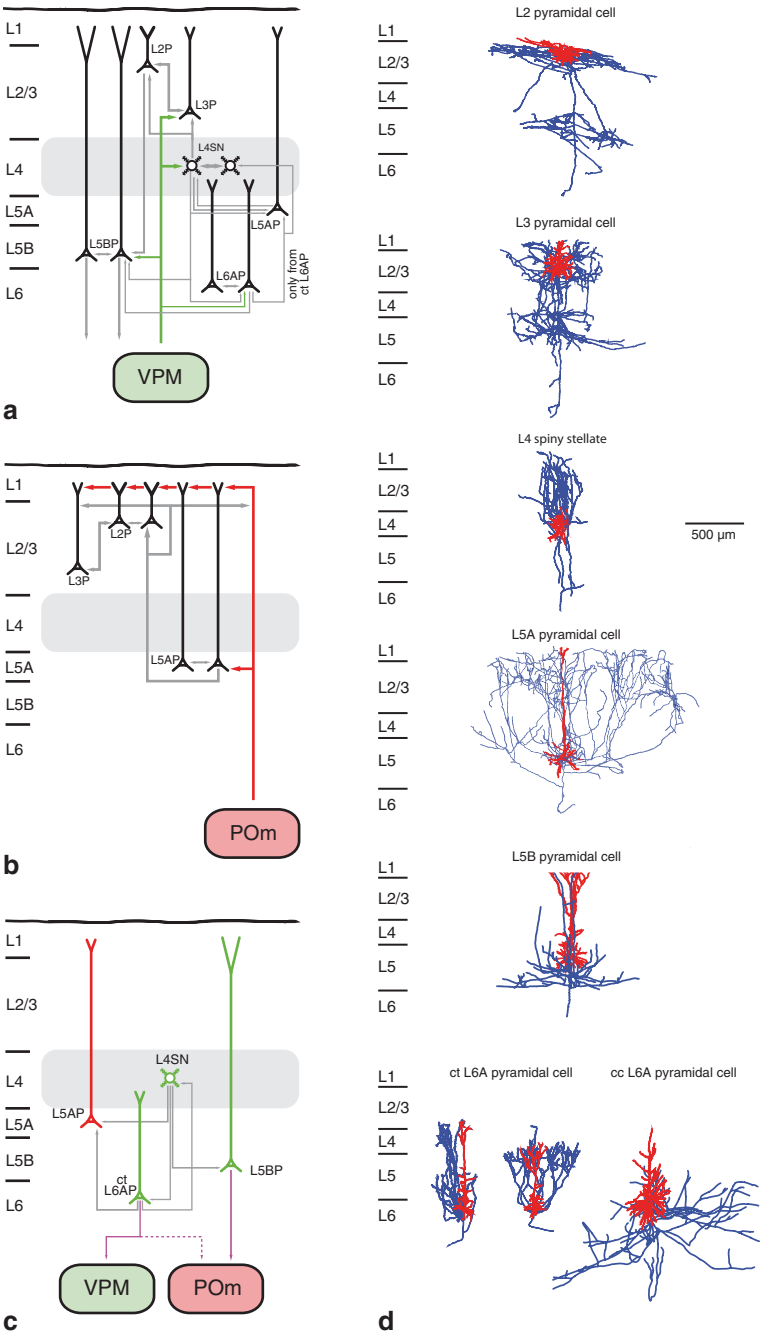

Fig. 4.5 Intracortical excitatory microcircuits in the lemniscal, paralemniscal and corticothalamic pathways. Synaptic signalling pathways in the neocortex. **a** Synaptic connections receiving input from the VPM (lemniscal) nucleus of the thalamus. **b** Synaptic connections receiving input from the POm (paralemniscal) nucleus of the thalamus. **c** Synaptic connections involved in the

ry neurons in the barrel cortex. Furthermore, long-range axonal projections form synaptic contacts with neurons in other ipsi- and contralateral cortical areas as well as subcortical targets.

Throughout this overview we will provide published 'connectivity ratios' for specific synaptic connections derived from recordings in acute slice preparations. Such connectivity estimates are subject to many errors: Most frequently, truncation of dendritic and axonal projection will result in underestimates of the connectivity. In addition, weak synaptic connection with a low release probability may not be resolved; also, dendritic filtering may attenuate substantially synaptic input to distal dendritic branches so that they remain undetected during somatic recordings. All these factors will affect the reliability and validity of cortical connectivity maps. When appropriate, such issues will be discussed below.

Layer 4 Serves to Distribute Intracortical Excitation

In layer 4 of the barrel cortex, the excitatory target neurons of VPM axons are spiny stellate cells, star pyramids and L4 pyramidal neurons [26, 27, 36]. There appear to be no major differences in the intrinsic electrical properties of these L4 spiny neuron types [37, 39; but see 40, 41].

The axons and dendrites of both spiny stellate and star pyramid neurons generally exhibit a 'barrel column'-related spatial arrangement (Fig. 4.3b and 4.5d; [37, 38]). The dendritic domain of spiny stellate cells is confined to a barrel in layer 4 and their axonal domain is largely columnar with a very high density of axonal collaterals in layers 4 and 2/3; projections to infragranular layers are sparse. Star pyramids, on the other hand have an untufted apical dendrite that project to layer 2/3; the density of axonal collaterals in layers 4 and 2/3 is significantly lower than that of spiny stellate cells while they appear to possess more axonal collaterals in deep cortical layers.

A subset of L4 spiny neurons send axonal collaterals into neighbouring barrels where they branch profusely, mostly within layer 4 [38]. Such axonal projections very likely contact other L4 spiny neurons as well as L4 interneurons thereby serving inter-barrel signal processing; this branching pattern may account for less focussed subthreshold receptive fields of L4 spiny neurons shown previously *in vivo* [26].

---

corticothalamic feedback loop. Note that VPM and POm inputs interdigitated at several different stations, *e.g.* in L5A which receives direct input from the POm and indirect input from the VPM (via L4 spiny neurons); a second example are are L5B neurons that receive input from the VPM and project to the POm. **d** Excitatory neuron types involved in these connections. L2 and L3 pyramidal cells are from Bruno et al. 2009 [67], the L5A pyramidal cell from Oberlaender et al. 2011 [93]. Three-dimensional axon morphologies of individual layer 5 neurons indicate cell type-specific intracortical pathways for whisker motion and touch. (modified from Proc. Natl. Acad. Sci. 108, 4188–4193 with permission) and corticothalamic (CT) and corticocortical (CC) L6A pyramidal cells (Zhang and Deschênes 1997 [56]; modified from Oxford University Press with permission) are from in vivo biocytin fillings; the L4 spiny neuron and the L5B pyramidal cell (Markram et al. 1997 [100]; modified from John Wiley and Sons Publisher with permission) from in vitro fillings. Somatodendritic domain in red, axonal arbour in blue

Within a barrel, L4 spiny neurons are organised in clusters of up to ~10 cells in which they are highly interconnected with other L4 spiny neurons in the same barrel; the connectivity ratios reported for this connection range from 25 to 36%; of those 20–30% are reciprocally coupled [24, 39; see also 42]. Until now, this synaptic coupling ratio is the highest reported for excitatory neurons. Excitatory connections between L4 spiny neurons in adjacent barrels may also exist: a few L4 spiny neurons have an axonal arbour showing a bifurcation in layer 5A that gives rise to collaterals projecting a neighbouring barrel [38].

Presynaptic L4 spiny neuron axons establish on average between two and five synaptic contacts on the postsynaptic L4 spiny neuron dendrites; the average geometric distance of these contacts from the soma was ~70 µm. The excitatory L4-L4 connections are of a relatively high efficacy (average unitary EPSP (uEPSP) amplitude of 1.6 mV) and a high reliability which suggests a high synaptic release probability [39]; however, the release probability of neocortical excitatory connections decreases in fully mature rodents [43]. Some unitary L4-L4 connections are exceptionally strong with uEPSPs > 10 mV that can initiate action potentials (APs) in the postsynaptic neurons. Such connections are also able to sustain disynaptic excitation [39].

L4 spiny neurons distribute thalamic excitation to other super- and infragranular layers. Of these, layer 2/3 is the main target region and exhibits a very high density of axon collaterals from L4 spiny neurons [37, 44]. The connectivity ratio for excitatory synaptic connections between L4 spiny neurons and L2/3 pyramidal cells is about 10–15% [24, 45]; such a high value in acute brain slice preparations is remarkable given the fact that the axonal pathway of the presynaptic neurons is in the order of several hundred µm.

The majority of L2/3 pyramidal neurons innervated by L4 spiny neuron axons are directly above the home barrel, i.e. within the home ‘barrel column’ (Fig. 4.4). This finding has been confirmed in studies using photo-release of caged glutamate which demonstrated that the most dominant input to L2/3 pyramidal neurons originates in layer 4; other cortical layers show significantly lower contributions [33, 36, 46]. The translaminar L4-L2/3 connection is exclusively unilateral, i.e. there are no reciprocal L4-L2/3 excitatory connections [24, 45].

The L4-L2/3 connection is relatively efficacious (uEPSPs between 0.6 and 1.0 mV; Fig. 4.4a) and exhibits a high release probability (P_r ~ 0.8; [45, 47]). Synaptic contacts established by the presynaptic L4 axon are mainly on the basal dendrites of the postsynaptic L2/3 pyramidal cells; the number of contacts per connection is between four and five and they are found at an average distance of ~70 µm from the soma (Fig. 4.4b, c).

In addition to innervating other L4 spiny neurons and L2/3 pyramidal cells, L4 spiny neurons have also been shown to form synaptic connections with L5A, L5B and L6A pyramidal cells in the same ‘barrel column’ [48, 49]. This suggests that direct, monosynaptic signalling pathways to infragranular layers exist, in addition to the well-known *indirect* excitatory synaptic connections from layer 4 via layer 2/3 to layer 5 (see below). The connectivity between L4 spiny neurons and pyramidal neurons in layers 5A and 5B is with ~10% also relatively high. However, the efficacy

of these connections is somewhat lower (average uEPSP amplitude ~0.6 mV) compared to that of L4-L4 and the L4-L2/3 connections [24, 48, 50–53]. It should be noted that the L4-L5A connection is the first convergence of the proposed 'lemniscal' and 'paralemniscal' synaptic signalling streams in the barrel cortex.

L4 spiny neurons contact L5A pyramidal cells mainly on the basal dendrites although synaptic contacts on the apical tuft branches have also been demonstrated [48]. The distribution of synaptic contacts at the L4-L5A connection overlaps largely with that calculated for the POm TC input to these neurons [13, 14, 52]. The fast EPSP time course at the L4-L5B connection suggests that synaptic contacts are also made on proximal, i.e. basal dendrites. Because L4 spiny neurons have a dense axonal projection in layer 2/3 it is also very likely that distal synaptic contacts are established on the apical tuft dendrites of L5B pyramidal cells. However, thick-tufted L5B pyramidal cells are electrotonically not very compact and EPSPs from such distal synaptic contacts are subject to strong dendritic filtering so that it is likely that they will be masked in somatic recordings; they can only be resolved by recording from apical dendrites.

L4 spiny neurons innervate also L6 pyramidal cells, at least those in sublamina 6A albeit at a very low connectivity ratio of ~3% [24, 49, 54, 55]. However, the innervation domain of L4 spiny stellate cells and L4 star pyramids with L6A pyramidal cells is distinct: the former establish synaptic contacts with apical tuft dendrites of L6 pyramidal cells (which terminate in layer 4) while the latter target predominately basal dendrites [54]. The differential innervation pattern by these L4 spiny neuron types is most likely due to their different axon projection pattern. This suggests different computational roles for the two types of L4 excitatory neurons in the L4-L6A excitatory synaptic pathway.

It should be noted that because of strong dendritic filtering EPSPs from distal synaptic inputs have a very slow time course and significantly attenuated amplitude when recorded at the soma. Therefore, only very large EPSPs originating at distal contacts will be detected; small EPSPs from these sites cannot be resolved. This will lead to a significant underestimation of the true connectivity rates.

L4 spiny neurons are connected to excitatory neurons in every cortical layer, which suggests that these neurons are responsible for the vertical distribution of incoming sensory signals. Although L4 spiny neuron axons project mainly within a 'barrel column' (and are therefore a kind of 'excitatory' interneuron) they are an integral part of several intracortical and cortical-subcortical neuronal networks and may serve to link and integrate different thalamocortical signalling streams such as the lemniscal and paralemniscal pathways (Fig. 4.5c). For example, they are involved in both feed-forward signalling within the S1 cortex and to other cortices via corticocortically projecting L2/3, L5 and L6 pyramidal neurons. In addition, they are also an element in synaptic feedback signalling structures between cortex and thalamus (via e.g. CT L6A pyramidal neurons, see Fig. 4.5c). In contrast, very few excitatory neuron types from other layers of the S1 barrel cortex establish synapses with L4 spiny neurons, with apparent connectivity ratios <1% [24]. The axonal arbour of CT L6A pyramidal neurons with its marked collateralisation at the level of a L4 barrel (see Fig. 4.2c) suggests that these neurons form synaptic connections

with L4 spiny neurons [56, 57]. This has been demonstrated for visual cortex [58, 59] and very recently also for barrel cortex [49, 60].

Vertical and Horizontal Spread of Synaptic Signalling in Layer 2/3 of the Barrel Cortex

Initially the spread of intracortical excitation is largely vertical from the VPM to a barrel in layer 4 and then to pyramidal cells in layer 2/3 of the home 'barrel column' [33, 44–46, 61]. In addition to this input from L4 spiny neurons, deep L2/3 pyramidal cells (also called L3 pyramidal cells; Fig. 4.5d) receive also direct input from the VPM [13, 14, 17, 62]. Input to the apical tufts of L2/3 pyramidal cells via POm afferents is also likely because these axons project to this layer (see above; [14, 63]). The prime target neurons for this input are probably L2 pyramidal cells because they have apical dendrites with a broad tuft region in layer 1 and are in a very good position to form synaptic contacts with POm axons running in that cortical layer (Fig. 4.5d). L3 pyramids have only slender apical tufts and thus are less likely to be contacted by POm axons [14, 36, 44, 46, 64; see also 65].

The majority of L2/3 pyramidal neurons have a main axon that exhibits (often long-range) horizontal collaterals predominately projecting in layers 2/3 and 5 over several 'barrel columns' in the S1 cortex and to other cortices such as the secondary somatosensory (S2) and the primary motor cortex (M1); in contrast, layer 4 is almost devoid of L2/3 axon collaterals [9, 64, 66, 67]. In addition to this more common type a small subset of L3 pyramidal cells in the barrel cortex show a much narrower axonal field span in supra- and infragranular layer and show some collaterals in layer 4 [66, 67]. Furthermore, some L2 pyramidal cell with an almost horizontal main ('apical') dendrite have been found; these neurons are located right at the border of layers 1 and 2. Thus, layer 2/3 contains several distinct pyramidal cell types with distinct morphologies. How this is related to different functions in the barrel cortex network remains to be determined.

Photostimulation of barrel cortex L2/3 pyramidal cells through glutamate uncaging demonstrated that these neurons have differential synaptic input patterns depending on their lamina depth [33, 46, 51]. These studies showed that both L2 and L3 pyramidal cells receive synaptic input from L4 spiny neurons in the same 'barrel column' (see above). However, L2 pyramidal cells above septa between two neighbouring L4 barrels are stronger excited by L5A pyramidal cells then 'septal' L3 pyramidal cells. Because L4 spiny neurons are the major targets of the 'lemniscal' (VPM) thalamic afferents and L5A pyramidal cells those of the 'paralemniscal' (POm) afferents it has been suggested that the L4-L2/3 connections and the L5A-septal L2 connections represent intracortical sections of the lemniscal and the paralemniscal pathways, respectively [33, 34, 36, 46]. These two pathways have been proposed to converge in layer 2. It should be noted, however, that layer 2 is not the only cortical layer where this takes place: L5A pyramidal cells receive direct POm (paralemniscal) and indirect lemniscal input via L4 spiny neurons and L3 and L6A pyramidal neurons, both of which are directly innervated by VPM (see above).

Furthermore, L4 septal neurons are targeted by both the lemniscal pathway [68] and the paralemniscal POm afferents [35, 69, 70]. Thus the septum between barrels may be considered as a third region were the two whisker-to-barrel cortex pathways converge. Finally, L5B pyramidal, that are innervated by the 'lemniscal' VPM nucleus of the thalamus [14, 15, 70], project back to the 'paralemniscal' POm nucleus where they synapse onto thalamic relay neurons [71–73]. A similar TC-CT projection may also be present in layer 6A [56]. In summary, this data suggests that the lemniscal and paralemniscal whisker-to-barrel pathways are not separate but interact at multiple stations, in particular in the barrel cortex but also at a thalamic level.

From L2/3 pyramidal cells intracortical excitation is distributed locally to other L2/3 pyramidal cells [64, 74, 75], vertically to infragranular layers (in particular to L5A and L5B pyramidal cells; [24, 51–53, 76–78]) and also across several S1 'barrel columns' both within layers 2/3 and 5 [79]. In addition, L2/3 pyramidal cells have long-range axonal projections to the S2, M1 and other cortices. Thus, L2/3 pyramidal cells will integrate the synaptic activity of several 'barrel columns' surrounding their home 'barrel column' as well as that from other cortical areas.

Detailed information of unitary synaptic connections with L2/3 pyramidal cells is only available for L2/3-L2/3 connections and to a lesser extent for L2/3-L5 connections. The connectivity ratio of local L2/3-L2/3 pyramidal cell connections has been reported to be ~10–20 %. The mean uEPSP amplitude at this connection is between ~0.7 and 1.0 mV with a relative high P_r of 0.7–0.8, a value comparable to that of excitatory L4-L2/3 connections [64, 75]; in mice, for which the L2/3-L2/3 connectivity ratio was similar (17 %) to that of rat, the synaptic efficacy was markedly lower (~0.4 mV; [78]). It is of note, however, that the synaptic connectivity and strength of this connection are not stable parameters but can be altered by processes such as sensory deprivation [80]. In L2/3-L2/3 connections, presynaptic L2/3 pyramidal cells establish two to four synaptic contacts at a mean distance of ~90 µm from the soma of the postsynaptic neuron. The majority of synaptic contacts are located on the basal dendrites with a few contacts being formed on proximal apical oblique dendrites [64, 81].

As stated above, L2/3 pyramidal cell axons descend to infragranular layers where they arborise extensively, in particular in layer 5. Here, they establish synaptic contacts with the basal dendrites of both L5A and L5B pyramidal cells [24, 51, 52, 76]. L2/3-L5 pyramidal cell connections are relatively weak (0.1 mV at postnatal day 28) and often display short-term facilitation indicative of a low release probability [76]. It has been reported that L2/3 pyramidal cells establish synaptic connections with two L5 pyramidal cells with a higher probability when these postsynaptic neurons are reciprocally coupled. In contrast, the probability of two L2/3 pyramidal cells being connected with a L5 pyramidal cell is lower when these two presynaptic neurons are reciprocally connected. This has been taken to suggest that L2/3 pyramidal cells converge onto 'subnetworks' of synaptically coupled L5 pyramidal cells while L5 pyramidal cells integrate the activity of different 'subnetworks' of L2/3 pyramidal cells which might code for different stimulus features [82]. Unfortunately, the study does not supply structural information on the L2/3-L5 connections which makes it difficult to judge whether there is a true 'connection specificity' as proposed there.

Thus, L2/3 pyramidal cells are in a position where the vertical signal transfer in the home 'barrel column' (via L4-L2/3 connection and L2/3-L5 connections; Fig. 4.5a) can expand in a horizontal direction in particular in layers 2/3 and 5. Here, they can establish synaptic connections with other pyramidal cells in different cortical domains (i.e. 'barrel columns') or areas. They may therefore coordinate the synaptic activity in the home 'barrel column' with that in neighbouring 'barrel columns' and other cortices. In addition, some L2/3 pyramidal cells project corticocallosally to the contralateral S1 barrel cortex [83, 84] and may thereby serve to integrate the sensory input to the two different hemispheres.

Layer 5 as the Main Cortical Output Layer

Layer 5 is considered to be the main output layer of neocortex; it contains pyramidal neurons with three distinct dendritic morphologies: those with slender apical tufts, those with thick, elaborate apical tufts and those with short, virtually untufted apical dendrites. Most slender-tufted pyramidal cells are located in lamina 5A; thick-tufted pyramidal cells, on the other hand, are mostly present in lamina 5B [64, 66, 85, 86] (Fig. 4.5d). Untufted pyramidal cells can be found in both lamina 5A and 5B, albeit at a low density [66]. Both the slender- and thick-tufted pyramidal cells have been shown to receive TC synaptic input [14, 52]. TC projections onto slender-tufted L5A pyramidal cells are almost exclusively from POm. In contrast, the TC input to thick-tufted L5B pyramidal cells arises mostly from VPM. However, POm afferents may also contribute to this input albeit to a significantly smaller degree (see Fig. 4.1; [14]). In addition, some of the POm TC input may also arrive in the terminal tuft dendrites via the POm afferents in layer 1.

The axons of the short, untufted L5 pyramidal cells project extensively to layer 2/3, in particular to the deeper portion of this layer (i.e. layer 3); the axon density in layers 5 and 6 is considerably lower [66]. At least a subset of the short, untufted L5 pyramidal cells projects via the corpus callosum to the contralateral S1 cortex [87, 88]. This is in accodance with findings on short L5 pyramidal cells in visual and auditory cortex (e.g. [89–92]).

Slender-tufted L5A pyramidal cells have a very characteristic axon with many branches ascending to layers 2/3 and 1 where they collateralise extensively [66, 87, 93] (Fig. 4.5d). The total intracortical axonal length of the L5A pyramidal cell exceeds that of L5B pyramidal cells by a factor of two. The L5A axon projects throughout the entire barrel field (both along rows and arcs) and beyond to ipsilateral cortical areas such as the whisker-related M1 cortex [93, 94] and to the contralateral S1 cortex [87].

The axon of thick-tufted L5B pyramidal cells projects largely (~60%) within layer 5; the length of supragranular axon collaterals is significantly lower than that of the slender-tufted or untufted L5 pyramidal cells. Thick-tufted L5B pyramidal cells target several cortical and subcortical brain regions such as the thalamic nuclei, the superior colliculi (tectum), the striatum, the trigeminal nuclei etc. both on the ipsi- and contralateral brain hemisphere [87, 94–97]. Different L5B pyramidal cell subtypes differ in their passive electrical properties, their AP firing characteristics

and their gene/protein expression profiles (e.g. [97, 98]) and are thus likely to process incoming sensory input differently.

L5A pyramidal cells receive most of intracortical synaptic inputs from cortical layers 2, 3, and 4 (connectivity ratios: ~10, ~6 and ~12%, respectively); the synaptic properties of these connections have been described above. The strongest excitatory synaptic input to the slender-tufted L5A pyramidal cells is from other L5A pyramidal cells. Here, the local intralaminar connectivity (within ~50–100 µm soma distance) is ~20% of which 15% are reciprocal. Synaptically coupled L5A pyramidal cell pairs form between one and six contacts most of which are located on the basal dendrites; however, there are also contacts established with the apical dendritic tuft in line with the axonal projection pattern of the L5A pyramidal cells. The L5A-L5A connection had a relatively high release probability and an average uEPSP amplitude of 0.3–0.6 mV [99]. Cell bodies and apical dendrites of synaptically connected L5A pyramidal cells were often found to be located below the border of 'barrel columns' and show a tendency towards vertical clustering [99]. Such an organisation is consistent with (but not necessarily proof of) the concept of a separate 'septal' neuronal network recruited (see above and [35] for a review). This network is recruited by POm and may play a role in the modulation of whisker motion.

In vitro paired recordings showed that L5A pyramidal cells establish synaptic connections with L2 and L3 pyramidal cells more frequently than the thick-tufted L5B pyramidal cells (connectivity ratio 2 and 4%, respectively, *vs*. 1 and 2%; [24]) reflecting the higher axonal density of L5A pyramidal cells in layer 2/3 [93]. Studies using either photostimulation by glutamate uncaging or activation of channelrhodopsin 2 (ChR2) obtained similar results [33, 34, 46, 52].

L5B pyramidal cell pairs have a connectivity ratio of ~5–10% with some of them showing reciprocal connectivity [15, 24, 76, 88, 100–102]. The connectivity probability was lower for thick-tufted L5B-L5B connections than for slender-tufted L5A-L5A connections; however, the number of L5B-L5B synaptic contacts (established both on basal dendrites and apical dendritic tufts at a mean distance of ~150 µm) was higher than reported for L5A-L5A pyramidal cell pairs. L5B-L5B connections have a high synaptic efficacy with mean uEPSP amplitudes ranging from 0.7 to 1.3 mV [24, 88, 100] and a release probability of 0.45 under near-physiological conditions [103], i.e. lower than that of L4-L4 and L4-L2/3 connections. It has also been postulated that L5B pyramidal neurons are organised in clusters with a high connectivity and efficacy [104]. Furthermore, L5 pyramidal cells with different projection targets supposedly form distinct neuronal subnetworks with differential connectivity patterns. So far, this has been proposed for visual, frontal and motor cortex [97, 105–108]. The connectivity ratio and strength within these networks is specific and non-random, although it remains unclear how such a specificity might be achieved. However, in these studies, the apparent specificity of synaptic connections was not based morphological properties of the *individual* synaptic connection types because these were not determined. Therefore, the above-mentioned studies do not disprove the hypothesis that synaptic connectivity follows a non-specific probability of axodendritic overlap [109–112].

Ascending L5B-L5A connections appear to be rare [24] because of the sparse ascending axonal domain of thick-tufted L5B pyramidal cells [93, 113]. In contrast axonal collaterals of L5A pyramidal cells establish synaptic contacts with thick-tufted L5B pyramidal cell dendrites with a significantly higher connection probability suggesting a directed signal flow between the two sublaminae. Given that the axonal projection of L5A pyramidal cells is broad and dense at the layer 1/layer 2 border, it is highly probable that synaptic contacts are predominantly made on the apical tuft dendrites [93]. However, somatic recordings in slice preparations would result in an underestimate of the true connectivity not only because of axonal truncations but also because uEPSPs from tuft dendrites would largely disappear in the electrical and synaptic 'noise' in somatic recordings from these neurons.

It has been suggested that L5A and L5B pyramidal cells interact via the following mechanisms [93]: Slender-tufted L5A pyramidal cells respond to changes in the motion and phase of whiskers but fire very little after passive touch [114, 115]. Because of their profuse axonal arborisation at the layer 1 and 2 border these neurons may integrate the synaptic activity of several 'barrel columns' thereby 'phase-locking' the membrane potential in L2/3 pyramidal cell dendrites to the whisking cycle. Slender-tufted L5A pyramidal cells will also recruit thick-tufted L5B pyramidal neurons which are very responsive to passive whisker touch [116], most likely through direct synaptic input from the VPM [13, 14, 34, 52, 117, 118]. Furthermore, during exploratory behaviour of the rodent e.g. during object location, the slender-tufted L5A pyramidal cells and the VPM afferents are activated almost simultaneously. In turn, L5B pyramidal cells will be depolarised at both the basal dendrites (by VPM afferents) and the apical tufts (by the L5A pyramidal cell axons). This will lead to an increased excitation which is subsequently conveyed to other intra- but also subcortical targets.

A subset of the thick-tufted L5B pyramidal cells is innervated by VPM and projects back to the POm. It has been suggested that this VPM-L5B-POm connection is part of the TC-CT feedback system (see also below): L5B pyramidal cell axons generate one or two clusters of large diameter (2–8 μm) presynaptic boutons in POm and form excitatory synapses with POm relay neurons [71, 73, 119–121]. According to another hypothesis the L5B-POm connection is part of a feed-forward, trans-thalamic signalling pathway from VPM via L5B pyramidal cells of barrel cortex to POm and from where it 'drives' higher order cortical areas such as the S2 cortex (see e.g. [122–124]; for a review see [125]). However, it is likely that the CT L5B pyramidal cells are elements in both the feedforward and the feed-back pathways described above.

The large L5B-POm synapses have a high release probability ($P_r \sim 0.8$) and are highly efficacious so that uEPSPs can elicit several APs in the thalamic relay neurons thereby acting as 'drivers' of the POm. Spontaneous activity of the L5B pyramidal cells on the other hand significantly reduces this 'driving' action through a strong short-term synaptic depression. Therefore, it has been proposed that the L5B-POm synapse has two functional modes: during high spontaneous activity the synapse is largely suppressed and only synchronous activity of several L5B inputs will induce spiking of the POm neurons: the synapse acts as a detector of coincident activity. However, when the spontaneous activity is low-e.g. during active whisking

or cortical silence (see e.g. [126])-a single input will result in AP firing of the postsynaptic POm neuron. Thus, the degree of spontaneous activity determines whether the CT L5B-POm synapse acts as a detector of synchronous neuronal activity or of cortical silence [73].

Synaptic connections of pairs of 'untufted' pyramidal cells in both layers 5A and 5B of the S1 cortex that project via the corpus callosum to the contralateral brain hemisphere are very different from those between other L5A or L5B pyramidal cell types [88]. The connection probability of pairs of corticocallosal L5 pyramidal cells has been reported to be only ~3 %; this is considerably lower than that of L5A-L5A and L5B-L5B connections (e.g. [24, 97, 99, 100]). The release probability at this connection was also comparatively low (P_r ~0.4) while the average uEPSP amplitude was similar to that of other L5 connections. Corticocallosally projecting L5 pyramidal cell pairs established between one and six synaptic contacts, mainly on basal dendrites at an average distance of ~130 µm. In addition, corticocallosal L5 pyramidal cells exhibit a dense axonal projection to upper layer 2/3 [66]. It is therefore very likely that they synapse onto neurons and dendrites in this layer; although such connections have not been described until now.

The excitatory synaptic connectivity in layer 5 is highly complex. L5 pyramidal cells receive synaptic inputs from virtually every cortical layer; however not all of these connections have been analysed in detail. A further complication is added by the fact that in particular L5B pyramidal cells project to several distinct subcortical brain areas; these different L5B pyramidal cell types may differ with respect to their structural and functional synaptic characteristics and may have different connectivity patterns as a result of different dendritic and (in particular 'long-range') axonal geometries.

Layer 6

Layer 6 of the somatosensory barrel cortex and other cortical areas has been divided into two distinct sublaminae with layer 6A being derived from the cortical plate (like layers 2–5). It contains mainly pyramidal cells with short, sparsely or even untufted apical dendrites that terminate predominantly in layers 3 to 5A (Fig. 4.5d). In addition, a small population of L6A pyramidal cells with apical dendrites ascending to layer 1 or those with obliquely oriented main dendrites were also found [49, 56, 57, 127]. L6A pyramidal cells can be subdivided into at least two major groups: those with a predominantly intracortical axonal projection pattern and those with an axon that projects back to the thalamic nuclei [55–57, 128, 129; see also [130] for a review). A very small (~10 %) population of L6A local circuit excitatory neurons may also exist.

Layer 6A pyramidal neurons receive synaptic input from VPM as shown by current stimulation or laser-activation of channelrhodopsin-expressing TC axons [131, 132]. TC synaptic responses recorded in L6 pyramidal cells were always depressing.

A large fraction of L6A pyramidal cells send axonal projections back to their related thalamic nuclei [1, 130, 133–135, 136]. In sensory cortices, these CT

projections are generally considered to be elements of a feed-back loop that modulates the response of thalamic relay neurons to incoming peripheral stimuli. CT L6A pyramidal cells can be further subdivided with respect to the innervated thalamic nucleus i.e. whether they target only VPM, POm or both [56, 57, 128]. L6A pyramidal cells projecting exclusively to VPM reside mostly in the upper half of layer 6. They have very short axons that terminate in layer 4 or lower layer 3 and are almost completely confined to the home 'barrel column'; few if any collaterals project to neighbouring 'columns' (see (Fig. 4.5d; CT L6AP (VPM)). Their axons have been described to be extremely short, as found both *in vitro* and *in vivo* studies. This type of CT L6A pyramidal cells has been proposed to receive a strong and focussed synaptic input from L4 spiny neurons in their home 'barrel column', indicating that neurons in this layer are involved in shaping the cortical modulation of activity in the somatosensory thalamus [54, 55].

Pyramidal cells that project to both VPM *and* POm are found in the lower half of layer 6A (Fig. 4.5d; CT L6AP (VPM and POm)). Their axonal domain is rather broad and not confined to a single 'barrel column' [56]. The axon is significantly longer than that of VPM-projecting L6A pyramidal cells; it terminates either in layer 5A or 4 in several barrel-related clusters that ramify profusely. These neurons may also project laterally within layer 6 of the barrel cortex [57]. CT L6A pyramidal cells that innervate exclusively POm neurons are relatively rare and have not been described in detail [56, 119]; their axons reside largely within layer 6 with a few collaterals ascending to layers 5 and 4.

The majority of axonal collaterals of CC L6A pyramidal cells remains predominantly within layers 5 and 6 of the S1 cortex [56, 57, 128]. The axon of CC L6A pyramidal cells is very extensive and projects over many 'barrel columns' thereby mediating transcolumnar interactions in the infragranular layers of the barrel cortex (Fig. 4.5d; CC L6AP). Most CC L6A axonal collaterals remain in the barrel field of the S1 cortex but some long-range projections targeting S2 and/or M1 cortex have also been found. Subcortical targets of CC L6A pyramidal cells axons have so far not been identified. It is not unlikely that different subtypes of CC L6A pyramidal cells exist that can be differentiated on the basis of their dendritic and axonal projection patterns [56, 57, 128].

One study showed that L6 pyramidal cells have a low synaptic connectivity with all excitatory neurons in other cortical layers (0–3 %; [24]). L6A pyramidal cells, in particular those projecting corticocortically, appear to establish synaptic contacts predominantly with L5B pyramidal cells (with a reported connectivity ratio of ~7 %; [137]). These findings are surprising given the extensive axonal arborisation of CC L6A pyramidal cells. In addition, an apparent connection specificity of L6A pyramidal cells has also been described: CC L6A pyramidal cells can be presynaptic to CT L6A pyramidal cells but not the other way round. However, this 'specificity' is not the result of a target neuron selectivity but due to the different axonal domains of CC and CT L6 pyramidal cells which are narrow and broad, respectively.

Furthermore, studies of cat visual cortex have established the existence of L6-L4 connections. These connections are weak and show paired pulse facilitation [58,

59]. Similar unreliable connections showing paired pulse EPSP facilitation have also been found in rat barrel cortex for connections onto both L4 spiny neurons and L5A pyramidal cells; all EPSPs at these connections showed a fast time course indicative of proximal synaptic contacts [49, 60]. Corticothalamic L6A-L5A connections (activated by light-induced activation of ChR2) were substantially stronger than CT L6A-L4 connections. Activation of multiple CT L6A pyramidal cells could even evoke APs in the L5A pyramidal cells [60]. Since L6A pyramidal cells receive synaptic input from the VPM, the CT L6A-L5A connection is another cortical microcircuit where the intracortical VPM ('lemniscal') and POm ('paralemniscal') interdigitate.

In addition, the release probability is lower at synaptic connections between two CC L6A pyramidal cells than between a CC and a (postsynaptic) CT L6A pyramidal cells (c.v.: ~0.6 *vs* ~0.2; [137]). L6A pyramidal neurons have also been found to be presynaptic to L5B pyramidal cells and receive excitatory input from layers 4, 5A and 5B [24, 54, 137].

Layer 6B is more complex than layer 6A because it contains both neurons derived from the subplate but also neurons that have migrated there from the cortical plate [138]. Excitatory L6 neurons are markedly more heterogenous than those of other cortical layers, both with respect to their dendritic and axonal morphology. In particular excitatory L6B neurons in the barrel cortex have many distinct morphologies ranging from short, untufted pyramids with apical dendrites that terminate in layer 5, those with atypically oriented (oblique, horizontal or inverted) 'apical' dendrites to multipolar neurons without a main dendrite [127, 139]. This is in accordance with L6B neuronal morphologies described for other cortical areas [140–142]. In the barrel cortex, most excitatory L6B neurons have a dominant intralaminar L6 projection [139]. L6B pyramidal cells possess also a strong axonal projection into the white matter; this projection has been proposed to innervate the POm [122]. In addition, a small subpopulation of L6B neurons sends axonal collaterals to layer 1 [139, 142] where they may innervate L1 GABAergic interneurons and/or the apical dendritic tufts of L2-L5 pyramidal cells. However, the synaptic connectivity pattern of the different excitatory L6B neurons has received little attention to date and the functional properties of L6B connections remains poorly understood.

Interneuron Connections in the Barrel Cortex

While excitatory connections have been described in some detail for the barrel cortex, significantly less is know about interneuron connections in this brain region. A major problem for a correlated morphological and functional description of inhibitory connections is their relative low number (~8–15% of neurons in the 'barrel column' [25]). Furthermore, interneurons are notoriously diverse with respect to molecular, structural and functional properties [143–145]. This makes it very difficult to identify interneuron synaptic connections and determine their functional roles in the neuronal network of the barrel cortex.

Many classification schemes for cortical GABAergic interneurons have been proposed until today. One frequently used scheme to distinguish different interneuron subtypes is based on the expression of certain marker peptides/proteins such as the Ca^{2+}-binding proteins parvalbumin (PV), calbindin (CB) or calretinin (CR), the peptide hormones somatostatin (SOM), neuropeptide Y (NPY) and vasoactive intestinal peptide (VIP), reelin etc.; this classification has often been linked to the AP firing properties of a neuron, e.g. PV expressing (PV^+) neurons such as basket cells (BCs) and the axo-axonic chandelier cells are fast-spiking (FS) interneurons. In recent studies, it has been proposed that the vast majority of cortical GABAergic interneurons belong to one of three major classes: interneurons that express either PV, SOM or the serotonin 3a receptor ($5\text{-}HT_{3a}R$; [146–148]); subgroups in particular of SOM and $5\text{-}HT_{3a}R$ may also express other cellular markers. Other research groups have proposed that five or even more different subtypes of interneurons exist (see e.g. [144, 145, 149–151]). Whether these classifications adequately describe the function of an interneuron subtype in the cortical neuronal network is still a matter of debate. Moreover, in some studies it has been shown that e.g. PV expression and/or a fast spiking pattern is a feature for several morphologically very distinct interneuron subtypes or is not correlated with a FS pattern at all (see below). In particular, the axonal projection pattern of these interneurons had markedly different target regions suggesting a differential function and connectivity within the cortical network. For the barrel cortex, interneurons with clearly distinct morphologies but the same antigenicity and/or similar firing properties have been identified [152–156]. Furthermore, many interneuron connections in the barrel cortex have been described in which the interneuron type has been identified only qualitatively; the terminology used is often not reproducible (see below).

For a description of the inhibitory network in the barrel cortex it is therefore of paramount importance to identify the dendritic and axonal morphology of different interneuron types because they determine the structural and functional connectivity. Thus, in the remainder of this section we will focus mainly but not exclusively on synaptic connections involving barrel cortex interneurons with identified pre- *and* postsynaptic neurons. Table 4.1 gives a brief summary of the synaptic connections mentioned in this section. Gap junction connections between barrel cortex interneurons have been described for various cortical layers. These connection are not in the focus of this review and will only be mentioned in passing; they are not included in Table 4.1

The available information on the different barrel cortex interneuron types and their structural and functional connectivity is rather limited to date. Because of this, this section of the chapter can only provide an incomplete overview of the intricacies of interneuronal microcircuits of the barrel cortex. It is very likely to change significantly in the coming years.

To provide a framework, we will begin with the description of the TC recruitment of barrel cortex interneurons and proceed then as described for excitatory neurons. We will outline the recruitment or inhibition of interneurons in other cortical layers by feed-forward, feed-back inhibitory and disinhibitory mechanisms

Table 4.1 Synaptic connections involving barrel cortex interneurons discussed in this chapter*

Layer	presynaptic neuron	postsynaptic neuron	Mode of action	Comment	Reference
4	VPM afferent	*PV^+, FS L4 interneuron*	feed-forward inhibition		Porter et al. 2001 [157] Beierlein et al. 2003 [165]
	VPM afferent	*SOM^+ L4 interneuron*	feed-forward inhibition		
	VPM afferent	*5-HT_{3A}R + L4 interneuron*	feed-forward inhibition		Lee et al. 2010 [153]
	L4 spiny neuron	*PV^+, FS L4 interneuron*[a]	feed-forward inhibition		Koelbl et al. 2013 [154]
	PV^+, FS L4 interneuron[a]	L4 spiny neuron	feedback inhibition		
	CT L6A pyramidal cell	*PV^+, FS L4 interneuron*	feed-forward inhibition		Kim et al. 2014 [60]
	SOM^+ L4 interneuron	L4 spiny neuron	feedback inhibition		Xu et al. 2013 [155]
	SOM^+ L4 interneuron	*PV^+, FS L4 interneuron*	disinhibition		
	5-HT_{3A}R + L4 NGFC	L4 spiny neuron	feedback inhibition		Chittajallu et al. 2013 [169]
	L4 spiny neuron	*L2/3 local inhibitor*[b]	feed-forward inhibition		Helmstaedter et al. 2008 [170]
		L2/3 lateral inhibitor[b]			
		L2/3 translaminar inhibitor[b]			
2/3	L2/3 pyramidal cell	*FS L2/3 interneuron*	feed-forward inhibition		Holmgren et al., 2003 [75] Avermann et al. 2012 [78]
	FS L2/3 interneuron	L2/3 pyramidal cell	feedback inhibition		
	L2/3 Martinotti cell	L2/3 pyramidal cell	feed-foward inhibition		Kapfer et al. 2007 [185]
	L2/3 chandelier cell	axon initial segment and different dendritic compartments of L2 pyramidal cell L3 pyramidal cell L5A pyramidal cell L5B pyramidal cell	feed-forward inhibition	postsynaptic L2/3 interneurons are presynaptic to L1 interneurons (L1 ENGC, L1 SBC)	Jiang et al. 2013 [186] Lee et al. 2014 [187]
	L2/3 Martinotti cell				
	L2/3 NGFC				
	L2/3 DBC				
	L2/3 BTC				
	L2/3 BPC				
	L2/3 BC				

Table 4.1 (continued)

Layer	presynaptic neuron	postsynaptic neuron	Mode of action	Comment	Reference
	VIP + 5-HT$_{3a}$R + L2/3 interneuron	*SOM + L2/3interneuron*			Lee et al. 2013 [189]
	PV + L2/3 MB interneuron	L2/3 pyramidal cell			Blatow et al. 2003 [183]
	CR$^+$ L2/3 BCR interneuron	*FS L2/3 interneuron*			Caputi et al. 2009 [199]
	CR$^+$L2/3 MCR interneuron				
1	L2/3 pyramidal cells	*FS L1 interneuron L1 interneuron with accomodating firing pattern L1 interneuron with burst firing pattern*	feed-forward inhibition		Wozny and Williams 2011 [203]
	FS L1 interneuron L1 interneuron with adapting firing pattern L1 NGFC	L2/3 pyramidal cell	feedback inhibition		
	L1 SBC	*L2/3 chandelier cell L2/3 Martinotti cell L2/3 NGFC L2/3 DBC L2/3 BTC L2/3 BPC L2/3 BC*	disinhibition	L1 interneurons are presynaptic to postsynaptic L2/3 interneurons (L1 ENGC, L1 SBC)	Jiang et al. 2013 [186] Lee et al. 2014 [187]
	L1 ENGC	*L2/3 Martinotti cell L2/3 NGFC L2/3 BTC*			
	L1 ENGC	L2 pyramidal cell L3 pyramidal cell L5A pyramidal cell L5B pyramidal cell	feed-forward inhibition		
5	VPM afferent	*PV$^+$, FS L5 interneuron*	feed-forward inhibition		Tan et al. 2008 [168]
		SOM$^+$L5 interneuron			

Table 4.1 (continued)

Layer	presynaptic neuron	postsynaptic neuron	Mode of action	Comment	Reference
	L5 Martinotti cell	L5B pyramidal cell	feed-foward inhibition		Siberberg and Markram 2007 [206] Berger et al. 2010 [207]
	CT L6A pyramidal cell	*FS L5A interneuron*	feed-foward inhibition		Kim et al. 2014 [60]
6	VPM afferent	*FS L6 interneuron*	feed-foward inhibition		Beierlein and Connors 2002 [131] Cruikshank et al. 2010 [132]
		SOM$^+$(GIN) L6 interneuron			
	CT L6A pyramidal cell	*PV$^+$, FS L6 interneuron*	feed-foward inhibition		Mercer et al. 2005 [137] West et al. 2006 [210]
	CC L6A pyramidal cell				
	PV$^+$, FS L6 interneuron	CT L6A pyramidal cell			

Pre- and/or postsynaptic interneuron types are shown in bold typeface

[a] mostly so-called 'barrel inhibitor' interneurons (BIn, see Koelbl et al. 2013 [154])

[b] see also Helmstaedter et al. 2009 a,b,c [171–173]

Abbreviations: *FS* fast spiking; *PV* parvalbumin; *SOM* somatostatin; 5-HT_{3A}R, serotonin 3 A receptor, *CR* calretinin; *NGFC* neurogliaform cell; *ENGC* elongated neurogliaform cell; *SBC* single bouquet cell; *DBC* double bouquet cell; *BTC* bitufted cell; *BPC* bipolar cell; *MB* multipolar bursting; *BCR* bipolar calretinin-positive; *MCR* multipolar calretinin-positive; *CT*: corticothalamic; *CC* corticocortical

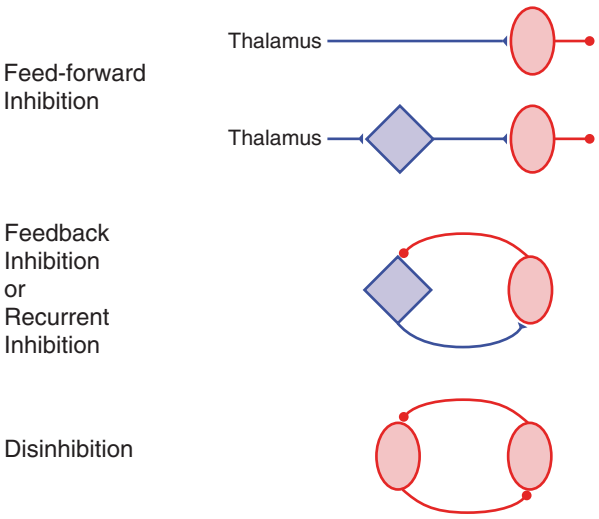

Fig. 4.6 Types of interneuron synaptic connections. Different types of synaptic microcircuit configurations involving GABAergic interneurons. The *feed-forward inhibition* may be direct or via one (as shown here) or more excitatory synapses. *Feedback inhibition* is shown as inhibition of an excitatory neuron that activates the same inhibitory neuron type (recurrent inhibition). *Disinhibition* is the inhibition of another inhibitory interneuron type

(Fig. 4.6) based on the presently available data. In this overview all synaptic connections involving barrel cortex interneurons will be included, i.e. connections in which interneurons are either pre- or postsynaptic or both.

Layer 4

In layer 4 of the somatosensory barrel cortex VPM afferents recruit several distinct types of L4 interneurons which in turn synapse onto excitatory neurons in the same or other cortical layers (see below) thereby mediating feed-forward inhibition. Given that interneurons comprise only 8.1 % (rat, Meyer et al. 2011)or 8.5 % (mouse, [24]) of the total neuron population in layer 4 of the barrel cortex the number of TC afferents innervating L4 interneurons is relatively large [21].

A major group of L4 interneurons targeted by TC afferents are the so-called FS, PV^+interneurons [131, 157–159]. They appear to be more readily recruited by TC input than excitatory neurons and are the major source of rapid intracortical inhibition in layer 4 [25, 158, 160, 161] and the infragranular cortical layers (e.g. [25, 146, 162]). Monosynaptic TC input to $5\text{-}HT_{3A}R^+$ interneurons has also been demonstrated [150] but their response to thalamic stimulation was considerably smaller than that of FS, PV^+ L4 interneurons. Furthermore, at least a subset of SOM^+ L4 interneurons (often showing a low-threshold or adapting firing pattern; [152, 163, 164]) appears to receive thalamic input. However, as observed for $5\text{-}HT_{3A}R^+$ interneurons their response is markedly weaker than that of PV^+, FS L4 interneurons and shows paired-pulse facilitation indicating a low release probability and a late recruitment of inhibition via these interneurons [132, 165].

FS L4 interneurons show a high maximal AP firing frequency (>100 Hz) that shows little if any adaptation. FS L4 interneurons in the barrel cortex are not a morphologically homogeneous class but have rather diverse axonal and dendritic

morphologies, ranging from FS L4 interneurons with a dense local axonal network to those projecting strongly into supra- and/or infragranular layers [154, 157]. Based on their axonal domain, FS L4 interneurons fall into three separate groups. Two of those show translaminar axonal projections; a few had axons that projected even into adjacent barrel 'columns'. However, the most prominent type is the FS L4 interneuron the axon of which is almost exclusively (>90%) confined to a barrel in layer 4 (Fig. 4.7). Therefore, this type has been coined 'L4 barrel inhibitor interneuron' (L4 BIn) and is probably a BC with a very dense, spatially confined axonal plexus. PV^+, FS L4 interneurons receive input from the VPM [157] and innervate excitatory L4 spiny neurons with a very high degree of connectivity (connectivity ratio ~70%; [154]). Notably, the connectivity remains high even when pre- and postsynaptic cell bodies are ~200 μm apart. IPSPs at this connection showed a short latency about 0.6 ms which is significantly smaller than that of L4 excitatory neurons onto other excitatory or inhibitory neurons. At the resting membrane potential of the L4 spiny neurons, the unitary IPSP amplitude is ~0.5 mV. The low c.v. (0.5) of IPSP amplitude and failure rate (14%) as well as the pronounced paired pulse depression of the IPSP indicate that the L4 BIn-L4 spiny neuron connection is reliable, i.e. it has a high release probability. The average number of inhibitory synaptic contacts in this connection was 3.5. These contacts were not only located on proximal dendrites but also at distal dendritic locations (>100 μm) which is at variance with the general view that this interneuron type forms only proximal synaptic contacts ([154]; Fig. 4.7).

Thus, L4 BIns are not only rapidly recruited by TC afferents but inhibit L4 spiny neurons at short latency thereby limiting excitation in barrel. Therefore, L4 BIns and other FS L4 interneurons may 'reset' the cortex rapidly and hence increase the temporal resolution of sensory stimuli. Because of the high degree of recurrent connectivity, they may also serve to maintain the excitatory-inhibitory balance in layer 4 of the barrel cortex. Furthermore, FS interneurons have also been implicated in the generation of oscillatory activity in neocortical neuronal networks.

In addition to the high inhibitory L4BIn-L4 spiny connection probability, there is also a large fraction (almost 70%) of reciprocally connected L4 BIn-L4 spiny neuron connections. EPSPs at this reciprocal connection have a longer latency than IPSPs, a mean amplitude of ~2 mV and were more reliable than IPSPs as the lower c.v. (0.34) and the lower failure rate (7%) indicate. In that respect they were similar to the excitatory L4-L4 spiny neuron and the L4 spiny neuron-L2/3 pyramidal cell connections [39, 45]; however their efficacy was somewhat higher and their time course faster. Thus, the L4 BIn-L4 spiny neuron connection is not only an integral element of a disynaptic feed-forward inhibition pathway in barrel cortex layer 4 (via direct TC activation of the PV^+, FS interneurons) but provides also a trisynaptic feedback control of the feed-forward inhibition. Furthermore, it has been demonstrated recently that L4 FS interneurons receive also rapid and powerful synaptic input from corticothalamic L6A pyramidal cells; EPSCs at this connection showed short-term depression with ongoing stimulation. Excitatory synaptic responses in L4 FS interneurons were markedly stronger than that in L4 spiny neurons indicative of a strong recruitment of these neurons. In concert with the synaptic input *via*

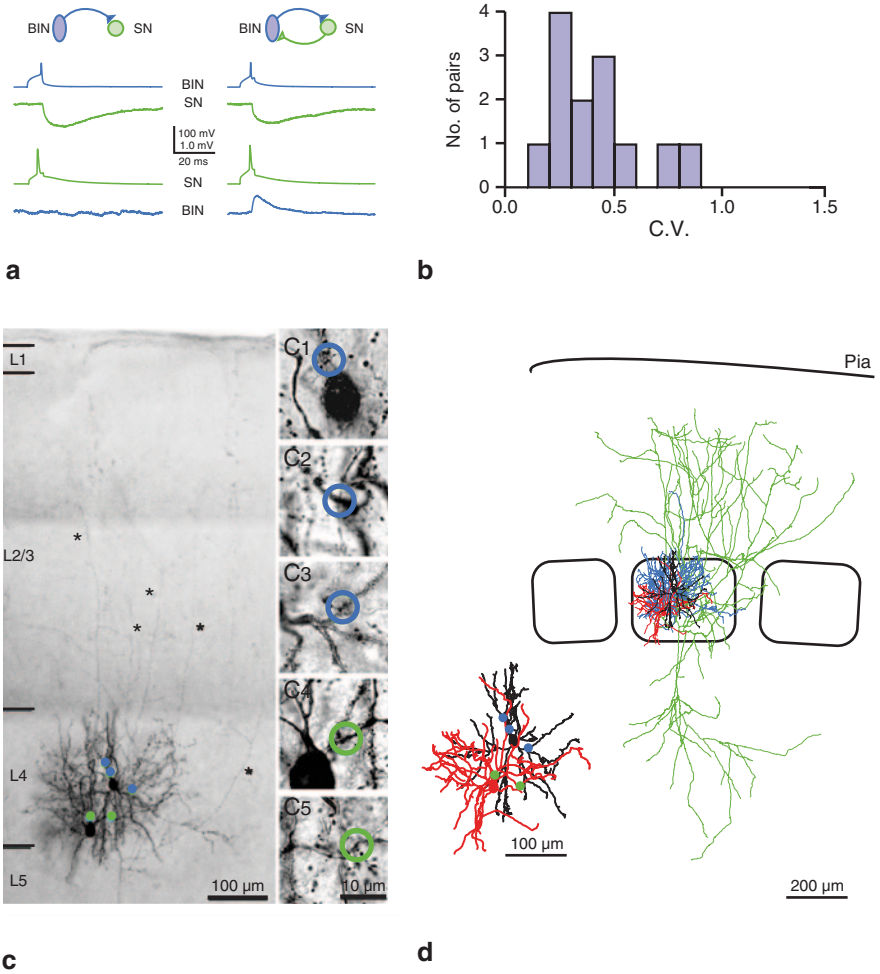

Fig. 4.7 Inhibitory synaptic microcircuit in layer 4 of the barrel cortex. Example of a feed-forward/feedback inhibitory synaptic microcircuit in layer 4 of the barrel cortex. a Paired recordings from an inhibitory connection between a PV^{+}, FS L4 interneuron (BIn, Koelbl et al. 2013 [154]) and a L4 spiny neuron. Left, monosynaptic connection; right recurrent connection, pre- and postsynaptic L4 neurons are reciprocally connected. Blue, recordings from the L4 interneuron, green; recordings from the L4 spiny neuron. b Coefficient of variation (c.v.) of L4 interneuron-L4 spiny neuron pairs. A low c.v. (< 0.5) signifies a reliable synaptic connection. c Biocytin labelling of a L4 interneuron-L4 spiny neuron pair in a barrel cortex slice preparation. Note that the two neurons are reciprocally coupled. Synaptic contacts established by the L4 interneuron, blue dots; synaptic contact established by the L4 spiny neuron, green dots. (C1-C5) High magnification images of dendritic and axonal appositions showing putative inhibitory (blue circles) and excitatory contacts (green circles). d Morphological reconstruction of the same L4 neuron pair. L4 interneuron, red dendrites, blue axon; L4 spiny neuron, white dendrites, green axon. Inhibitory and excitatory synaptic contacts are colour-coded as in panel C. Inset, enlarged image of the somatodendritic domain of the two reconstructed neurons showing the distribution of the synaptic contacts. Modified from Koelbl et al. 2013 [154] with permission from Oxford University Press

VPM afferents, the CT L6A input will strongly drive synaptic inhibition *via* L4 FS interneurons [60].

Barrel cortex layer 4 is one of the layers with a high density of SOM^+ interneurons. These L4 SOM^+ interneurons showed an adapting AP firing pattern with maximal mean firing frequencies of 70–150 Hz. Using different mouse lines (so called X94, X98 and GIN lines) several distinct types of SOM^+ interneurons have been identified that vary in their neurochemical, electrophysiological, morphological properties and their layer location [146, 152, 155]. Two major types of SOM^+ neurons have been identified in layer 4: interneurons with axon collaterals that ascend to layer 1 (which are probably SOM^+ L1-projecting Martinotti cells of the GIN subtype; [152, 166]) and those with a local, dense axonal domain that remains largely within a barrel (SOM^+ L4 interneurons of the X94 subtype [152]). SOM^+(X94) L4 interneurons are the dominant SOM^+ L4 interneuron type. These locally projecting SOM^+ L4 interneurons establish functional synaptic contacts with both FS L4 interneurons and L4 spiny neurons in the same barrel. However, SOM^+-FS L4 interneuron connections showed a significantly higher efficacy than SOM^+ interneuron-L4 spiny neuron connections. The connectivity ratio for SOM^+ L4 interneuron—FS L4 interneuron connections was reported to be 62 % and thus significantly larger than that for L4 spiny neurons [155].

These properties of SOM^+ L4 interneurons suggest a disinhibitory action on the excitatory network in layer 4. In recurrent intracortical networks, SOM^+ interneurons receive facilitating synaptic input from neocortical excitatory neurons [167]. This may contribute to an enhancement of disinhibition of a network silenced by FS interneurons. However, this action may be counteracted by SOM^+ interneurons in layer 5 (see below; [168]).

The third major group of interneurons, the $5\text{-}HT_{3A}R^+$ interneurons are not frequently found in layer 4. In this layer the major type of $5\text{-}HT_{3A}R^+$ interneuron is the so-called neurogliaform cell (NGFC) which express $5\text{-}HT_{3A}R$ and reelin [146, 153]. L4 NGFCs receive no direct thalamic excitation. They have a dense axonal plexus in layer 4 and exhibit a late AP firing pattern distinct from that of FS interneurons. The connectivity between L4 NGFCs and L4 spiny neurons is with 91 % extremely high [169]. AP firing of L4 NGFCs results in $GABA_B$ receptor-mediated unitary IPSPs in L4 spiny neurons with an extremely slow time course. This slow inhibition attenuates thalamic feed-forward inhibition by PV^+ FS L4 interneurons via $GABA_B$ receptors so that inhibition of L4 spiny neurons is reduced; it does, however, not affect thalamo- and intracortical excitation directly. The authors suggested that this slow inhibition serves as a mechanism to counteract a prolonged imbalance of excitation and inhibition in layer 4 of the barrel cortex. Thus, L4 FS interneurons ensure a high temporal resolution of sensory signals by rapidly inhibiting L4 spiny neuron recruitment. In contrast, L4 NGFCs enlarge the temporal window for synaptic coding thereby enhancing the integrative properties of the thalamic-L4 microcircuit necessary for plastic changes such as the refinement of receptive fields.

L4 spiny neurons do not only target L4 interneurons but also interneurons in supragranular layers [170–173]. Based on the axonal projection pattern, the dendritic geometry and the AP firing pattern eleven L2/3 interneuron types were identified

in the barrel cortex. Two of them had a highly distinctive structure: The chandelier cell, an FS interneuron type that innervates axon initial segments and the L1-inhibiting Martinotti cell. Using an unsupervised cluster analysis, additional four interneuron types with a local axonal domain, three with a lateral domain (with the axon projecting laterally over several barrel column) and two with a translaminar axon (with an axon projecting throughout several cortical layers) were identified (see Fig. 4.8). L4 spiny neurons made contacts with L2/3 interneurons belonging to all these three classes (i.e. those with local, lateral and translaminar axonal projection). This can also be considered as a feed-forward inhibition pathway where the interneuron is disynaptically recruited. However, no L4 spiny neuron connection with either the axo-axonic L2/3 chandelier cells (PV^+; [174, 175]) or L1-inhibiting L2/3 Martinotti cells (SOM^+; see also [152]) were found in this study.

The properties of different L4 spiny neuron-L2/3 interneuron connections were not identical and varied both with respect to efficacy, failure rate and paired-pulse ratio. This has been studied in a more detailed fashion for three connection types. Both putative local type 2 and lateral type 1 L2/3 interneurons (putative L2/3 neurogliaform and FS large BCs; see Fig. 4.8) show a high to intermediate efficacy (mean uEPSP amplitude of 1.2 and 0.6 mV); in addition the failure rate for these connection is low and the paired pulse ratio (PPR) is below 1.0, i.e. depressing. These properties are markedly different from L4-L2/3 connections with a postsynaptic local type 3 interneuron which may be a bitufted/bipolar, so-called low threshold spiking (LTS) interneuron. The mean uEPSP amplitude is with ~0.3 mV rather small while the failure rate is high (~50%) and the PPR is large, i.e. facilitating (PPR: ~2.0). Such a facilitating synaptic response was also observed in connection between L2/3 pyramidal cells and bitufted L2/3 interneurons [176]. Thus, while L4 spiny neurons connect to many different L2/3 interneurons there is a clear sign that the properties of synaptic transmission are target neuron specific on the functional level.

Gap junction connections between FS interneurons on the one hand and LTS interneurons on the other have been described for both layer 4 and 5 [163, 177, 178–180]. These connections were homotypic only, *i.e.* the gap junction connections between different L4 interneuron types were not been reported; however, for other brain regions heterotypic coupling has been shown to reported (*e.g.* [181–183]). Therefore, two distinct subnetworks of gap junction-coupled interneurons have been proposed to exist that serve to maintain oscillatory activity and synchronization of synaptic activity.

Layer 2/3

The total interneuron density varies in layer 2/3 with the top lamina ('layer 2') having a very high fraction of interneurons (17% of all neurons) which is significantly larger than that of either layer 3 or layer 4 (~9 and ~8%, respectively; [25]). Layer 2/3 contains interneurons of all major histochemical groups, i.e. PV^+, SOM^+ and

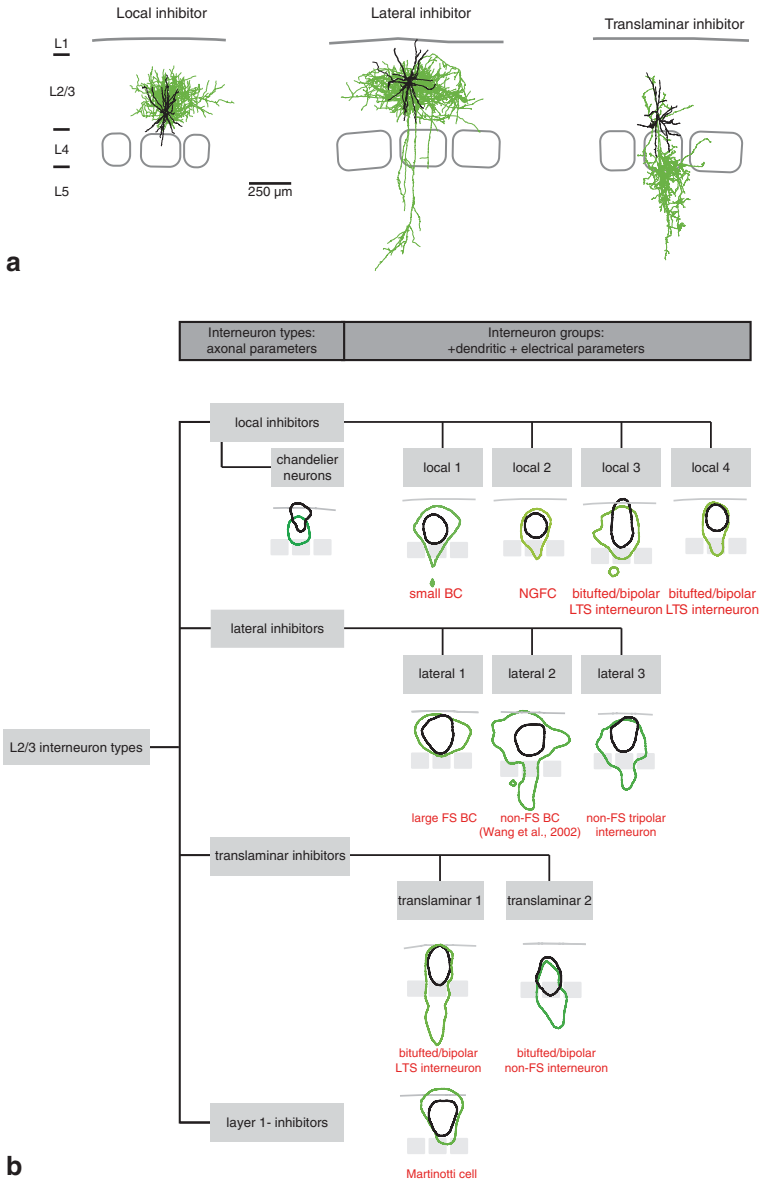

Fig. 4.8 L2/3 interneurons in the barrel cortex. L2/3 interneuron types identified by their laminar position and the relationship of the somatodendritic and axonal domain with respect to the underlying barrel structure. **a** Three example reconstructions of L2/3 interneurons with a local, a lateral and a translaminar axonal domain, respectively. The axon is in green, the dendrite in black. **b** Classification of the different types of L2/3 interneurons with a local, lateral and translaminar axonal domain, respectively, as well as the axo-axonic chandelier cells and the L1-inhibiting Martinotti cells. The 80 % extent of the axonal domains are outlined in different shades of green. Modified from Helmstaedter et al. 2009c with permission from Oxford University Press. For details see text and Helmstaedter et al. 2008 [170], Helmstaedter et al. 2009 a,b,c [171–173]

5-$HT_{3a}R^+$ interneurons [184]. However, in contrast to deep cortical layers the fraction of PV^+ interneurons is substantially lower and 5-$HT_{3a}R^+$ interneurons represent the predominant fraction, comprising about 50 % of all L2/3 interneurons [146; see also 162].

L2/3 interneurons are mainly recruited by L4 spiny neurons (see above) but also by L2 and L3 pyramidal cells in a feed-forward manner. L2/3 interneurons synaptically coupled to L4 spiny neurons have been described above. Synaptic connections between L2 and L3 pyramidal cells and L2/3 interneurons have to date not been characterised to such an extent. Holmgren and coworkers have analysed synaptic connections between L2 and L3 pyramidal cells and FS L2/3 interneurons, i.e. putative PV^+ BCs [75]. The observed connectivity probability was 80–90 %. The majority of these connections was reciprocal and thus recurrent: the L2/3 pyramidal cells exite L2/3 interneurons and in turn their activity is inhibited. Kapfer and coworkers also report a high connectivity ratio of 66.7 % for the FS L2/3 interneuron-L2/3 pyramidal cell connection [185]. Compared to unitary excitatory connections between L2/3 pyramidal cells, unitary excitatory connections onto an FS L2/3 interneuron were substantially more efficacious (0.7 vs. 3.5 mV) and show a stronger paired-pulse depression (10 Hz stimulation; 0.9 vs. 0.7) indicating a high release probability. Similarly, inhibitory connections from a FS L2/3 interneuron onto a L2/3 pyramidal cell showed also a high efficacy (3.0 mV with 20 mM K^+ and −2.3 mV with physiological K^+ at a resting membrane potential of about −70 mV) and reliability (PPR = 0.7) indicating that local inhibition is powerful and activated rapidly.

Two recent and very detailed studies [186, 187] (see below) described the disynaptic interaction between L1 interneurons and L2/3 interneuron types.The authors of this work also investigated synaptic connections established between different L2/3 interneuron types and pyramidal cells in layers 2/3 and 5. Several distinct L2/3 interneuron types were identified: Martinotti cells, chandelier cells, NGFCs, double bouquet cells (DBCs), bitufted cells (BTCs), bipolar cells (BPCs), as well as BCs (Fig. 4.9). It should be noted that the identification of interneuron types was based only on a limited number of quantitative parameters; the possible pitfalls of this approach for interneuron terminology have been discussed in depth recently [145; see also 171].

All L2/3 interneurons studied by Jiang et al. [186] and Lee et al. [187] project onto L2, L3, L5A and L5B pyramidal cells but apparently not L6 pyramidal cells. However, they target different cellular compartments (see Fig. 4.9c). Chandelier cells are known to target axon initial segments; in layer 2/3 the majority are likely to target axons of L2/3 pyramidal cells with a (small) subset innervating L5 pyramidal cells. L2/3 BCs and L2/3 DBCs establish synaptic contacts with the basal dendrites. L2/3 BPCs target the proximal apical dendrite and L2/3 BTCs its middle portion and apical tuft. Similarly, NGFCs in superficial layer 2/3 (i.e. layer 2) establish also synaptic contacts with the distal apical dendrite and the tuft; however, there are also deep L2/3 NGCs which are in a position to innervate basal dendrites of the L2/3 pyramidal cells. Finally, L2/3 Martinotti cells innervate mainly the apical dendritic tuft. L5 pyramidal cells showed an L2/3 interneuron innervation profile similar to that of L2/3 pyramidal cells. It is of note that different types of L2/3 interneurons

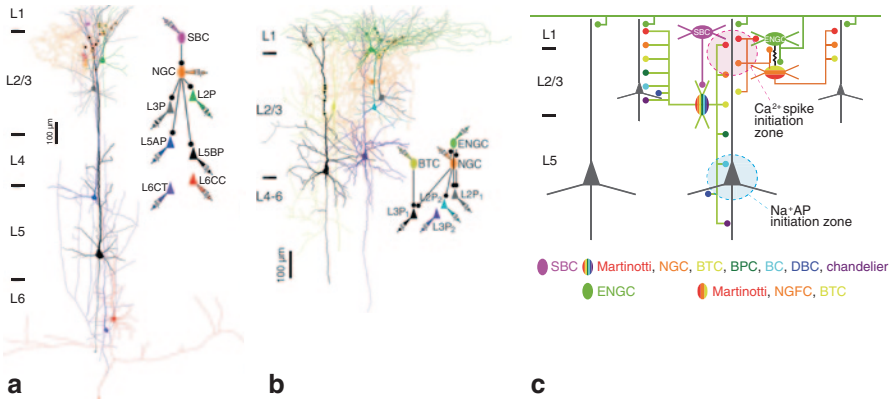

Fig. 4.9 L1 interneuron synaptic connections. **a** Octuple recording of the synaptic microcircuitry between L1 SBC, L2/3 NGC (*i.e.* NGFC) and L2, L3, L5A, L5B and CC and CT L6A pyramidal cells. **b** Septuple recording of the synaptic microcircuitry between L1 ENGC, L2/3 NGC (*i.e.* NGFC) and two L2 and two L2/3 pyramidal cells. **c** Schematic of the synaptic connectivity of L1 SBC and L1 ENGC with the different types of L2/3 interneurons projecting to the axon-initial segment and different compartments of the axosdendritic domain of pyramidal cells. Colour code for the different interneuron types is shown below the schematic; for panels A and B the same colour code applies. Modified from Lee *et al*., 2014 (with permission from Oxford University press). For further details see text and Lee *et al*., 2014 [187]

contact pyramidal cells in layers 2/3 and 5 along the entire axodendritic domain of these neurons. Axo-axonic chandelier cells, on the other hand, are a special case. By innervating the axon initial segment these interneurons are in an ideal position to control the AP output of pyramidal cells. However, they do not hyperpolarise but depolarise the axon initial segment of the postsynaptic pyramidal cells thereby increasing their gain [188]. The reason for this effect is a lack of a potassium chloride co-transporter (KCC2) at the axon initial segment which results in an increased intracellular chloride concentration which in turn will result in depolarising GABAergic postsynaptic potentials.

L2/3 interneurons establish between 3 and 6 synaptic contacts with L2/3 pyramidal cells. These numbers are similar for postsynaptic L5A pyramidal cells (4–6 synapses) but somewhat higher for L5B pyramidal cells (4–8 synapses). The synaptic efficacy of synaptic connections between single L2/3 interneuron and either L2/3 or L5 pyramidal cells is in the range of 0.27–0.67 mV and 0.15–0.45 mV, respectively, and thus relatively low; the synaptic dynamics and reliability of these connections were not studied [186, 187].

VIP^+ L2/3 interneurons, a subtype of $5\text{-}HT_{3a}R^+$ interneurons [146], have an adapting firing pattern like other $5\text{-}HT_{3a}R^+$ interneurons, a narrow axonal domain in layer 2/3 and dendritic projections in both layer 2/3 and layer 1. VIP^+, $5\text{-}HT_{3a}R^+$ interneurons in layer 2/3 target mainly SOM^+ interneurons that in turn inhibit the distal dendrites and apical tufts of pyramidal cells [189]. The inhibition of FS L2/3 interneurons and L2/3 pyramidal cells by VIP^+ L2/3 interneurons is weak; in marked contrast, SOM^+interneurons are strongly inhibited by VIP^+, $5\text{-}HT_{3a}R^+$ interneurons in layer 2/3. These SOM^+ interneurons are located in layer 2 and have a local axonal

domain that innervates preferentially the distal portion of the apical dendrites of pyramidal cells.

L2/3 and L5 pyramidal cells have two spike generation zones, the Ca^{2+} spike generation zone near the apical dendritic tuft of pyramidal cells and the AP initiation zone in the axon initial segment (Fig. 4.9c; for reviews see [190, 191]). These inherent 'active' properties of L2/3 and L5 pyramidal cells permit the coupling of excitatory synaptic inputs that simultaneously arrive at the apical dendritic tuft and the basal dendrites. Thereby they can function as 'coincidence' detectors, a mechanism that has been implicated in the association and integration synaptic inputs from different origins [192–194].

Because VIP^+ L2/3 interneuron dendrites project into layer 1 they can be targeted by long-range axonal projections from other cortical areas and subcortical regions [159, 195–197]. Using an optogenetic approach, Lee and coworkers [189] were able to demonstrate that VIP^+ L2/3 interneurons receive strong input from the primary vibrissal motor cortex (vM1), while non-VIP^+ 5-$HT_{3a}R^+$ interneurons do not. Hence, axons from the vM1 recruit VIP^+ L2/3 interneurons that in turn exert a powerful inhibitory influence over SOM^+ interneurons. Thus, activation of vM1 axons establishes a strong VIP^+ L2/3 interneuron-mediated disynaptic disinhibition of L2/3 pyramidal cells. In accordance with this, *in vivo* recordings showed that during whisking the AP firing of VIP^+ L2/3 interneurons strongly increases while that of SOM^+ L2/3 interneurons decreases. Because the preferential target region of SOM^+ interneurons is the apical tuft of L2/3 pyramidal cells this will selectively facilitate the generation of burst of Ca^{2+} spikes in the apical dendritic tufts of pyramidal cells and hence increase the synaptic gain at this compartment. Such burst of Ca^{2+} spikes have been shown to occur during the interaction of whisker sensory input into S1 cortex and vM1 activity induced by whisking behaviour as shown in layer 5 pyramidal cells [198].

Furthermore, several unusual interneuron types have also been identified in layer 2/3 that do not fit the widely used terminologies (see e. g. [144, 149]). Using transgenic animals in which either PV- or CR-expressing interneurons were labelled, novel types of PV^+ and CR^+ interneuron types were identified in the S1 barrel cortex [183, 199]. The PV^+ L2/3 interneuron was coined multipolar bursting (MB) interneuron and the CR^+ interneuron types bipolar and multipolar CR^+ interneurons (BCR and MCR). These three L2/3 interneuron types differed substantially in their functional and structural properties from previously described PV^+ or CR^+ interneurons. PV is generally expressed in FS interneurons such as BC or the axo-axonic chandelier cells. However, PV^+ MB interneurons show no FS firing pattern but an initial AP burst when depolarised; they have a dense axonal plexus in upper layer 2/3 with a few collaterals descending to layer 5 [183]. This axonal morphology resembles that of so-called 'nest' or 'large' BCs [143, 200]. BCR have a small and narrow axonal domain projecting down to layer 5; their AP firing pattern shows an initial high-frequency burst. In contrast, MCRs have a horizontal axonal domain that remains within layer 2/3; they have an adapting firing pattern. The morphology and functional properties of both BCR and MCR interneurons differed markedly from SOM^+Martinotti cells, which express also CR.

MB, BCR and MCR interneuron types are synaptically connected with L2/3 pyramidal cells and receive input from them. PV^+ MB L2/3 interneurons showed a high connectivity with L2/3 pyramidal cells (connectivity ratio = 0.41) but not CR^+ BCRs and CR^+ MCRs (0.1). BCRs and MCRs are reciprocally connected with FS L2/3 interneurons; however, only MCRs receive synaptic input from PV^+ MBs. The connectivity ratios of MCRs and BCRs with each other and the MB and FS L2/3 interneuron types range between ~10–30% which is low for interneuron connections. Only MCR-BCR, BCR-MCR and MCR-MB connections show significantly higher connectivity ratios (>40%). Furthermore, MCRs appear to receive monosynaptic input from layer 4 while MBs are only activated disynaptically.

In addition, these synaptic connections showed markedly different synaptic dynamics. While L2/3 pyramidal cell-BCR connections are strongly depressing those onto MBs and MCRs are facilitating. Conversely, BCR-pyramidal cell connections are facilitating while MCR-pyramidal cell connections are depressing. In addition, BCRs and MBs form local gap junction networks with each other (so-called homotypic electrical coupling). For MB interneurons it has been shown that these gap junctions persist into adulthood; they have been implicated in the synchronisation of activity in other MB interneurons and the synaptically coupled L2/3 pyramidal cells. In contrast, MCRs are electrically coupled not with each other but with the PV^+ MB interneurons. However, the functional roles of these novel interneuron types remains elusive [182, 183, 199]. In addition, heterotypic electrical coupling between PV^+ MB interneurons and L2/3 pyramidal cells has also been observed but this was developmentally down-regulated and virtually absent after the fourth postnatal week.

While these two studies on L2/3 interneurons are very interesting and of note they also pinpoint the difficulties inherent to the study of cortical interneuron connectivity. The terminology used by the authors is not commonly used; it is therefore difficult to place these interneuron types in the neuronal network of layer 2/3 and assess their functional roles. Nevertheless, the studies suggest that the diversity of interneurons may be even higher than anticipated and that previously held assumptions may not be entirely correct.

Layer 1

Cortical layer 1 is unique because it contains almost exclusively GABAergic interneurons—with the possible exception of Cajal-Retzius cells which are probably glutamatergic. The majority of L1 interneurons express 5-HT_{3a}Rs, with the exception of a small group (~5%) of SOM^+ L1 interneurons [146; see also 162]. However, a consensus on the classification of L1 interneuron has not been achieved and between two and six different types have been proposed [cf. 201–204, 183]. A quantitative morphological and electrophysiological analysis of L1 interneurons revealed the existence of four interneuron types: FS L1 interneurons, L1 interneurons with an adapting or burst-firing pattern as well as L1 NGFCs with a delayed AP firing mode [203]. Apart from L1 NGFCs, the other L1 interneuron types received

synaptic input from L2/3 pyramidal cells. The connectivity between L2/3 pyramidal cells and FS L1 interneurons was reported to be markedly higher (0.35) than that of adapting and burst-firing L1 interneurons (0.16 and 0.12, respectively). Unitary EPSPs at the L2/3 pyramidal cell-FS L1 interneuron connections were significantly faster than those at the other connection types and showed paired pulse facilitation. Although L1 NGFCs did not receive excitatory input from L2/3 pyramidal cells, they are the dominant source of inhibition of these neurons (connectivity probability of 0.44). Inhibition at this connection was mediated by $GABA_A$ and $GABA_B$ receptors as shown for NGFCs in other cortical layers [205; see also 186]. FS L1 interneurons also showed a relatively high inhibitory connectivity with L2/3 pyramidal cells (0.33) and exclusively $GABA_A$ receptor-mediated IPSPs. In contrast adapting L1 interneurons had only a low connection probability with L2/3 pyramidal cells (0.06); as for FS L1 interneuron uIPSPs were mediated by $GABA_A$ receptors only.

Zhu and co-workers (see above; [186, 187]) recently described inhibitory and disinhibitory interneuron microcircuits that are driven by the activity of L1 interneurons. They identified two major types of L1 interneurons, the L1 single bouquet cells (L1 SBCs) and the L1 elongated neurogliaform cells (termed L1 ENGCs; however this classification has not been used by any of the other research groups studying L1 interneurons). L1 SBCs have a narrow axonal domain which projects within layer 1 but also into layer 2/3 while the axonal domain of L1 ENGCs is broad but confined to layer 1 (Fig. 4.9a, b). The firing pattern of SBCs and ENGCs was not distinct adapting burst-spiking and non-adapting, delayed-spiking patterns were found for both neuron types. This observation is in marked contrast to that made for L1 NGFC by other research groups [202, 203, 205]. In addition, the late-spiking, putative L1 NGFCs have been shown to form gap junction networks between each other [202].

L1 SBCs establish unidirectional inhibitory connections with virtually every interneuron type in layer 2/3 (see above) with connectivity ratios ranging from 0.05 to 0.28 but with a low synaptic strength (mean IPSP amplitude: 0.34 mV; averaged over all L2/3 interneuron types). They only form monosynaptic connections with L2 and L3 but not with L5A/L5B pyramidal cells. However, L1 SBC disynaptically target L5 pyramidal cells via L2/3 pyramidal cells and L2/3 interneurons (see above).

Unlike L1 SBCs, L1 ENGCs were found to form *reciprocal* inhibitory and gap junction connections with a subset of L2/3 interneurons, namely L2/3 (SOM^+) Martinotti cells, L2 NGCs and L2/3 BTC with connectivity ratios of 0.18, 0.43 and 0.32, respectively. The mean IPSP amplitude was 0.68 mV averaged over all three L1 ENGC-L2/3 interneuron connection types. L1 ENGCs establish also direct inhibitory synapses with L2/3 and-in contrast to L1 SBCs-L5 pyramidal cells located in both the home and neighbouring 'barrel columns', thereby inhibiting a large population of these neurons.

The two L1 interneuron types display highly distinct connectivity patterns: The disynaptic L1 SBC-L2/3 interneuron-L5 pyramidal cell connections have a *disinhibitory* influence on L5 pyramidal cells at all dendritic compartments targeted by different L2/3 interneurons. In contrast, L1 ENGC-L2/3 interneuron connections supposedly exert a *largely inhibitory* influence over the disynaptically connected

L2/3 and L5 pyramidal cells. This is because the monosynaptic L1 ENGC-L2/3 interneurons connections are strongly recurrent and thus act through a feedback inhibitory mechanism. Synaptic contacts established by the three L2/3 interneuron types innervated by L1 ENGCs are located mainly on apical dendritic tuft dendrites, near the Ca^{2+} spike generation zone. The various L2/3 interneuron types (see above and Fig. 4.9c), with specific influences on different compartments of the apical dendritic tree of L5 pyramidal cells can affect this interaction either by blocking dendritic Ca^{2+} spikes directly or by altering the synergistic coupling between the somatic/basal dendritic and apical dendritic compartment. Nevertheless, the L1-L2/3 interneuron-L5 pyramidal cell pathway described in these studies [186, 187] does not take into account possible interactions between the different L2/3 interneurons and the excitatory input from L2/3 and possibly also from L5A pyramidal cells. Both these mechanisms may interfere with the proposed L1 inhibitory and disinhibitory mechanisms.

Layer 5

By now, interneuron function has been studied to some extent for supragranular layers. However, significantly less is known with respect to infragranular layers. However, for layer 5A and B the relative fraction of interneurons (interneurons/total neurons) was with 20 and 16 % relatively high compared to other barrel cortex layers with the exception of layer 2 (see above). The majority of L5 interneurons belong to the PV^+ type; in particular in layer 5A, the fraction of SOM^+ interneurons is also relatively high. Only few studies on the functional role of L5B interneurons and its special position in the neocortical microcircuitry in either the barrel cortex or the somatosensory cortex exist. Tan and co-workers studied the synergistic action of PV^+, FS and SOM^+ interneurons in layer 5B. During early phases of thalamic excitation PV^+ FS L5 interneurons are activated; this activation is initially strong and will result in rapid but only transient AP firing (Fig. 4.10). Persistent AP firing of TC afferents (as it may occur during active whisking of the rodent) leads to a pronounced paired-pulse depression of the TC EPSPs at FS, PV^+ interneuron synapses; this will effectively silence FS, PV^+ L5B interneurons. The reduction in fast feed-forward inhibition would result in a run-away excitation which, however, has not been observed *in vivo*. Thus, the rapidly depressing fast feed-forward inhibition needs to be replaced by a slow-onset inhibition provided by a different interneuron type.

Unlike most other SOM^+ interneurons (see above) those in layer 5B do not synapse onto distal portions of the apical dendrite of pyramidal neurons but have a dominant barrel-related axonal domain (Fig. 4.10a, b); this is at least the case for the X94-subtype of SOM^+ interneurons [152]. They receive TC input (like SOM^+(X94) interneurons in layer 4; see above and [167]). The target structures of these SOM^+ L5 interneurons are dendrites of L4 spiny neurons [168]. In contrast to PV^+ FS L5B interneurons, adapting-firing SOM^+ L5B interneurons respond with facilitating EPSPs during ongoing thalamic stimulation. When TC axons fire at a high presynaptic spiking frequency, EPSP facilitation will occur and result in progressively larger

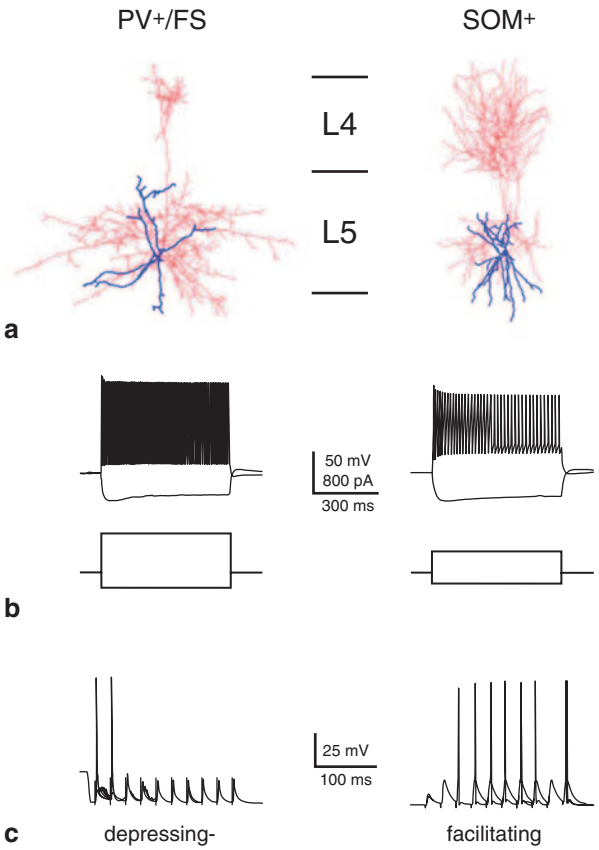

Fig. 4.10 SOM$^+$ and PV$^+$ L5 interneuron morphology and function. Reconstructions of the axo-dendritic domain of a PV$^+$, FS interneuron and a SOM$^+$ interneuron in deep layer 5 (layer 5B); dendrites blue, axons red. Note the different axonal projection patterns. (b) Different AP firing patterns of the PV$^+$, FS and the SOM$^+$ L5 interneurons. (c) On repetitive stimulation of the VPM, PV$^+$, FS and the SOM$^+$ L5 interneuron EPSPs show a depression and facilitation, respectively. In PV$^+$, FS L5 interneurons the first few EPSPs are superthreshold and result in APs. In contrast, in SOM$^+$ L5 interneurons, the AP threshold is reached only after prolonged VPM stimulation and the resulting EPSP facilitation is necessary to reach AP threshold; AP firing in SOM$^+$ L5 interneurons is therefore 'delayed'. Modified from Tan et al. (2008) [168]. Robust but delayed thalamocortical activation of dendritic-targeting inhibitory interneurons. Proc. Natl. Acad. Sci. U S A 105:2187–2192 with permission, Copyright (2008) National Academy of Sciences U.S.A

EPSPs in the SOM$^+$ L5B interneurons; in turn, they will eventually reach the AP threshold and fire APs (Fig. 4.10c). Inhibition of SOM$^+$ L5B interneurons is not recruited in response to brief stimuli; rather it requires ongoing TC input to induce SOM$^+$ interneuron firing. Thus, there is a shift in the rapid-onset feed-forward inhibition of L4 spiny neurons by PV$^+$ FS L5B interneurons (and also FS L4 interneurons; [157, 163]) to a late-onset inhibition via SOM$^+$ L5B interneurons. The latter interneurons will be the main source of inhibition in the late phase of TC excitation because their synaptic efficacy is maximal at this point in time. Such change in the

recruitment of inhibition will also occur at stimulation frequencies of 10–20 Hz, which are behaviourally relevant whisking frequencies in rodents [168]. It should be noted, however, that in layer 4 of the barrel cortex SOM^+-FS interneuron connections have been shown to exert a disinhibitory effect on the excitatory neuronal network. This is in marked contrast to the delayed inhibitory action proposed for L5 SOM^+-FS interneuron connections.

A hyperpolarising, i.e. inhibitory synaptic response can be occasionally observed between two neighbouring thick-tufted L5 pyramidal cells [206, 207]. A similar phenomenon was also found for L2/3 pyramidal cells [185]. This inhibition is disynaptic: one L5 pyramidal cell fires an interneuron that in turn inhibits the second pyramidal cell. Disynaptic inhibitory connections are significantly more frequent than direct, monosynaptic excitatory connection between L5 pyramidal cells, at least at the age of animal used for this study (postnatal day 14–16). The inhibitory response increases with the frequency and duration of the AP train in the 'presynaptic' pyramidal cell. The L5 interneurons that mediates this frequency-dependent disynaptic inhibition are SOM^+, L1-targeting Martinotti cells located in layer 5. L5 Martinotti cells have ascending axonal collaterals with a narrow axonal domain; they target apical oblique and tuft dendrites of the thick-tufted L5 pyramidal cells. Synaptic connections between L5 thick-tufted pyramidal cells and L5 Martinotti cells showed a high degree of convergence with ~70% of neighbouring pyramidal cells contacting the same interneuron. The degree of divergence was even higher: a single L5 Martinotti cell established synaptic contacts with ~80% of the neighbouring L5 pyramidal cells. The authors argue that the mechanism of interaction between L5 pyramidal cells and L5 Martinotti cells is AP rate dependent. At low AP frequency the main effect of two neighbouring pyramidal cells is largely excitatory because the membrane potential in Martinotti cells does not reach the AP threshold. When the AP firing frequency and duration in the L5 pyramidal cell increase, Martinotti cells start to fire APs due to EPSP summation and an inhibitory response in neighbouring pyramidal cells will occur. Because most Martinotti cells target distal dendrites they may also act to suppress Ca^{2+} spikes in the apical tuft of the neighbouring L5 thick-tufted pyramidal cells. The powerful inhibition exerted by Martinotti cells may also act by correlating membrane potential fluctuations, leading to synchronous spiking between L5 pyramidal cells that simultaneously receive frequency-dependent disynaptic inhibition. This disynaptic inhibitory mechanism is not exclusive to the somatosensory (barrel) cortex but appears to be ubiquitous in the neocortex and has been observed also in other cortices such as motor, visual and prefrontal cortex [208].

Recently it has been demonstrated that like L4 FS interneurons those in layer 5A receive strong synaptic input from corticothalamic L6A pyramidal cells [60; see above]. Thus, CT L6A pyramidal cells activate L5A FS interneurons which in turn target local L5A pyramidal cells thereby curtailing excitation of L5A neurons by a feed-forward inhibition mechanism. However, support for this hypothesis based on anatomical data is still missing.

L5A SOM^+ interneurons are also activated by CT L6A pyramidal cells. However, L6A input to this interneuron type is much weaker than that to L5A FS interneu-

rons; it also shows a pronounced EPSP facilitation, indicating that the CT L6A-L5A SOM^+ interneuron connection is not very reliable. Given its short-term dynamics one may hypothesise that L5A SOM^+ interneurons are only recruited following prolonged synaptic input; the functional implication of this is so far unknown because the connectivity profile for pyramidal cells, FS and SOM^+ interneurons in layer 5A is not clear.

Layer 6

Inhibition in layer 6 of the neocortex has so far not been in the focus of current research activity. A recent study by Perrenoud and co-workers provided a first description of L6A and L6B interneurons [209] showing that there are at least four different types: PV^+ FS L6 interneurons, SOM^+ L6 interneurons with an adapting firing pattern as well as VIP-expressing and NPY-expressing L6 interneurons which also show an adapting firing pattern and are both subgroups of the 5-$HT3aR^+$ interneurons. All L6 interneuron types were found in layers 6A and 6B, albeit with somewhat different morphological features.

The synaptic connectivity of L6 interneurons has only been investigated for FS and SOM^+(GIN) L6 LTS interneurons [132]. Both interneuron types receive TC input from the VPM but show significant differences in the efficacy of the synaptic response, reminiscent of the situation found for L4 interneurons. FS L6 interneurons (which are responsible for rapid feed-forward inhibition) received strong TC input that showed pronounced paired pulse depression. In contrast, TC EPSPs in SOM^+ L6 interneurons of the GIN subtype [166] were significantly weaker than those recorded in either excitatory L6 neurons or FS L6 interneurons. PV^+ FS L6 interneurons and SOM^+interneurons have been reported to receive excitatory input from CT and—to a significantly smaller extent—CC L6 pyramidal cells [137, 210]. The excitatory input shows weak or pronounced facilitation, respectively. A rapid recruitment of PV^+ FS L6 interneurons by CT L6 pyramidal cells has also been reported for visual cortex [210, 211]. There, CT L6 pyramidal cells recruit widespread inhibition throughout all cortical layers by activating visual cortex FS interneurons with L1-to-L6 translaminar axonal projections; these FS L6 interneurons are different from locally-projecting FS interneurons in layer 6. So far, a comparable type of FS L6 interneuron and a similar translaminar inhibitory mechanism have not been reported for barrel cortex.

Conclusion

As this chapter shows it is still premature to draw a combined and interdigitated map of the local excitatory and inhibitory microcircuits in the barrel cortex. For excitatory synaptic connections in the barrel cortex several schemes for the excitatory

neuronal network in a barrel 'column' have been proposed. However, emerging data on the cellular short- and in particular long-range axonal geometry of excitatory neurons and a hitherto unknown diversity in pyramidal cell types suggest that this picture is likely to change in the future, in particular with respect to signal propagation in the vertical plane of the neocortex.

The picture is even more difficult for synaptic connections involving barrel cortex inhibitory interneurons. This is in part due to the extremely high diversity of interneurons with respect to action potential firing, gene expression and morphology. Furthermore, the database on the synaptic connectivity of the different types of barrel cortex interneurons is still very limited and the functional roles of the different excitatory-inhibitory, inhibitory-excitatory and inhibitory-inhibitory connections remain poorly understood. A number of studies on cortical interneuron function argue for a 'preferential' or 'selective' targeting of one interneuron type by another. However, so far no direct proof for such a selectivity exist. In recent years some studies have actually shown that the connectivity of PV^+ FS and SOM^+ interneurons with excitatory neurons in the same layer is very high but unspecific [154, 212–214]. To date, no data concerning this point is available for interneuron-interneuron connections but it is likely that a similar picture will emerge. In addition, the high degree of recurrent interneuron connectivity makes it difficult to dissect predominantly inhibitory or disinhibitory action of an interneuron connection. Furthermore, the dynamic properties of cortical interneuron connections determine their functional connectivity and temporal sequence of activation, processes that are highly dependent on the dynamic properties of the synaptic connection. Inhibitory and disinhibitory actions of a defined microcircuit may therefore occur in the same inhibitory microcircuit during the duration of their activation. Thus, it is at present too premature to draw even an approximate schematic of the inter- and translaminar interneuronal network in a barrel 'column'. More structural *and* functional data is needed to understand the role that monosynaptic interneuron connections but also of di- and polysynaptic interneuron circuits play in synaptic signalling in the barrel cortex.

References

1. Fox KD (2008) Barrel Cortex. 1st edition edn. Cambridge University Press, Cambridge
2. Bosman LW, Houweling AR, Owens CB, Tanke N, Shevchouk OT, Rahmati N, Teunissen WH, Ju C, Gong W, Koekkoek SK, De Zeeuw CI (2011) Anatomical pathways involved in generating and sensing rhythmic whisker movements. Front Integr Neurosci 5:53. doi:10.3389/fnint.2011.00053
3. Feldmeyer D, Brecht M, Helmchen F, Petersen CC, Poulet JF, Staiger JF, Luhmann HJ, Schwarz C (2013) Barrel cortex function. Prog Neurobiol 103:3–27. doi:10.1016/j.pneurobio.2012.11.002
4. Helmstaedter M, de Kock CP, Feldmeyer D, Bruno RM, Sakmann B (2007) Reconstruction of an average cortical column in silico. Brain Res Brain Res Rev 55(2):193–203. doi:10.1016/j.brainresrev.2007.07.011

5. Douglas RJ, Martin KA (1991) A functional microcircuit for cat visual cortex. J Physiol 440:735–769
6. Thomson AM, Morris OT (2002) Selectivity in the inter-laminar connections made by neocortical neurones. J Neurocytol 31(3–5):239–246
7. Douglas RJ, Martin KA (2004) Neuronal circuits of the neocortex. Annu Rev Neurosci 27:419–451
8. Lübke J, Feldmeyer D (2007) Excitatory signal flow and connectivity in a cortical column: focus on barrel cortex. Brain Struct Funct 212(1):3–17. doi:10.1007/s00429-007-0144-2
9. Aronoff R, Matyas F, Mateo C, Ciron C, Schneider B, Petersen CC (2010) Long-range connectivity of mouse primary somatosensory barrel cortex. Eur J Neurosci 31(12):2221–2233. doi:10.1111/j.1460-9568.2010.07264.x
10. Feldmeyer D (2012) Excitatory neuronal connectivity in the barrel cortex. Front Neuroanat 6:24. doi:10.3389/fnana.2012.00024
11. Vitali I, Jabaudon D (2014) Synaptic biology of barrel cortex circuit assembly. Semin Cell Dev Biol. doi:10.1016/j.semcdb.2014.07.009
12. Constantinople CM, Bruno RM (2013) Deep cortical layers are activated directly by thalamus. Science 340(6140):1591–1594. doi:10.1126/science.1236425
13. Meyer HS, Wimmer VC, Hemberger M, Bruno RM, de Kock CP, Frick A, Sakmann B, Helmstaedter M (2010a) Cell type-specific thalamic innervation in a column of rat vibrissal cortex. Cereb Cortex 20(10):2287–2303. doi:10.1093/cercor/bhq069
14. Oberlaender M, de Kock CP, Bruno RM, Ramirez A, Meyer HS, Dercksen VJ, Helmstaedter M, Sakmann B (2012) Cell type-specific three-dimensional structure of thalamocortical circuits in a column of rat vibrissal cortex. Cereb Cortex 22(10):2375–2391. doi:10.1093/cercor/bhr317
15. Groh A, Meyer HS, Schmidt EF, Heintz N, Sakmann B, Krieger P (2010) Cell-type specific properties of pyramidal neurons in neocortex underlying a layout that is modifiable depending on the cortical area. Cereb Cortex 20(4):826–836. doi:10.1093/cercor/bhp152
16. Bernardo KL, Woolsey TA (1987) Axonal trajectories between mouse somatosensory thalamus and cortex. J Comp Neurol 258(4):542–564
17. Jensen KF, Killackey HP (1987) Terminal arbors of axons projecting to the somatosensory cortex of the adult rat. I. The normal morphology of specific thalamocortical afferents. J Neurosci 7(11):3529–3543
18. Chmielowska J, Carvell GE, Simons DJ (1989) Spatial organization of thalamocortical and corticothalamic projection systems in the rat SmI barrel cortex. J Comp Neurol 285(3):325–338
19. Pierret T, Lavallée P, Deschênes M (2000) Parallel streams for the relay of vibrissal information through thalamic barreloids. J Neurosci 20(19):7455–7462
20. White EL, Rock MP (1979) Distribution of thalamic input to different dendrites of a spiny stellate cell in mouse sensorimotor cortex. Neurosci Lett 15(2–3):115–119. doi:0304–3940(79)96099-3 [pii]
21. White EL, Rock MP (1981) A comparison of thalamocortical and other synaptic inputs to dendrites of two non-spiny neurons in a single barrel of mouse SmI cortex. J Comp Neurol 195(2):265–277
22. White EL, Benshalom G, Hersch SM (1984) Thalamocortical and other synapses involving nonspiny multipolar cells of mouse SmI cortex. J Comp Neurol 229(3):311–320
23. White EL (2007) Reflections on the specificity of synaptic connections. Brain Res Brain Res Rev 55(2):422–429. doi:S0165-0173(06)00139-1 [pii] 10.1016/j.brainresrev.2006.12.004
24. Lefort S, Tomm C, Floyd Sarria JC, Petersen CC (2009) The excitatory neuronal network of the C2 barrel column in mouse primary somatosensory cortex. Neuron 61(2):301–316. doi:10.1016/j.neuron.2008.12.020
25. Meyer HS, Schwarz D, Wimmer VC, Schmitt AC, Kerr JN, Sakmann B, Helmstaedter M (2011) Inhibitory interneurons in a cortical column form hot zones of inhibition in layers 2 and 5A. Proc Natl Acad Sci U S A 108(40):16807–16812. doi:10.1073/pnas.1113648108

26. Brecht M, Sakmann B (2002) Dynamic representation of whisker deflection by synaptic potentials in spiny stellate and pyramidal cells in the barrels and septa of layer 4 rat somatosensory cortex. J Physiol 543(Pt 1):49–70
27. Bruno RM, Sakmann B (2006) Cortex is driven by weak but synchronously active thalamocortical synapses. Science 312(5780):1622–1627
28. Benshalom G, White EL (1986) Quantification of thalamocortical synapses with spiny stellate neurons in layer IV of mouse somatosensory cortex. J Comp Neurol 253(3):303–314
29. Brumberg JC, Pinto DJ, Simons DJ (1999) Cortical columnar processing in the rat whisker-to-barrel system. J Neurophysiol 82(4):1808–1817
30. Miller KD, Pinto DJ, Simons DJ (2001) Processing in layer 4 of the neocortical circuit: new insights from visual and somatosensory cortex. Curr Opin Neurobiol 11(4):488–497
31. Jia H, Varga Z, Sakmann B, Konnerth A (2014) Linear integration of spine Ca2+ signals in layer 4 cortical neurons in vivo. Proc Natl Acad Sci USA 111(25):9277–9282. doi:10.1073/pnas.1408525111
32. Schoonover CE, Tapia JC, Schilling VC, Wimmer V, Blazeski R, Zhang W, Mason CA, Bruno RM (2014) Comparative strength and dendritic organization of thalamocortical and corticocortical synapses onto excitatory layer 4 neurons. J Neurosci 34(20):6746–6758. doi:10.1523/JNEUROSCI.0305–14.2014
33. Shepherd GM, Stepanyants A, Bureau I, Chklovskii D, Svoboda K (2005) Geometric and functional organization of cortical circuits. Nat Neurosci 8(6):782–790
34. Bureau I, von Saint PF, Svoboda K (2006) Interdigitated paralemniscal and lemniscal pathways in the mouse barrel cortex. PLoS Biol 4(12):e382
35. Alloway KD (2008) Information processing streams in rodent barrel cortex: the differential functions of barrel and septal circuits. Cereb Cortex 18(5):979–989. doi:10.1093/cercor/bhm138
36. Staiger JF, Bojak I, Miceli S, Schubert D (2014) A gradual depth-dependent change in connectivity features of supragranular pyramidal cells in rat barrel cortex. Brain Struct Funct. doi:10.1007/s00429-014-0726-8
37. Lübke J, Egger V, Sakmann B, Feldmeyer D (2000) Columnar organization of dendrites and axons of single and synaptically coupled excitatory spiny neurons in layer 4 of the rat barrel cortex. J Neurosci 20(14):5300–5311
38. Egger V, Nevian T, Bruno RM (2008) Subcolumnar dendritic and axonal organization of spiny stellate and star pyramid neurons within a barrel in rat somatosensory cortex. Cereb Cortex 18(4):876–889. doi:10.1093/cercor/bhm126
39. Feldmeyer D, Egger V, Lübke J, Sakmann B (1999) Reliable synaptic connections between pairs of excitatory layer 4 neurones within a single 'barrel' of developing rat somatosensory cortex. J Physiol 521(Pt 1):169–190
40. Cowan AI, Stricker C (2004) Functional connectivity in layer IV local excitatory circuits of rat somatosensory cortex. J Neurophysiol 92(4):2137–2150
41. Staiger JF, Flagmeyer I, Schubert D, Zilles K, Kötter R, Luhmann HJ (2004) Functional diversity of layer IV spiny neurons in rat somatosensory cortex: quantitative morphology of electrophysiologically characterized and biocytin labeled cells. Cereb Cortex 14(6):690–701
42. Sarid L, Bruno R, Sakmann B, Segev I, Feldmeyer D (2007) Modeling a layer 4-to-layer 2/3 module of a single column in rat neocortex: interweaving in vitro and in vivo experimental observations. Proc Natl Acad Sci 104(41):16353–16358
43. Feldmeyer D, Radnikow G (2009) Developmental alterations in the functional properties of excitatory neocortical synapses. J Physiol 587(Pt 9):1889–1896. doi:jphysiol.2009.169458 [pii]10.1113/jphysiol.2009.169458
44. Lübke J, Roth A, Feldmeyer D, Sakmann B (2003) Morphometric analysis of the columnar innervation domain of neurons connecting layer 4 and layer 2/3 of juvenile rat barrel cortex. Cereb Cortex 13(10):1051–1063
45. Feldmeyer D, Lübke J, Silver RA, Sakmann B (2002) Synaptic connections between layer 4 spiny neurone-layer 2/3 pyramidal cell pairs in juvenile rat barrel cortex: physiology and anatomy of interlaminar signalling within a cortical column. J Physiol 538(3):803–822

46. Shepherd GM, Svoboda K (2005) Laminar and columnar organization of ascending excitatory projections to layer 2/3 pyramidal neurons in rat barrel cortex. J Neurosci 25(24):5670–5679
47. Silver RA, Lübke J, Sakmann B, Feldmeyer D (2003) High-probability uniquantal transmission at excitatory synapses in barrel cortex. Science 302(5652):1981–1984. doi:10.1126/Science.1087160
48. Feldmeyer D, Roth A, Sakmann B (2005) Monosynaptic connections between pairs of spiny stellate cells in layer 4 and pyramidal cells in layer 5A indicate that lemniscal and paralemniscal afferent pathways converge in the infragranular somatosensory cortex. J Neurosci 25(13):3423–3431
49. Qi G, Radnikow G, Feldmeyer D (2014) Electrophysiological and morphological characterization of neuronal microcircuits in acute brain slices using paired patch-clamp recordings. J Vis Exp :e52358. doi:10.3791/52358
50. Schubert D, Staiger JF, Cho N, Kötter R, Zilles K, Luhmann HJ (2001) Layer-specific intracolumnar and transcolumnar functional connectivity of layer V pyramidal cells in rat barrel cortex. J Neurosci 21(10):3580–3592
51. Schubert D, Kötter R, Luhmann HJ, Staiger JF (2006) Morphology, electrophysiology and functional input connectivity of pyramidal neurons characterizes a genuine layer Va in the primary somatosensory cortex. Cereb Cortex 16(2):223–236
52. Petreanu L, Mao T, Sternson SM, Svoboda K (2009) The subcellular organization of neocortical excitatory connections. Nature 457(7233):1142–1145. doi:10.1038/nature07709
53. Hooks BM, Hires SA, Zhang YX, Huber D, Petreanu L, Svoboda K, Shepherd GM (2011) Laminar analysis of excitatory local circuits in vibrissal motor and sensory cortical areas. PLoS Biol 9(1):e1000572. doi:10.1371/journal.pbio.1000572
54. Qi G, Feldmeyer D (2015) Dendritic target region-specific formation of synapses between excitatory layer 4 neurons and layer 6 pyramidal cells. Cereb Cortex. doi:10.1093/cercor/bhu334
55. Tanaka YR, Tanaka YH, Konno M, Fujiyama F, Sonomura T, Okamoto-Furuta K, Kameda H, Hioki H, Furuta T, Nakamura KC, Kaneko T (2011) Local connections of excitatory neurons to corticothalamic neurons in the rat barrel cortex. J Neurosci 31(50):18223–18236. doi:10.1523/JNEUROSCI.3139-11.2011
56. Zhang ZW, Deschênes M (1997) Intracortical axonal projections of lamina VI cells of the primary somatosensory cortex in the rat: a single-cell labeling study. J Neurosci 17(16):6365–6379
57. Pichon F, Nikonenko I, Kraftsik R, Welker E (2012) Intracortical connectivity of layer VI pyramidal neurons in the somatosensory cortex of normal and barrelless mice. Eur J Neurosci 35(6):855–869. doi:10.1111/j.1460-9568.2012.08011.x
58. Stratford KJ, Tarczy-Hornoch K, Martin KA, Bannister NJ, Jack JJ (1996) Excitatory synaptic inputs to spiny stellate cells in cat visual cortex. Nature 382(6588):258–261. doi:10.1038/382258a0
59. Tarczy-Hornoch K, Martin KA, Stratford KJ, Jack JJ (1999) Intracortical excitation of spiny neurons in layer 4 of cat striate cortex in vitro. Cereb Cortex 9(8):833–843
60. Kim J, Matney CJ, Blankenship A, Hestrin S, Brown SP (2014) Layer 6 corticothalamic neurons activate a cortical output layer, layer 5a. J Neurosci 34(29):9656–9664. doi:10.1523/JNEUROSCI.1325-14.2014
61. Laaris N, Keller A (2002) Functional independence of layer IV barrels. J Neurophysiol 87(2):1028–1034
62. Arnold PB, Li CX, Waters RS (2001) Thalamocortical arbors extend beyond single cortical barrels: an in vivo intracellular tracing study in rat. Exp Brain Res 136(2):152–168
63. Ohno S, Kuramoto E, Furuta T, Hioki H, Tanaka YR, Fujiyama F, Sonomura T, Uemura M, Sugiyama K, Kaneko T (2012) A morphological analysis of thalamocortical axon fibers of rat posterior thalamic nuclei: a single neuron tracing study with viral vectors. Cereb Cortex 22(12):2840–2857. doi:10.1093/cercor/bhr356
64. Feldmeyer D, Lübke J, Sakmann B (2006) Efficacy and connectivity of intracolumnar pairs of layer 2/3 pyramidal cells in the barrel cortex of juvenile rats. J Physiol 575(Pt 2):583–602. doi:10.1113/jphysiol.2006.105106

65. van Aerde KI, Qi G, Feldmeyer D (2013) Cell type-specific effects of adenosine on cortical neurons. Cereb Cortex. doi:10.1093/cercor/bht274
66. Larsen DD, Callaway EM (2006) Development of layer-specific axonal arborizations in mouse primary somatosensory cortex. J Comp Neurol 494(3):398–414
67. Bruno RM, Hahn TT, Wallace DJ, de Kock CP, Sakmann B (2009) Sensory experience alters specific branches of individual corticocortical axons during development. J Neurosci 29(10):3172–3181. doi:10.1523/JNEUROSCI.5911-08.2009
68. Furuta T, Kaneko T, Deschênes M (2009) Septal neurons in barrel cortex derive their receptive field input from the lemniscal pathway. J Neurosci 29(13):4089–4095. doi:10.1523/JNEUROSCI.5393-08.2009
69. Koralek KA, Jensen KF, Killackey HP (1988) Evidence for two complementary patterns of thalamic input to the rat somatosensory cortex. Brain Res 463(2):346–351
70. Wimmer VC, Bruno RM, de Kock CP, Kuner T, Sakmann B (2010) Dimensions of a projection column and architecture of VPM and POm axons in rat vibrissal cortex. Cereb Cortex 20(10):2265–2276. doi:bhq068 [pii] 10.1093/cercor/bhq068
71. Hoogland PV, Wouterlood FG, Welker E, van der Loos H (1991) Ultrastructure of giant and small thalamic terminals of cortical origin: a study of the projections from the barrel cortex in mice using Phaseolus vulgaris leuco-agglutinin (PHA-L). Exp Brain Res 87(1):159–172
72. Hoogland PV, Welker E, van der Loos H (1987) Organization of the projections from barrel cortex to thalamus in mice studied with Phaseolus vulgaris-leucoagglutinin and HRP. Exp Brain Res 68(1):73–87
73. Groh A, de Kock CP, Wimmer VC, Sakmann B, Kuner T (2008) Driver or coincidence detector: modal switch of a corticothalamic giant synapse controlled by spontaneous activity and short-term depression. J Neurosci 28(39):9652–9663. doi:10.1523/JNEUROSCI.1554-08.2008
74. Egger V, Feldmeyer D, Sakmann B (1999) Coincidence detection and changes of synaptic efficacy in spiny stellate neurons in rat barrel cortex. Nat Neurosci 2(12):1098–1105. doi:10.1038/16026
75. Holmgren C, Harkany T, Svennenfors B, Zilberter Y (2003) Pyramidal cell communication within local networks in layer 2/3 of rat neocortex. J Physiol 551(Pt 1):139–153
76. Reyes A, Sakmann B (1999) Developmental switch in the short-term modification of unitary EPSPs evoked in layer 2/3 and layer 5 pyramidal neurons of rat neocortex. J Neurosci 19(10):3827–3835
77. Hardingham NR, Read JC, Trevelyan AJ, Nelson JC, Jack JJ, Bannister NJ (2010) Quantal analysis reveals a functional correlation between presynaptic and postsynaptic efficacy in excitatory connections from rat neocortex. J Neurosci 30(4):1441–1451. doi:10.1523/JNEUROSCI.3244-09.2010
78. Avermann M, Tomm C, Mateo C, Gerstner W, Petersen CC (2012) Microcircuits of excitatory and inhibitory neurons in layer 2/3 of mouse barrel cortex. J Neurophysiol 107(11):3116–3134. doi:10.1152/jn.00917.2011
79. Adesnik H, Scanziani M (2010) Lateral competition for cortical space by layer-specific horizontal circuits. Nature 464(7292):1155–1160. doi:10.1038/nature08935
80. Cheetham CE, Hammond MS, Edwards CE, Finnerty GT (2007) Sensory experience alters cortical connectivity and synaptic function site specifically. J Neurosci 27(13):3456–3465. doi:10.1523/JNEUROSCI.5143-06.2007
81. Sarid L, Feldmeyer D, Gidon A, Sakmann B, Segev I (2013) Contribution of intracolumnar layer 2/3-to-layer 2/3 excitatory connections in shaping the response to whisker deflection in rat barrel cortex. Cereb Cortex. doi:10.1093/cercor/bht268
82. Kampa BM, Letzkus JJ, Stuart GJ (2006) Cortical feed-forward networks for binding different streams of sensory information. Nat Neurosci 9(12):1472–1473. doi:10.1038/nn1798
83. White EL, Czeiger D (1991) Synapses made by axons of callosal projection neurons in mouse somatosensory cortex: emphasis on intrinsic connections. J Comp Neurol 303(2):233–244. doi:10.1002/cne.903030206

84. Petreanu L, Huber D, Sobczyk A, Svoboda K (2007) Channelrhodopsin-2-assisted circuit mapping of long-range callosal projections. Nat Neurosci 10(5):663–668
85. Manns ID, Sakmann B, Brecht M (2004) Sub- and suprathreshold receptive field properties of pyramidal neurones in layers 5A and 5B of rat somatosensory barrel cortex. J Physiol 556(Pt 2):601–622. doi:10.1113/jphysiol.2003.053132
86. de Kock CP, Sakmann B (2008) High frequency action potential bursts (> or = 100 Hz) in L2/3 and L5B thick tufted neurons in anaesthetized and awake rat primary somatosensory cortex. J Physiol 586(14):3353–3364. doi:10.1113/jphysiol.2008.155580
87. Larsen DD, Wickersham IR, Callaway EM (2007) Retrograde tracing with recombinant rabies virus reveals correlations between projection targets and dendritic architecture in layer 5 of mouse barrel cortex. Front Neural Circuits 1:5. doi:10.3389/neuro.04.005.2007
88. Bé JV L, Silberberg G, Wang Y, Markram H (2007) Morphological, electrophysiological, and synaptic properties of corticocallosal pyramidal cells in the neonatal rat neocortex. Cereb Cortex 17(9):2204–2213. doi:10.1093/cercor/bhl127
89. Games KD, Winer JA (1988) Layer V in rat auditory cortex: projections to the inferior colliculus and contralateral cortex. Hear Res 34(1):1–25
90. Hübener M, Bolz J (1988) Morphology of identified projection neurons in layer 5 of rat visual cortex. Neurosci Lett 94(1–2):76–81
91. Hübener M, Schwarz C, Bolz J (1990) Morphological types of projection neurons in layer 5 of cat visual cortex. J Comp Neurol 301(4):655–674. doi:10.1002/cne.903010412
92. Koester SE, O'Leary DD (1992) Functional classes of cortical projection neurons develop dendritic distinctions by class-specific sculpting of an early common pattern. J Neurosci 12(4):1382–1393
93. Oberlaender M, Boudewijns ZS, Kleele T, Mansvelder HD, Sakmann B, de Kock CP (2011) Three-dimensional axon morphologies of individual layer 5 neurons indicate cell type-specific intracortical pathways for whisker motion and touch. Proc Natl Acad Sci USA 108(10):4188–4193. doi:10.1073/pnas.1100647108
94. Mao T, Kusefoglu D, Hooks BM, Huber D, Petreanu L, Svoboda K (2011) Long-range neuronal circuits underlying the interaction between sensory and motor cortex. Neuron 72(1):111–123. doi:10.1016/j.neuron.2011.07.029
95. Veinante P, Lavallée P, Deschênes M (2000) Corticothalamic projections from layer 5 of the vibrissal barrel cortex in the rat. J Comp Neurol 424(2):197–204
96. Kozloski J, Hamzei-Sichani F, Yuste R (2001) Stereotyped position of local synaptic targets in neocortex. Science 293(5531):868–872
97. Brown SP, Hestrin S (2009) Intracortical circuits of pyramidal neurons reflect their long-range axonal targets. Nature 457(7233):1133–1136. doi:10.1038/nature07658
98. Hattox AM, Nelson SB (2007) Layer V neurons in mouse cortex projecting to different targets have distinct physiological properties. J Neurophysiol 98(6):3330–3340. doi:10.1152/jn.00397.2007
99. Frick A, Feldmeyer D, Helmstaedter M, Sakmann B (2008) Monosynaptic connections between pairs of L5A pyramidal neurons in columns of juvenile rat somatosensory cortex. Cereb Cortex 18(2):397–406
100. Markram H, Lübke J, Frotscher M, Roth A, Sakmann B (1997) Physiology and anatomy of synaptic connections between thick tufted pyramidal neurones in the developing rat neocortex. J Physiol 500(Pt 2):409–440
101. Krieger P, Kuner T, Sakmann B (2007) Synaptic connections between layer 5B pyramidal neurons in mouse somatosensory Cortex are independent of apical dendrite bundling. J Neurosci 27(43):11473–11482. doi:10.1523/jneurosci.1182-07.2007
102. Perin R, Berger TK, Markram H (2011) A synaptic organizing principle for cortical neuronal groups. Proc Natl Acad Sci U S A 108(13):5419–5424. doi:10.1073/pnas.1016051108
103. Loebel A, Silberberg G, Helbig D, Markram H, Tsodyks M, Richardson MJ (2009) Multiquantal release underlies the distribution of synaptic efficacies in the neocortex. Front Comput Neurosci 3:27. doi:10.3389/neuro.10.027.2009

104. Song S, Sjöström PJ, Reigl M, Nelson S, Chklovskii DB (2005) Highly nonrandom features of synaptic connectivity in local cortical circuits. PLoS Biol 3(3):e68. doi:04-PLBI-RA-0489R2 [pii]10.1371/journal.pbio.0030068
105. Morishima M, Kawaguchi Y (2006) Recurrent connection patterns of corticostriatal pyramidal cells in frontal cortex. J Neurosci 26(16):4394–4405. doi:26/16/4394 [pii] 10.1523/JNEUROSCI.0252-06.2006
106. Anderson CT, Sheets PL, Kiritani T, Shepherd GM (2010) Sublayer-specific microcircuits of corticospinal and corticostriatal neurons in motor cortex. Nat Neurosci 13(6):739–744. doi:10.1038/nn.2538
107. Morishima M, Morita K, Kubota Y, Kawaguchi Y (2011) Highly differentiated projection-specific cortical subnetworks. J Neurosci 31(28):10380–10391. doi:10.1523/JNEUROSCI.0772-11.2011
108. Otsuka T, Kawaguchi Y (2011) Cell diversity and connection specificity between callosal projection neurons in the frontal cortex. J Neurosci 31(10):3862–3870. doi:10.1523/JNEUROSCI.5795-10.2011
109. Peters A, Feldman ML (1976) The projection of the lateral geniculate nucleus to area 17 of the rat cerebral cortex. I. General description. J Neurocytol 5(1):63–84
110. Braitenberg V, Schüz A (1991) Anatomy of the Cortex. Statistics and Geometry (Studies of Brain Function), vol 18. Anatomy of the Cortex. Springer, Heidelberg
111. Peters A, Payne BR (1993) Numerical relationships between geniculocortical afferents and pyramidal cell modules in cat primary visual cortex. Cereb Cortex 3(1):69–78
112. Binzegger T, Douglas RJ, Martin KA (2004) A quantitative map of the circuit of cat primary visual cortex. J Neurosci 24(39):8441–8453
113. Lübke J, Markram H, Frotscher M, Sakmann B (1996) Frequency and dendritic distribution of autapses established by layer 5 pyramidal neurons in the developing rat neocortex: comparison with synaptic innervation of adjacent neurons of the same class. J Neurosci 16(10):3209–3218
114. Curtis JC, Kleinfeld D (2009) Phase-to-rate transformations encode touch in cortical neurons of a scanning sensorimotor system. Nat Neurosci 12(4):492–501. doi:10.1038/nn.2283
115. de Kock CP, Sakmann B (2009) Spiking in primary somatosensory cortex during natural whisking in awake head-restrained rats is cell-type specific. Proc Natl Acad Sci USA 106(38):16446–16450. doi:10.1073/pnas.0904143106
116. de Kock CP, Bruno RM, Spors H, Sakmann B (2007) Layer- and cell-type-specific suprathreshold stimulus representation in rat primary somatosensory cortex. J Physiol 581(Pt 1):139–154
117. Yu C, Derdikman D, Haidarliu S, Ahissar E (2006) Parallel thalamic pathways for whisking and touch signals in the rat. PLoS Biol 4(5):e124. doi:05-PLBI-RA-0916R3 [pii] 10.1371/journal.pbio.0040124
118. Meyer HS, Wimmer VC, Oberlaender M, de Kock CP, Sakmann B, Helmstaedter M (2010b) Number and laminar distribution of neurons in a thalamocortical projection column of rat vibrissal cortex. Cereb Cortex 20(10):2277–2286. doi:10.1093/cercor/bhq067
119. Bourassa J, Pinault D, Deschênes M (1995) Corticothalamic projections from the cortical barrel field to the somatosensory thalamus in rats: a single-fibre study using biocytin as an anterograde tracer. Eur J Neurosci 7(1):19–30
120. Liao CC, Chen RF, Lai WS, Lin RC, Yen CT (2010) Distribution of large terminal inputs from the primary and secondary somatosensory cortices to the dorsal thalamus in the rodent. J Comp Neurol 518(13):2592–2611. doi:10.1002/cne.22354
121. Groh A, Bokor H, Mease RA, Plattner V, Hangya B, Stroh A, Dêschenes M, Acsády L (2013) Convergence of cortical and sensory driver inputs on single thalamocortical cells. Cereb Cortex. doi:10.1093/cercor/bht173
122. Killackey HP, Sherman SM (2003) Corticothalamic projections from the rat primary somatosensory cortex. J Neurosci 23(19):7381–7384
123. Theyel BB, Llano DA, Sherman SM (2010) The corticothalamocortical circuit drives higher-order cortex in the mouse. Nat Neurosci 13(1):84–88. doi:10.1038/nn.2449

124. Sherman SM, Guillery RW (2011) Distinct functions for direct and transthalamic corticocortical connections. J Neurophysiol 106(3):1068–1077. doi:10.1152/jn.00429.2011
125. Guillery RW, Sherman SM (2011) Branched thalamic afferents: what are the messages that they relay to the cortex? Brain Res Rev 66(1–2):205–219. doi:10.1016/j.brainresrev.2010.08.001
126. Gentet LJ, Avermann M, Matyas F, Staiger JF, Petersen CC (2010) Membrane potential dynamics of GABAergic neurons in the barrel cortex of behaving mice. Neuron 65:422–435. doi:10.1016/j.neuron.2010.01.006
127. Chen CC, Abrams S, Pinhas A, Brumberg JC (2009) Morphological heterogeneity of layer VI neurons in mouse barrel cortex. J Comp Neurol 512(6):726–746. doi:10.1002/cne.21926
128. Kumar P, Ohana O (2008) Inter- and intralaminar subcircuits of excitatory and inhibitory neurons in layer 6a of the rat barrel cortex. J Neurophysiol 100(4):1909–1922. doi:10.1152/jn.90684.2008
129. Mease RA, Krieger P, Groh A (2014) Cortical control of adaptation and sensory relay mode in the thalamus. Proc Natl Acad Sci USA. doi:10.1073/pnas.1318665111
130. Thomson AM (2010) Neocortical layer 6, a review. Front Neuroanat 4:13. doi:10.3389/fnana.2010.00013
131. Beierlein M, Connors BW (2002) Short-term dynamics of thalamocortical and intracortical synapses onto layer 6 neurons in neocortex. J Neurophysiol 88(4):1924–1932
132. Cruikshank SJ, Urabe H, Nurmikko AV, Connors BW (2010) Pathway-specific feedforward circuits between thalamus and neocortex revealed by selective optical stimulation of axons. Neuron 65(2):230–245. doi:10.1016/j.neuron.2009.12.025
133. Peters A, Jones EG (1984) Cellular components of the cerebral cortex, vol 1. Cerebral Cortex Plenum Press, New York
134. Deschênes M, Veinante P, Zhang ZW (1998) The organization of corticothalamic projections: reciprocity versus parity. Brain Res Brain Res Rev 28(3):286–308
135. Sherman SM (2005) Thalamic relays and cortical functioning. Prog Brain Research 149:107–126. doi:S0079-6123(05)49009-3 [pii] 10.1016/S0079-6123(05)49009-3
136. Jones EG (2009) Synchrony in the interconnected circuitry of the thalamus and cerebral cortex. Ann NY Acad Sci 1157(1):10–23. doi:10.1111/j.1749-6632.2009.04534.x
137. Mercer A, West DC, Morris OT, Kirchhecker S, Kerkhoff JE, Thomson AM (2005) Excitatory connections made by presynaptic cortico-cortical pyramidal cells in layer 6 of the neocortex. Cereb Cortex 15(10):1485–1496
138. Marín-Padilla M (1978) Dual origin of the mammalian neocortex and evolution of the cortical plate. Anat Embryol (Berl) 152(2):109–126
139. Marx M, Feldmeyer D (2013) Morphology and physiology of excitatory neurons in layer 6b of the somatosensory rat barrel cortex. Cereb Cortex 23(12):2803–2817. doi:10.1093/cercor/bhs254
140. Tömböl T, Hajdu F, Somogyi G (1975) Identification of the Golgi picture of the layer VI cortic-geniculate projection neurons. Exp Brain Res 24(1):107–110
141. Tömböl T (1984) Layer VI cells. In: Peters A, Jones EG (eds) Cerebral Cortex, vol 1. Plenum Press, New York, pp 479–519
142. Clancy B, Cauller LJ (1999) Widespread projections from subgriseal neurons (layer VII) to layer I in adult rat cortex. J Comp Neurol 407(2):275–286. doi:10.1002/(SICI)1096-9861(19990503)407:2<275::AID-CNE8>3.0.CO;2-0 [pii]
143. Gupta A, Wang Y, Markram H (2000) Organizing principles for a diversity of GABAergic interneurons and synapses in the neocortex. Science 287(5451):273–278
144. Ascoli GA, Alonso-Nanclares L, Anderson SA, Barrionuevo G, Benavides-Piccione R, Burkhalter A, Buzsáki G, Cauli B, DeFelipe J, Fairén A, Feldmeyer D, Fishell G, Fregnac Y, Freund TF, Gardner D, Gardner EP, Goldberg JH, Helmstaedter M, Hestrin S, Karube F, Kisvárday ZF, Lambolez B, Lewis DA, Marín O, Markram H, Muñoz A, Packer A, Petersen CC, Rockland KS, Rossier J, Rudy B, Somogyi P, Staiger JF, Tamás G, Thomson AM, Toledo-Rodríguez M, Wang Y, West DC, Yuste R (2008) Petilla terminology: nomen-

clature of features of GABAergic interneurons of the cerebral cortex. Nat Rev Neurosci 9(7):557–568. doi:10.1038/nrn2402
145. DeFelipe J, López-Cruz PL, Benavides-Piccione R, Bielza C, Larrañaga P, Anderson S, Burkhalter A, Cauli B, Fairén A, Feldmeyer D, Fishell G, Fitzpatrick D, Freund TF, González-Burgos G, Hestrin S, Hill S, Hof PR, Huang J, Jones EG, Kawaguchi Y, Kisvárday Z, Kubota Y, Lewis DA, Marín O, Markram H, McBain CJ, Meyer HS, Monyer H, Nelson SB, Rockland K, Rossier J, Rubenstein JL, Rudy B, Scanziani M, Shepherd GM, Sherwood CC, Staiger JF, Tamás G, Thomson A, Wang Y, Yuste R, Ascoli GA (2013) New insights into the classification and nomenclature of cortical GABAergic interneurons. Nat Rev Neurosci 14(3):202–216. doi:10.1038/nrn3444
146. Rudy B, Fishell G, Lee S, Hjerling-Leffler J (2011) Three groups of interneurons account for nearly 100 % of neocortical GABAergic neurons. Dev Neurobiol 71(1):45–61. doi:10.1002/dneu.20853
147. Kepecs A, Fishell G (2014) Interneuron cell types are fit to function. Nature 505(7483):318–326. doi:10.1038/nature12983
148. Taniguchi H (2014) Genetic dissection of GABAergic neural circuits in mouse neocortex. Front Cell Neurosci 8:8. doi:10.3389/fncel.2014.00008
149. Markram H, Toledo-Rodriguez M, Wang Y, Gupta A, Silberberg G, Wu C (2004) Interneurons of the neocortical inhibitory system. Nat Rev Neurosci 5(10):793–807
150. Kawaguchi Y, Kondo S (2002) Parvalbumin, somatostatin and cholecystokinin as chemical markers for specific GABAergic interneuron types in the rat frontal cortex. J Neurocytol 31(3–5):277–287
151. Gelman DM, Marín O (2010) Generation of interneuron diversity in the mouse cerebral cortex. Eur J Neurosci 31(12):2136–2141. doi:10.1111/j.1460-9568.2010.07267.x
152. Ma Y, Hu H, Berrebi AS, Mathers PH, Agmon A (2006) Distinct subtypes of somatostatin-containing neocortical interneurons revealed in transgenic mice. J Neurosci 26(19):5069–5082. doi:10.1523/JNEUROSCI.0661-06.2006
153. Lee S, Hjerling-Leffler J, Zagha E, Fishell G, Rudy B (2010) The largest group of superficial neocortical GABAergic interneurons expresses ionotropic serotonin receptors. J Neurosci 30(50):16796–16808. doi:10.1523/JNEUROSCI.1869-10.2010
154. Koelbl C, Helmstaedter M, Lübke J, Feldmeyer D (2013) A barrel-related interneuron in layer 4 of rat somatosensory cortex with a high intrabarrel connectivity. Cereb Cortex. doi:10.1093/cercor/bht263
155. Xu H, Jeong H-Y, Tremblay R, Rudy B (2013) Neocortical somatostatin-expressing GABAergic interneurons disinhibit thethalamorecipient layer 4. Neuron 77(1):155–167. doi:http://dx.doi.org/10.1016/j.neuron.2012.11.004
156. Li P, Huntsman MM (2014) Two functional inhibitory circuits are comprised of a heterogeneous population of fast-spiking cortical interneurons. Neuroscience 265C:60–71. doi:10.1016/j.neuroscience.2014.01.033
157. Porter JT, Johnson CK, Agmon A (2001) Diverse types of interneurons generate thalamus-evoked feedforward inhibition in the mouse barrel cortex. J Neurosci 21(8):2699–2710
158. Cruikshank SJ, Lewis TJ, Connors BW (2007) Synaptic basis for intense thalamocortical activation of feedforward inhibitory cells in neocortex. Nat Neurosci 10(4):462–468. doi:10.1038/nn1861
159. Cruikshank SJ, Ahmed OJ, Stevens TR, Patrick SL, Gonzalez AN, Elmaleh M, Connors BW (2012) Thalamic control of layer 1 circuits in prefrontal cortex. J Neurosci 32(49):17813–17823. doi:10.1523/JNEUROSCI.3231–12.2012
160. Staiger JF, Zuschratter W, Luhmann HJ, Schubert D (2009) Local circuits targeting parvalbumin-containing interneurons in layer IV of rat barrel cortex. Brain Struct Funct 214(1):1–13. doi:10.1007/s00429-009-0225-5
161. Hu H, Ma Y, Agmon A (2011) Submillisecond firing synchrony between different subtypes of cortical interneurons connected chemically but not electrically. J Neurosci 31(9):3351–3361. doi:10.1523/JNEUROSCI.4881-10.2011

162. Xu X, Roby KD, Callaway EM (2010) Immunochemical characterization of inhibitory mouse cortical neurons: three chemically distinct classes of inhibitory cells. J Comp Neurol 518(3):389–404. doi:10.1002/cne.22229
163. Gibson JR, Beierlein M, Connors BW (1999) Two networks of electrically coupled inhibitory neurons in neocortex. Nature 402(6757):75–79
164. Fanselow EE, Richardson KA, Connors BW (2008) Selective, state-dependent activation of somatostatin-expressing inhibitory interneurons in mouse neocortex. J Neurophysiol 100(5):2640–2652. doi:10.1152/jn.90691.2008
165. Beierlein M, Gibson JR, Connors BW (2003) Two dynamically distinct inhibitory networks in layer 4 of the neocortex. J Neurophysiol 90(5):2987–3000
166. Oliva AA Jr, Jiang M, Lam T, Smith KL, Swann JW (2000) Novel hippocampal interneuronal subtypes identified using transgenic mice that express green fluorescent protein in GABAergic interneurons. J Neurosci 20(9):3354–3368
167. Ma Y, Hu H, Agmon A (2012) Short-term plasticity of unitary inhibitory-to-inhibitory synapses depends on the presynaptic interneuron subtype. J Neurosci 32(3):983–988. doi:10.1523/JNEUROSCI.5007-11.2012
168. Tan Z, Hu H, Huang ZJ, Agmon A (2008) Robust but delayed thalamocortical activation of dendritic-targeting inhibitory interneurons. Proc Natl Acad Sci U S A 105(6):2187–2192. doi:0710628105 [pii]10.1073/pnas.0710628105
169. Chittajallu R, Pelkey KA, McBain CJ (2013) Neurogliaform cells dynamically regulate somatosensory integration via synapse-specific modulation. Nat Neurosci 16(1):13–15. doi:10.1038/nn.3284
170. Helmstaedter M, Staiger JF, Sakmann B, Feldmeyer D (2008) Efficient recruitment of layer 2/3 interneurons by layer 4 input in single columns of rat somatosensory cortex. J Neurosci 28(33):8273–8284. doi:10.1523/JNEUROSCI.5701-07.2008
171. Helmstaedter M, Sakmann B, Feldmeyer D (2009a) Neuronal correlates of local, lateral, and translaminar inhibition with reference to cortical columns. Cereb Cortex 19(4):926–937. doi:10.1093/cercor/bhn141
172. Helmstaedter M, Sakmann B, Feldmeyer D (2009b) The relation between dendritic geometry, electrical excitability, and axonal projections of L2/3 interneurons in rat barrel cortex. Cereb Cortex 19(4):938–950. doi:10.1093/cercor/bhn138
173. Helmstaedter M, Sakmann B, Feldmeyer D (2009c) L2/3 interneuron groups defined by multiparameter analysis of axonal projection, dendritic geometry, and electrical excitability. Cereb Cortex 19(4):951–962. doi:10.1093/cercor/bhn130
174. Fairén A, Valverde F (1980) A specialized type of neuron in the visual cortex of cat: a Golgi and electron microscope study of chandelier cells. J Comp Neurol 194(4):761–779. doi:10.1002/cne.901940405
175. Somogyi P, Freund TF, Cowey A (1982) The axo-axonic interneuron in the cerebral cortex of the rat, cat and monkey. Neuroscience 7(11):2577–2607
176. Reyes A, Lujan R, Rozov A, Burnashev N, Somogyi P, Sakmann B (1998) Target-cell-specific facilitation and depression in neocortical circuits. Nat Neurosci 1(4):279–285
177. Galarreta M, Hestrin S (1999) A network of fast-spiking cells in the neocortex connected by electrical synapses. Nature 402(6757):72–75
178. Beierlein M, Gibson JR, Connors BW (2000) A network of electrically coupled interneurons drives synchronized inhibition in neocortex. Nat Neurosci 3(9):904–910
179. Amitai Y, Gibson JR, Beierlein M, Patrick SL, Ho AM, Connors BW, Golomb D (2002) The spatial dimensions of electrically coupled networks of interneurons in the neocortex. J Neurosci 22(10):4142–4152. doi:20026371
180. Galarreta M, Hestrin S (2002) Electrical and chemical synapses among parvalbumin fast-spiking GABAergic interneurons in adult mouse neocortex. Proc Natl Acad Sci USA 99(19):12438–12443
181. Bittman K, Becker DL, Cicirata F, Parnavelas JG (2002) Connexin expression in homotypic and heterotypic cell coupling in the developing cerebral cortex. J Comp Neurol 443(3):201–212

182. Meyer AH, Katona I, Blatow M, Rozov A, Monyer H (2002) In vivo labeling of parvalbumin-positive interneurons and analysis of electrical coupling in identified neurons. J Neurosci 22(16):7055–7064
183. Blatow M, Rozov A, Katona I, Hormuzdi SG, Meyer AH, Whittington MA, Caputi A, Monyer H (2003) A novel network of multipolar bursting interneurons generates theta frequency oscillations in neocortex. Neuron 38(5):805–817
184. Gentet LJ (2012) Functional diversity of supragranular GABAergic neurons in the barrel cortex. Front Neural Circuits 6:52. doi:10.3389/fncir.2012.00052
185. Kapfer C, Glickfeld LL, Atallah BV, Scanziani M (2007) Supralinear increase of recurrent inhibition during sparse activity in the somatosensory cortex. Nat Neurosci 10(6):743–753. doi: 10.1038/nn1909
186. Jiang X, Wang G, Lee AJ, Stornetta RL, Zhu JJ (2013) The organization of two new cortical interneuronal circuits. Nat Neurosci 16(2):210–218. doi:10.1038/nn.3305
187. Lee AJ, Wang G, Jiang X, Johnson SM, Hoang ET, Lante F, Stornetta RL, Beenhakker MP, Shen Y, Julius Zhu J (2014) Canonical Organization of Layer 1 Neuron-Led Cortical Inhibitory and Disinhibitory Interneuronal Circuits. Cereb Cortex. doi:10.1093/cercor/bhu020
188. Szabadics J, Varga C, Molnár G, Oláh S, Barzó P, Tamás G (2006) Excitatory effect of GABAergic axo-axonic cells in cortical microcircuits. Science 311(5758):233–235. doi:10.1126/science.1121325
189. Lee S, Kruglikov I, Huang ZJ, Fishell G, Rudy B (2013) A disinhibitory circuit mediates motor integration in the somatosensory cortex. Nat Neurosci. doi:10.1038/nn.3544
190. Spruston N (2008) Pyramidal neurons: dendritic structure and synaptic integration. Nat Rev Neurosci 9(3):206–221. doi:10.1038/nrn2286
191. Major G, Larkum ME, Schiller J (2013) Active properties of neocortical pyramidal neuron dendrites. Annu Rev Neurosci 36:1–24. doi:10.1146/annurev-neuro-062111-150343
192. Larkum ME, Zhu JJ, Sakmann B (1999) A new cellular mechanism for coupling inputs arriving at different cortical layers. Nature 398(6725):338–341
193. Larkum ME, Zhu JJ (2002) Signaling of layer 1 and whisker-evoked Ca^{2+} and Na^{+} action potentials in distal and terminal dendrites of rat neocortical pyramidal neurons in vitro and in vivo. J Neurosci 22(16):6991–7005
194. Larkum M (2013) A cellular mechanism for cortical associations: an organizing principle for the cerebral cortex. Trends Neurosci 36(3):141–151. doi:10.1016/j.tins.2012.11.006
195. Cauller L (1995) Layer I of primary sensory neocortex: where top-down converges upon bottom-up. Behav Brain Res 71(1–2):163–170
196. Mitchell BD, Cauller LJ (2001) Corticocortical and thalamocortical projections to layer I of the frontal neocortex in rats. Brain Res 921(1–2):68–77. doi:S0006-8993(01)03084-0 [pii]
197. Rubio-Garrido P, Pérez-de-Manzo F, Porrero C, Galazo MJ, Clascá F (2009) Thalamic input to distal apical dendrites in neocortical layer 1 is massive and highly convergent. Cereb Cortex 19(10):2380–2395. doi:10.1093/cercor/bhn259
198. Xu NL, Harnett MT, Williams SR, Huber D, O'Connor DH, Svoboda K, Magee JC (2012) Nonlinear dendritic integration of sensory and motor input during an active sensing task. Nature 492(7428):247–251. doi:10.1038/nature11601
199. Caputi A, Rozov A, Blatow M, Monyer H (2009) Two calretinin-positive GABAergic cell types in layer 2/3 of the mouse neocortex provide different forms of inhibition. Cereb Cortex 19(6):1345–1359. doi:10.1093/cercor/bhn175
200. Wang Y, Gupta A, Toledo-Rodriguez M, Wu CZ, Markram H (2002) Anatomical, physiological, molecular and circuit properties of nest basket cells in the developing somatosensory cortex. Cereb Cortex 12(4):395–410
201. Zhou FM, Hablitz JJ (1996) Layer I neurons of the rat neocortex. II. Voltage-dependent outward currents. J Neurophysiol 76(2):668–682
202. Chu Z, Galarreta M, Hestrin S (2003) Synaptic interactions of late-spiking neocortical neurons in layer 1. J Neurosci 23(1):96–102
203. Wozny C, Williams SR (2011) Specificity of synaptic connectivity between layer 1 inhibitory interneurons and layer 2/3 pyramidal neurons in the rat neocortex. Cereb Cortex 21(8):1818–1826. doi:10.1093/cercor/bhq257

204. Muralidhar S, Wang Y, Markram H (2013) Synaptic and cellular organization of layer 1 of the developing rat somatosensory cortex. Front Neuroanat 7:52. doi:10.3389/fnana.2013.00052
205. Tamás G, Lőrincz A, Simon A, Szabadics J (2003) Identified sources and targets of slow inhibition in the neocortex. Science 299(5614):1902–1905. doi:10.1126/science.1082053 299/5614/1902 [pii]
206. Silberberg G, Markram H (2007) Disynaptic inhibition between neocortical pyramidal cells mediated by Martinotti cells. Neuron 53(5):735–746
207. Berger TK, Silberberg G, Perin R, Markram H (2010) Brief bursts self-inhibit and correlate the pyramidal network. PLoS Biol 8(9). doi:10.1371/journal.pbio.1000473
208. Berger TK, Perin R, Silberberg G, Markram H (2009) Frequency-dependent disynaptic inhibition in the pyramidal network: a ubiquitous pathway in the developing rat neocortex. J Physiol 587(Pt 22):5411–5425. doi: 10.1113/jphysiol.2009.176552
209. Perrenoud Q, Rossier J, Geoffroy H, Vitalis T, Gallopin T (2013) Diversity of GABAergic interneurons in layer VIa and VIb of mouse barrel cortex. Cereb Cortex 23(2):423–441. doi:10.1093/cercor/bhs032
210. West DC, Mercer A, Kirchhecker S, Morris OT, Thomson AM (2006) Layer 6 cortico-thalamic pyramidal cells preferentially innervate interneurons and generate facilitating EPSPs. Cereb Cortex 16(2):200–211. doi:bhi098 [pii] 10.1093/cercor/bhi098
211. Bortone DS, Olsen SR, Scanziani M (2014) Translaminar inhibitory cells recruited by layer 6 corticothalamic neurons suppress visual cortex. Neuron. doi:10.1016/j.neuron.2014.02.021
212. Fino E, Yuste R (2011) Dense inhibitory connectivity in neocortex. Neuron 69(6):1188–1203. doi:10.1016/j.neuron.2011.02.025
213. Packer AM, Yuste R (2011) Dense, unspecific connectivity of neocortical parvalbumin-positive interneurons: a canonical microcircuit for inhibition? J Neurosci 31(37):13260–13271. doi:10.1523/JNEUROSCI.3131-11.2011
214. Packer AM, McConnell DJ, Fino E, Yuste R (2013) Axo-dendritic overlap and laminar projection can explain interneuron connectivity to pyramidal cells. Cereb Cortex 23(12):2790–2802. doi:10.1093/cercor/bhs210

Chapter 5
Imaging the Cortical Representation of Active Sensing in the Vibrissa System

Fritjof Helmchen and Jerry L. Chen

Abstract Rodents explore the environment with their facial whiskers using active whisking to collect information about object location and identity. The sensory information gathered is processed in the vibrissa system, a hierarchical network of interacting brain regions, comprising brainstem nuclei, thalamus subdivisions and neocortical regions. In the neocortex, neural representations of whisking and touch are formed to guide and adapt behavior given the environmental context. The exact features of these representations and their spatiotemporal dynamics still remain elusive. In this chapter, we provide an overview of in vivo functional imaging techniques that enable the study of spatiotemporal profiles of cortical activity during whisking-based behavior. We discuss imaging applications covering the large scale as well as the level of local cellular circuits, with a special focus on studies employing two-photon calcium imaging. We summarize recent findings on the cortical representation of passive and active sensation and of task-relevant whisker dynamics.

Keywords Barrel cortex · Active whisking · Neocortical regions · Voltage imaging · Two-photon calcium imaging · Object localization · Texture discrimination

Introduction

For multiple reasons the rodent whisker system is a well suited model for studying tactile information processing in the mammalian brain. Touching objects or conspecifics with facial whiskers is a highly behaviorally relevant sensing modality for rats and mice [1]. Rodents intentionally move their whiskers in characteristic ways to touch and gather tactile information, an example *par excellence* of active sensing [2]. The processing of tactile stimuli is organized in neural pathways at all

F. Helmchen (✉) · J. L. Chen
Laboratory of Neural Circuit Dynamics, Brain Research Institute, University of Zurich, Winterthurerstrasse 190, 8057 Zurich, Switzerland
e-mail: helmchen@hifo.uzh.ch

J. L. Chen
e-mail: jerry.chen@hifo.uzh.ch

P. Krieger, A. Groh (eds.), *Sensorimotor Integration in the Whisker System,*
DOI 10.1007/978-1-4939-2975-7_5

key levels of mammalian somatosensory computation, including brainstem loops, relay pathways through thalamic nuclei, thalamocortical loops, and especially cortical representations that feed into descending pathways for behavior control [3, 4]. Further, the importance of tactile sensation is reflected in the disproportionally large representation of the whisker pad in the barrel field (BF) of the primary somatosensory area (S1), with a well-defined somatotopic layout. This clear anatomy has invited numerous studies of cortical signal flow, the underlying synaptic interactions, and neural circuit mechanisms related to whisker motion and touch, within S1 and beyond. Another advantageous feature of the whisker system is the ease with which whiskers can be mechanically stimulated in a controlled manner (or, alternatively, trimmed or plucked to deprive the brain from this sensory input). Such manipulations have been widely adopted to investigate mechanisms of neural plasticity [5–7]. Finally, rats and mice can be well trained in whisker-dependent tasks, enabling studies of the neural basis of learning, decision making and other high-level brain functions.

In this chapter we focus on the neocortical level of the whisker system. The S1 barrel field connects to multiple other cortical areas via cortico-cortical axonal projections. For example, a strong connecting pathway exists to the contralateral S1 via the corpus callosum. In addition, S1 connects ipsilaterally to the smaller, more laterally positioned secondary somatosensory area (S2) and to the more anterior, medial primary motor cortex region (M1) (Fig. 5.1a). The S1-S2-M1 triangle forms the core of cortical sensorimotor integration, tied together by reciprocal connections but also connecting to further cortical areas [8–11]. Because of the widespread connectivity pattern among cortical regions, it can be expected that signal processing does not occur in isolation in individual areas but rather is likely to be governed by the interplay of all these areas. For the topic of this chapter, we note that the key cortical areas are located on the dorsal surface of the mouse brain and thus are accessible for imaging, either by implanting chronic glass windows or by thinning the overlaying skull. S1 and M1 thus presumably have come into the focus of imaging research not only because of their conceptual importance as primary cortical areas but also for this ease of access.

On the local-circuit level, six-layered barrel cortex has been dissected in considerable detail, yet our understanding of this microcircuit is still incomplete. Similar to other primary sensory areas of the neocortex, the major neuronal cell types in the BF have been characterized in terms of their morphologies and anatomical distributions, their intrinsic biophysical properties, and their synaptic connections with neighboring cells or cells in other layers [12–15]. Electrophysiological recordings have been particularly informative in this respect, including extensive studies in brain slice preparations [5, 16] and more recently intracellular recordings in vivo, in anesthetized animals and in head-restrained awake, behaving animals [17–20]. A special focus has been the investigation of the functional relevance of specific subtypes of GABAergic interneurons [21], including prominently the parvalbumin(PV)-positive interneurons [22], the somatostatin(SOM)-positive interneurons [23, 24] and the interneurons positive for the vasoactive intestinal polypeptide (VIP). The latter group is a subgroup of the larger, recently identified group of interneurons

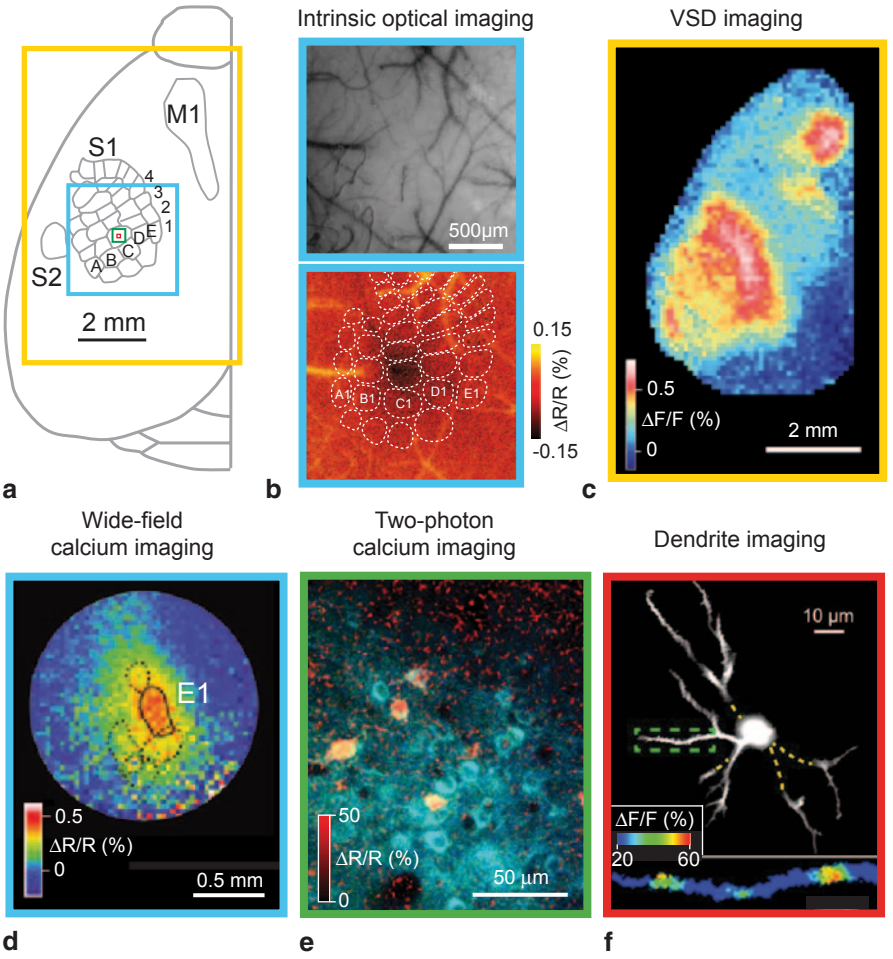

Fig. 5.1 Various imaging modalities to study barrel cortex function. **a** Overview of the different spatial scales covered by various imaging techniques, including hemisphere-wide field of views (*yellow*), barrel cortex imaging (*blue*), cellular imaging within a barrel column (*green*) and single-cell imaging (*red*). **b** Intrinsic optical imaging is performed by illuminating the cortical surface (*top*) with light (typically using 630-nm wavelength) and mapping the relative percentage changes in reflectance (ΔR/R; *bottom*) upon whisker stimulation. Adapted from Petersen, 2007 [16]. **c** Wide-field VSD imaging. The example image was recorded in a urethane-anesthetized mouse with the voltage-sensitive dye RH1691 and shows the activity pattern 30 ms after a single-whisker stimulation, displaying the spread in S1 and a secondary activation spot in motor cortex (average of 10 trials; adapted from Ferezou et al. 2007 [36]). **d** Functional imaging across the barrel field can be performed by using wide-field calcium imaging with a camera. This example shows the onset activation map after stimulation of the E1 whisker, measured through a chronic cranial window with the ratiometric GECI YC3.60 following viral induction of indicator expression. ΔR/R indicates the changes in fluorescence ratio (mean of 20 trials). Adapted from Minderer et al. 2012 [58] with permission from John Wiley and Sons. **e** Two-photon calcium imaging of L2/3 neuronal activity in barrel cortex in an awake mouse performing a texture discrimination task. The image was acquired with the ratiometric indicator YCNano-140 and shows strong activation of a subset

expressing the ionotropic serotonin receptor 5HT3aR [25]. VIP-positive interneurons have been functionally implicated in cortical disinhibition [26, 27].

While electrophysiological studies provided a wealth of functional data on neuronal activity in barrel cortex, and continue to do so, here we focus on the application of imaging techniques to study cortical dynamics in the whisker system. Imaging methods are complementary to electrophysiological methods in many ways and often these two activity measures can be combined in beneficial ways. Important advantages of imaging methods are that they enable (1) a large-scale view of cortical signal flow; (2) population recordings from identified neurons in relatively large networks of up to hundreds of neurons; and (3) functional measurements from subcellular structures such as axons, dendrites, and dendritic spines that are hardly accessible with electrophysiology. This chapter provides an overview of in vivo imaging approaches and highlights results that were obtained over the past decade for cortical dynamics in adult animals. We put special emphasis on imaging studies in awake, behaving animals, which have become feasible only recently.

Imaging Global and Local Cortical Representations of Whisker Dynamics

A variety of optical imaging methods can be applied to measure in vivo cortical activity evoked by active whisker movements or mechanical whisker stimulation. These methods cover distinct spatial scales, ranging from very local measurements at individual synaptic contacts to a global view of activity patterns across an entire hemisphere (Fig. 5.1a). They also differ with respect to their capability to resolve individual neurons and their temporal resolution for measuring subthreshold and/or suprathreshold activity. In the following we summarize the principles of the imaging techniques that are used to study the rodent vibrissa system.

Wide-Field Imaging of Intrinsic Signals

Large-scale imaging with sensitive CCD cameras has a long tradition in barrel cortex research, starting with optical imaging of intrinsic signals [28, 29]. The exposed cortical surface is illuminated with light (typically red light at around 630-nm wavelength) and the reflected light is imaged with a large field-of-view objective and a sensitive camera, capturing areas of several square millimeters. The degree of reflectance depends on the absorptive and scattering properties of the tissue, which change upon neuronal activation in part due to associated blood flow changes. Stimulation of a single whisker results in a localized, albeit blurry reflectance change, making it possible to determine where the barrel column is located that receives the

of neurons upon touching a presented texture with the whiskers. (Adapted From Chen et al. 2013b [80] with permission). **f** Calcium imaging of dendritic activity following single-neuron loading with Alexa Fluor 594 and the calcium indicator Oregon Green BAPTA-1. The Alexa-filled neuron with its dendrites is shown at the top. Localized ΔF/F changes in a selected dendrite following whisker stimulation are shown at the bottom. (Adapted from Varga et al. 2011 [84])

principal input from the stimulated whisker (Fig. 5.1b). Intrinsic signal changes are small (< 1 %) and rather slow and therefore cannot resolve cortical dynamics with high temporal resolution. On the other hand, no dye-labeling is required and signal changes can be detected through the intact (thinned) skull. Because of its simplicity, intrinsic signal optical imaging has developed into a standard method for functional mapping of the barrel field in vivo, which is especially useful for targeting a specific barrel column [30]. In addition, imaging of intrinsic signal changes has contributed to studies of map plasticity, revealing expansion or shrinkage of single-whisker maps following sensory deprivation of surround whiskers and exposure to natural habitats, respectively [6, 31, 32]. More recently, map changes have been assessed in various transgenic mouse models of diseases [33, 34].

Wide-Field Fluorescence Imaging of Voltage Indicators

Whereas intrinsic signal imaging does not require previous dye labeling, staining cortical tissue with fluorescent indicators provides further opportunities to measure the spread of cortical activity related to whisker use. A direct visualization of electrical activity in neuronal populations is possible with voltage-sensitive dye (VSD) imaging, which is a classical experimental approach to measure cortical maps with high temporal resolution [35]. Various organic dyes have been developed that label cellular membranes and report membrane potential changes. For in vivo imaging, the cortical surface is soaked in a VSD-containing solution so that dye molecules penetrate the tissue and stain neuronal membranes. The measured fluorescence signal corresponds to the bulk average of the local membrane potential changes in the tissue (for cortical measurements originating mainly from supragranular layers) [18]. This method lacks cellular resolution but can reveal fast signal dynamics (up to kHz frequency range) with a sufficiently fast VSD and a high-speed camera.

VSD imaging of barrel cortex in the anesthetized rat revealed that following a single-whisker stimulation an initially highly localized cortical activity (at the location of the principal barrel column) rapidly spreads across the entire barrel field within 50 ms, with particularly high speed along the whisker row representation [18]. In follow-up studies on mouse neocortex, the field-of-view of VSD imaging was expanded to comprise nearly the entire dorsal surface of the neocortex, covering even both hemispheres [36, 37]. This global view uncovered that shortly after the S1 activation in the hemisphere contralateral to the single-whisker stimulus, another focal activation spot appears in the motor cortex, triggering a secondary wave of activity in frontal regions (Fig. 5.1c). In addition, S1 regions in the hemisphere ipsilateral to the stimulus are activated with a delay too. These examples demonstrate the brain-wide dimension of cortical processing, even following a simple brief stimulus, mediated via the dense cortico-cortical connections, here particularly from S1 to M1 [36, 38]. While high temporal resolution and direct read out of membrane potential changes are clear advantages of the VSD imaging technique, it is difficult to perform repeated measurements over long time periods using synthetic organic VSDs, which may also present potential pharmacological side effects [39].

The development and application of voltage-sensitive fluorescent proteins (VSFPs) represents a highly promising alternative to organic dyes. Stable and long-

term expression of these genetically-encoded voltage indicators (GEVIs) can be achieved using either viral delivery or in transgenic mice (e.g., VSFP-Butterfly1.2, JAX® Mice, Stock Nr. 023528), potentially even targeting specific cellular subtypes. VSFPs have been applied, for example, to resolve whisker-evoked single-trial responses in the barrel cortex map [40, 41]. Further transgenic mouse lines have now become available [42]. Recently, new sensitive and fast VFSPs have been introduced, e.g., 'Arch' [43], 'ArcLight' [44], 'MacQ' [45], or 'ASAP1' [46]; in vivo applications of these new indicators are currently gaining momentum with great prospects of novel opportunities to chronically study fast cortex-wide signal flow patterns and oscillatory phenomena during behavior.

Wide-Field Fluorescence Imaging of Calcium Indicators

Besides fluorescent voltage indicators, the most prominent indicators of neuronal activity are calcium indicators. In fact, fluorescent calcium indicators still are the best characterized and most widely used indicators due to their large dynamic range and superior signal-to-noise ratio. In all neurons, the generation of an action potential is associated with the activation of voltage-gated calcium channels, causing a brief influx of calcium ions and thus allowing calcium indicators to serve as 'action potential detectors'. The action-potential evoked change in intracellular calcium concentration is reported as a transient fluorescence change, typically lasting for a few hundred milliseconds in the cell soma [47, 48]. Calcium indicators furthermore can uncover localized calcium influx in dendrites, axons, and in pre- and postsynaptic structures, where calcium ions also exert important physiological functions as second messenger.

Since the introduction of the first genetically-encoded calcium indicator (GECI) 'cameleon' [49], the palette of available GECIs has largely expanded. Indicators have steadily become more sensitive, meanwhile outperforming the best traditional small-molecule indicators such as Oregon Green BAPTA-1. One class of GECIs is composed of a single fluorescent protein (FP) attached to a calcium-binding domain that triggers a conformational switch and thus translates calcium binding into a fluorescence change. A second class of GECIs consists of two FPs linked via a calcium-binding domain such that the distance and relative orientation between the FPs—and therefore the 'fluorescence resonance energy transfer' (FRET) between them—are modulated in a calcium concentration-dependent manner. By reading out the fluorescence signal emissions in two spectral windows, these indicators enable ratiometric measurements, which normalize for various factors including motion artifacts and can be calibrated in terms of absolute calcium concentrations. At present, the most popular GECIs are the newest single-FP GCaMP indicators [50, 51] and the best variants of ratiometric dual-FP GECIs, designed with a linker derived from either calmodulin [52, 53] or troponin [54, 55].

Following up on earlier work using the synthetic calcium indicator Oregon Green BAPTA-1 [56] GECIs are now employed for wide-field fluorescence imaging of cortical activity. A standard method to induce GECI expression is viral delivery, especially using adeno-associated virus (AAV) constructs with neuron-specific promoters [57]. For example, virally induced expression of 'yellow cameleon 3.60' (YC-3.60) in mouse barrel cortex was employed to repeatedly map the location

and spread of whisker-evoked activity in the barrel cortex over several weeks [58] (Fig. 5.1d). Using a transgenic GCaMP3 reporter line [59], large-scale calcium signals were mapped across even larger areas of the somatomotor cortex using a similar approach [60]. Care had to be taken in this study to separate the green calcium indicator fluorescence changes from confounding autofluorescence and intrinsic optical signals. Recently, transgenic mice with widespread GECI expression (e.g., GCaMP6f line, JAX® Mice, Stock Nr. 024107) have been introduced that will be extremely useful for wide-field in vivo imaging, in particular when additional specificity is achieved by restricting expression to only particular cortical layers or neuronal subtypes [42].

Cellular Resolution Two-Photon Calcium Imaging

Two-photon excited fluorescence imaging is the key technology that enables high-resolution imaging at substantial depths in cortical tissue [61]. Two-photon calcium imaging is widely used to study neuronal population activity as well as subcellular calcium dynamics in dendrites and dendritic spines in mouse neocortex [48, 62, 63] (Fig. 5.1e and f). Two major paradigm shifts have occurred during the past decade and are still ongoing. First, after an initial phase, in which studies were mainly carried out in anesthetized rats or mice [64–67] the field by now has largely shifted towards imaging in awake, head-restrained animals, following the initial key demonstrations of the feasibility of such experiments [68, 69]. Crucially, cortical imaging in awake animals enables direct observation of neocortical microcircuit dynamics while the brain is in action, best when it is performing a meaningful, task-relevant computation [70] (see below). The second shift seen over the past years is the progressive transition from synthetic calcium indicators to GECIs, fostered by continual improvements of the latter and the advent of sophisticated expression strategies. While bulk-loading with small-molecule indicators continues to be highly suitable for revealing population activity patterns [65, 71, 72], the game-changing advantage of GECIs is the possibility of long-term monitoring of the same neurons and populations over weeks and months [73]. This feature has enabled for instances the investigation of how neuronal activity in mouse barrel cortex reorganizes during sensory deprivation induced by whisker trimming [32] or during learning of a whisker-dependent task [74]. Besides opening the door for such longitudinal studies of changes in network dynamics during plasticity and learning, long-term repeated imaging also turns out helpful in a practical sense for working with well-habituated mice over extended time periods and for making the efforts to train mice in specific behavioral tasks worthwhile.

Local network activity is usually assessed by imaging field-of-views containing tens to several hundred neurons and acquiring time series of two-photon images with frame rates of about 10 Hz for standard and >50 Hz for resonant scanning systems. Free laser scanning techniques for visiting soma after soma can acquire population data with even higher temporal resolution [75, 76]. Irrespective of which laser scanning technique is applied, population calcium imaging in the end provides a multivariate time series data set, containing the time course of action potential-evoked calcium signals for all measured neurons and thus reflecting network dynamics in a high-dimensional state space (with the number of neurons as number

of dimensions). In principle, the neural spike patterns underlying the calcium signals can be estimated from the indicator fluorescence traces using deconvolution techniques [77–80], but much of the analysis can also be carried out on the calcium signals directly. With increasing numbers of neurons being monitored, i.e., sampling network dynamics in even higher-dimensional state space, the demand is now increasing for (semi-)automatized methods for data pre-processing (motion correction, temporal alignment, ROI selection, etc.) and for the application of more sophisticated population analysis tools [81, 82], e.g., for decoding behavioral variables in awake mice [79, 83].

Finally, the high spatial resolution of two-photon microscopy enables in vivo imaging of subcellular events, in particular of localized activity in dendrites and at individual synapses (Fig. 5.1f). Thereby, it has become feasible to reveal the spatiotemporal pattern of dendritic activation in the living brain [48], which is essential in order to understand single-neuron computation, i.e., the input-output transformation of a particular cell type. A first goal is to map the spatial distribution of activated synapses by analyzing sensory-evoked subthreshold calcium signals in dendritic spines over substantial portions of the dendritic tree, e.g., following stimulation of different whiskers [84]. Early mapping studies of this sort utilized classical synthetic calcium indicators loaded via whole-cell recording pipettes, but the newest generation of GECIs clearly is capable of resolving single spine activity [50]. Therefore, extended studies of mapping synaptic input patterns, especially during behavior, can be expected for the coming years. A second major goal is to determine in how far and under what conditions the non-linear properties of dendrites become essential. Many neuronal dendrites in principle are capable of producing localized regenerative potentials (‘dendritic spikes’), especially when synaptic inputs are clustered and arrive synchronously. If, how and when this special mode of dendritic integration is relevant is still being worked out in current studies. For example, while most studies agree that NMDA-type glutamate receptors are crucially involved in localized dendritic excitability and calcium signaling, it is still debated under what conditions synaptic integration is rather linear or non-linear, as illustrated by two recent studies on layer 4 neurons in barrel cortex reaching opposite conclusions [85, 86]. Further in vivo imaging studies are required to uncover the rules for integration of sensory inputs during specific behavioral conditions in the different neuronal cell types.

Spontaneous Activity and Whisker-Evoked Responses During Anesthesia

Using these various imaging methods, what have we learned about the neocortical representation of whisker movements and touch at the level of cells, local circuits, and cortical hemispheres? Before considering active whisker movements and touch-induced mechanical stimulation, let us first ask what type of spontaneous activity is found in the neocortical network because it is continually active,

whether during sleep, anesthesia, or wakefulness. VSD imaging studies revealed spontaneous waves of activity that travel across cortex, encompassing the barrel field and other areas beyond [36, 37, 87]. During anesthesia, these waves occur at a slow frequency (~1 Hz) and correlate well with local field potential (LFP) measurements and with UP and DOWN state membrane potential fluctuations as observed in pyramidal neurons with whole-cell patch pipettes [87]. Interestingly, the spatial dynamics sometimes closely resembles the whisker-evoked activation patterns, an observation that also holds for other sensory modalities and presumably reflects the underlying large-scale functional connectivity across cortical areas [37]. On the cellular level, a consistent finding of electrophysiological and imaging studies is that spontaneous action potential firing rates in layer 2/3 pyramidal neurons are low, typically below 0.5 Hz [66, 88], and that baseline rates increase only slightly (~30%) in awake animals [68]. Juxtacellular recordings from deeper L5 neurons revealed higher baseline firing rates [88], which is hard to compare to optical studies at present because calcium imaging of infragranular layers has remained more challenging (but see [89, 90]).

On all scales, neural responses to whisker stimulation have been measured under anesthesia. Wide-field imaging studies confirm the spatial activation patterns mentioned above, showing an initial activation spot in S1 followed by a second wave of activity emerging from M1 (Fig. 5.2a). Zooming in on the local circuitry in S1 two salient response characteristics have been identified: sparseness and heterogeneity. Layer 2/3 neurons elicit action potentials in response to a whisker stimulus only with a low probability of 0.1–0.4 [66, 67]. Consistently, only a fraction of neurons exhibit suprathreshold responses for a given trial. Moreover, this sparse population activity is quite heterogeneous, it is not normally distributed but displays a skewed, long-tailed distribution with only few percent of strongly responding cells [32]; many neurons show weaker and less reliable responses and a substantial pool mostly remains silent. The functional implications and potential underlying mechanisms of such a sparse and heterogeneous distribution of neuronal network activity are currently being worked out (for review see for example [73, 91, 92]). On the subcellular level, dendritic spine calcium imaging of layer 2 neurons revealed distinct synaptic input patterns when neighboring whiskers of anesthetized mice were stimulated [84]. However, a substantial number of spines were activated by both whiskers, suggesting that these ‘shared inputs’ arrive from neurons that have already integrated the two streams of information.

An important question that so far has been primarily examined under anesthesia is whether feature selectivity maps, analogous to orientation preference maps in visual cortex, exist in the barrel cortex. One possibility is that the cortical responses depend on the direction of whisker deflection (rostro-caudal, ventral-dorsal). Indeed, whisker direction selectivity maps were found inside individual barrel columns using two-photon calcium imaging in rats [93], consistent with earlier electrophysiological work [94]; such maps, however, appeared only in adult animals (with enriched environment) and were not found in young animals [66, 93]. Recently, another type of feature selectivity was described: Population responses of layer 2/3 neurons were examined with two-photon calcium imaging when whiskers were

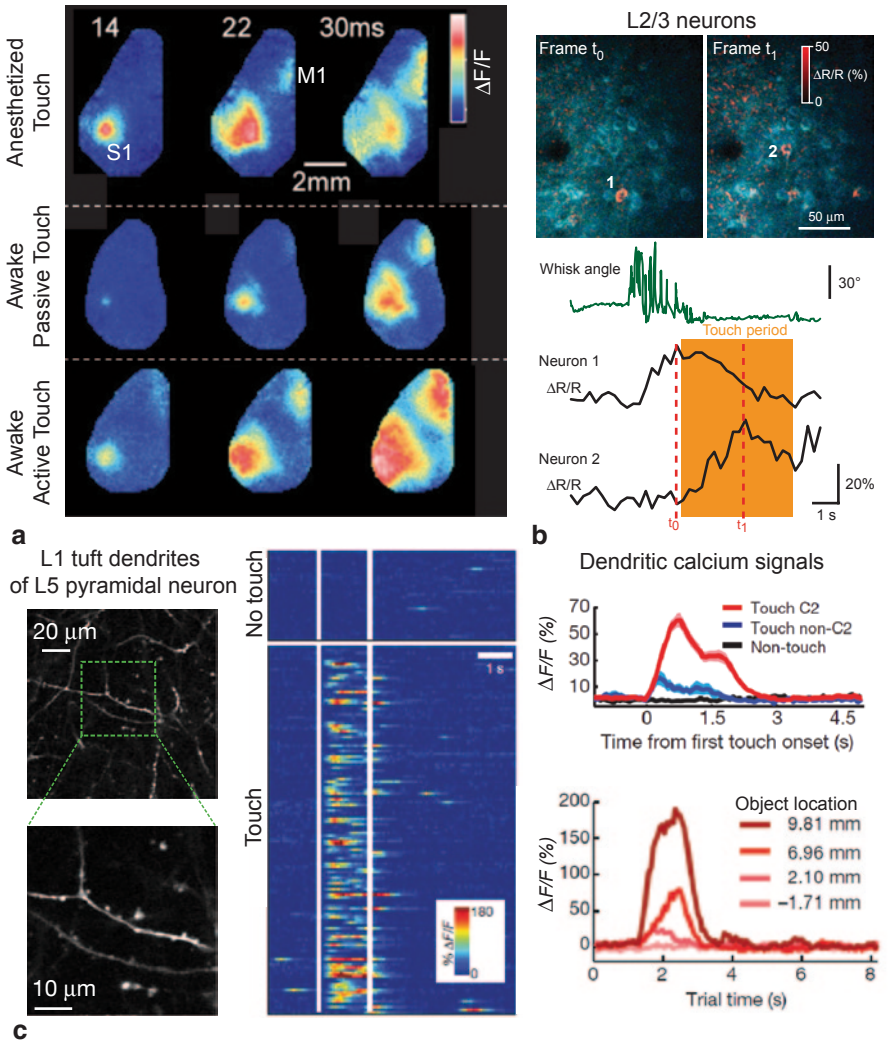

Fig. 5.2 Cortical representations of passive and active whisker touch. **a** Hemisphere-wide cortical activation pattern as revealed with VSD imaging in response to contralateral C2 whisker stimulation (three time points after stimulation shown). A similar pattern of first S1 then M1 activation is seen under three different conditions (3 different mice). (Adapted from Ferezou et al. 2007 [36] with permission). **b** Local circuit activation in layer 2/3 in mouse barrel cortex in response to active texture touch of a sandpaper. ΔR/R changes of the GECI YC-Nano140 are shown at two time points t_0 and t_1, just before and during touch. The whiskers are pushed backwards upon contact and the animal stops rhythmic whisking during the touch period. Neuron 1 shows activity correlated with whisking whereas another neuronal subset, including neuron 2, responds during the contact period. (Unpublished data from the Chen et al. 2013b study [80]). **c** Two-photon imaging of distal dendrites of L5 pyramidal neurons in barrel cortex of an awake, head-fixed mouse. The mouse touched with its whiskers a vertical pole presented at different positions as part of a object localization task. *Left*: Zoomed-in two-photon images from L1 dendrites. *Middle*: Dendritic calcium transients with color-coded amplitude in many trials (each row one trial), sorted according to

made to contact textures of different coarseness using artificial whisking [95]. The results suggest that distinct subsets of neurons exhibit preference for different texture coarseness and that these subsets could be organized in spatial clusters and in a columnar fashion. It will be interesting in the future to relate these findings obtained under anesthesia to neuronal response patterns evoked by texture touches in awake animals.

Cortical Representations of Free Whisking and Touch Events in Awake Mice

Several studies have started to apply in vivo imaging methods to investigate cortical activity in the whisker system of awake animals. Most of these studies are now taking advantage of head-fixed paradigms as it turns out that both rats and mice can be well trained to tolerate head fixation [69, 96]. A first question is what activity patterns occur during spontaneous 'active whisking' in free air. Calcium imaging of neurons in M1 revealed a relative high fraction of active layer 2/3 neurons, which were classified as 'whisking neurons' based on their increased activity during whisking and their ability to decode this behavioral feature [79]; other neurons correlated better with different behavioral features such as object touch or licking. In contrast, using virally induced YC GECIs, we found that the majority of active layer 2/3 neurons in S1 was down-modulated in their activity during free-air whisking but we could also detect a small fraction of neurons (< 10 %) exhibiting increased activity [97]. Presumably excitatory as well as inhibitory neurons are among these up-modulated neurons but there is also evidence for some cell-type specificity. For example, PV-positive interneurons were always down-modulated, which is consistent with a whole-cell recording study showing reduced firing of fast-spiking interneurons during whisking [22]. Thus, in the supragranular layers of S1 barrel cortex a heterogeneous picture is observed and the same can be expected for other cortical layers and areas. It will be highly informative to employ calcium imaging techniques to determine the sign and strength of modulation for all major cell types throughout S1, M1, and further areas during the simple behavior of voluntary free-air whisking.

During whisker touch events, either 'passive' for a quiescent mouse or 'active' as induced by whisking, VSD imaging across brain hemispheres has shown a sequential pattern of first S1 and then M1 activation in awake mice similar to the one observed during anesthesia (Fig. 5.2a) [36]. The exact pattern of activation did,

whether a touch occurred or not. *Right top*: Averaged calcium signals aligned to onset of touch for trials with C2 whisker touch (Touch C2), with touch from whiskers other than C2 (Touch non-C2) and with no touch (Non-touch). *Right bottom*: Averaged calcium signals for trials with different object locations. Colors correspond to object locations (measured as the distance of the pole from the centre of the whisker pad along the anterior–posterior axis). (Adapted from Xu et al. 2012 [98] with permission)

however, depend on the behavioral state such that the spread of activity in S1 and particularly the activation of M1 and frontal regions was decreased in trials in which the mouse was either whisking or when the stimulus did not induce a whisking reaction [36]. The tight interplay between S1 and M1 has also been observed in cellular imaging studies. For example, in layer 2/3 of barrel cortex, distinct sparse subsets of neurons are activated upon active touch of a sandpaper, some tightly correlated with the touch period but others correlated with whisking behavior (Fig. 5.2b) [80]. A two-photon imaging study of activity in distal apical tuft dendrites of L5 pyramidal neurons showed a clear correlation of dendritic calcium signals with touch events and interestingly an additional dependency on the object location (Fig. 5.2c) [98]. These studies of neural touch responses in awake mice thus have uncovered functional correlations of the activity in areas, neurons, or dendrites with particular aspects of a touch event. As for free-whisking, it will be essential in the coming years to expand such types of studies to other cortical regions, layers, and cell types in order to obtain a more comprehensive picture of the neural representation of whisker touch in the cortical circuitry. The question remains whether neuronal correlations simply reflect sensory or motor variables or whether neuronal activities are causative for driving behavior. Addressing this issue will be important to fully understand how the neural circuit controlling and processing whisker touches operates. Specific manipulations such as infraorbital nerve transection, localized lesions, or controlled silencing of neural elements using optogenetics and pharmacogenetics will help to dissect causal relationships in the dynamic neural network of the whisker system.

Cortical Dynamics During Tactile Behavioral Tasks

In order to understand sensory processing in the cortex, it is necessary to observe activity patterns under experimental conditions, in which tactile information is used to drive behavior. In order to study how cortical circuits determine behaviorally-relevant parameters such as “where” a stimulus is in the environment and “what” it represents, tasks have been developed for object localization and object discrimination [1]. Since mechanical stability is a fundamental requirement for imaging calcium dynamics in awake animals with standard two-photon microscopes, these tasks have been adopted to head-fixed conditions, which also provide a high degree of stimulus control and behavioral read-out. The mouse is presented with sensory stimuli belonging to two different categories (e.g. anterior vs. posterior position or smooth vs. rough texture). The task of the mouse is to determine the category of a given stimulus and respond with predefined actions such as licking a water port or pressing a lever to obtain reward. During a “go/no-go” task, the animal must initiate an action to obtain a reward following “go” stimuli and withhold the action upon “no-go” stimuli [99]. During a two-alternative forced choice (2AFC) task [100,

101], the animal makes one out of two actions based on the stimuli, e.g., licking one of two water ports positioned to the left or right of the mouth. Each task has its experimental advantages and disadvantages. In the go/no-go task, only the stimuli in "go" trials are potentially rewarding, thus no-go trials can be useful in isolating sensory responses without the potential influence of reward anticipation or response. On the other hand, it can be hard to judge whether no-go trials may also result from a lack of engagement in the task. In 2AFC tasks both categories of stimuli have similar reward predicting values which allows a better readout of reaction time and behavioral state where trials, in which animals fail to respond, can signal lack of motivation or attention. As the animal is supposed to actively respond in each trial, assessment of pure sensory representations may be more difficult, however.

Thus far, object localization during head-fixed tasks has been assessed by presenting a pole along different positions relative to mouse's head. Population imaging in layer 2/3 of S1during this task has verified that tactile responses to touch are sparse in this layer with only 10–20% of neurons showing touch-related activity on average [19, 80]. In layer 2/3 of M1, neurons showed correlations with sensory or behavior variables and in well-trained mice neuronal subsets were discriminative for distinguishing trial types such as hits, false alarms, and correct rejections (Fig. 5.3a, b, c) [79]. The sub-cellular resolution of two-photon microscopy provides the unique opportunity to directly observe axonal and dendritic activity during behavior. Activity of long-range inputs can be isolated by imaging spiking-related calcium signals of axons in a region innervated by projection neurons from distant cortical or subcortical areas (Fig. 5.3d, e, f). Calcium imaging of M1 axons innervating S1 has demonstrated that M1 sends information about whisking motor behavior directly to S1 during active tactile sensation [83]. How motor information is integrated into S1 has been studied by complementary work, in which calcium signals were measured in dendritic apical tufts of L5 neurons in S1 [98]. The results suggest that dendrites can non-linearly integrate M1 input carrying information about whisker position with ascending sensory input conveying touch information in order to compute the object position (see Fig. 5.2c).

Object identification has been studied using a texture discrimination task in which mice are trained to report between different panels of sandpaper with different degrees of coarseness (Fig. 5.3g). Calcium imaging of retrogradely labeled S2-projecting and M1-projecting neurons demonstrate that the activity of patterns of these subsets of neurons during texture discrimination differed compared to during object localization (Fig. 5.3h, i). This finding provides a cellular basis for how S1 can support different modes of sensory processing as demanded upon by behavior [80].

It is an open question as to whether the responses observed in sensorimotor cortex during behavior are hardwired within the cortical circuitry or are shaped during learning. Chronic calcium imaging using genetically-encoded calcium indicators provides new opportunities for observing potential changes in cellular responses during perceptual or procedural learning. Initial studies monitoring L2/3 activity in whisker M1 during learning of an object localization task suggest that individual

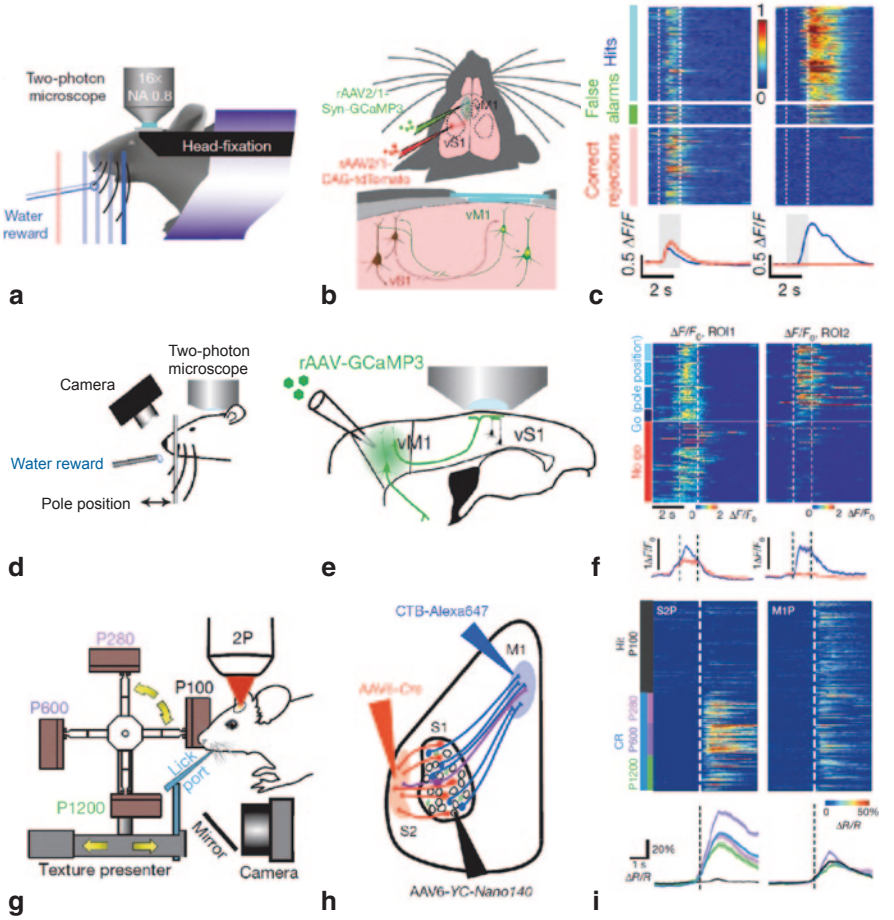

Fig. 5.3 Behavior-related activity of specific elements in cortical circuitry during whisker-based go/no-go tasks. **a** Object detection task. The head-fixed mouse has to detect the presence of a pole presented along the antero-posterior axis. Whisker movements are monitored with a high-speed camera, neuronal population activity in whisker M1 with two-photon calcium imaging. **b** In this study M1 was targeted for GCaMP3 calcium imaging by first injecting a virus causing expression of the red marker tdTomato and then guiding GCaMP3-virus injection by imaging the area of the red axonal projections in M1. **c** Example calcium transients (normalized in amplitude) for two example M1 neurons, sorted according to behavioral outcome. Cell A is active during the whisker sampling period (grey-shaded time period) and shows little trial-type dependence, cell B is active after sensory sampling during licking. (**a-c**) adapted from Huber et al. 2012 [79] with permission. **d** Object localization task in another study, with several go positions and a single no-go pole position in front, similar to (a). **e** In this case axonal projections to S1 originating from M1 were made to express GCaMP3 and the terminal axonal arborizations were imaged in S1. **f** Calcium transients for two example ROIs representing two axons, sorted according to trial type (only correct trials shown). While axon 1 shows activity before and during whisking sampling periods, axon 2 is mainly active in trials with strong whisker touches. (**d-f**) adapted from Petreanu et al. 2012 [83] with permission. **g** Texture discrimination task. The mouse has to judge the coarseness of presented sandpapers and lick for a water reward when the target P100 texture is presented. Whisker movements are monitored with a high-speed camera, neuronal population activity in

L2/3 neurons seem to be pre-wired to represent particular motor variables such as whisking or licking through activation of subsets of neurons [79]. However, while population-level representations were stable, the timing and reliability of single neuron responses were dynamic and tracked with motor behavior changes associated with improved task performance. This suggests that a broad repertoire of neuronal responses exist in M1 that is selected for during learning. To what extent S1 responses are shaped in a similar manner during learning remains to be determined.

Conclusions

Looking forward, the imaging methods and molecular techniques developed thus far now presents new opportunities to obtain a comprehensive understanding of vibrissa function in the neocortex during behavior that is integrative along multiple spatial and temporal scales. On the single-neuron level, imaging synaptic activation patterns during behaviors, either by functional measurements of axonal pathways [83, 102] or by direct observation of postsynaptic signals in dendrites with single spine resolution [50], should be highly informative. Such experiments could shed light on the principles of dendritic integration under relevant behavioral conditions. Population imaging of specific neuronal cell types as defined by molecular profile, laminar location, and anatomical connectivity will reveal the functional properties of individual circuit components and their interactions that can be used to determine the computations they perform across different behavioral contexts. Wide-field or large-scale imaging across cortical areas may allow us to better resolve the actual signal flow and understand how local circuit information is exchanged and transformed for sensorimotor integration or feature extraction.

Acknowledgements The authors' work has been supported by the Swiss National Science Foundation (SNSF) (grant 310030-127091 and Sinergia project CRSII3_147660/1; F.H.), a 'Forschungskredit' of the University of Zurich (grant 541541808, J.L.C.) and a fellowship from the U.S. National Science Foundation, International Research Fellowship Program (grant 1158914, J.L.C.).

barrel cortex with two-photon calcium imaging. **h** Labeling strategy to identify projection neurons from S1 to S2 and M1, respectively, using injection of a retrograde infecting AAV6 construct and fluorescently-labeled cholera toxin B subunit (CTB), respectively. In this study the GECI yellow cameleon-Nano140 was applied. **i** Example calcium transients for two neurons in one session, sorted according to behavioral condition. Each row represents the color-coded $\Delta R/R$ change in one trial, aligned to the first moment of touch (dashed line). Average calcium transients are shown at the bottom. Note that the S2-projecting neuron (S2P) is highly discriminative for correct rejection (CR) versus Hit trials, while the M1-projecting neuron (M1P) shows no discriminative power. (**g-i**) adapted from Chen et al. 2013b [80] with permission

References

1. Diamond ME, von Heimendahl M, Knutsen PM, Kleinfeld D, Ahissar E (2008) 'Where' and 'what' in the whisker sensorimotor system. Nat Rev Neurosci 9:601–612
2. Petersen CC (2014) Cortical control of whisker movement. Annu Rev Neurosci 37:183–203
3. Ahissar E, Kleinfeld D (2003) Closed-loop neuronal computations: focus on vibrissa somatosensation in rat. Cereb Cortex 13:53–62
4. Bosman LW, Houweling AR, Owens CB, Tanke N, Shevchouk OT, Rahmati N, Teunissen WH, Ju C, Gong W, Koekkoek SK, De Zeeuw CI (2011) Anatomical pathways involved in generating and sensing rhythmic whisker movements. Front Integr Neurosci 5:53
5. Feldman DE (2009) Synaptic mechanisms for plasticity in neocortex. Annu Rev Neurosci 32:33–55
6. Feldman DE, Brecht M (2005) Map plasticity in somatosensory cortex. Science 310:810–815
7. Margolis DJ, Lütcke H, Helmchen F (2014) Microcircuit dynamics of map plasticity in barrel cortex. Curr Opin Neurobiol 24:76–81
8. Aronoff R, Matyas F, Mateo C, Ciron C, Schneider B, Petersen CC (2010) Long-range connectivity of mouse primary somatosensory barrel cortex. Eur J Neurosci 31:2221–2233
9. Chakrabarti S, Alloway KD (2006) Differential origin of projections from SI barrel cortex to the whisker representations in SII and MI. J Comp Neurol 498(5):624–636
10. Zingg B, Hintiryan H, Gou L, Song MY, Bay M, Bienkowski MS, Foster NN, Yamashita S, Bowman I, Toga AW, Dong HW (2014) Neural networks of the mouse neocortex. Cell 156:1096–1111
11. Oh SW, Harris JA, Ng L, Winslow B, Cain N, Mihalas S, Wang QX, Lau C, Kuan L, Henry AM, Mortrud MT, Ouellette B, Nguyen TN, Sorensen SA, Slaughterbeck CR, Wakeman W, Li Y, Feng D, Ho A, Nicholas E, Hirokawa KE, Bohn P, Joines KM, Peng HC, Hawrylycz MJ, Phillips JW, Hohmann JG, Wohnoutka P, Koch C, Bernard A, Dang C, Jones AR, Zeng HK, Gerfen CR (2014) A mesoscale connectome of the mouse brain. Nature 508:207
12. Oberlaender M, de Kock CP, Bruno RM, Ramirez A, Meyer HS, Dercksen VJ, Helmstaedter M, Sakmann B (2012) Cell type-specific three-dimensional structure of thalamocortical circuits in a column of rat vibrissal cortex. Cereb Cortex 22:2375–2391
13. Meyer HS, Egger R, Guest JM, Foerster R, Reissl S, Oberlaender M (2013) Cellular organization of cortical barrel columns is whisker-specific. Proc Natl Acad Sci U S A 110:19113–19118
14. Feldmeyer D (2012) Excitatory neuronal connectivity in the barrel cortex. Front Neuroanat 6:24
15. Feldmeyer D, Brecht M, Helmchen F, Petersen CCH, Poulet JFA, Staiger JF, Luhmann HJ, Schwarz C (2013) Barrel cortex function. Prog Neurobiol 103:3–27
16. Petersen CC (2007) The functional organization of the barrel cortex. Neuron 56:339–355
17. Crochet S, Petersen CC (2006) Correlating whisker behavior with membrane potential in barrel cortex of awake mice. Nat Neurosci 9:608–610
18. Petersen CC, Grinvald A, Sakmann B (2003) Spatiotemporal dynamics of sensory responses in layer 2/3 of rat barrel cortex measured in vivo by voltage-sensitive dye imaging combined with whole-cell voltage recordings and neuron reconstructions. J Neurosci 23:1298–1309
19. O'Connor DH, Peron SP, Huber D, Svoboda K (2010b) Neural activity in barrel cortex underlying vibrissa-based object localization in mice. Neuron 67:1048–1061
20. Sachidhanandam S, Sreenivasan V, Kyriakatos A, Kremer Y, Petersen CCH (2013) Membrane potential correlates of sensory perception in mouse barrel cortex. Nat Neurosci 16:1671–1677
21. Gentet LJ (2012) Functional diversity of supragranular GABAergic neurons in the barrel cortex. Front Neural Circuits 6:52
22. Gentet LJ, Avermann M, Matyas F, Staiger JF, Petersen CC (2010) Membrane potential dynamics of GABAergic neurons in the barrel cortex of behaving mice. Neuron 65:422–435

23. Wang Y, Toledo-Rodriguez M, Gupta A, Wu C, Silberberg G, Luo J, Markram H (2004) Anatomical, physiological and molecular properties of Martinotti cells in the somatosensory cortex of the juvenile rat. J Physiol 561:65–90
24. Gentet LJ, Kremer Y, Taniguchi H, Huang ZJ, Staiger JF, Petersen CC (2012) Unique functional properties of somatostatin-expressing GABAergic neurons in mouse barrel cortex. Nat Neurosci 15:607–612
25. Rudy B, Fishell G, Lee S, Hjerling-Leffler J (2011) Three groups of interneurons account for nearly 100% of neocortical GABAergic neurons. Dev Neurobiol 71:45–61
26. Pi HJ, Hangya B, Kvitsiani D, Sanders JI, Huang ZJ, Kepecs A (2013) Cortical interneurons that specialize in disinhibitory control. Nature 503:521
27. Karnani MM, Agetsuma M, Yuste R (2014) A blanket of inhibition: functional inferences from dense inhibitory connectivity. Curr Opin Neurobiol 26:96–102
28. Grinvald A, Lieke E, Frostig RD, Gilbert CD, Wiesel TN (1986) Functional architecture of cortex revealed by optical imaging of intrinsic signals. Nature 324:361–364
29. Masino SA, Frostig RD (1996) Quantitative long-term imaging of the functional representation of a whisker in rat barrel cortex. Proc Natl Acad Sci U S A 93:4942–4947
30. Petersen CCH, Crochet S (2013) Synaptic computation and sensory processing in neocortical layer 2/3. Neuron 78:28–48
31. Polley DB, Kvasnak E, Frostig RD (2004) Naturalistic experience transforms sensory maps in the adult cortex of caged animals. Nature 429:67–71
32. Margolis DJ, Lütcke H, Schulz K, Haiss F, Weber B, Kügler S, Hasan MT, Helmchen F (2012) Reorganization of cortical population activity imaged throughout long-term sensory deprivation. Nat Neurosci 15:1539–1546
33. Arnett MT, Herman DH, McGee AW (2014) Deficits in tactile learning in a mouse model of fragile X syndrome. PLoS ONE 9(10):e109116
34. Guy J, Wagener RJ, Mock M, Staiger JF (2014) Persistence of functional sensory maps in the absence of cortical layers in the somsatosensory cortex of reeler mice. Cereb Cortex. (Epub ahead of print)
35. Grinvald A, Hildesheim R (2004) VSDI: a new era in functional imaging of cortical dynamics. Nat Rev Neurosci 5:874–885
36. Ferezou I, Haiss F, Gentet LJ, Aronoff R, Weber B, Petersen CC (2007) Spatiotemporal dynamics of cortical sensorimotor integration in behaving mice. Neuron 56:907–923
37. Mohajerani MH, Chan AW, Mohsenvand M, LeDue J, Liu R, McVea DA, Boyd JD, Wang YT, Reimers M, Murphy TH (2013) Spontaneous cortical activity alternates between motifs defined by regional axonal projections. Nat Neurosci 16:1426
38. Porter LL, White EL (1983) Afferent and efferent pathways of the vibrissal region of primary motor cortex in the mouse. J Comp Neurol 214:279–289
39. Grandy TH, Greenfield SA, Devonshire IM (2012) An evaluation of in vivo voltage-sensitive dyes: pharmacological side effects and signal-to-noise ratios after effective removal of brain-pulsation artifacts. J Neurophysiol 108:2931–2945
40. Akemann W, Mutoh H, Perron A, Rossier J, Knöpfel T (2010) Imaging brain electric signals with genetically targeted voltage-sensitive fluorescent proteins. Nat Methods 7:643–649
41. Akemann W, Mutoh H, Perron A, Park YK, Iwamoto Y, Knöpfel T (2012) Imaging neural circuit dynamics with a voltage-sensitive fluorescent protein. J Neurophysiol 108:2323–2337
42. Madisen L, Garner AR, Shimaoka D, Chuong AS, Klapoetke NC, Li L, van der Bourg A, Niino Y, Egolf L, Monetti C, Gu H, Mills M, Cheng A, Tasic B, Nguyen TN, Sunkin SM, Benucci A, Nagy A, Miyawaki A, Helmchen F, Empson RM, Knöpfel T, Boyden ES, Reid RC, Carandini M, Zeng H (2015) Transgenic mice for intersectional targeting of neural sensors and effectors with high specificity and performance. Neuron 85:942–958
43. Kralj JM, Douglass AD, Hochbaum DR, Maclaurin D, Cohen AE (2012) Optical recording of action potentials in mammalian neurons using a microbial rhodopsin. Nat Methods 9:90
44. Jin L, Han Z, Platisa J, Wooltorton JRA, Cohen LB, Pieribone VA (2012) Single action potentials and subthreshold electrical events imaged in neurons with a fluorescent protein voltage probe. Neuron 75:779–785

45. Gong YY, Wagner MJ, Li JZ, Schnitzer MJ (2014) Imaging neural spiking in brain tissue using FRET-opsin protein voltage sensors. Nat Commun 5:3674
46. St-Pierre F, Marshall JD, Yang Y, Gong YY, Schnitzer MJ, Lin MZ (2014) High-fidelity optical reporting of neuronal electrical activity with an ultrafast fluorescent voltage sensor. Nat Neurosci 17:884–889
47. Göbel W, Helmchen F (2007a) In vivo calcium imaging of neural network function. Physiology 22:358–365
48. Grienberger C, Konnerth A (2012) Imaging calcium in neurons. Neuron 73:862–885
49. Miyawaki A, Llopis J, Heim R, McCaffery JM, Adams JA, Ikura M, Tsien RY (1997) Fluorescent indicators for Ca^{2+} based on green fluorescent proteins and calmodulin. Nature 388:882–887
50. Chen TW, Wardill TJ, Sun Y, Pulver SR, Renninger SL, Baohan A, Schreiter ER, Kerr RA, Orger MB, Jayaraman V, Looger LL, Svoboda K, Kim DS (2013c) Ultrasensitive fluorescent proteins for imaging neuronal activity. Nature 499:295–300
51. Ohkura M, Sasaki T, Sadakari J, Gengyo-Ando K, Kagawa-Nagamura Y, Kobayashi C, Ikegaya Y, Nakai J (2012) Genetically encoded green fluorescent Ca^{2+} indicators with improved detectability for neuronal Ca^{2+} signals. PLoS ONE 7:e51286
52. Nagai T, Yamada S, Tominaga T, Ichikawa M, Miyawaki A (2004) Expanded dynamic range of fluorescent indicators for Ca^{2+} by circularly permuted yellow fluorescent proteins. Proc Natl Acad Sci U S A 101:10554–10559
53. Horikawa K, Yamada Y, Matsuda T, Kobayashi K, Hashimoto M, Matsu-ura T, Miyawaki A, Michikawa T, Mikoshiba K, Nagai T (2010) Spontaneous network activity visualized by ultrasensitive Ca^{2+} indicators, yellow Cameleon-Nano. Nat Methods 7:729–732
54. Mank M, Santos AF, Direnberger S, Mrsic-Flogel TD, Hofer SB, Stein V, Hendel T, Reiff DF, Levelt C, Borst A, Bonhoeffer T, Hubener M, Griesbeck O (2008) A genetically encoded calcium indicator for chronic in vivo two-photon imaging. Nat Methods 5:805–811
55. Thestrup T, Litzlbauer J, Bartholomaus I, Mues M, Russo L, Dana H, Kovalchuk Y, Liang YJ, Kalamakis G, Laukat Y, Becker S, Witte G, Geiger A, Allen T, Rome LC, Chen TW, Kim DS, Garaschuk O, Griesinger C, Griesbeck O (2014) Optimized ratiometric calcium sensors for functional in vivo imaging of neurons and T lymphocytes. Nat Methods 11:175
56. Berger T, Borgdorff A, Crochet S, Neubauer FB, Lefort S, Fauvet B, Ferezou I, Carleton A, Lüscher HR, Petersen CCH (2007) Combined voltage and calcium epifluorescence Imaging in vitro and in vivo reveals subthreshold and suprathreshold dynamics of mouse barrel cortex. J Neurophysiol 97:3751–3762
57. Lütcke H, Murayama M, Hahn T, Margolis DJ, Astori S, Zum Alten Borgloh SM, Göbel W, Yang Y, Tang W, Kügler S, Sprengel R, Nagai T, Miyawaki A, Larkum ME, Helmchen F, Hasan MT (2010) Optical recording of neuronal activity with a genetically-encoded calcium indicator in anesthetized and freely moving mice. Front Neural Circuits 4:9
58. Minderer M, Liu W, Sumanovski LT, Kügler S, Helmchen F, Margolis DJ (2012) Chronic imaging of cortical sensory map dynamics using a genetically encoded calcium indicator. J Physiol 590:99–107
59. Zariwala HA, Borghuis BG, Hoogland TM, Madisen L, Tian L, De Zeeuw CI, Zeng H, Looger LL, Svoboda K, Chen TW (2012) A Cre-dependent GCaMP3 reporter mouse for neuronal imaging in vivo. J Neurosci 32:3131–3141
60. Vanni MP, Murphy TH (2014) Mesoscale transcranial spontaneous activity mapping in GCaMP3 transgenic mice reveals extensive reciprocal connections between areas of somatomotor cortex. J Neurosci 34:15931–15946
61. Helmchen F, Denk W (2005) Deep tissue two-photon microscopy. Nat Methods 2:932–940
62. Grewe BF, Helmchen F (2009) Optical probing of neuronal ensemble activity. Curr Opin Neurobiol 19:520–529
63. Lütcke H, Helmchen F (2011) Two-photon imaging and analysis of neural network dynamics. Rep Prog Phys 74(8):086602
64. Ohki K, Chung S, Ch'ng Y, Kara P, Reid R (2005) Functional imaging with cellular resolution reveals precise micro-architecture in visual cortex. Nature 433:597–603

65. Kerr JND, Greenberg D, Helmchen F (2005) Imaging input and output of neocortical networks in vivo. Proc Natl Acad Sci U S A 102:14063–14068
66. Kerr JN, de Kock CP, Greenberg DS, Bruno RM, Sakmann B, Helmchen F (2007) Spatial organization of neuronal population responses in layer 2/3 of rat barrel cortex. J Neurosci 27:13316–13328
67. Sato TR, Gray NW, Mainen ZF, Svoboda K (2007) The functional microarchitecture of the mouse barrel cortex. PLoS Biol 5:e189
68. Greenberg DS, Houweling AR, Kerr JN (2008) Population imaging of ongoing neuronal activity in the visual cortex of awake rats. Nature Neurosci 11(7):749–751
69. Dombeck DA, Khabbaz AN, Collman F, Adelman TL, Tank DW (2007) Imaging large-scale neural activity with cellular resolution in awake, mobile mice. Neuron 56:43–57
70. Chen JL, Andermann ML, Keck T, Xu NL, Ziv Y (2013a) Imaging neuronal populations in behaving rodents: paradigms for studying neural circuits underlying behavior in the mammalian cortex. J Neurosci 33:17631–17640
71. Stosiek C, Garaschuk O, Holthoff K, Konnerth A (2003) In vivo two-photon calcium imaging of neuronal networks. Proc Natl Acad Sci USA 100:7319–7324
72. Dombeck DA, Graziano MS, Tank DW (2009) Functional clustering of neurons in motor cortex determined by cellular resolution imaging in awake behaving mice. J Neurosci 29:13751–13760
73. Lütcke H, Margolis DJ, Helmchen F (2013b) Steady or changing? Long-term monitoring of neuronal population activity. Trends Neurosci 36:375–384
74. Chen JL, Margolis DJ, Stankov A, Sumanovski LT, Schneider BL, Helmchen F (2015) Pathway-specific reorganization of projection neurons in somatosensory cortex during learning. Nat Neurosci 2015 Jun 22, (Epub ahead of print)
75. Göbel W, Helmchen F (2007b) New angles on neuronal dendrites in vivo. J Neurophysiol 98:3770–3779
76. Lillis KP, Eng A, White JA, Mertz J (2008) Two-photon imaging of spatially extended neuronal network dynamics with high temporal resolution. J Neurosci Methods 172:178–184
77. Vogelstein JT, Packer AM, Machado TA, Sippy T, Babadi B, Yuste R, Paninski L (2010) Fast nonnegative deconvolution for spike train inference from population calcium imaging. J Neurophysiol 104:3691–3704
78. Lütcke H, Gerhard F, Zenke F, Gerstner W, Helmchen F (2013a) Inference of neuronal network spike dynamics and topology from calcium imaging data. Front Neural Circuits 7:201
79. Huber D, Gutnisky DA, Peron S, O'Connor DH, Wiegert JS, Tian L, Oertner TG, Looger LL, Svoboda K (2012) Multiple dynamic representations in the motor cortex during sensorimotor learning. Nature 484:473–478
80. Chen JL, Carta S, Soldado-Magraner J, Schneider BL, Helmchen F (2013b) Behaviour-dependent recruitment of long-range projection neurons in somatosensory cortex. Nature 499:336–340
81. Mukamel EA, Nimmerjahn A, Schnitzer MJ (2009) Automated analysis of cellular signals from large-scale calcium imaging data. Neuron 63:747–760
82. Freeman J, Vladimirov N, Kawashima T, Mu Y, Sofroniew NJ, Bennett DV, Rosen J, Yang CT, Looger LL, Ahrens MB (2014) Mapping brain activity at scale with cluster computing. Nat Methods 11:941–950
83. Petreanu L, Gutnisky DA, Huber D, Xu NL, O'Connor DH, Tian L, Looger L, Svoboda K (2012) Activity in motor-sensory projections reveals distributed coding in somatosensation. Nature 489:299–303
84. Varga Z, Jia HB, Sakmann B, Konnerth A (2011) Dendritic coding of multiple sensory inputs in single cortical neurons in vivo. Proc Natl Acad Sci U S A 108:15420–15425
85. Lavzin M, Rapoport S, Polsky A, Garion L, Schiller J (2012) Nonlinear dendritic processing determines angular tuning of barrel cortex neurons in vivo. Nature 490:397–401
86. Jia HB, Varga Z, Sakmann B, Konnerth A (2014) Linear integration of spine Ca^{2+} signals in layer 4 cortical neurons in vivo. Proc Natl Acad Sci U S A 111:9277–9282
87. Ferezou I, Bolea S, Petersen CC (2006) Visualizing the cortical representation of whisker touch: voltage-sensitive dye imaging in freely moving mice. Neuron 50:617–629

88. de Kock CP, Sakmann B (2009) Spiking in primary somatosensory cortex during natural whisking in awake head-restrained rats is cell-type specific. Proc Natl Acad Sci U S A 106:16446–16450
89. Mittmann W, Wallace DJ, Czubayko U, Herb JT, Schaefer AT, Looger LL, Denk W, Kerr JN (2011) Two-photon calcium imaging of evoked activity from L5 somatosensory neurons in vivo. Nat Neurosci 14:1089–1093
90. Andermann ML, Gilfoy NB, Goldey GJ, Sachdev RN, Wolfel M, McCormick DA, Reid RC, Levene MJ (2013) Chronic cellular imaging of entire cortical columns in awake mice using microprisms. Neuron 80:900–913
91. Barth AL, Poulet JFA (2012) Experimental evidence for sparse firing in the neocortex. Trends Neurosci 35:345–355
92. Buzsaki G, Mizuseki K (2014) The log-dynamic brain: how skewed distributions affect network operations. Nat Rev Neurosci 15:264–278
93. Kremer Y, Leger JF, Goodman D, Brette R, Bourdieu L (2011) Late emergence of the vibrissa direction selectivity map in the rat barrel cortex. J Neurosci 31:14831–14831
94. Andermann ML, Moore CI (2006) A somatotopic map of vibrissa motion direction within a barrel column. Nat Neurosci 9:543–551
95. Garion L, Dubin U, Rubin Y, Khateb M, Schiller Y, Azouz R, Schiller J (2014) Texture coarseness responsive neurons and their mapping in layer 2–3 of the rat barrel cortex in vivo. Elife 3:e03405
96. Schwarz C, Hentschke H, Butovas S, Haiss F, Stuttgen MC, Gerdjikov TV, Bergner CG, Waiblinger C (2010) The head-fixed behaving rat–procedures and pitfalls. Somatosens Mot Res 27:131–148
97. Schulz K, Schrepfer I, Margolis DJ, Lütcke H, Kügler S, Hasan MT, Helmchen F (2010) Whisking-induced modulation of L2/3 population activity imaged in awake head-fixed mice. Society of Neuroscience abstract. Program No 58718, 2010, Neuroscience Meeting Planner, San Diego, CA
98. Xu NL, Harnett MT, Williams SR, Huber D, O'Connor DH, Svoboda K, Magee JC (2012) Nonlinear dendritic integration of sensory and motor input during an active sensing task. Nature 492:247–251
99. O'Connor DH, Clack NG, Huber D, Komiyama T, Myers EW, Svoboda K (2010a) Vibrissa-based object localization in head-fixed mice. J Neurosci 30:1947–1967
100. Mayrhofer JM, Skreb V, von der Behrens W, Musall S, Weber B, Haiss F (2013) Novel two-alternative forced choice paradigm for bilateral vibrotactile whisker frequency discrimination in head-fixed mice and rats. J Neurophysiol 109:273–284
101. O'Connor DH, Hires SA, Guo ZV, Li N, Yu J, Sun QQ, Huber D, Svoboda K (2013) Neural coding during active somatosensation revealed using illusory touch. Nat Neurosci 16:958–965
102. Glickfeld LL, Andermann ML, Bonin V, Reid RC (2013) Cortico-cortical projections in mouse visual cortex are functionally target specific. Nat Neurosci 16:219–226

Chapter 6
The Rodent Vibrissal System as a Model to Study Motor Cortex Function

Shubhodeep Chakrabarti and Cornelius Schwarz

Abstract The function of mammalian motor cortex was one of the first problems studied in neuroscience. But until today, the major principles of the workings of motor cortex have remained conjectural. It is clear that motor cortex holds a topographic map of body parts. However, does that necessarily imply that motor cortex itself undertakes the challenging task of converting movement plans (i.e. intended trajectories and effects of actions) into low level motor commands appropriate for driving the muscles? Many decades of research on motor function has shown that this is not entirely true by revealing the existence of dedicated networks, the so-called central pattern generators (CPGs). Many, if not all of them, are located subcortically, and are likely to take over this task. Unfortunately the detailed circuitry and cellular elements of CPGs are only vaguely known. More recent work has elucidated continuous as well as discontinuous (discrete) mapping of motor cortex to movement. In the quest to understand motor cortex-CPG interactions, discontinuities are important because they allow us to dissect how neighboring motor cortex sites connect to different CPGs for different purposes—driving the very same muscles. The rodent whisker motor system is a decidedly modular system. Neighboring cortical areas drive very distinct whisker movements used by the animals in different contexts. We review the state of art in this system and argue that the modularity of the whisker system together with its great accessibility makes it a promising candidate for a model system for the investigation of motor cortex—CPG interactions on the cellular and network level—a highly valuable tool for the subsequent understanding of the more complex and continuously organized motor cortex of the arm/hand/finger system in primates.

C. Schwarz (✉) · S. Chakrabarti
Systems Neurophysiology Group, Department of Cognitive Neurology, Werner Reichardt Center for Integrative Neuroscience, University of Tübingen, Hertie Institute for Clinical Brain Research, Bernstein Center for Computational Neuroscience, Otfried Müller Straße 25, 72076 Tübingen, Germany
e-mail: cornelius.schwarz@uni-tuebingen.de

S. Chakrabarti
e-mail: shubo.chakrabarti@gmail.com

P. Krieger, A. Groh (eds.), *Sensorimotor Integration in the Whisker System,*
DOI 10.1007/978-1-4939-2975-7_6

Keywords Motor cortex · Whisking · Central pattern generator · Topography · Motor planning · Rhythmic whisking region

Motor Cortex Organization -General Principles

Introduction

The idea of the existence of a cortical region responsible for the control of different muscle groups was first promulgated by Hughlings Jackson in the 1870s [1], based on his observation of seizures or muscle twitches travelling across adjacent body parts in epileptic patients. These 'marching spasms', led him to postulate that the representation of these muscle groups were related to each other in the brain. Such a cortical area was indeed demonstrated by Gustav Fritsch and Eduard Hitzig [2] in their pioneering experiments involving electrical stimulation in dogs. Their experiments, as well as later work by David Ferrier [3, 4], showed that the electrical stimulation of the surface of the pre-central gyrus caused twitching or muscle contractions in various body parts, with movements elicited *'which vary in distribution as the electrodes are moved from place to place in the region, but remain very regularly similar under repeated application of the stimulus to any one and the same spot*' [5]. This attractive idea of functional topography or 'localization' in the cortex was enthusiastically received [4–7]) and soon became the established view amongst neurophysiologists and anatomists investigating the motor functions of the cerebral cortex. However, since the early days the exact nature of the observed topography or functional localization in primary motor cortex (M1), as we now know it, was intensely debated. For example, even in his very early manuscripts, Ferrier noted that the areas of electrical stimulation '*have no exact line of demarcation from each other and where they adjoin, stimulation is apt to produce conjoint the effect peculiar to each*' [8], thus suggesting that these topographically organized functional modules were by no means mutually exclusive but characterized by considerable convergence and overlap. Further, the anatomical classification of the pre-central gyrus as motor cortex was found to be simplistic and the gyrus was soon sub-divided, based on histological parameters, into pre-motor and motor cortices [9].

The Nature of Topography in the Motor Cortex

The improvement and refining of stimulation techniques over the next 50 years and the establishment of intracortical microstimulation (ICMS) by Hiroshi Asanuma and colleagues in the 1960s and 1970s, allowed cortical motor maps to become increasingly refined and a number of motor map representations were described in

different species such as the human [10, 11], the monkey [12, 13], the dog [14], the cat [15, 16], the mouse [17–19], and the rat [20]. Using ICMS, Asanuma and his coworkers were able to evoke movement of body parts by advancing an electrode to layer V of the motor cortex and using only micro-ampere current levels, thus limiting the current spread within cortex [12, 21–23]. The detailed cortical motor maps elucidated using ICMS, clearly showed that M1 consisted of a heterogeneous 'mosaic of small discrete zones' with particular muscles receiving convergent input from a wide area of cortical surface. Further, from an anatomical perspective, the existence of long range horizontal connections in motor cortex [24, 25], and the large divergence/convergence of widespread cortico-spinal motor cortex neurons onto motoneurons [26–32], presumably integrating diverse inputs to diverse sets of muscles, strongly argue against the presence of a precise map of muscles in M1. Marc Schieber postulated that the cortical representations on the larger scale that had been described earlier could have in fact been due to the concurrent excitation of many such scattered zones with high currents [22].

The Progression from Topography to Functional Modules

Thus, the nature of the M1 representation and specifically its output map has been the subject of intense speculation following the studies in the late 1970s and early 1980s demonstrating the mosaic like pattern of the motor cortical map which possessed only a very basic topography. These findings led to the idea that movements (rather than muscles) were represented in the vertebrate motor cortex. An expression of this notion was the idea, first formulated by Apostolos Georgopoulos and colleagues, that variables describing the trajectories of movements, like the direction of movement, rather than patterns of muscle activity are coded by motor cortex [33–36]. Michael Graziano and colleagues addressed this debate in the early 2000s by demonstrating that long trains of electrical stimulation elicit complex, behaviorally relevant, multi-joint movements such as feeding and defensive postures and that the sites evoking these various movements were clustered on the surface of M1. Comparing trajectory endpoints of those complex movements evoked from neighboring points on the cortical surface, they suggested that large parts of primary motor and premotor areas map trajectory endpoints in 3D space surrounding the body [37–41]. This phenomenon is unlikely to be generated by direct connections of motor cortex to spinal motoneurons, because activation patterns of ICMS are bound to be highly artificial, and therefore not appropriate for coordinating movements from the animals' own natural repertoire. Which and where, then, are the downstream circuits that can be activated by ICMS to evoke naturalistic movements? A possible solution to this problem comes from the observation that the movements described by the Graziano group resemble the force fields obtained in the work of Emilio Bizzi by direct spinal stimulation in frogs. Force fields are movements that end at a certain end point irrespective of the initial position of the moved limb [42, 43]. It is therefore feasible that functional modules characterized

by their specific connections to varied and dedicated (subcortical) central pattern generators (CPGs) contribute to the ICMS-evoked movements. Another possibility is that cortico-cortical projections are part of the CPG and are able to drive muscles in a meaningful way by activating cortico-spinal projections remote from the directly stimulated site. The latter is, however, a conceptually difficult view as it reduces the local cortical circuits in M1 to an on/off switch that merely activates other cortical circuits. The reason is the already mentioned fact that ICMS severely disrupts local cortical activity: highly synchronous rhythmic activity directly evoked by the electrical pulses is accompanied by a strong activation of inhibitory circuits leaving no room for the devolution of naturalistic local neuronal dynamics [44]. Thus, if cortico-cortical projections are involved, the ICMS-evoked movements are the expression of activity in coupled cortical sites *minus* the one that is directly activated. Further, it fails to explain why the local disruptive activity has no impact on the performance of the movement at all. We therefore support the more parsimonious explanation that subcortical CPGs take the major part in generating these movements. The existence of subcortical CPGs is well documented and their circuitries are thought to be hardwired, a factor that adds weight to the view that they are a major contributor to the generation of naturalistic movements as seen with long ICMS.

CPGs have long been known to drive rhythmic movements such as sniffing, whisking, licking, mastication, and locomotion in different mammals [45–47]. In more simple examples of rhythmic movement, like mastication and whisking, it has been demonstrated that cortical microstimulation is able to drive the CPG [46, 48]. The CPG dedicated to generate whisking movements in rats, has now been discovered and its sub-cortical location has been confirmed [47]. The exciting part of this discovery—to be elaborated in more detail below and in Chap. 7 by Moore, Deschênes and Kleinfeld—is that the CPG is confined to a small cluster of cells in the reticular formation, thereby affording an excellent opportunity to be targeted and studied in its entirety on the cellular and micro-circuit level. The case of locomotion is more complex. Although not activated by simple microstimulation in M1, a large body of work, originating with Charles Sherrington and Graham Brown, making use of spinalized and deafferented animals, indicates that a CPG for locomotion exists on the spinal level in vertebrates including cats, dogs and monkeys [49, 50]. Further, the performance of the spinal CPG for locomotion can be improved by electrical stimulation and pharmacological intervention [45, 51, 52]. The situation in the monkey arm and hand motor system is even more elaborate. The challenge here is that arm/hand and finger movements generate trajectories that are continuously mapped in 3D space and that a respective continuous mapping has been found in the motor cortex [38]. Thus, if CPGs for these movements exist, they would have to be organized in a continuous fashion as well: an incremental change in location within M1 would result in an incremental change of activation and/or recruited subset of a presumed reaching CPG. With respect to the quest to prove the existence of CPGs and to elucidate their properties, these are complicating factors and do not constitute favorable experimental

preconditions, because incremental changes can always be interpreted as incremental different neuronal activity in motor cortex driving the muscles directly. For instance, it has been recently demonstrated that motor cortex population activity shows signs of quasi-rhythmicity expressed as rotatory components in the state space trajectory of population firing [53, 54]. These findings clearly liken what can be called motor cortex attractor dynamics to rhythmic activity classically attributed to CPGs. For hand reaching movements in primates at least, these results therefore, could be interpreted in favor of motor cortex participation in CPG activity (i.e. transforming motor plans to concrete patterns of muscle activity and sending such signals directly to the muscles), an idea fitting the mentioned existence of direct connections between motor cortex and motoneurons in these animals. However, the fact that complex and naturalistic arm and hand movements can be readily evoked by ICMS in M1 [38], omitting any preparatory activity and completely disrupting local neuronal dynamics, speaks against this view. Thus, whatever the reason might be for rotatory attractor dynamics during preparation and execution of reaching movements in motor cortex, rotatory attractor dynamics do not seem to be necessary for the type of arm/hand movements observed with long ICMS in motor cortex.

In summary, at present it is not clear which signals M1 holds—ideas and convincing underlining evidence range from abstract variables within an attractor network [54], via dynamic variables [55, 56] to kinematic variables [33]. Whatever M1 does, it becomes increasingly clear that it organizes movements on a rather abstract control level. The detailed conversion of M1 signals into detailed muscular commands is largely done by sub-cortical CPG networks of quite variable degrees of complexity. In primates this statement seems to be generally true as well, despite the existence of direct connections of M1 (and S1) to motoneurons [32]. Our lack of knowledge about the organization of even the simplest of these CPGs may thus be the main reason why deciphering the M1 signals strikes us as an insurmountable problem. The general abstinence of M1 from direct muscular activation does not mean that the mentioned signals—from attractor to kinematics—are not needed on its level of organization. They all are plausible constituent parts of sensorimotor and cognitive processes leading to the generation of flexible and meaningful movement. However, we still do not know whether and in which form each of these signals must be fed to the varied CPGs to realize the intended movement. The consequence in the search for promising experimental strategies is that we need simple model systems in which CPGs are organized in a very simple, accessible fashion. Also we deem it advantageous if motor cortex mapping is discrete with quite different classes or types of movement mapped within the confines of motor cortex topography. This would allow us to find out if discontinuous changes of movements evoked from neighboring cortical sites are matched by corresponding changes of sub-cortical connections to entirely different CPGs—greatly increasing the chances to identify their existence. In the rest of this article we will review the rat vibrissal motor system and argue that its modularity offers great potential to be highly useful for the outlined experimental strategy.

The Organization of the Rat Vibrissal Motor Cortex (VMCx)

Spatial Extent and Motor Map of Rat Motor Areas

The rat M1 was first studied using surface stimulation [57] before several investigators further elucidated these maps in great detail using ICMS [20, 58, 59–62]. The first ICMS-based map of rat M1 [20] confirmed the location of M1 to be in the frontal and dorsomedial areas of neocortex and a movement map that represents large body parts in a topographical fashion (Fig. 6.1). M1 agranular cortex is composed of a lateral and medial agranular area (AGl and AGm). AGm occupies an area of ca. 1.5 mm along the midline and stretches down the medial bank bordering there to cingulate cortex. AGl is a wedge-shaped patch of motor cortex sandwiched by AGm medially and S1 laterally. AGm and AGl differ in the relative thickness of layers 3 and 5. Layer 3 is prominent in AGl, but thins toward AGm within a transition zone (TZ). Layer 5 shows the reverse tendency—it is relatively thick in AGl and then thins down in TZ to reach medium thickness in AGm [63–65]. An ICMS study [60] and an in vivo intracellular study [66] revealed that the border between AGm and AGl aligns with the border between the vibrissal and the trunk/paw representations. Matching this observation, AGm sends its major projection to the superior colliculus while AGl's main target is the spinal cord [60].

The degree to which M1 extends toward the frontal pole and its functional boundaries with either premotor [60, 67–69] or prefrontal [70] cortices are yet to be determined. The rostral parts of AGm and medially adjoining dorsal anterior cingulate area (ACd) have been referred to as 'dorsal shoulder region' [70]. The dorsal shoulder includes regions with cortico-spinal projections from which forelimb, hindlimb and vibrissal motor responses can be evoked using low threshold ICMS [60, 61, 71] but otherwise show connectivity patterns to other cortical areas, the thalamus, amygdala and basal ganglia and functional properties, that align well with those reported from prefrontal and premotor areas in primates [70]. We will refer to this area as the premotor and prefrontal area (PMPF) acknowledging that more detailed work has to be done to delineate possible subareas and identify its specific functions. The rostral extent of M1 is farthest on the lateral convexity reaching approx. 5 mm anterior to Bregma with large representations of tongue and jaw movements. Closer to the midline, the anterior limit of M1 reaches to approx. 3 mm anterior to Bregma with vibrissae and neck representations bordering PMPF. On the medial bank AGm is delimited along its total rostro-caudal extent by the ACd holding eyelid and oculomotor representations that have been likened to the frontal eyefield in primates [20, 60, 72].

The representation of the vibrissae within M1 (VMCx) is confined to the AGm, and appears to be largely magnified, occupying around 20% of the motor cortical area. Some authors have found single vibrissae responses, but no study so far has been able to come up with a generally accepted topographic map of the vibrissal

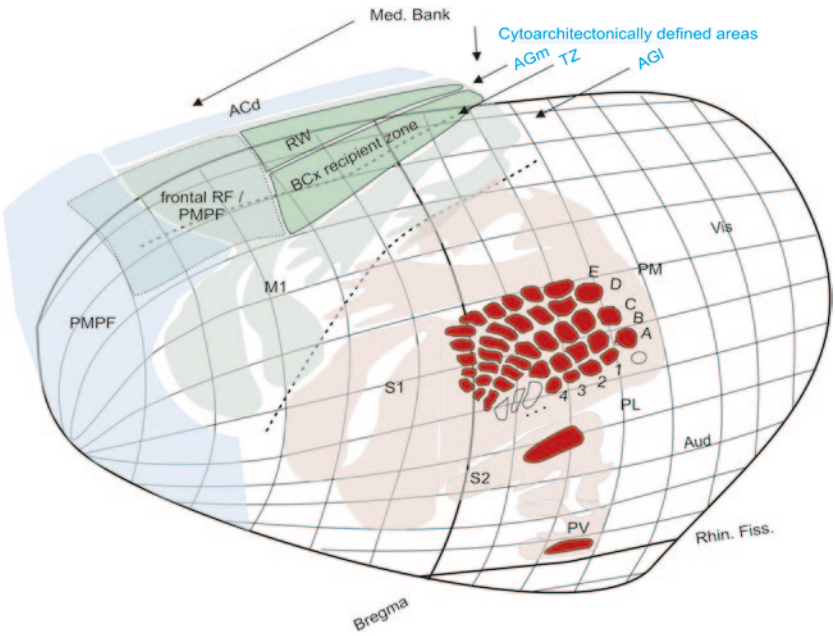

Fig. 6.1 A surface map of the rat sensorimotor cortex. The primary somatosensory cortex (*S1*) and tactile, partly multimodal, association areas are depicted in *light red*. Motor areas are in *light green* and premotor/prefrontal areas in *light blue*. Classification of areas using functional criteria has been shown in black and that using cytoarchitectonic criteria in blue. The strong colors indicate whisker representations. The modularity of the primary motor cortex (*M1*) whisker representation (*VMCx*) is indicated. The rhythmic whisker area (*RW*) reaches the dorsal surface of the neocortex but likely extends well into the medial bank. The barrel cortex recipient transition zone (*TZ*) is located on the dorsal surface of the neocortex. Frontal RF and whisker representations in the premotor/prefrontal cortex (*PMPF*) are little investigated. Their delineation is unclear and within *PMPF* the detailed topography of limb and head representations is not consistent in the data available today. To indicate this uncertainty, these modules have been paled in color and limits are depicted by broken lines. *ACd* dorsal anterior cingulate cortex, *AGm* medial agranular cortex, *AGl* lateral agranular cortex. Thick broken lines indicate borders between *AGm* and *AGl* and between *AGl* and *S1*. *S2* secondary somatosensory cortex, *AGm* houses the head and whisker representations while *AGl* houses trunk and limb representations (indicated by arrows), *PV*, *PL*, *PM* posterior ventral, lateral and medial cortex, Aud auditory cortex, Vis visual cortex. Med. Bank medial bank of the hemisphere (the parts of the map extending into the medial bank are folded up for clarity. Rhin. Fiss. rhinal fissure. The coronal section line corresponding to anterior–posterior coordinate 0 is labeled Bregma

pad. Rather the number of moving whiskers was reported to depend on the type and depth of anesthesia. Evoked movements in awake animals and lightly ketamine anesthetized animals were observed to encompass many if not all whiskers while other anesthetics, and generally deep anesthesia decreased number of moving whiskers [48, 72]. Even single cell intracellular stimulation in vivo consistently yielded movement of several whiskers, supporting the hypothesis that muscle synergies rather than individual muscles are represented in VMCx [66].

The Connectivity of the Rodent Vibrissal Motor Cortex (VMCx)

Cortical Connections

Rodent vibrissal motor cortex (VMCx) is densely connected with virtually all other vibrissal representations in the cortex including the primary and secondary somatosensory areas (S1 and S2), the multimodal areas located around S1 (posterolateral, PL, -medial, PM, -ventral, PV, and perirhinal areas PR), and VMCx in the contralateral hemisphere. The arguably most important afferent projection to VMCx originates from S1 barrel cortex (BCx). The predominant source of these afferents are septal columns, the slabs of barrel cortex that separate barrel columns from each other and receive signals from the paralemniscal pathway [64, 73–83]. The BCx-VMCx projection is likely the main source of tactile inputs to the VMCx as tactile responses are largely abolished after inactivation of BCx [74, 76, 84]. There is an interesting anisotropy of projection with respect to rows and arcs of barrel columns that correspond to the rows and arcs of whiskers on the whisker pad [85]. Septal regions located along rows show significantly greater convergence of afferent fields in VMCx, than the one along arcs [86]. The BCx-VMCx projection is reciprocal and involves L2/3 and L5a neurons in both structures [76, 80, 84, 87, 88]. Importantly, BCx projections do not reach the whole VMCx but are limited to an area of about 1 mm extent in the medio-lateral direction straddling TZ [64]. VMCx regions medial to TZ, like the so-called rhythmic whisking area (RW), do not respond to whisker touch [89]. These facts will be discussed in detail in the next chapter.

S2 terminals intermingle with the ones originating from S1 in the TZ [64, 77, 82] while projections from the posterior parietal cortex (PPC, some refer to this area as posterior-lateral and/or posterior-medial areas PL, PM) terminate in AGm adjoining the TZ [64, 77, 90, 91]. VMCx connections to other somatosensory areas located lateral to S2, PV and PR, have been reported as well, but the exact termination zone within AGm, TZ and AGl has not been determined [77, 79, 82, 92, 93].

The VMCx on both hemispheres are strongly interconnected with each other [81, 94]. When compared in detail [77] the bilateral interconnection of VMCx is significantly stronger than the one found in M1 forelimb representation. This may well have implications for the bilateral co-ordination of whisking as has been observed in many behavioral studies [95–97].

Thalamic Connections

Apart from its extensive cortical connections, VMCx has both afferent and efferent connections with various thalamic nuclei. The main thalamic nuclei which are reciprocally connected with the ipsilateral VMCx are the mediodorsal group of nuclei (MD), the centrolateral group (CL) and the medial aspect of the posterior nucleus

(POm). In addition, mirroring the extensive reciprocal connections between VMCx of both hemispheres, the ventrolateral group of thalamic nuclei (VL) receive projections from both ipsilateral as well as contralateral VMCx [81, 98–102], perhaps related to the need to bilaterally coordinate whisker movements [98, 99].

The reciprocal projections between the POm and the VMCx have been hypothesized to play a vital role for the gating of ascending information via the paralemniscal pathway by descending motor commands—an example of sensorimotor integration occurring at the corticothalamic level. VMCx might be involved in the gating of sensory transmission through the thalamic station of the paralemniscal pathway (POm) by releasing it from the inhibitory drive of the zona incerta [103–105].

Other Sub-Cortical Connections

In addition to the thalamus, VMCx also projects to several other sub-cortical structures such as the ponto-cerebellum [106], dorsolateral neostriatum [99, 107], and the claustrum [108, 109]. Which then are the critical pathways conveying VMCx activity to the vibrissal musculature? Direct connections of the VMCx to the motoneurons in facial nucleus innervating the vibrissal pad have been reported to be either absent or extremely sparse [81, 110–112], so that, in our view, direct control of motoneurons can be assumed to be of minor importance. VMCx, however, does project strongly to a number of intermediate structures in the midbrain and brainstem that project in turn to the facial nucleus and thus must be considered candidate projections connecting VMCx to distinct CPGs driving vibrissal movements and coordinating them with head and body movements. Specifically, candidates for an oligosynaptic connection between VMCx and the facial nucleus have been reported to be the reticular formation, superior colliculus, nucleus ambiguus and the deep mescencephalic nucleus, the periacqueductal gray, the interstitial nucleus of the medial longitudal fascicularis, and the red nucleus [81, 110, 112, 113].

Functional Modules in Rat Vibrissal Motor Cortex

As discussed for the primate motor cortex in the introduction, there is mounting evidence that VMCx is systematically connected to different CPGs, and thus, represents different types of whisker movement in a modular fashion. At present four such candidate modules can be distinguished. There are three presumptive modules in VMCx, two of which have been identified by the different kinds of movements evoked by long ICMS in awake animals, a smaller caudo-medial one evoking rhythmic whisking (RW) and a larger fronto-lateral one evoking whisker retraction accompanied with other face but also body movements (RF) [48]. RF as originally defined by the study of Haiss and Schwarz can be further sub-divided into two areas. One located between the AGm and AGl and therefore named the transitional

zone (TZ) is distinguished by sensorimotor connectivity [64] whereas a frontal area, frontal RF, is devoid of tactile inputs. Both give rise to retraction movements with long ICMS, but the TZ differs greatly from RW and frontal RF by the reception of the strong afferent inputs from BCx. A fourth possible module is located rostral to M1 in vibrissal representation of PMPF [61, 70] (Fig. 6.1).

It appears likely that the functional properties of frontal RF and its delineation from the whisker representations in the PMPF has never been studied in detail. The dorsal shoulder region shows clear separation of its limb representation from those in M1 but has confluent representations of the head and whiskers [61] (i.e. with frontal RF). Based on connectivity [61] and visuomotor function [114] PMPF may be analogous to the premotor cortex of primates. Others likened its connectivity and function to prefrontal areas in monkeys [70]. PMPF and frontal RF, and their delineation, continue to be poorly defined. Long ICMS stimulation in the awake animal in these frontal areas as well as more detailed experiments aimed at functional properties of these areas are missing. In the following we therefore focus on the two modules that were analyzed in functional terms by several studies, the RW and the TZ (Fig. 6.2).

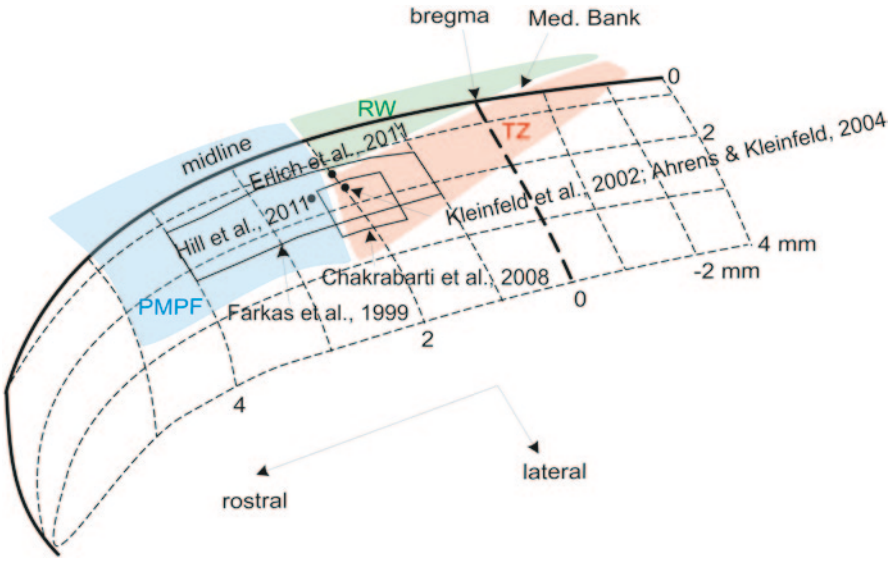

Fig. 6.2 Modules of VMCx as seen in the plane spanned by the anterior-posterior and the medial-lateral stereotactic axes. Coordinates used in previous studies to record VMCx neurons are indicated by *dots*,or rectangles, and functionally defined VMCx modules by colored patches. Other abbreviations as in Fig. 6.1. It is likely that most if not all previous studies that did not functionally characterize the recorded area using ICMS landed in *TZ*

RW

Guided by the work of Graziano in the monkey, and an earlier study in the rat, describing separate whisker protraction and retraction motor regions [71], Haiss and Schwarz [48] used long pulse trains at 60–100 Hz in awake, chronically implanted rats. They found that VMCx could be sub-divided into two distinct regions, that caused whisker retraction and complex face movements (RF), and another that caused naturalistic rhythmic whisking without any other movements (RW). The presence of RW and RF modules were confirmed also in the mouse VMCx [115].

The rhythmic whisking trajectories initiated by electrical stimulation in the RW region were virtually indistinguishable from self-initiated whisking and occurred at natural frequencies [48] (Fig. 6.3a). Under anesthesia, depending on the anesthetic, these rhythmic movements are either strongly reduced or absent [48, 116]. Electrophysiological recordings in RW in awake whisking rats [89] revealed that kinematics of whisker movement is coded exclusively on a slow time scale (in the range of seconds) excluding any contribution of RW to the computation of whisker trajectories on a stroke-by-stroke level which typically happens in the frequency range between 7 and 12 Hz (Fig. 6.3b). Two independent variables describing whisker movements are encoded. One is the whisker position and the other is either velocity, intensity or frequency (the three latter variables appeared highly correlated within a typical whisking trace). Preparatory activity before onset of whisker movement was not found (but see [117]) and many neurons are in fact active during whisker rest and decrease their firing rate during movement. These findings are not compatible with the notion of a low level motor function of RW and fit the known presence of a rhythmic whisking CPG located in the ventral part of the intermediate band of the reticular formation (vIRt, medial to the ambiguous nucleus pars semicompacta and near the pre-Bötzinger complex) [47] (Fig. 6.3c). The slow positional RW signals can be interpreted as coding for the set point (i.e. the average whisker position during a whisking bout) while slow velocity/intensity/frequency signals may set general parameters of rhythmic movements around that set point. Further, RW may provide a go (movement cells) and stop signal (rest cells). These high level movement signals together with the confined location of the rhythmic whisking CPG in the brainstem are promising cornerstones for future establishment of a model system of M1-CPG interaction. Neural activity in the rhythmic whisking CPG shows phase locking to different phases of the whisker rhythm. Following CPG inactivation, rhythmic whisking is abolished [47] (Fig. 6.3c). Once the connectivity of RW and/or other modules to the rhythmic whisking CPG is morphologically clarified, this model system has a good chance to be simple and confined enough to be amenable to decipher the functionality of local CPG circuits and their modulation by corticofugal terminals. The possibility that RW lacks significant preparatory activity and conveys information about the whisking trajectory of the past as well as the one in the future, suggests that RW may causally influence as well as monitor whisking movement [89]. An interesting further possibility would involve the reciprocal interaction of RW with the rhythmic whisking CPG.

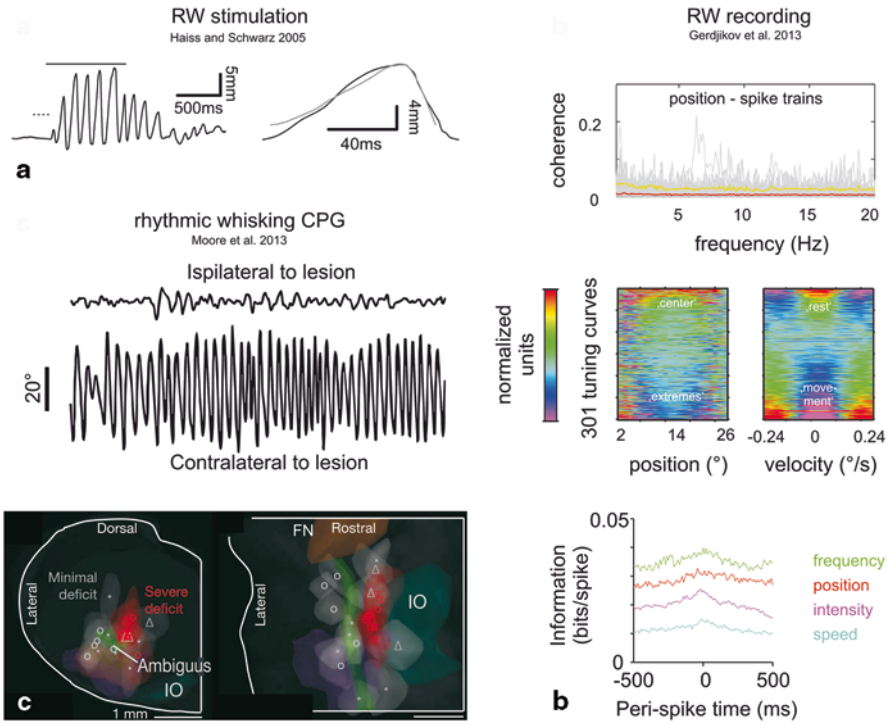

Fig. 6.3 Functional organization of *RW* and *rhythmic whisking CPG*. **a** Rhythmic whisking evoked by long ICMS in RW. The line above the whisker trace on the left indicates the duration of 60 Hz ICMS. *Right*: Individual strokes, one evoked by ICMS (*thin line*) and another voluntarily generated by the rat (*thick line*). Note the close similarity between the two. Modified to demonstrate recent data from Haiss and Schwarz (2005). **b** Unitary recordings from *RW* in awake head-fixed animals engaged in a whisking task. Top: Coherence between the spike train and the whisker position trace. The coherence function of all *RW* units is low and flat, excluding any significant stroke-by-stroke coding in *RW* (line colors: *gray*: individual single ($n=301$) and multi units ($n=261$); *red*: median of distribution; *yellow* 90 % percentile). *Center*: Color coded tuning curves for position (*left*) and velocity (*right*) calculated from spike trains of 301 single units. The tuning strength (rainbow color code *violet-blue-green-yellow-red*) is scaled in normalized units. Note that the neurons' tuning curves were ordered according to the coefficient of the first principle component obtained from the sample of tuning curves to reveal different types of tuning (i.e. lines in the two panels do not correspond to the same cell). *Bottom*: Average Shannon information carried by a single *RW* spike about the whisker trajectory at a certain latency. Information transferred from different whisking variables is shown. A bootstrap procedure using scrambled spike trains indicated that the majority of *RW* neurons convey significant information about the whisker trajectory. Importantly, information about a large interval around the spike (time 0) is present, making a pure causal role of RW for whisker movement unlikely. Modified to demonstrate recent data Gerdjikov et al., (2013)**c** The rhythmic whisking CPG. *To*p: Two whisking traces ipsilateral and contralateral of the electrolytic lesion in the medulla are shown. Rhythmic whisking requires intactness of the lesioned site in the medulla. *Bottom*: Effective lesion (*red* symbols) sites in the medulla as seen in the frontal (*left*) and horizontal plane (*right*). The location of the rhythmic whisking CPG is in the ventral intermediate band of the reticular formation (vIRt). *Abbr.*: FN: facial nucleus, *IO*: inferior olive. *Ambiguus*: Nucleus ambiguous. Modified to demonstrate recent data from Moore et al., (2013). See Chap. 10 in this volume for more detailed discussion

Another phenomenon that deserves clarification arose from experiments in RW of awake mice. Rhythmic whisking evoked from ICMS responses [115] has been shown to dependent on the function of the barrel cortex [118]. If barrel cortex function is blocked, ICMS at sites within VMCx, hitherto eliciting retraction typical for RF, changed to elicit rhythmic whisking typical for RW. A systematical assessment of this finding across M1 sites that do and do not receive BCx projections has not been performed, so it is not clear if the BCx dependent RF sites were located within TZ.

TZ

We define TZ as a zone that responds to long ICMS with whisker retraction movements, and receives direct tactile inputs originating from septal columns in BCx as described using tract tracing and electrophysiology [64, 73–83]. Judged from reported coordinates of electrode penetration all of the studies discussed below are likely to have recorded TZ activity (Fig. 6.2). We therefore discuss them tentatively here, under the heading of TZ. The inactivation of S1 barrel cortex has been shown to abolish sensory responses from M1 of anaesthetized rats to peripheral whisker stimulation [74, 76, 84]. Such responses were reported to be either low-pass filtered version of BCx responses [119], or fast transients followed by a strong inhibition, like the responses known from BCx [76, 84]. Whether these discrepancies are due to differences in preparation (anesthesia) or differences in recorded sites within M1 must await experimental clarification. Using LFP recordings, M1 neurons, most likely located also in TZ were reported to represent the rhythmicity of the movement [120]. Unit recordings at around the same sites, did not confirm that whisker rhythm was a major determinant of M1 neurons' activity. Modulation of unit firing rate with the whisker rhythm was weak and infrequent [121]. Over-representing the best of these rare units in a probabilistic model enabled Hill and coauthors to reconstruct the detailed whisker trajectory from synthesized population activity. However, whether such a biased read-out is actually realized in M1 remains an open question. It is further not clear how the suggested coding for detailed whisker trajectory [121] can be reconciled with the whisker retraction and other body movements observed with long ICMS form this area [48]. A closer match between ICMS-evoked movements and the neuron's movement representation was found in a study employing an orientation task [122] that likely reports about TZ recordings as well (Fig. 6.2). These authors found that individual neurons coded well for the direction of an orientation response, which typically consisted in whole body orientation movements with concomitant whisker retraction. Inactivation of the studied M1 site resulted in deficits of task related orientation movements. Further, the significant correlation of spike activity with orientation direction, present even in a memory period before execution of the movement found by Erlich and coauthors, together with the earlier results with long ICMS [48] argues in favor of a role of this area in the coordination of whisker, head and body movements. The CPG intercalating

these movement signals with muscles is likely to be spread out more widely involving brainstem (whiskers, face, neck) as well as spinal circuits (body). Differential analysis of brainstem connectivity of RW and TZ should help to clarify this question in the future.

Summary and Outlook

We hold that the VMCx in rodents promises to be a relatively simple and useful model system for understanding how motor cortex contributes to, and realizes movements. A widely accepted view is that motor cortex acts on diverse sub-cortical circuits, the CPGs, which take over the task to interpret the rather abstract, high level motor commands issued by motor cortex and transform them to low level motor instructions driving the muscles. It is worth pointing out that this view originates from studies in the primate motor system, which does show direct projections from M1 to motoneurons, and thus does not require to posit the existence of neuronal structures intercalated between M1 and motoneurons. The reason for the unique presence of the direct projection in primates and its detailed function is unknown. But the naturalistic movements in primates observed with long ICMS which disrupts local neuronal dynamics, is a clear indication that the main bulk of low level control of motoneurons/muscles is carried out by external CPGs. In monkeys the trajectories of reaching movements evoked by long ICMS are mapped in a continuous fashion on the surface of the cortex. However, there are instances, in which the mapping becomes discrete and modular because entirely different types of movements are mapped. In the primate motor system such an instance is an area in which defensive movements are mapped next to reaching movements involving the same muscles. Further, discrete modules may be mapped on a scale too small to be differentiated by ICMS. Arguably, such discontinuities are most promising as these are the instances where neighboring cortical sites likely take effect on disjunctive CPGs, and thus allow to dissect these connections and the associated CPGs. The VMCx offers a model system to investigate just that in great detail. Albeit the VMCx is only in the course of being established as model system, and a lot of detailed knowledge is still lacking, it seems clear that the simple whisker movement are not mapped continuously in M1 but in a modular fashion. Two modules controlling two different modes of whisker movements, rhythmic explorative whisking (RW), and whole body orientation movements together with whisker retraction (RF/TZ), have been outlined. The respective cortical modules coding for these different movement contexts are adjoining on the cortical surface but must be assumed to connect to widely differing CPG networks. Two other possible modules (frontal RF and PMPF) await to be characterized in greater detail. The modularity and discreteness of this motor system offers great promise to make headway in the understanding how motor cortex interacts with CPGs to realize the intended movement. The roadmap to make use of the vibrissal motor system for this purpose, is first a detailed and complete mapping of connectivity of the mentioned cortical

modules to sub-cortical structures. Second, the simplicity of the rhythmic whisking CPG recently found (Moore et al., 2013) needs to be exploited—best combining in vivo work with an in vitro slice preparation—to find out in detail how the CPG is internally organized and how motor cortex connects to identified cellular elements of the CPG.

References

1. Jackson JH (1958) On the anatomical and physiological localisation of movements in the brain. In: Taylor J, Holmes G, Walsche FMR (eds) Selected writings of John Hughlings Jackson on epilepsy and epileptiform convulsions. Basic Books, New York, pp 37–76
2. Fritsch G, Hitzig E (1870) Über die elektrische Erregbarkeit des Grosshirns. Arch Anat Physiol Med Wiss, 37, 300–332
3. Ferrier D (1873) Experimental researches in cerebral physiology and pathology. J Anat Physiol 8:152–155
4. Ferrier D (1874) On the localisation of the functions of the brain. Br Med J 2:766–767
5. Sherrington CS, Grunbaum AS (1901) An ADDRESS on LOCALISATION in the "MOTOR" CEREBRAL CORTEX: Delivered to the Pathological Society of London, December 17th, 1901. Br Med J 2:1857–1859
6. Beevor CE (1903) The Croonian Lectures ON MUSCULAR MOVEMENTS AND THEIR REPRESENTATION IN THE CENTRAL NERVOUS SYSTEM: Delivered before the Royal College of Physicians of London. Br Med J 2:12–16
7. Horsley V, Schäfer EA (1886) Experiments on the character of the muscular contractions which are evoked by excitation of the various parts of the motor tract. J Physiol 7:96–110
8. Ferrier D (1876) Functions of the brain. Smith, Elder & Co, London
9. Campbell AW (1905) Histological studies on the localization of cerebral function. Cambridge University Press, New York
10. Rasmussen T, Penfield W (1947) The human sensorimotor cortex as studied by electrical stimulation. Fed Proc 6:184
11. Schott GD (1993) Penfield's homunculus: a note on cerebral cartography. J Neurol Neurosurg Psychiatry 56:329–333
12. Asanuma H, Rosen I (1972) Topographical organization of cortical efferent zones projecting to distal forelimb muscles in the monkey. Exp Brain Res 14:243–256
13. Woolsey CN, Settlage PH, Meyer DR, Sencer W, Pinto Hamuy T, Travis AM (1952) Patterns of localization in precentral and "supplementary" motor areas and their relation to the concept of a premotor area. Res Publ Assoc Res Nerv Ment Dis 30:238–264
14. Buxton DF, Goodman DC (1967) Motor function and the corticospinal tracts in the dog and raccoon. J Comp Neurol 129:341–360
15. Delgado JM (1952) Responses evoked in waking cat by electrical stimulation of motor cortex. Am J Physiol 171:436–446
16. Delgado JM, Livingston RB (1955) Motor representation in the frontal sulci of the cat. Yale J Biol Med 28:245–252
17. Li CX, Waters RS (1991) Organization of the mouse motor cortex studied by retrograde tracing and intracortical microstimulation (ICMS) mapping. Can J Neurol Sci 18:28–38
18. Pronichev IV, Lenkov DN (1996) Functional mapping of the motor cortex in the white mouse by microstimulation. Fiziol Zh Im I M Sechenova 82:28–35
19. Pronichev IV, Lenkov DN (1998) Functional mapping of the motor cortex of the white mouse by a microstimulation method. Neurosci Behav Physiol 28:80–85
20. Hall RD, Lindholm EP (1974) Organization of motor and somatosensory neocortex in the albino rat. Brain Res 66:23–38

21. Asanuma H, Arnold A, Zarzecki P (1976) Further study on the excitation of pyramidal tract cells by intracortical microstimulation. Exp Brain Res 26:443–461
22. Schieber MH (2001) Constraints on somatotopic organization in the primary motor cortex. J Neurophysiol 86:2125–2143
23. Stoney SD Jr, Thompson WD, Asanuma H (1968) Excitation of pyramidal tract cells by intracortical microstimulation: effective extent of stimulating current. J Neurophysiol 31:659–669
24. Capaday C, Ethier C, Brizzi L, Sik A, van Vreeswijk C, Gingras D (2009) On the nature of the intrinsic connectivity of the cat motor cortex: evidence for a recurrent neural network topology. J Neurophysiol 102:2131–2141
25. Murthy VN, Fetz EE (1996) Synchronization of neurons during local field potential oscillations in sensorimotor cortex of awake monkeys. J Neurophysiol 76:3968–3982
26. Buys EJ, Lemon RN, Mantel GW, Muir RB (1986) Selective facilitation of different hand muscles by single corticospinal neurones in the conscious monkey. J Physiol 381:529–549
27. Fetz EE, Cheney PD (1978) Muscle fields of primate corticomotoneuronal cells. J Physiol (Paris) 74:239–245
28. Fetz EE, Cheney PD (1979) Muscle fields and response properties of primate corticomotoneuronal cells. Prog Brain Res 50:137–146
29. Lemon R (1988) The output map of the primate motor cortex. Trends Neurosci 11:501–506
30. Lemon RN, Mantel GW, Muir RB (1986) Corticospinal facilitation of hand muscles during voluntary movement in the conscious monkey. J Physiol 381:497–527
31. McKiernan BJ, Marcario JK, Karrer JH, Cheney PD (1998) Corticomotoneuronal postspike effects in shoulder, elbow, wrist, digit, and intrinsic hand muscles during a reach and prehension task. J Neurophysiol 80:1961–1980
32. Rathelot JA, Strick PL (2006) Muscle representation in the macaque motor cortex: an anatomical perspective. Proc Natl Acad Sci U S A 103:8257–8262
33. Georgopoulos AP, Kalaska JF, Caminiti R, Massey JT (1982) On the relations between the direction of two-dimensional arm movements and cell discharge in primate motor cortex. J Neurosci 2:1527–1537
34. Moran DW, Schwartz AB (1999a) Motor cortical activity during drawing movements: population representation during spiral tracing. J Neurophysiol 82:2693–2704
35. Moran DW, Schwartz AB (1999b) Motor cortical representation of speed and direction during reaching. J Neurophysiol 82:2676–2692
36. Schwartz AB, Moran DW (1999) Motor cortical activity during drawing movements: population representation during lemniscate tracing. J Neurophysiol 82:2705–2718
37. Aflalo TN, Graziano MS (2006) Possible origins of the complex topographic organization of motor cortex: reduction of a multidimensional space onto a two-dimensional array. J Neurosci 26:6288–6297
38. Graziano M (2006) The organization of behavioral repertoire in motor cortex. Annu Rev Neurosci 29:105–134
39. Graziano MS, Aflalo TN (2007) Mapping behavioral repertoire onto the cortex. Neuron 56:239–251
40. Graziano MS, Taylor CS, Moore T (2002a) Complex movements evoked by microstimulation of precentral cortex. Neuron 34:841–851
41. Graziano MS, Taylor CS, Moore T (2002b) Probing cortical function with electrical stimulation. Nat Neurosci 5:921
42. Bizzi E, Cheung VC, d'Avella A, Saltiel P, Tresch M (2008) Combining modules for movement. Brain Res Rev 57:125–133
43. Bizzi E, Mussa-Ivaldi FA, Giszter S (1991) Computations underlying the execution of movement: a biological perspective. Science 253:287–291
44. Butovas S, Schwarz C (2003) Spatiotemporal effects of microstimulation in rat neocortex: a parametric study using multielectrode recordings. J Neurophysiol 90:3024–3039
45. Grillner S (2006) Biological pattern generation: the cellular and computational logic of networks in motion. Neuron 52:751–766

46. Huang CS, Hiraba H, Murray GM, Sessle BJ (1989) Topographical distribution and functional properties of cortically induced rhythmical jaw movements in the monkey (Macaca fascicularis). J Neurophysiol 61:635–650
47. Moore JD, Deschenes M, Furuta T, Huber D, Smear MC et al (2013) Hierarchy of orofacial rhythms revealed through whisking and breathing. Nature 497:205–210
48. Haiss F, Schwarz C (2005) Spatial segregation of different modes of movement control in the whisker representation of rat primary motor cortex. J Neurosci 25:1579–1587
49. Brown TG (1911) The intrinsic factors in the act of progression in the mammal. Proc R Soc Lond 84:308–319
50. Sherrington CS (1947) The integrative action of the nervous system. Yale University Press, New Haven. p. xxiv, 433 pp
51. Grillner S (1975) Locomotion in vertebrates: central mechanisms and reflex interaction. Physiol Rev 55:247–304
52. Shik ML, Orlovsky GN (1976) Neurophysiology of locomotor automatism. Physiol Rev 56:465–501
53. Churchland MM, Cunningham JP, Kaufman MT, Foster JD, Nuyujukian P et al (2012) Neural population dynamics during reaching. Nature 487:51–56
54. Shenoy KV, Sahani M, Churchland MM (2013) Cortical control of arm movements: a dynamical systems perspective. Annu Rev Neurosci 36:337–359
55. Kalaska JF, Cohen DA, Hyde ML, Prud'homme M (1989) A comparison of movement direction-related versus load direction-related activity in primate motor cortex, using a two-dimensional reaching task. J Neurosci 9:2080–2102
56. Scott SH (2000) Role of motor cortex in coordinating multi-joint movements: is it time for a new paradigm? Can J Physiol Pharmacol 78:923–933
57. Settlage PH, Bingham WG, Suckle HM, Borge AF, Woolsey CN. (1949) The pattern of localization in the motor cortex of the rat. Fed Proc 8, 144
58. Gioanni Y, Lamarche M (1985) A reappraisal of rat motor cortex organization by intracortical microstimulation. Brain Res 344:49–61
59. Hicks SP, D'Amato CJ (1977) Locating corticospinal neurons by retrograde axonal transport of horseradish peroxidase. Exp Neurol 56:410–420
60. Neafsey EJ, Bold EL, Haas G, Hurley-Gius KM, Quirk G et al (1986) The organization of the rat motor cortex: a microstimulation mapping study. Brain Res 396:77–96
61. Neafsey EJ, Sievert C (1982) A second forelimb motor area exists in rat frontal cortex. Brain Res 232:151–156
62. Sapienza S, Talbi B, Jacquemin J, Albe-Fessard D (1981) Relationship between input and output of cells in motor and somatosensory cortices of the chronic awake rat. A study using glass micropipettes. Exp Brain Res 43:47–56
63. Donoghue JP, Wise SP (1982) The motor cortex of the rat: cytoarchitecture and microstimulation mapping. J Comp Neurol 212:76–88
64. Smith JB, Alloway KD (2013) Rat whisker motor cortex is subdivided into sensory-input and motor-output areas. Front Neural Circuits 7:4
65. Zilles K, Zilles B, Schleicher A (1980) A quantitative approach to cytoarchitectonics. VI. The areal pattern of the cortex of the albino rat. Anat Embryol (Berl) 159:335–360
66. Brecht M, Schneider M, Sakmann B, Margrie TW (2004b) Whisker movements evoked by stimulation of single pyramidal cells in rat motor cortex. Nature 427:704–710
67. Conde F, Audinat E, Maire-Lepoivre E, Crepel F (1990) Afferent connections of the medial frontal cortex of the rat. A study using retrograde transport of fluorescent dyes. I. Thalamic afferents. Brain Res Bull 24:341–354
68. Conde F, Maire-Lepoivre E, Audinat E, Crepel F (1995) Afferent connections of the medial frontal cortex of the rat. II. Cortical and subcortical afferents. J Comp Neurol 352:567–593
69. Preuss TM (1995) Do rats have prefrontal cortex? The rose-woolsey-akert program reconsidered. J Cogn Neurosci 7:1–24
70. Uylings HB, Groenewegen HJ, Kolb B (2003) Do rats have a prefrontal cortex? Behav Brain Res 146:3–17

71. Sanderson KJ, Welker W, Shambes GM (1984) Reevaluation of motor cortex and of sensorimotor overlap in cerebral cortex of albino rats. Brain Res 292:251–260
72. Brecht M, Krauss A, Muhammad S, Sinai-Esfahani L, Bellanca S, Margrie TW (2004a) Organization of rat vibrissa motor cortex and adjacent areas according to cytoarchitectonics, microstimulation, and intracellular stimulation of identified cells. J Comp Neurol 479:360–373
73. Alloway KD, Zhang M, Chakrabarti S (2004) Septal columns in rodent barrel cortex: functional circuits for modulating whisking behavior. J Comp Neurol 480:299–309
74. Aronoff R, Matyas F, Mateo C, Ciron C, Schneider B, Petersen CC (2010) Long-range connectivity of mouse primary somatosensory barrel cortex. Eur J Neurosci 31:2221–2233
75. Chakrabarti S, Alloway KD (2006) Differential origin of projections from SI barrel cortex to the whisker representations in SII and MI. J Comp Neurol 498:624–636
76. Chakrabarti S, Zhang M, Alloway KD (2008) MI neuronal responses to peripheral whisker stimulation: relationship to neuronal activity in si barrels and septa. J Neurophysiol 100:50–63
77. Colechio EM, Alloway KD (2009) Differential topography of the bilateral cortical projections to the whisker and forepaw regions in rat motor cortex. Brain Struct Funct 213:423–439
78. Koralek KA, Olavarria J, Killackey HP (1990) Areal and laminar organization of corticocortical projections in the rat somatosensory cortex. J Comp Neurol 299:133–150
79. Krubitzer LA, Sesma MA, Kaas JH (1986) Microelectrode maps, myeloarchitecture, and cortical connections of three somatotopically organized representations of the body surface in the parietal cortex of squirrels. J Comp Neurol 250:403–430
80. Mao T, Kusefoglu D, Hooks BM, Huber D, Petreanu L, Svoboda K (2011) Long-range neuronal circuits underlying the interaction between sensory and motor cortex. Neuron 72:111–123
81. Miyashita E, Keller A, Asanuma H (1994) Input-output organization of the rat vibrissal motor cortex. Exp Brain Res 99:223–232
82. Reep RL, Goodwin GS, Corwin JV (1990) Topographic organization in the corticocortical connections of medial agranular cortex in rats. J Comp Neurol 294:262–280
83. Tennant KA, Adkins DL, Donlan NA, Asay AL, Thomas N et al (2011) The organization of the forelimb representation of the C57BL/6 mouse motor cortex as defined by intracortical microstimulation and cytoarchitecture. Cereb Cortex 21:865–876
84. Farkas T, Kis Z, Toldi J, Wolff JR (1999) Activation of the primary motor cortex by somatosensory stimulation in adult rats is mediated mainly by associational connections from the somatosensory cortex. Neuroscience 90:353–361
85. Petersen CC (2007) The functional organization of the barrel cortex. Neuron 56:339–355
86. Hoffer ZS, Hoover JE, Alloway KD (2003) Sensorimotor corticocortical projections from rat barrel cortex have an anisotropic organization that facilitates integration of inputs from whiskers in the same row. J Comp Neurol 466:525–544
87. Sato TR, Svoboda K (2010) The functional properties of barrel cortex neurons projecting to the primary motor cortex. J Neurosci 30:4256–4260
88. Zagha E, Casale AE, Sachdev RN, McGinley MJ, McCormick DA. (2013) Motor cortex feedback influences sensory processing by modulating network state. Neuron 79(3):567–78
89. Gerdjikov TV, Schwarz C (2013) Rhythmic whisking area (RW) in rat primary motor cortex: an internal monitor of movement-related signals. J Neurosci 33(35):14193–14204
90. Fabri M, Burton H (1991) Ipsilateral cortical connections of primary somatic sensory cortex in rats. J Comp Neurol 311:405–424
91. Reep RL, Chandler HC, King V, Corwin JV (1994) Rat posterior parietal cortex: topography of corticocortical and thalamic connections. Exp Brain Res 100:67–84
92. Kyuhou S, Gemba H (2002) Projection from the perirhinal cortex to the frontal motor cortex in the rat. Brain Res 929:101–104
93. McIntyre DC, Kelly ME, Staines WA (1996) Efferent projections of the anterior perirhinal cortex in the rat. J Comp Neurol 369:302–318

94. Porter LL, White EL (1983) Afferent and efferent pathways of the vibrissal region of primary motor cortex in the mouse. J Comp Neurol 214:279–289
95. Gao P, Hattox AM, Jones LM, Keller A, Zeigler HP (2003) Whisker motor cortex ablation and whisker movement patterns. Somatosens Mot Res 20:191–198
96. Mitchinson B, Martin CJ, Grant RA, Prescott TJ (2007) Feedback control in active sensing: rat exploratory whisking is modulated by environmental contact. Proc Biol Sci 274:1035–1041
97. Towal RB, Hartmann MJ (2006) Right-left asymmetries in the whisking behavior of rats anticipate head movements. J Neurosci 26:8838–8846
98. Alloway KD, Olson ML, Smith JB (2008) Contralateral corticothalamic projections from MI whisker cortex: potential route for modulating hemispheric interactions. J Comp Neurol 510:100–116
99. Alloway KD, Smith JB, Beauchemin KJ, Olson ML (2009) Bilateral projections from rat MI whisker cortex to the neostriatum, thalamus, and claustrum: forebrain circuits for modulating whisking behavior. J Comp Neurol 515:548–564
100. Cicirata F, Angaut P, Cioni M, Serapide MF, Papale A (1986) Functional organization of thalamic projections to the motor cortex. An anatomical and electrophysiological study in the rat. Neuroscience 19:81–99
101. Hooks BM, Mao T, Gutnisky DA, Yamawaki N, Svoboda K, Shepherd GM (2013) Organization of cortical and thalamic input to pyramidal neurons in mouse motor cortex. J Neurosci 33:748–760
102. Rouiller EM, Liang FY, Moret V, Wiesendanger M (1991) Patterns of corticothalamic terminations following injection of Phaseolus vulgaris leucoagglutinin (PHA-L) in the sensorimotor cortex of the rat. Neurosci Lett 125:93–97
103. Lavallee P, Urbain N, Dufresne C, Bokor H, Acsady L, Deschenes M (2005) Feedforward inhibitory control of sensory information in higher-order thalamic nuclei. J Neurosci 25:7489–7498
104. Trageser JC, Burke KA, Masri R, Li Y, Sellers L, Keller A (2006) State-dependent gating of sensory inputs by zona incerta. J Neurophysiol 96:1456–1463
105. Urbain N, Deschenes M (2007) A new thalamic pathway of vibrissal information modulated by the motor cortex. J Neurosci 27:12407–12412
106. Schwarz C, Mock M (2001) Spatial arrangement of cerebro-pontine terminals. J Comp Neurol 435:418–432
107. Alloway KD, Lou L, Nwabueze-Ogbo F, Chakrabarti S (2006) Topography of cortical projections to the dorsolateral neostriatum in rats: multiple overlapping sensorimotor pathways. J Comp Neurol 499:33–48
108. Smith JB, Alloway KD (2010) Functional specificity of claustrum connections in the rat: interhemispheric communication between specific parts of motor cortex. J Neurosci 30:16832–16844
109. Smith JB, Radhakrishnan H, Alloway KD (2012) Rat claustrum coordinates but does not integrate somatosensory and motor cortical information. J Neurosci 32:8583–8588
110. Alloway KD, Smith JB, Beauchemin KJ (2010) Quantitative analysis of the bilateral brainstem projections from the whisker and forepaw regions in rat primary motor cortex. J Comp Neurol 518:4546–4566
111. Grinevich V, Brecht M, Osten P (2005) Monosynaptic pathway from rat vibrissa motor cortex to facial motor neurons revealed by lentivirus-based axonal tracing. J Neurosci 25:8250–8258
112. Hattox AM, Priest CA, Keller A (2002) Functional circuitry involved in the regulation of whisker movements. J Comp Neurol 442:266–276
113. Reep RL, Corwin JV, Hashimoto A, Watson RT (1987) Efferent connections of the rostral portion of medial agranular cortex in rats. Brain Res Bull 19:203–221
114. Passingham RE, Myers C, Rawlins N, Lightfoot V, Fearn S (1988) Premotor cortex in the rat. Behav Neurosci 102:101–109

115. Ferezou I, Haiss F, Gentet LJ, Aronoff R, Weber B, Petersen CC (2007) Spatiotemporal dynamics of cortical sensorimotor integration in behaving mice. Neuron 56:907–923
116. Cramer NP, Keller A (2006) Cortical control of a whisking central pattern generator. J Neurophysiol 96:209–217
117. Friedman WA, Zeigler HP, Keller A (2012) Vibrissae motor cortex unit activity during whisking. J Neurophysiol 107:551–563
118. Matyas F, Sreenivasan V, Marbach F, Wacongne C, Barsy B et al (2010) Motor control by sensory cortex. Science 330:1240–1243
119. Kleinfeld D, Sachdev RN, Merchant LM, Jarvis MR, Ebner FF (2002) Adaptive filtering of vibrissa input in motor cortex of rat. Neuron 34:1021–1034
120. Ahrens KF, Kleinfeld D (2004) Current flow in vibrissa motor cortex can phase-lock with exploratory rhythmic whisking in rat. J Neurophysiol 92:1700–1707
121. Hill DN, Curtis JC, Moore JD, Kleinfeld D (2011) Primary motor cortex reports efferent control of vibrissa motion on multiple timescales. Neuron 72:344–356
122. Erlich JC, Bialek M, Brody CD (2011) A cortical substrate for memory-guided orienting in the rat. Neuron 72:330–343

Chapter 7
The Central Pattern Generator for Rhythmic Whisking

David Kleinfeld, Martin Deschênes and Jeffrey D. Moore

Abstract Whisking and sniffing are predominant aspects of exploratory behavior in rodents. We review evidence that these motor rhythms are coordinated by the respiratory patterning circuitry in the ventral medulla. A region in the intermediate reticular zone, dorsomedial to the preBötzinger inspiratory complex, provides rhythmic input to the facial motoneurons that drive protraction of the vibrissae. Neuronal output from this region is reset at each inspiration by direct input from the preBötzinger complex. High frequency breathing, or sniffing, has a one-to-one coordination with whisking while basal respiration is accompanied by intervening whisks that occur between breaths. We conjecture that the preBötzinger complex, which projects to neighboring premotor regions for the control of other orofacial muscles, functions as a master clock to coordinate orofacial behaviors with breathing.

Keywords Whisking · Sniffing · Exploratory behavior · Respiratory patterning circuitry · Ventral medulla · preBötzinger complex

Some 50 years ago Welker [1] observed that whisking and sniffing by rodents appeared to be synchronous. More than a curious observation, it leads to the suggestion that breathing may be at the root of all rhythmic orofacial behaviors. We now

D. Kleinfeld (✉)
Department of Physics and Section on Neurobiology, University of California San Diego, 9500 Gilman Drive, La Jolla, CA 92093, USA
e-mail: dk@physics.ucsd.edu

M. Deschênes
Department of Psychiatry and Neuroscience,
Laval University, 2601 de la Canardière, Quebec City, QC G2B 2Y2, Canada
e-mail: martin.deschenes@crulrg.ulaval.ca

J. D. Moore
Graduate Program in Neuroscience, University of California San Diego, 9500 Gilman Dr., La Jolla, CA 92093, USA
e-mail: jeffrey.moore.428@gmail.com

P. Krieger, A. Groh (eds.), *Sensorimotor Integration in the Whisker System,*
DOI 10.1007/978-1-4939-2975-7_7

understand the basis for Welker's observation and, in this review, summarize the hunt for the neuronal circuitry that controls rhythmic exploratory whisking by rats [2]. This is followed by a discussion of the potential role of sniffing as carrier signal that binds different orofacial sensory inputs.

Before we begin our narrative on whisking, it is worth considering an abbreviated wiring diagram of the anatomy of the vibrissa sensorimotor system [3] (Fig. 7.1), as such circuit maps can constrain the potential mechanisms that generate behavior. The business end of the rodent vibrissa system is the mystacial pad, which includes the muscles that drive the follicles and the sensory fibers that innervate the follicles. Each follicle holds one vibrissa, a long hair, the compresses the follicle upon deflection. We see that the nervous system already forms a feedback loop at the level of the brainstem, from the trigeminal ganglion inputs through interneurons in the trigeminal nuclei and back to the facial motoneurons that drive the muscles. This di-

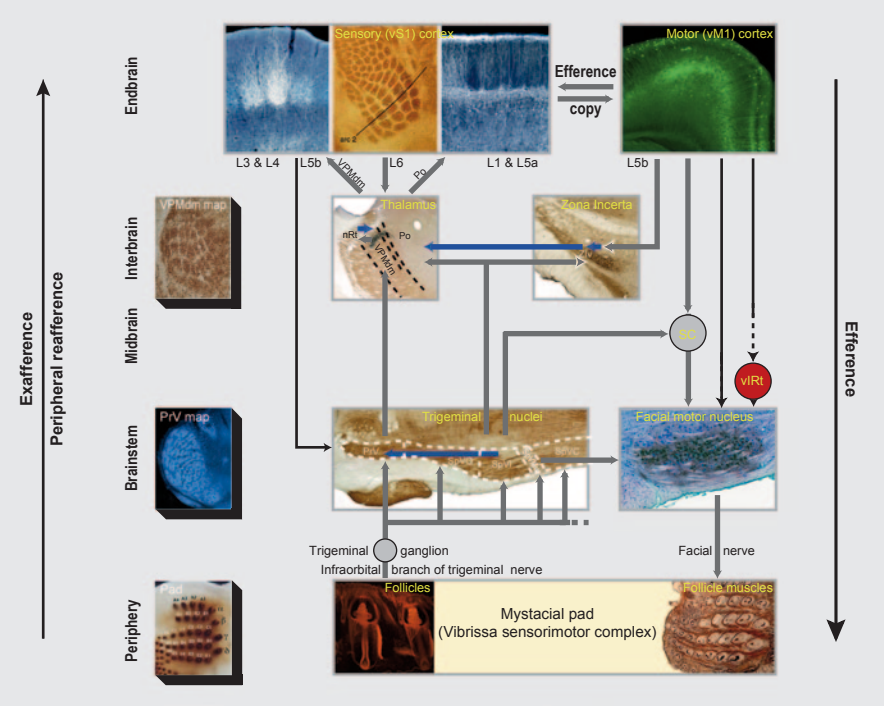

Fig. 7.1 The anatomy of the vibrissa somatosensorimotor system. Major pathways from the vibrissae to the brainstem and up through neocortex are shown. Abbreviations: PrV, principal trigeminal nucleus; SpVO, SpVI, SpVM, and SpVC, spinal nuclei oralis, interpolaris, muralis, and caudalis, respectively; VPMdm, dorsomedial aspect of the ventral posterior medial nucleus of dorsal thalamus; Po, medial division of the posterior group nucleus; nRt, nucleus reticularis; ZIv, ventral aspect of the zona incerta; SC, superior colliculus; and vIRT, the vibrissa region of the intermediate reticular zone and the central pattern generator for whisking. Black arrows indicate excitatory projections while red arrows are inhibitory projections. Adapted from [3]

synaptic feedback loop is the shortest sensorimotor pathway [4], and it is paralleled by loops that involve the cerebellum, by loops that involved the midbrain, *e.g.*, the superior colliculus, and by loops that involve the forebrain, the most extensive of which includes vibrissa primary sensory (vS1) and primary motor cortices (vM1).

What is the nature of whisking? Rodents will whisk in air as they explore a novel environment and search for objects and conspecifics [5]. The nature of whisking can change upon contact with a surface, especially as the animal turns and whisking is no longer symmetric [6, 7]. Here we focus on the case of rhythmic symmetric whisking by rats [8], in which an epoch of whisking appears almost periodic (Fig. 7.2). This suggests that, from a mathematical perspective, whisking may be conceived as a rhythmic process, with a rapidly evolving phase and a slowly evolving envelope, *i.e.*, amplitude and midpoint, much like the signals in AM radio. Formally, we can define the angle of a vibrissa relative to the face as $\theta(t)$, which evolves according to $\theta(t) = \theta_{amplitude}(t) \cdot cos\ [\varphi(t)] + \theta_{midpoint}(t)$ with $d\varphi(t)/dt = 2\pi f_{whisk}$, where f_{whisk} is the instantaneous whisking frequency [9]. This definition raises an interesting question. Does the brain drive whisking through a

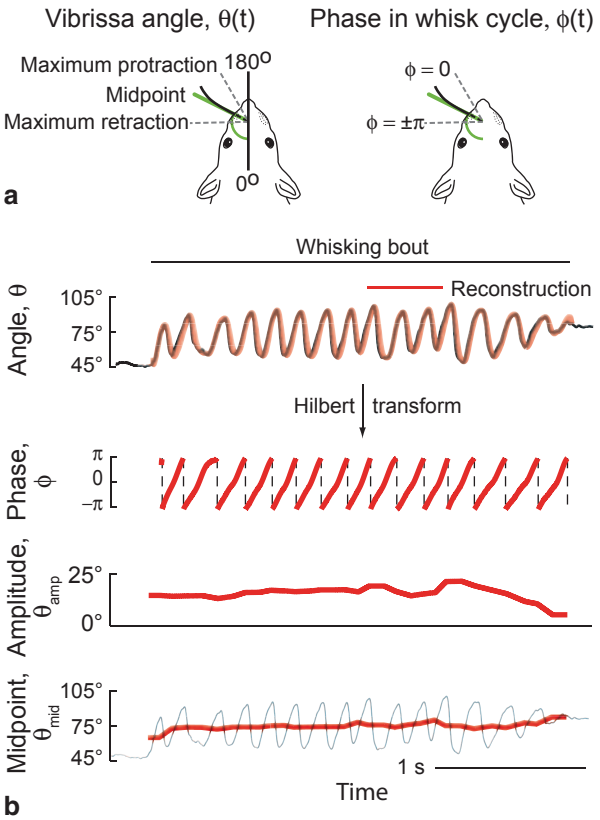

Fig. 7.2 Decomposition of rhythmic whisking into a varying phase component and slowly varying envelope parameters. **a** Schematic of the angular parameters and the representation of phase in the whisk cycle. **b** Top panel shows vibrissa angular position, $\theta(\tau)$. Lower panels show the phase, $\varphi(\tau)$, as calculated from the Hilbert transform, along with the amplitude, $\theta_{amplitude}$, and midpoint, $\theta_{midpoint}$, of the whisking angle calculated from individual whisk cycles. Broken vertical lines indicate wrapping of phase from π to $-\pi$. The red line in the top panel is the reconstruction calculated from $\theta = \theta_{amplitude} \bullet cos[\varphi] + \theta_{midpoint}$ at each time point. Adapted [11]

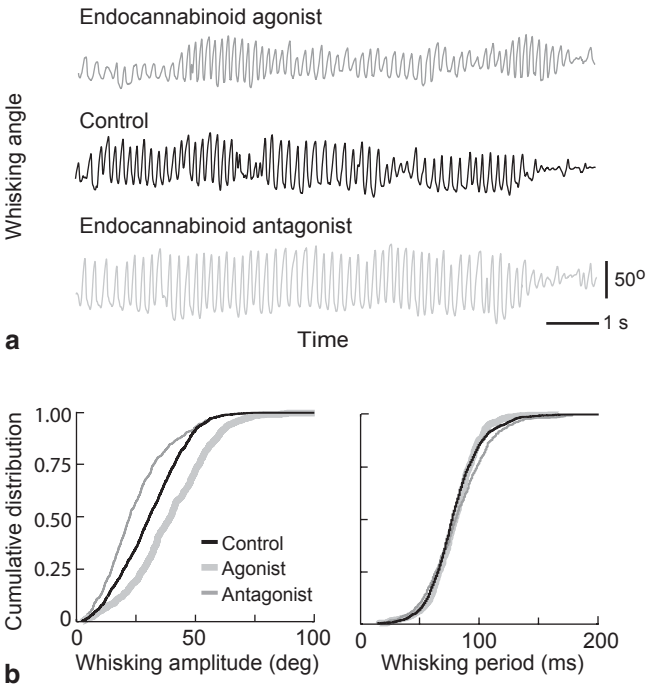

Fig. 7.3 Effect of a cannabinoid receptor type 1 agonist and an antagonist on whisking kinematics. **a** Typical traces of vibrissa angle executed by an animal four hours after administration of Δ^9-THC, an agonist (dark gray), vehicle (black), or SR141716A, an antagonist (light gray). Vertical calibration bar corresponds to 50°. **b** Cumulative probability distribution functions of protraction amplitudes and whisking durations across all animals. Adapted [10]

combination of signals, each with a different time-scale as implied by the mathematical decomposition, or is there a single control signal with a broad range of frequencies? Past experimental results suggest that nature has chosen to control whisking through narrow band signals that code on the scale of the fast rhythm, *i.e.*, roughly 10 Hz, and the slowly evolving envelope, *i.e.*, roughly 1 Hz. First, Pietr et al. [10] showed that systemic infusion of an agonist of endocannabinoid receptors leads to a decrease in the amplitude of whisking, while infusion of an antagonist to these same receptors leads to high-amplitude whisking without variation in amplitude (Fig. 7.3a). Critically, in both cases the pharmacological interventions had no effect on the frequency of whisking (Fig. 7.3b). Second, Hill et al. [11] showed that the firing patterns of neurons in vM1 cortex preferentially report the slowly varying amplitude and midpoint of a whisking bout independent of the rapidly varying phase (Fig. 7.4). These data suggest that the rapidly varying phase and the slowly varying change in the envelope of whisking are controlled by separate mechanisms.

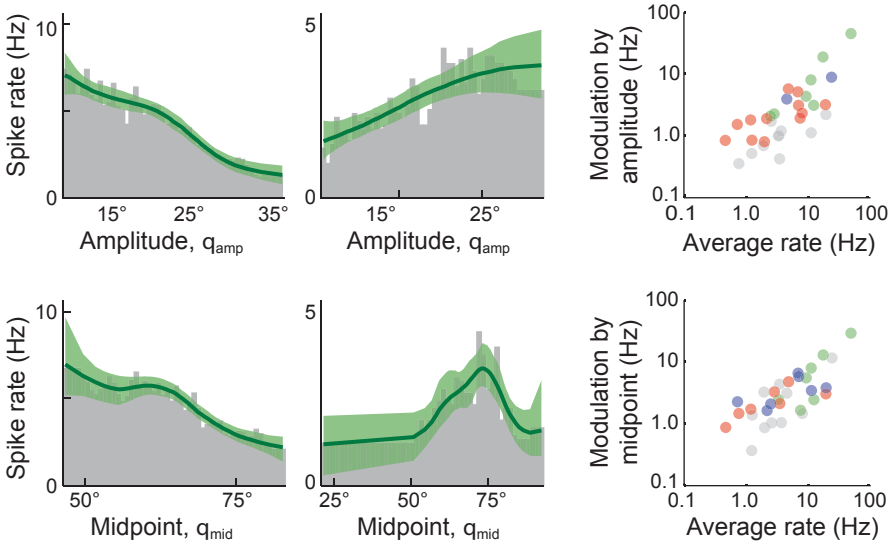

Fig. 7.4 Neurons in vM1 cortex report the amplitude and midpoint of rhythmic whisking. Firing rate profiles for two example units in vM1 cortex as a function of slowly varying parameters, *i.e.*, amplitude and midpoint, of vibrissa motion (Fig. 7.2). The left and middle columns are profiles of units that show different relative modulation. Each plot is calculated by dividing the distribution of the respective signal at spike time by the distribution of that signal over the entire behavioral session. Green lines are fits from a smoothing algorithm along with the 95% confidence band. The right column shows composite data across units and illustrates that, on average, the rate is unaffected by whisking, consistent with the presence of units that both increase (*green*) and decrease (*red*) their rate with increasing angle; blue dots correspond to a non-monotonic change. Adapted [11]

We now revisit Welker's [1] observation regarding the synchrony of whisking and sniffing. Quantitative, concurrent measurements of breathing and whisking in head-restrained and freely moving rats reveal key aspects of their coordination [2, 12] (insert in Fig. 7.5). First, breathing over a wide range of rates can occur without substantial whisking (Fig. 7.5a). To test whether whisking can also occur without breathing, a puff of ammonia was applied to the snout to inactivate the central inspiratory drive [13] and temporarily inhibit respiration. Critically, rats can whisk during such a disruption in breathing (Fig. 7.5b), which implies that the oscillator for breathing and the putative oscillator for whisking are separately gated. While sniffing is indeed accompanied by a one-to-one relation with whisking (Fig. 7.5a), basal breathing is accompanied by whisks that are coincident with an inspiration, which we denote "inspiratory-locked whisks", and also "intervening whisks" that occur between successive breaths and successively decrease in amplitude (Fig. 7.5c). Therefore there is an incommensurate many-to-one relation between whisking and breathing. These data imply that there are separate, or separable, oscillators for breathing and whisking.

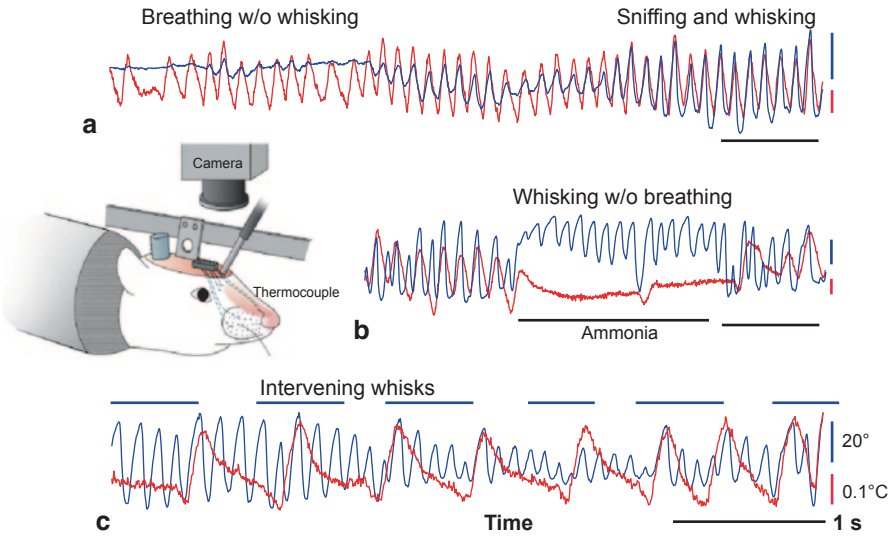

Fig. 7.5 Simultaneous measurements of vibrissa angular position (blue) and breathing (red). **a** Measurement showing epochs of breathing without whisking and sniffing with whisking. **b** Measurement showing an epoch of whisking without breathing. **c** Measurement showing breathing with intervening whisks between inspirations. These data illustrate phase resetting of whisking by breathing (Fig. 7.6). (insert) Procedure to measure whisking via videography and breathing via a thermocouple in a head-restrained rat. The additional chamber is a port for electrode measurements. Adapted [2]

The detailed timing between whisking and breathing was quantified though a frequency-ordered plot of the correlation of whisking with breathing across a large data set of whisks (Fig. 7.6). Vibrissa protractions are time-locked to the onset of inspiration across the entire range of breathing frequencies. Basal respiration cycles are accompanied by multiple whisks per breath, with an instantaneous whisking frequency of approximately 8 Hz for the intervening whisks. These data imply a unidirectional connection from the breathing oscillator [14–16] to a putative CPG for whisking and that the breathing rhythm can reset the whisking rhythm.

Where is the pattern generator for the fast, rhythmic vibrissa motion? One possibility is that rapid whisking is generated by the previously discussed disynaptic feedback loop in the brainstem. That is, sensory signals generated by the motion of the vibrissa could directly drive the facial motoneurons, which would in turn generate a new sensory signal, and so on. The frequency of whisking would depend on the presence of propagation delays in this circuit. Against this hypothesis, lesion of the sensory nerve (infraorbital nerve in Fig. 7.1) has minimal effect on whisking [1, 8, 17]; in fact the rhythmic pattern becomes more stable [8]! Similarly, lesioning of any of a large number of midbrain and forebrain nuclei only minimally interrupt whisking [1, 18]. This leads to the hypothesis that an oscillator which drives

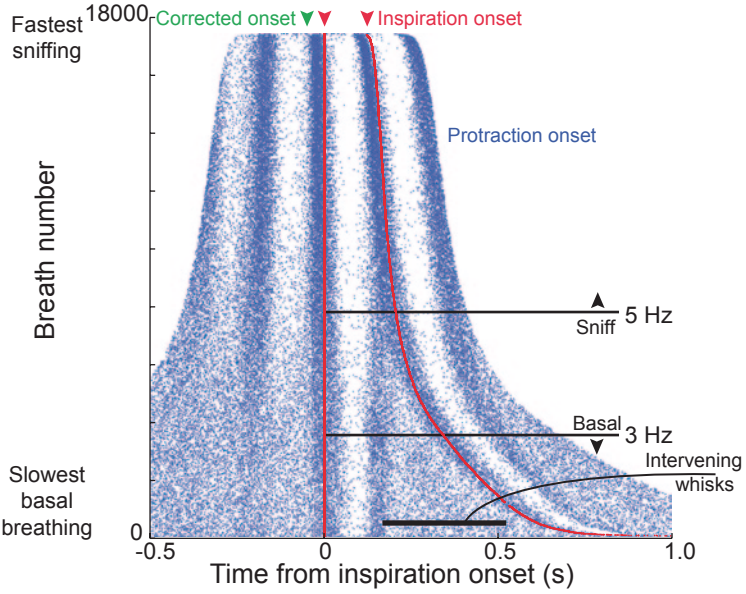

Fig. 7.6 *Reset of whisking by inspiration*. Rasters of inspiration onset times (*red*) and protraction onset times (*blue*) relative to the onset of inspiration for individual breaths are ordered by the duration of the breath; green arrow accounts for the 30 ms lead of inspiratory drive to facial muscles as opposed to the measured inspiration [46]. Whisk and inspiration onset times are significantly correlated during both sniffing and basal respiration. Adapted [2]

whisking is located in the brainstem. But where? Given the close phase relationship between whisking and breathing, the neighborhood of the ventral respiratory column in the medulla [19] is a parsimonious guess. A role for breathing in the control of whisking is further suggested by the shared facial musculature between the two behaviors [20, 21]. Lastly, the CPGs for chewing, *i.e.*, the oral portion of the gigantocellular reticular nucleus [22], for airway control, *i.e.*, the *ambiguus* nucleus [23], and for licking, *i.e.*, the medial edge of the parvocellular reticular formation bordering the IRt, are located near each other [24] and near the preBötzinger complex, which has been demonstrated to generate the inspiratory breathing rhythm [14, 25]. This collective proximity is consistent with the need to synchronize orofacial behaviors [26]. In particular, the coordination of whisking with breathing and the resetting of whisking by inspiration suggests that a brainstem whisking CPG is reset, and possibly driven, by the preBötzinger complex.

The difference in the basal respiration, at frequencies < 3 Hz, and whisking patterns provides a signature to discriminate between breathing and potential whisking neuronal centers [2] (Fig. 7.5c). As a control, we first recorded multiunit spiking activity within the preBötzinger complex as well as the rostral ventral respiratory group in awake rats,. We observed units whose spiking occurred in phase with inspi-

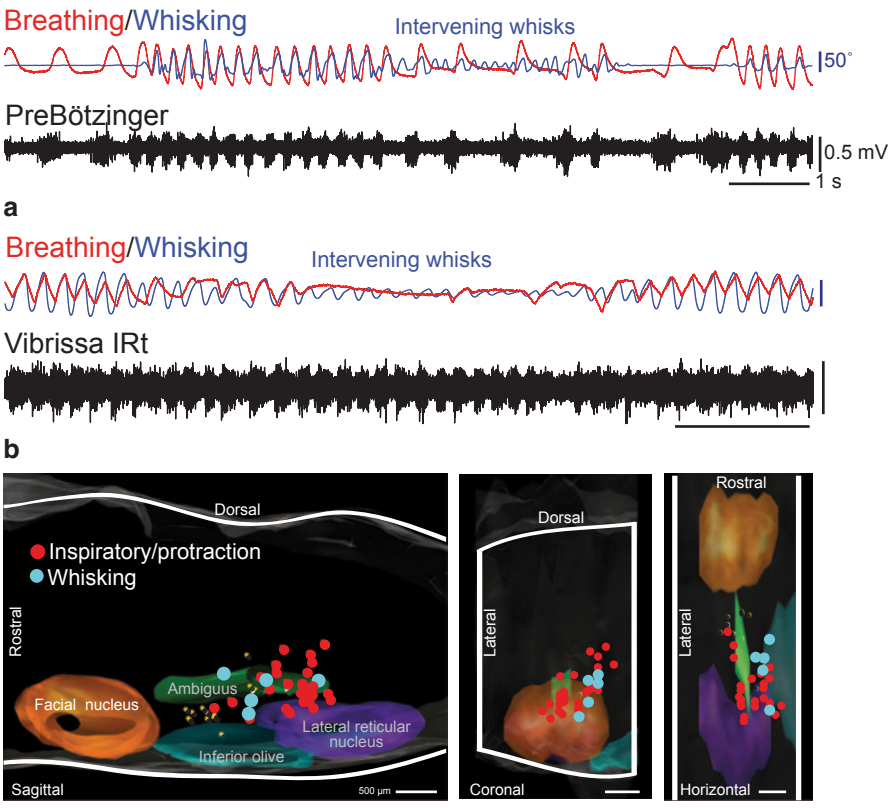

Fig. 7.7 Units in the intermediate reticular formation (IRt) that report inspiration versus protraction. **a** Concurrent recordings of breathing (*red*), whisking (*blue*), and multiunit activity (*black*) in the preBötzinger complex. The location of the recording site is labeled with Chicago sky blue and is shown in a sagittal section counterstained with neutral red. LRt denotes the lateral reticular nucleus, FN the facial nucleus, Amb the *ambiguus* nucleus, and IO the inferior olive. **b** Multiunit spike activity in the vibrissa zone of the intermediate reticular formation. The section is counterstained with neutral red. **c** The recording sites for all data imposed on a three dimensional reconstruction of the medulla. Whisking units are located medial to the preBötzinger complex in the IRt. Adapted [2]

ration and with vibrissa protraction during inspiratory-locked whisks (Fig. 7.7a and red dots in Fig. 7.7c). Critically, the activity did not track the intervening whisks. In contrast, we located a subset of units in the intermediate band of the reticular formation (IRt) whose spiking was tightly phase-locked to the protraction of both inspiratory-locked and intervening whisks (Fig. 7.7b and blue dots in Fig. 7.7c). These units are potential pre-motor drivers of the intrinsic muscles that serve rhythmic whisking (Fig. 7.2a) and are henceforth referred to as "whisking units". They are located in the ventral part of the IRt, medial to the *ambiguus* nucleus and immediately dorsomedial to the preBötzinger complex. We denote this new region the vibrissa zone of the IRt (vIRt) (Fig. 7.1).

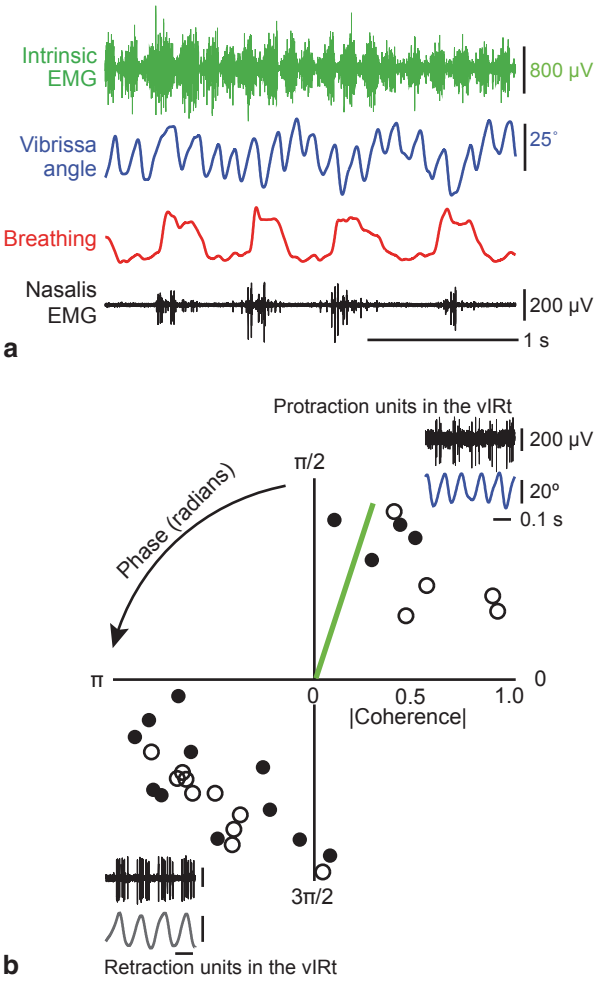

Fig. 7.8 Injection of kainic acid activates the vIRt, which drives facial motoneurons and induces whisking. **a** Vibrissa motion (*blue*), breathing (*red*), intrinsic (*green*) and extrinsic (*black*) electromyogram (EMG). **b** Polar plots of the coherence between spiking activity and vibrissa motion at the peak frequency of whisking. Open circles represent multiunit activity and closed circles represent single units. The green bar represents the coherence of the EMG for the intrinsic muscle (panel b) with vibrissa motion. **(Inserts)** Spiking activity of neuronal units in the vIRt (*black*) in relation to vibrissa motion (*blue*). Adapted [2]

The hypothesis that whisking units in the vIRt constitute the oscillator for whisking predicts that activation of this region will lead to prolonged, autonomous rhythmic whisking [2]. Indeed, microinjection of the glutamate receptor agonist kainic acid in the vicinity of the vIRt is a salutary means to induce prolonged rhythmic vibrissa movement, near 10 Hz, in the lightly anesthetized rat (Fig. 7.8a). The frequency of whisking decreases over time as the effect of the intravenous anesthesia declines, while the frequency of breathing remains a constant basal rate. This implies that the chemical activation is sufficiently strong to decouple rhythmic protraction from breathing. The ability to induce whisking in an immobile animal further provides a means to stably record from units whose firing times were coherent with rhythmic protraction (Fig. 7.8b). We identified neuronal units that spiked in

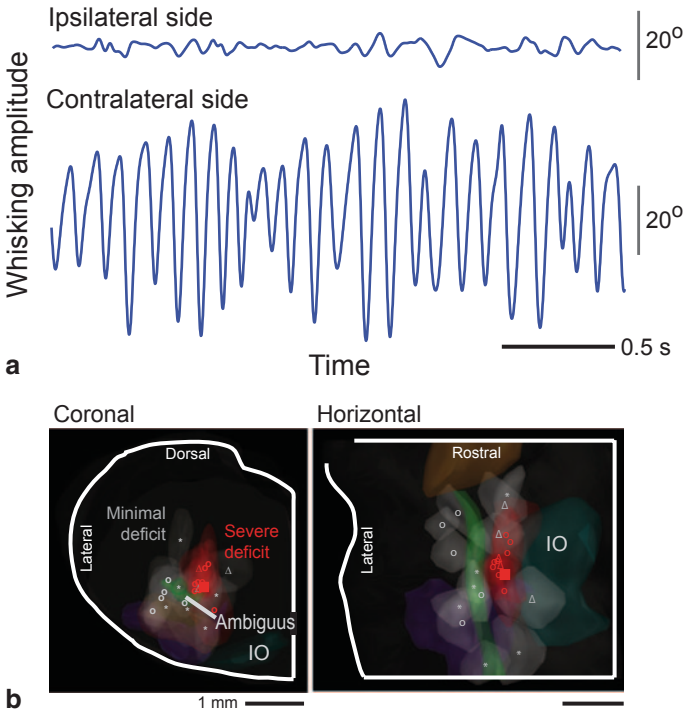

Fig. 7.9 Lesion of the vIRt impairs ipsilateral whisking. **a** Example of whisking bout following an electrolytic lesion. **b** Composite histological results across all lesion sites were mapped onto a three dimensional reconstruction of the medulla and selected anatomical substructures. The lesion centroids are denoted with symbols, with circles for electrolytic lesions, triangles for lesion via transport of Sindbis virus, and squares for chemical lesion by ibotenic acid. Adapted [2]

synchrony with protraction, as in the case of the units identified during intervening whisks in the behaving animal (Fig. 7.7c), as well as units that spiked in anti-phase. Injection of an anterograde tracer in the vIRt led to labeling of axon terminals in the ventrolateral part of the facial nucleus, where motoneurons that innervate the intrinsic muscles are clustered [2].

The above results provide evidence for the sufficiency of neurons in the vIRt to drive rhythmic protraction. We now consider the necessity of the vIRt for rhythmic motion and test if a lesion to this zone suppresses whisking [2]. First, small electrolytic lesions of the vIRt abolish whisking on the side of the lesion, while whisking persists on the contralateral side (Fig. 7.9a). Critically, lesions within the vIRt that were as small as 200 μm in diameter were sufficient to severely impair whisking on the ipsilateral side, whereas off-site lesions have minimal effects on whisking (Fig. 7.9c). Qualitatively similar results were found with ibotenic acid or Sindbis viral lesions (Fig. 7.9c). These data lead to the conclusion that units in the vIRt play an obligatory role in the generation of whisking.

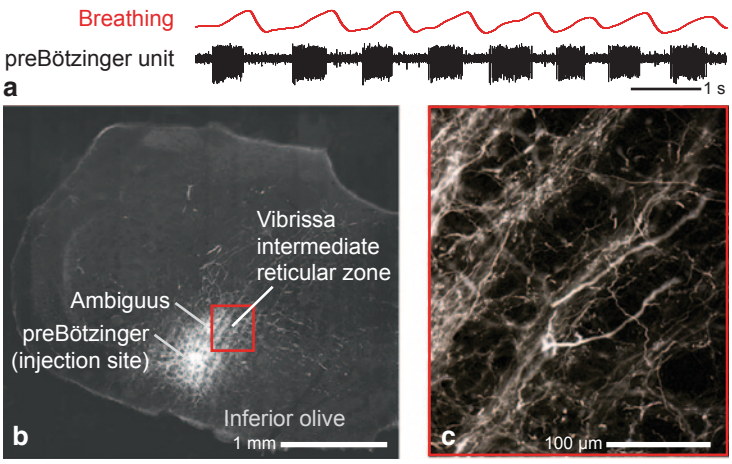

Fig. 7.10 Anatomical evidence that preBötzinger units project to the vibrissa zone of the IRt. **a** Recording of a single inspiratory unit in the preBötzinger complex, together with breathing. **b** Injection of the anterograde tracer biotinylated dextran amine through the same pipette used to record (panel a). **c** Labeling of axons and terminals in the vIRt from cells in the preBötzinger complex. Adapted [2]

The behavioral (Figs. 7.5 and 7.6) and physiological (Figs. 7.7 and 7.8) data suggest that neurons in the inspiratory CPG reset an oscillatory network of whisking units in the vIRt that can drive protraction of the vibrissa concurrent with each inspiration. We assessed this hypothesized connection by tract tracing methods [2]. Injections of tracer into the preBötzinger complex (Fig. 7.10a), identified by the phase relation of units relative to breathing (Fig. 7.10b), led to dense anterograde labeling of terminals in the vIRt, in the same region where we observed whisking units and where lesions extinguished ipsilateral whisking (Fig. 7.10c). These results support a direct connection from the preBötzinger complex to the vIRt.

We next delineated the projections from neurons in the vIRt to facial motoneurons [2]. Tracer was injected in the lateral aspect of the facial nucleus (Fig. 7.11a), and we observed a number of retrogradely labeled cells in the vIRt (Fig. 7.11b). A detailed map of the location of cells that were retrogradely labeled from this injection reveals the spatial extent of the high-density cluster of facial projecting vIRt cells (Fig. 7.11c). *In toto*, these and previous [27, 28] patterns of neuronal labeling in the IRt support a direct connection from the vIRt to the facial nucleus and thus substantiate the role of the vIRt as a premotor nucleus. This zone functions as the premotor pattern generator for rhythmic whisking and is part of a larger circuit whereby cells in nuclei that are obligatory for inspiration [25, 29, 30] reset the phase of vIRt units with each breath (Fig. 7.12).

We conclude that whisking concurrent with sniffing is effectively driven on a cycle-by-cycle basis by the inspiratory rhythm generator, while intervening whisks between successive inspirations result from oscillations of the whisking units in

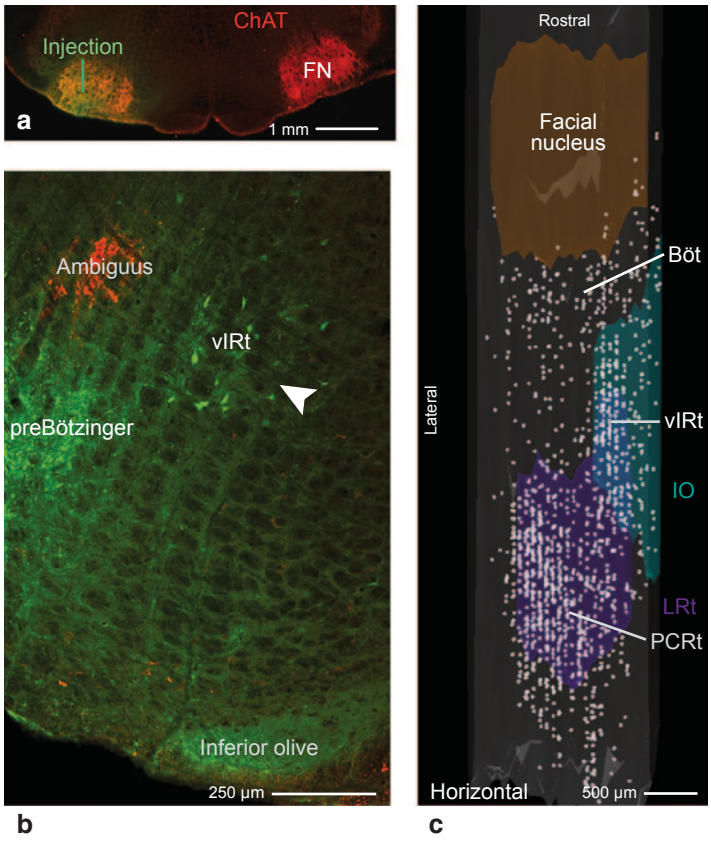

Fig. 7.11 Anatomical evidence that the facial nucleus receives input from the vibrissa zone of the IRt. **a** Injection of retrograde tracer Neurobiotin™ (*green*) into the facial nucleus (FN). Labeling with α-choline acetyl-transferase highlights motoneurons in the facial nucleus (*red*). **b** Retrograde labeling of neurons in the vIRt (*white arrow*). Labeling with α-choline acetyl-transferase highlights neurons in the *ambiguus* nucleus (*red*). **c** Compendium of the locations of cells that were retrogradely labeled from the facial nucleus with Neurobiotin™, superimposed on a three dimensional reconstruction of the medulla. Note labeled cells in the vIRt, located between coronal planes spaced 500 µm apart and that span 200 µm along the lateral-medial axis. pFRG denotes the parafacial respiratory group and PCRt the parvocellular reticular nucleus. Adapted [2]

vIRt [2]. This result bears on the generation of other rhythmic orofacial behaviors, for which licking is particularly well described. First, tongue protrusions are coordinated with the respiratory cycle [31]. Second, like the vIRt facial premotoneurons, a cluster of hypoglossal premotoneurons are concentrated dorsomedially to the pre-Bötzinger complex within the IRt [24, 32] and, further, are driven by bursts of spikes that are locked to inspiration [33]. Third, the output of units in the hypoglossal IRt zone locks to rhythmic licking [34]. Lastly, infusion of an inhibitory agonist into

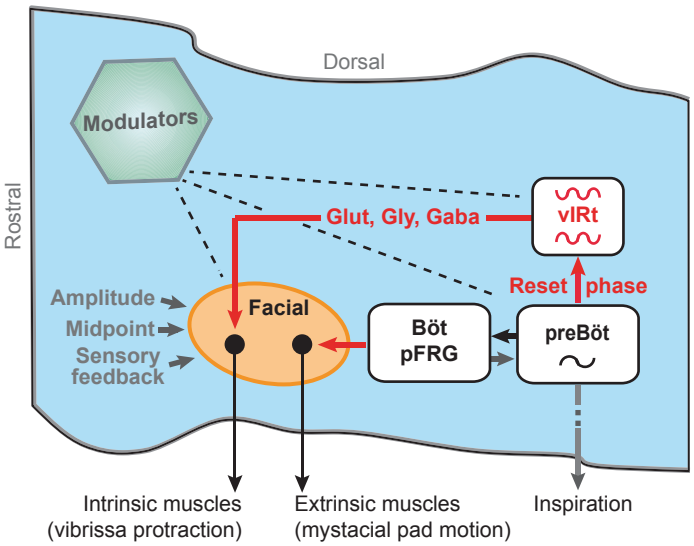

Fig. 7.12 Schematic of the brainstem circuitry that generates whisking in coordination with breathing. The neurotransmitters refer to glycine (Gly), glutamate (Glu), and γ-aminobutyric acid (Gaba) that were found from *in situ* hybridization measurements [2]

the IRt blocks licking [35]. These past results are consistent with a model in which preBötzinger units reset the onset of bursting in a network of hypoglossal premotor neurons in the IRt zone, in parallel with our circuit for whisking (Fig. 7.12).

A final issue concerns the potential binding of touch-based and olfaction-based sensory inputs. In the vibrissa system, the spike rate of neurons in vS1 cortex (Fig. 7.1) is modulated by the phase of the vibrissa in the whisk cycle [36–40]. In particular, the spike rate of neurons in layers 4 and 5a is most pronounced when the vibrissae contact an objects at a particular phase [38] (Fig. 7.13, b). Different neurons have different preferred phases so that all phases in the whisk cycle, corresponding to contact upon retraction as well as protraction, are covered. In contrast, the output of the same neurons appears untuned when contact is plotted as a function of absolute contact angle (Fig. 7.13c).

Tuning of the neuronal response in terms of phase implies that the rodent codes touch in a coordinate system that is locked to the CPG for whisking. It is of interest that neurons in the olfactory bulb tend to spike in phase with breathing, as opposed to spiking in a manner time-locked to the presentation of an odorant [41] (Fig. 7.14). When rodents are actively exploring, the precise one-to-one phase locking between whisking and sniffing (Fig. 7.5a) could ensure that spikes induced by both tactile and olfactory stimuli occur with a fixed temporal relationship to one another, with a delay that corresponds to a particular location and smell. This implies that sensory inputs from touch, which enter the brain at the level of the brainstem, and inputs from smell, which enter the brain at the rostral pole, can in principle be linked by the

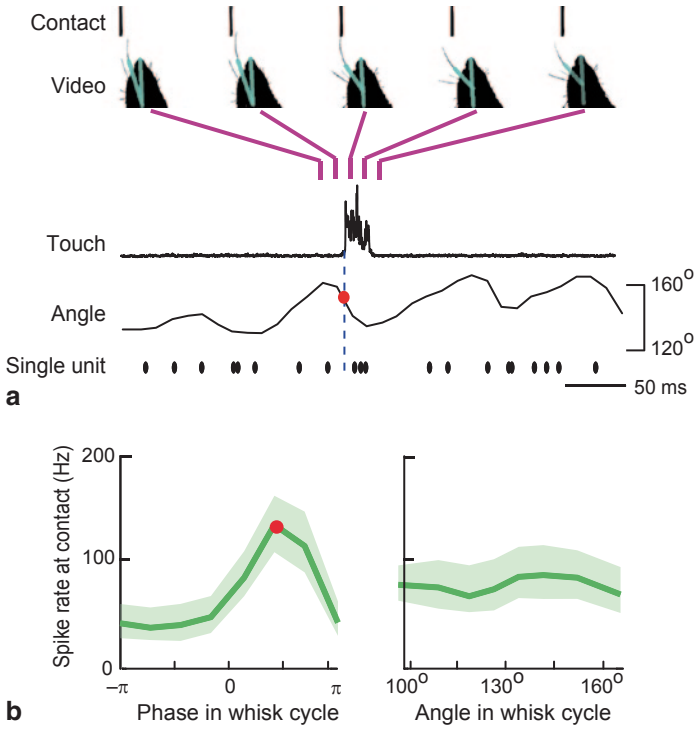

Fig. 7.13 Evidence that neurons in vS1 cortex encode contact with an object relative to the phase of the vibrissae in the whisk cycle **a** The scheme used to measure the spike response of units in vS1 cortex as animals rhythmically whisk first in air then whisk to touch a contact sensor. Vibrissa position is determined from videography while contact is determined via displacement of the sensor. A critical aspect of this behavioral task is that touch is recorded across all phases of the whisk cycle; the case shown here is touch soon after the onset of retraction (*red dot*). **b** The left plot shows the peak values of the touch response as a function of phase in the whisk cycle (*left panel* in Fig. 7.2a). The uncertainty represents the 95 % confidence interval. A smooth curve through this data defines the phase of maximal touch response, (red dot and corresponding dot in panel a). The right plot is the same data parsed according to the angular position of the vibrissa upon contact. The angle is measured relative to the midline of the animal's head (*right panel* in Fig. 7.2a). Unlike the case for phase, there is no significant tuning for angle. Adapted [38]

breathing rhythm via computations in downstream neurons [42]. Thus, coordination by the output of the preBötzinger complex can ensure that orofacial behaviors do not confound each other as well as serve to perceptually bind concurrent tactile and olfactory inputs [43]. Whether the binding mechanism further involves coherent transient theta-band oscillations in neocortical and hippocampal circuits remains an open issue [44, 45].

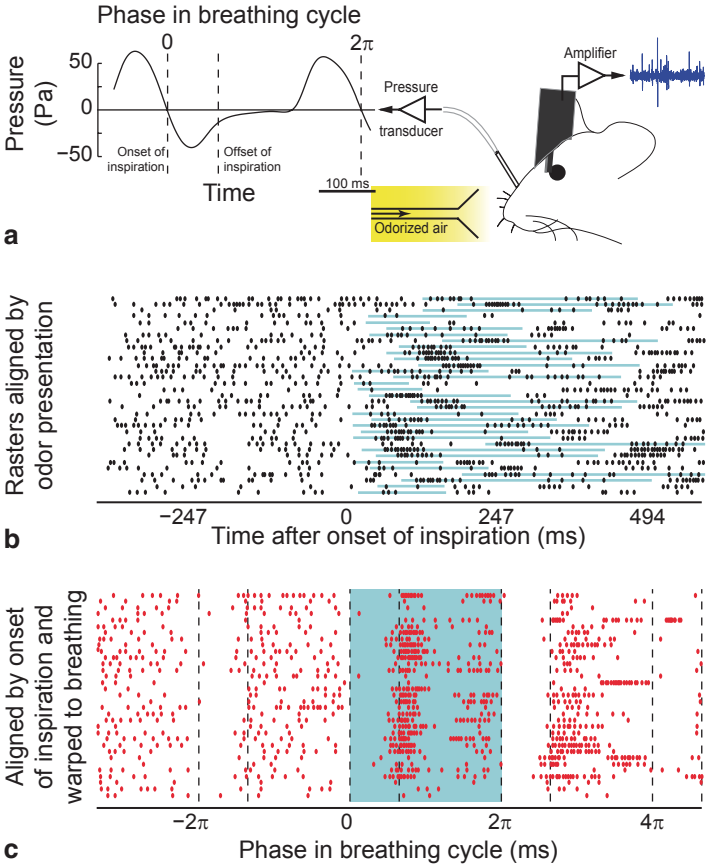

Fig. 7.14 Odor response in olfactory bulb in a representative neuron in the olfactory bulb of an awake mouse. **a** Schematic of the experiment. A head-fixed animal was positioned in front of the odor delivery port. It was implanted with intranasal cannula to derive the breathing cycle from the measured pressure and a multi-electrode chamber. **b** Raster plots for single unit spikes from a mitral or tufted neuron in the olfactory bulb in response to an odor stimulus. The data is displayed as synchronized by odor onset. The blue bands show the respiration cycles for each trace. **c** The same data as used for panel b after alignment to the onset of inspiration and temporally warped by breathing, so that it is now in phase coordinates. The uniformity of the blue bands indicates that the individual respiration cycles are now aligned. Adapted [41]

Acknowledgements Our work was funded by the Canadian Institutes of Health Research (grant MT-5877), the United States National Institutes of Health (grants NS058668, NS066664 and NS047101), the United States National Science Foundation (grant PHY-1451026), and the US-Israeli Binational Science Foundation (grant 2003222).

References

1. Welker WI (1964) Analysis of sniffing of the albino rat. Behaviour 12:223–244
2. Moore* JD, Deschênes* M, Furuta T, Huber D, Smear MC, Demers M, Kleinfeld D (2013) Hierarchy of orofacial rhythms revealed through whisking and breathing. Nature 469:53–57
3. Kleinfeld D, Deschênes M (2011) Neuronal basis for object location in the vibrissa scanning sensorimotor system. Neuron 72:455–468
4. Nguyen Q-T, Kleinfeld D (2005) Positive feedback in a brainstem tactile sensorimotor loop. Neuron 45:447–457
5. Deschênes M, Moore JD, Kleinfeld D (2012) Sniffing and whisking in rodents. Curr Opin Neurobiol 22:243–250
6. Mitchinson B, Martin CJ, Grant RA, Prescott TJ (2007) Feedback control in active sensing: Rat exploratory whisking is modulated by environmental contact. Proc Royal Soc Lond Biol Sci 274:1035–1041
7. Towal RB, Hartmann MJ (2006) Right-left asymmetries in the whisking behavior of rats anticipate movements. J Neurosci 26:8838–8846
8. Berg RW, Kleinfeld D (2003) Rhythmic whisking by rat: Retraction as well as protraction of the vibrissae is under active muscular control. J Neurophysiol 89:104–117
9. Hill DN, Bermejo R, Zeigler HP, Kleinfeld D (2008) Biomechanics of the vibrissa motor plant in rat: Rhythmic whisking consists of triphasic neuromuscular activity. J Neurosci 28:3438–3455
10. Pietr MD, Knutsen PM, Shore DI, Ahissar E, Vogel Z (2010) Cannabinoids reveal separate controls for whisking amplitude and timing in rats. J Neurophysiol 104:2532–2542
11. Hill DN, Curtis JC, Moore JD, Kleinfeld D (2011) Primary motor cortex reports efferent control of vibrissa position on multiple time scales. Neuron 72:344–356
12. Ranade S, Hangya B, Kepecs A (2013) Multiple modes of phase locking between sniffing and whisking during active exploration. J Neurosci 33:8250–8256
13. Lawson EE, Richter DW, Czyzyk-Krzeska MF, Bischoff A, Rudesill RC (1991) Respiratory neuronal activity during apnea and other breathing patterns induced by laryngeal stimulation. J Appl Ohysiol 70:2742–2749
14. Smith JC, Ellenberger HH, Ballanyi K, Richter DW, Feldman JL (1991) Pre-Botzinger complex: a brainstem region that may generate respiratory rhythm in mammals. Science 254:726–729
15. Feldman JL, Del Negro CA, Gray PA (2013) Understanding the rhythm of breathing: so near, yet so far. Annu Rev Physiol 75:423–452
16. Garcia AJ, Zanella S, Koch H, Doi A, Ramirez JM (2011) Networks within networks: the neuronal control of breathing. Prog Brain Res 188:31–50
17. Gao P, Bermejo R, Zeigler HP (2001) Vibrissa deaffentation and rodent whisking patterns: behavioral evidence for a central pattern generator. J Neurosci 21:5374–5380
18. Lovick TA (1972) The behavioural repertoire of precollicular decerebrate rats. J Physiol 226:4P–6P
19. Smith JC, Abdala APL, Rybak IA, Paton JFR (2009) Structural and functional architecture of respiratory networks in the mammalian brainstem. Philos Trans Royal Soc Lond B 364:2577–2587
20. Sherrey JH, Megirian D (1977) State dependence of upper airway respiratory motoneurons: functions of the cricothyroid and nasolabial muscles of the unanesthetized rat. Electroencephalogr Clin Neurophysiol 43:218–228
21. Haidarliu S, Golomb D, Kleinfeld D, Ahissar E (2012) Dorsorostral snout muscles in the rat subserve coordinated movement for whisking and sniffing. Anat Rec 295:1181–1191
22. Nakamura Y, Katakura N (1995) Generation of masticatory rhythm in the brainstem. Neurosci Res 23:1–19
23. Bieger D, Hopkins DA (1987) Viscerotopic representation of the upper alimentary tract in the medulla oblongata in the rat: the nucleus ambiguus. J Comp Neurol 262:546–562

24. Travers JB, Dinardo LA, Karimnamazi H (1997) Motor and premotor mechanisms of licking. Neurosci Biobehav Rev 21:631–647
25. Tan W, Janczewski WA, Yang P, Shao XM, Callaway EM, Feldman JL (2008) Silencing preBötzinger complex somatostatin-expressing neurons induces persistent apnea in awake rat. Nat Neurosci 11:538–540
26. Travers JB (1995) Oromotor nuclei *In* The rat nervous system - second edition. Paxinos G (ed) 239–255, Academic Press
27. Takatoh J, Nelson A, Zhou X, Bolton MM, Ehlers MD, Arenkiel BR, Mooney R, Wang F (2013) New modules are added to vibrissal premotor circuitry with the emergence of exploratory whisking. Neuron 77:346–360
28. Isokawa-Akesson M, Komisaruk BR (1987) Difference in projections to the lateral and medial facial nucleus: anatomically separate pathways for rhythmical vibrissa movement in rats. Exp Brain Res 65:385–398
29. Gray PA, Hayes JA, Ling GY, Llona I, Tupal S, Picardo MC, Ross SE, Hirata T, Corbin JG, Eugenín J, Del Negro CA (2010) Developmental origin of preBötzinger complex respiratory neurons. J Neurosci 30:14883–148895
30. Bouvier J, Thoby-Brisson MNR, Dubreuil V, Ericson J, Champagnat J, Pierani AAC, Fortin G (2010) Hindbrain interneurons and axon guidance signaling critical for breathing. Nat Neurosci 13:1066–1074
31. Welzl H, Bures J (1977) Lick-synchronized breathing in rats. Physiol Behav 18:751–753
32. Koizumi H, Wilson CG, Wong S, Yamanishi T, Koshiya N, Smith JC (2008) Functional imaging, spatial reconstruction, and biophysical analysis of a respiratory motor circuit isolated in vitro. J Neurosci 28:2353–2365
33. Ono T, Ishiwata Y, Inaba N, Kuroda T, Nakamura Y (1998) Modulation of the inspiratory-related activity of hypoglossal premotor neurons during ingestion and rejection in the decerebrate cat. J Neurophysiol 80:48–58
34. Travers JB, DiNardo LA, Karimnamazi H (2000) Medullary reticular formation activity during ingestion and rejection in the awake rat. Exp Brain Res 130:78–92
35. Chen Z, Travers SP, Travers JB (2001) Muscimol infusions in the brain stem reticular formation reversibly block ingestion in the awake rat. Am J Physiol Regul Intergr Comp Physiol 280:R1085–R1094
36. de Kock CP, Sakmann B (2009) Spiking in primary somatosensory cortex during natural whisking in awake head-restrained rats is cell-type specific. Proc Natl Acad Sci U S A 106:16446–16450
37. Fee MS, Mitra PP, Kleinfeld D (1997) Central versus peripheral determinates of patterned spike activity in rat vibrissa cortex during whisking. J Neurophysiol 78:1144–1149
38. Curtis JC, Kleinfeld D (2009) Phase-to-rate transformations encode touch in cortical neurons of a scanning sensorimotor system. Nat Neurosci 12:492–501
39. Crochet S, Petersen CCH (2006) Correlating membrane potential with behaviour using whole-cell recordings from barrel cortex of awake mice. Nat Neurosci 9:608–609
40. Gentet LJ, Avermann M, Matyas F, Staiger JF, Petersen CCH (2010) Membrane potential dynamics of GABAergic neurons in the barrel cortex of behaving mice. Neuron 65:422–435
41. Shusterman R, Smear MC, Koulakov AA, Rinberg D (2011) Precise olfactory responses tile the sniff cycle. Nat Neurosci 14:1039–1044
42. Kleinfeld D, Deschênes M, Wang F, Moore JD (2014) More than a rhythm of life: breathing as a binder of orofacial sensation. Nat Neuroci 15:647–651
43. Moore JD, Kleinfeld D, Wang F (2014) How the brainstem controls orofacial behaviors comprised of rhythmic actions. Trends Neurosci 27:370–380
44. Berg RW, Whitmer D, Kleinfeld D (2006) Exploratory whisking by rat is not phase-locked to the hippocampal theta rhythm. J Neurosci 26:6518–6522
45. Lisman JE, Jensen O (2013) The q-g neural code. Neuron 77:1002–1016
46. Fukuda Y, Honda Y (1982) Differences in respiratory neural activities between vagal (superior laryngeal), hypoglossal, and phrenic nerves in the anesthetized rat. Jpn J Physiol 32:387–398

Part III
Computations of the Whisker System

Chapter 8
Functional Principles of Whisker-Mediated Touch Perception

Miguel Maravall and Mathew E. Diamond

Abstract In the progression of events wherein the rodent whisker sensory system constructs a percept of the world around the animal, neurons exercise distinct functional roles; here we review recent progress in our understanding of the principles for response organization in the system. The whisker's mechanical properties and anchoring to the follicle shape the forces transmitted to specialized receptors. The sensory and motor systems are intimately interconnected, giving rise to two forms of whisker-mediated sensation: generative and receptive. The sensory pathway exemplifies fundamental concepts in computation and coding: hierarchical feature selectivity, sparseness, adaptive representations, and population coding. The central processing of signals can be considered a sequence of filters. At the level of cortex, neurons represent object features by a coordinated population code which encompasses cells with heterogeneous properties.

Keywords Feature selectivity · Sensory encoding · Decoding · Population code · Adaptation · Texture

Introduction

In the process that culminates in sensing and identifying an object, the starting point is the encoding of physical parameters by sensory receptors. A growing set of investigations focuses on transformations along sensory pathways as a means to understand the conversion from raw physical signals into sensations and percepts [1]. This review aims to identify computations mediating those transformations in the

M. Maravall (✉)
School of Life Sciences, University of Sussex,
Brighton BN1 9QG, United Kingdom
e-mail: m.maravall@sussex.ac.uk

M. E. Diamond (✉)
Tactile Perception and Learning Lab, International School for Advanced Studies-SISSA,
Via Bonomea 265, 34136 Trieste, Italy
e-mail: diamond@sissa.it

P. Krieger, A. Groh (eds.), *Sensorimotor Integration in the Whisker System,*
DOI 10.1007/978-1-4939-2975-7_8

rodent whisker system, an "expert" system [2], but which are likely to generalize across systems [3].

Each sensory system is optimized for collecting information in particular ways. Touch is a proximal sensing system—it entails putting sensors into contact with an object to determine its identity, properties or location. Recent reviews have emphasized computations specific to the whisker pathway [2, 4–6]. The intricate loops connecting "sensory" and "motor" circuits in the whisker system can be understood in terms of the need to meld sensory and motor information—motor output generates sensory input, sensory input modulates motor output [5, 7–11]. In contrast, the system's serial structure is comparatively simple: the sequential pathway from receptors to somatosensory cortex is only three synapses long—very short compared to the visual and auditory systems [7, 12]. In this review, we focus on computations along the receptor-to-cortex ascending pathway; nevertheless a complete picture of tactile sensation will only be achieved by understanding how sensory and motor computations are woven together [7, 13].

Mechanical Forces in the Follicle

As in any sensory pathway, transduction from physical entities into action potentials constrains all later processing. Input signals encounter the sensory fiber terminal at the whisker base, in the follicle of the mystacial pad [14–18] (Fig. 8.1a). The properties and position of an object contacted by a whisker are encoded into fluctuations in mechanical energy shaped by the interaction between the whisker's motion, its mechanical properties (e.g. compliance—the ability to flex or yield elastically to force) and properties of the contacted object. The whisker-follicle junction is rigid, allowing robust transmission and readout of the forces induced by whisker motion [19].

The form of whiskers (Fig. 8.1a) determines their mechanical behavior. Bending stiffness decreases from whisker base to tip due to taper [20], and the concomitant increase in flexibility enables the slippage of whiskers during object exploration [21, 22]. Additional flexibility is achieved by their hollow structure [23].

Methods for tracking whisker motion [24–29] have allowed detailed analysis of how whiskers interact with objects during behavior [30, 31]. Rodents modulate the duration and position of contact during exploration, maximizing the number of whiskers that touch the surface and minimizing "impingement": this favors contact near the tip and enhances the relative impact of vibrational stresses [32, 33]. The combination of whisker measurements with models of whisker deflection has begun to specify bending [22, 34] and changes in forces at the whisker base [19, 20, 22, 35]. Contact-induced whisker deformations can be decomposed into a slow bending component and a transient vibrational component [36]; the relative contributions of different components depend on the specific interaction of the whisker with the object of interest [19, 20, 37]. The nature of a whisker stimulus could therefore potentially be decoded by comparing the relative magnitudes of the slow and transient components over time. This would require those components to be effectively and

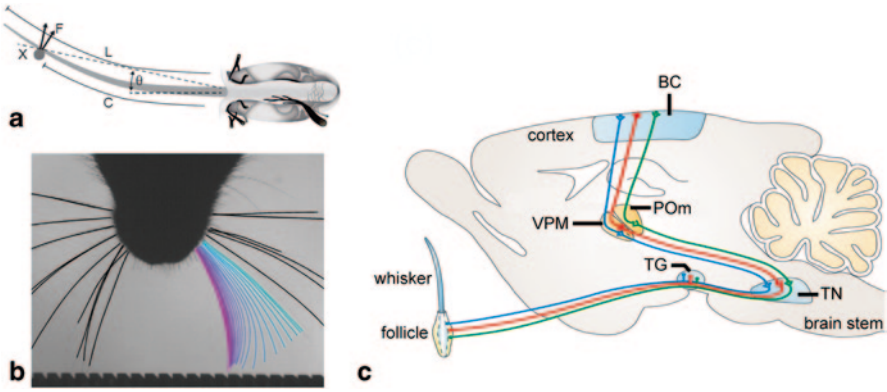

Fig. 8.1 Input forces to the sensory system and the ascending pathway. **a** The force acting upon a whisker during contact, and thus transmitted to the receptors in the follicle, is illustrated. The object at position X strikes a whisker of length L at a distance C from the skin and at angle θ away from the whisker's resting angle, inducing a force F. **b** Illustration of a single large stick-slip event. One frame from a high-speed (1000 frames/second) video is shown in *gray* scale. The whisker traces have been enhanced to increase their visibility. While the rat palpated the surface to judge the groove spatial frequency, one whisker was tracked through a sequence of frames and the traces, from *violet* to *light blue*, shows the whisker position over 1 ms timesteps. The whisker tip was blocked in a groove and then sprung free as the rat retracted the whisker shaft in the posterior direction. **c** Principal sensory pathways to the cortex are illustrated schematically. TG neurons send a peripheral branch to the skin and a central branch into the trigeminal nuclei (TN) of the brainstem. Axons from TN cross the midline to reach the thalamus, terminating in VPM and the posterior medial nucleus, POm. Thalamic neurons project to BC. *Blue*, *red*, and *green* lines represent parallel pathways that carry different sorts of tactile information, as reviewed elsewhere. (**a** adapted personal communication from A. Hires and K. Svoboda; **b** adapted from [45]; **c** adapted from [7])

separately transduced by mechanoreceptors: exactly which components are transduced, and how, is a crucial issue for future work [38].

When whiskers sweep across a textured surface (Fig. 8.1b), they are trapped and released by surface ridges and grains [28, 29, 39–45]. These brief (~2 ms) "stick-slip" events cause transient, high-frequency vibrations [41]. The consequent sequence of fluctuations in mechanical energy can provide a signature of texture [39, 41]. Stick-slip events excite primary sensory neurons and their targets [39, 41, 42, 45]. However, differences in "stick-slip" events across trials are not well-correlated with trial-to-trial choices in a texture discrimination task [45]; since "stick-slip" events do not account for perceptual choices, additional differences in whisker motion evoked by contact with the texture must therefore contribute to the choice as well.

Other physiological factors may also contribute to the mechanical forces that come into play during whisker motion. Follicle compliance likely varies during whisking and is modulated by the engorgement of the blood sinus that surrounds each follicle complex [18, 46–50]. Forces are also modulated by the intrinsic musculature of the whisker pad. Recently, models have been proposed for overall whis-

ker pad motion [49] and activation of the motor mechanical system consisting of whiskers, follicles and muscles [51].

Transduction of Touch into Neuronal Signals

Transduction is carried out at the terminals of neurons whose cell body resides in the trigeminal ganglion (TG; Fig. 8.1c). Each follicle is innervated by ~200 neurons [15, 52]; each TG neuron innervates a single follicle [53]. The many mechanoreceptor types, distributed differentially across the follicle, have diverse response properties and are best activated by distinct forces with particular (slower or faster) time courses.

Models for transduction in the follicle-sinus complex capture diverse responses of receptors [54, 55]. A simple model using a single process to account for the interaction between whisker and receptors predicts responses to passive stimulation of the main functional classes of primary afferent neurons (slowly and rapidly adapting, SA and RA) [55].

Given the diversity of receptor types and spatial distributions, it is not surprising that both of the principal functional classes of primary afferent neurons, slowly and rapidly adapting (SA and RA), in fact comprise a rich variety of feature combinations. Thus, each neuron displays distinct sensitivity to the location, direction and velocity of whisker displacements evoking lateral forces [39, 53, 56–64], to the pattern of axial forces [63], to whisking phase [60, 65, 66] and to contact, detachment or their combinations [60, 62].

As a population, TG neurons represent the space of dynamical features of one whisker through a high-dimensional code (~200, counting each neuron as a dimension) (see *Feature selectivity*) [67]. This permits rapid information encoding: specific patterns of forces (e.g. [20]) may engage subsets of neurons to "label" the stimulus. Whisker motion patterns are richly represented by the TG population, allowing several population-based decoding schemes for any task. For example, information present across the population likely permits instantaneous comparison of the relative magnitudes of different force components (see *Mechanical forces in the follicle*). Intriguingly, each TG neuron projects to multiple target neurons within a column of the principal trigeminal nucleus ("barrelette"), and individual barrelette neurons receive convergent inputs of different afferent types (SA, RA): thus, TG population signals are decoded in a "one-to-many" and "many-to-one" manner [68].

A requirement for TG to implement a fast population code based on relatively small numbers of spikes is that spike generation be precise. Indeed, TG neurons respond with highly reliable firing patterns [39, 53, 55, 56, 58, 60, 61, 69] and are among the most temporally precise neurons yet discovered in the animal kingdom [39, 67, 69]. Response jitter is on a timescale of tens of microseconds, comparable to that underlying bat echolocation or representations of interaural time difference (reviewed in [70]).

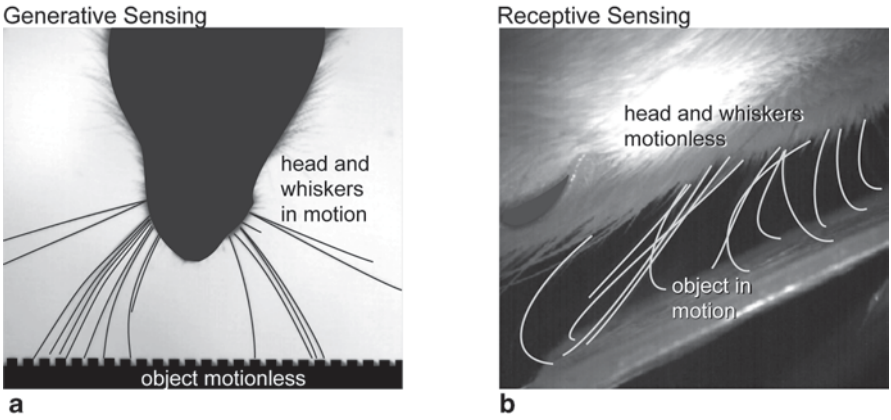

Fig. 8.2 Two modes in which rodents collect tactile information. Both panels are single frames from high-speed (1000 frames/s) video; the whisker traces have been enhanced to increase their visibility. **a** During generative sensing, the rat moves its head and whiskers to create dynamic interaction between the whisker tips and the object. This mode of sensing is critical when the object is immobile and the mechanical energy must originate in the animal's motor system. The image is taken as the rat judges the spatial frequency of grooves on the object surface. **b** During receptive sensing, the object provides mechanical energy. Since the rat's percept could be confounded by its own motor output, the head and whiskers remain motionless. The image is taken as the rat perceives the vibration of the flat plate. (**a** adapted from [45]; **b** adapted from [86])

To summarize, TG neurons convey information packaged in a high-temporal precision code where different neurons encode diverse physical properties. The speed of peripheral encoding and the small number of synapses—just three—from receptors to somatosensory cortex (Fig. 8.1c) are reflected in the finding that the responses of cortical neurons already carry texture information (i.e., correlate with the identity of a texture) within 20 ms after whisker contact [71, 72].

Active Sensing

Active sensing systems are purposive and information-seeking [73]: active sensing entails control of the sensor apparatus in whatever manner allows the brain to optimize the collection of task-relevant information. Although the concept of sensor apparatus control applies to all modalities, it is perhaps most evident in the modality of touch. Recent evidence indicates that whisker-mediated sensation occurs through two modes of operation.

In the generative mode (Fig. 8.2a), the animal moves its whiskers to actively seek contact with objects and palpate them: the animal generates the percept by its own motion [33]. Tasks involving the generative mode include wall following [74], gap measurement [75], texture discrimination [43–45, 72, 76], and object localization [77, 78]. In the generative mode, whisker-mediated perception has been

put forward as a process where sensory and motor systems dynamically converge, through repeated contacts, until both neuronal representations reach a stable state [77, 79].

In the receptive mode (Fig. 8.2b), the animal places its whiskers on an object and is frequently observed to immobilize its whiskers to optimize signal collection. Tasks include detection and discrimination of vibrations applied to whiskers [75, 80–86] and discrimination of the width of an aperture [87].

Feature Selectivity

Neurons early in sensory processing are sensitive to the presence of particular features in a stimulus. Feature selectivity can be approximated by treating the neuron as a device that (1) linearly filters its input and (2) responds by applying a nonlinear threshold function to the filtered stimulus [88, 89]. Variants and generalizations of such linear-nonlinear models predict trains of action potentials in TG [39, 61, 67, 90–92], the ventral posterior medial thalamic nucleus (VPM) [90, 93] and the barrel cortex (BC) [94, 95]. Neurons are selective to temporal features of whisker motion (Fig. 8.3). For subcortical neurons, filtering is typically simple in that a single, short-duration feature (e.g., instantaneous velocity) predicts a neuron's response [67, 93]. These features are conserved from TG [67] to VPM [93] (Fig. 8.3b, c), though VPM processing differs in other important aspects (discussed below). In contrast, BC neurons are also sensitive to temporal features (Fig. 8.3d, e), but have more complex, high-dimensional selectivity: multiple features, sometimes in combination, are necessary to explain a neuron's firing [94, 95]. Cortical neurons respond to nonlinear dynamical features such as speed (the absolute value of velocity) [39, 94, 95] and are sensitive to patterned or correlated motion between whiskers [95] (Fig. 8.3f). Subcortical tuning curves indicate faithful representation of filtered stimulus magnitude, while cortical curves indicate the detection of events that exceed background by some proportion [90, 93, 94]. Until there is evidence that can be explained only by alternative models, our view is that the high-dimensional selectivity of cortical neurons is, to a first approximation, the result of convergence of neurons with simpler properties.

Early studies described nonlinear integration of the motion of multiple whiskers in cortex (reviewed in [96]); such findings were given a new framework by recent research on multiwhisker correlations [95]. Multiwhisker selectivity allows neurons to construct "apparent global motion" (the appearance of overall coordinated motion of whiskers, such as that generated by multiple whiskers sliding across an object) from sequential deflection of adjacent whiskers. This may potentially permit neurons to extract information about macroscopic object shape and configuration—where macroscopic refers to objects whose size spans a large number of whisker tips [97]. Interestingly, a neuron's directional sensitivity to apparent motion is not predicted by its directional sensitivity to motion of its principal whisker. Neurons in VPM can also display selectivity to apparent global motion [98], although more weakly than in the cortex [98, 99].

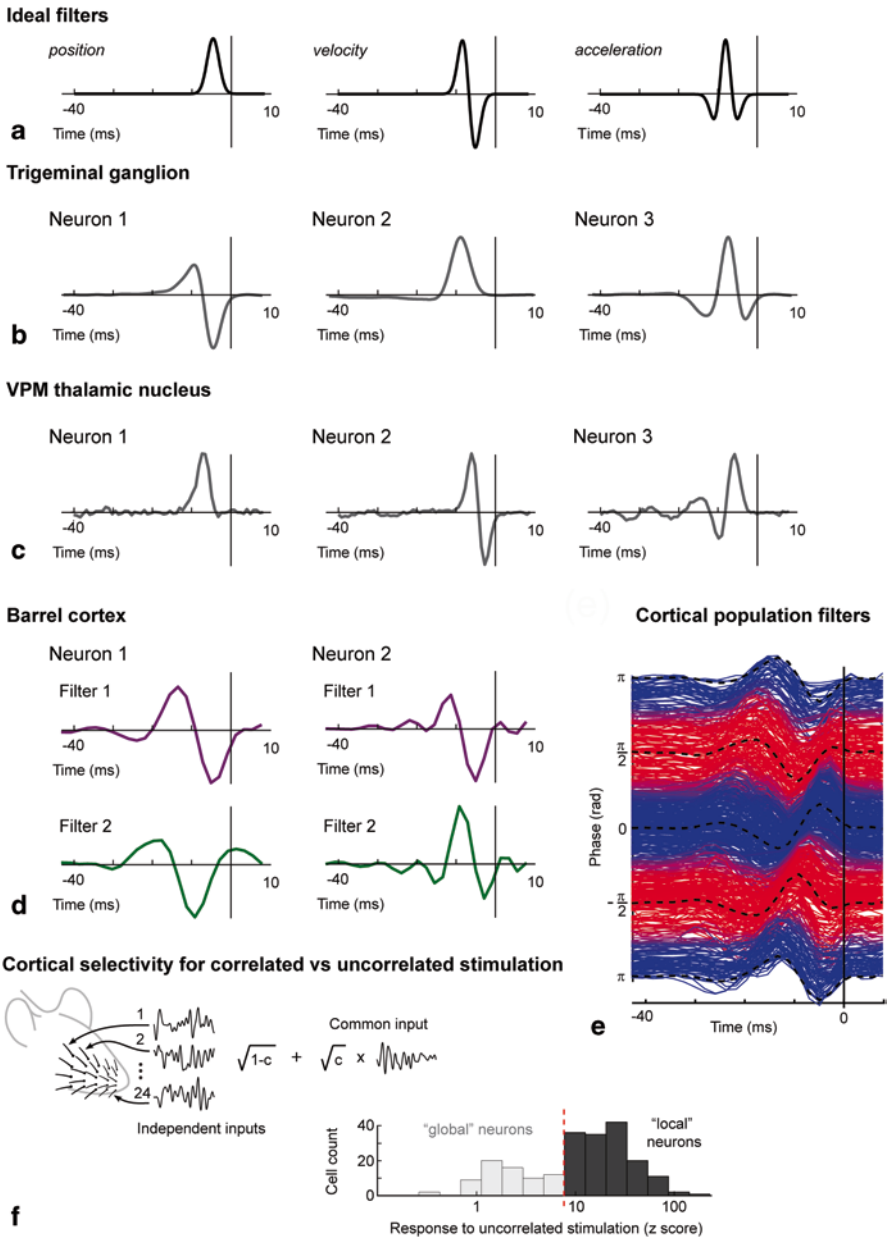

Fig. 8.3 Feature selectivity. **a** "Ideal" filters for extraction of position, velocity and acceleration values. Note similarity between these waveforms and those in the remaining panels. **b** Examples of filters for TG neurons in rats. Each neuron extracts a distinct, rapid feature. **c** Examples for VPM neurons. **d** BC neurons are sensitive to multiple features in combination. Features are of longer duration than those comprising subcortical filters, signifying longer temporal integration. **e** Dataset of linear filters for barrel cortex neurons sensitive to single-whisker stimulation, sorted by the relative phase of the filter waveform. **f** Distribution of barrel cortex sensitivity to stimuli with different degrees of interwhisker correlation. Each whisker received a stimulus waveform

Most studies of feature selectivity have relied on delivering controlled whisker stimulation to anesthetized animals; as yet, no study has directly compared tuning properties under anesthesia with response properties of the same cells during behavior. However, feature selectivity properties have strong parallels in animals performing discrimination tasks. Whisker contact modulates the firing rate of BC neurons in behaving animals [41, 72, 100–103] (S.A. Hires et al. abstract in *Soc Neurosci Abstr* 2012, 677.18): responses correlate with features including force magnitude, frequency of stick-slip events and maximum curvature. Similar sensory parameters are also represented in the primary motor cortex, where subsets of neurons encode touch and couple sensory input to learned motor programs [10, 11].

Sparsification

In the whisker pathway, activity levels change systematically from stage to stage, a change that can be quantified as "sparseness"—the fraction of neurons that are active and encoding information at any moment [102, 104–106] (Fig. 8.4a). The computational advantages of sparse activity have been reviewed elsewhere [106–109]. Sparseness can reduce overlap (correlation) between activity patterns, facilitate learning, discrimination and categorization, and limit energy expenditure. A representation where individual neurons are more sensitive to high-level features (*Feature selectivity*) is a step towards the "concept" representations found at the final stage of cortical processing [1, 110].

In whisker-mediated touch perception, activity in subcortical populations is relatively high and sparseness increases (i.e. the fraction of active neurons decreases) at more central stations of the sensory pathway, peaking in layers 2/3 of barrel cortex ([41, 102, 111–116]; reviewed in [106, 107]) (Fig. 8.4a). For example, in behaving animals, stick-slip events during texture exploration elicit low-probability, precisely timed cortical responses [41]. Mechanisms underlying sparsification are being examined [117].

Response Heterogeneity

A striking finding is that neurons responsive to the same whisker diverge markedly in their responses to a given peripheral event. Neurons within the same column can participate strongly, or not at all, in the encoding of objects contacted by the corresponding whisker [41, 72, 102, 103, 118]. This heterogeneity occurs from TG to

comprising a component shared with all other whiskers ("Common input") and an independent component ("Independent inputs"), with the degree of commonality controlled through correlation parameter c. Neurons could be classified into cells preferring stimuli with a strong common component ('global') or independent component ('local'). (**a** and **c** adapted from [93]; **b** from [67]; **d-f** from [95])

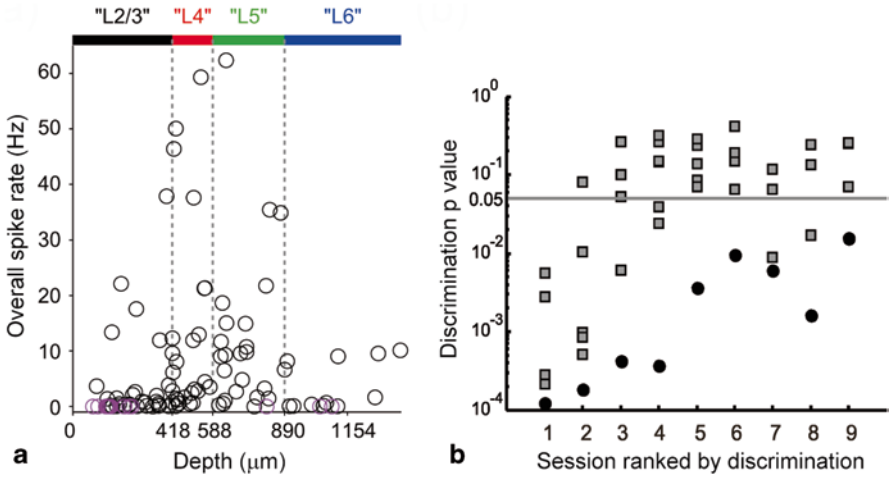

Fig. 8.4 Firing rate heterogeneity and population coding in BC. **a** Spike rates during pole localization in head-fixed mice. Each circle is one neuron and colored bars indicate *laminar boundaries*. Median activity level differs across cortical layers, yet within each layer there is marked variability. **b** Single-neuron and population discrimination performance for 9 experimental sessions of a texture discrimination task in freely moving rats. Each *gray square* corresponds to a separate neuronal cluster (a single unit or multiunit spike train that could not be further sorted into constituents); each *black circle*, to a population of simultaneously recorded clusters (3–7 separate clusters constituted each population). Sessions ranked in order of performance. P value is the probability that the discrimination performance of a neuron or population arose by chance; horizontal gray line, $p = 0.05$. Individual neuronal clusters are variable and often perform below chance ($p > 0.05$). However, every population performs well above chance. (**a** adapted from [102]; **b** from [118])

all layers of BC, with two important properties. First, neurons within each network (e.g. layer or sublayer of a column) are tuned to diverse stimulus properties. Second, neurons have diverse activity levels.

Diverse Tuning Properties

Tuning to stimulus features is heterogeneous at every stage where it has been assessed (*Feature selectivity*) [67, 93, 95] (Fig. 8.3). Since the preferred stimulus features of neurons in VPM are similar to those in TG, heterogeneity is partly inherited from stage to stage [67, 93]. Higher-level features in cortex are also heterogeneous across neurons, providing a rich representation of stimuli [95]. Neurons in animals performing sensory discrimination tasks also display diverse selectivity for sensory features, as do fibers projecting into BC from motor cortex [11, 103, 119] (S.A. Hires et al., abstract in *Soc Neurosci Abstr* 2012, 677.18). Neurons with different feature selectivity are spatially intermingled within each barrel column [120–122].

Diverse Activity Levels

Although mean activity levels differ systematically from stage to stage (*Sparsification*), within each stage there is a wide variability in activity and responsiveness among individual neurons [106] (Fig. 8.4a). For example, during a pole localization task in mice, the most active 10 % of BC neurons generated approximately 50 % of spikes [102]. In the supragranular layers, where activity is sparsest, studies under a range of conditions have nevertheless found a subset of highly active neurons numbering ~20–30 % of the population [102, 103, 121–124].

The fraction of responsive neurons in a particular condition could reflect selectivity to the stimuli presented. If so, sparse, heterogeneous responses would reflect the failure of stimuli to engage most neurons. However, the finding that many neurons exhibit low firing rate under a variety of behaviors and forms of stimulation [41, 102, 103, 116, 124], even when stimulation systematically explores a large region of parameter space [95], suggests that sparse firing is more a property of neurons than an outcome of inadequate stimulus sets.

Responsiveness correlates with spontaneous activity levels [116, 124]. Further, the relative activity level of strongly responding BC neurons is stable [116, 124], despite changes in tuning properties over time [124]. Thus, some neurons appear intrinsically more active and generate more spikes irrespective of their specific tuning. In layer 2/3, the more active neurons (those generating more spikes) receive more excitation and less inhibition [116, 123] and appear to lie at one extreme of a gradient of responsiveness and of excitatory synaptic input strength [125].

Some of the heterogeneity in responses correlates with differences in neuronal projection pattern: layer 2/3 cells that project to motor cortex have different excitability than those projecting to secondary somatosensory cortex [119] and respond differently during tactile tasks [103].

Spiking Precision, Timing-Based Representations, and Synchrony

As described above, TG responses display reliable and precise timing. Timing precision remains high across the pathway: typical response "jitter" (spike time standard deviation across trials) under equivalent conditions is ~0.2 ms in TG, ~0.4 ms in VPM and ~1–2 ms in BC [39, 67, 126].

The pressure driving temporal precision is unlikely to be a need to limit variation in absolute timing, because jitter is orders of magnitude smaller than the trial-to-trial variability observed in naturalistic exploratory behavior [2, 39, 45]. The requirement, instead, is for sharp *relative* timing, enabling precise temporal patterning of spikes across neurons—either to permit sensory responses to be referred to the animal's own whisking motion, or to facilitate activity propagation.

A sensory whisking signal, i.e., a response sensitive to the whisking motion, is found in at least a subset of TG neurons (*Transduction of touch into neuronal*

signals). Information about both whisking amplitude and midpoint is relayed to BC [10, 11, 127, 128]. BC neurons can show a small modulation of membrane potential by whisking phase [100, 129], allowing contact responses to vary with phase. The whisking phase signal combined with the amplitude and midpoint references could enable reconstruction of whisker position and of the location of objects relative to the animal's face [5, 101, 130].

Sensory codes based on temporally patterned spikes can convey more information than spike count-based codes [131, 132]. In BC, latency differences across populations can code for whisker identity [133, 134]; similarly, in other somatosensory pathways including human primary afferents, first-spike latencies can convey most of the relevant stimulus information [135, 136]. Spike patterns both in TG and in BC can discriminate texture in a manner decodable by an ideal observer [71].

Decoding spike timing information requires a temporal reference. When the system is in the generative mode, the reference can be the whisking signal, as above. A reference also present in receptive mode, or when a stimulus appears unpredictably, is the stimulus-evoked population activity itself, both in the form of collective activity oscillations (see *Interactions between emergent activity and tactile responses*) and of synchronous spiking across subsets of neurons [81, 131, 132, 137]. Which neuronal subsets become synchronously coactive in, e.g., VPM, depends on the particular stimulus [138, 139] (M. Bale et al. abstract in *Soc Neurosci Abstr* 2011, 704.14). Therefore, the identity of the synchronous subset can convey robust stimulus information [140, 141]. Dynamic changes in synchrony across subpopulations of neurons can likely be decoded downstream, as neurons are sensitive detectors of small changes in synchrony across an afferent population [141, 142].

Synchronous activation allows activity to propagate reliably in the thalamocortical pathway, where individual synaptic connections are weak on average [143]. However, full, precise synchrony across a large part of the presynaptic population is unlikely to be required, as some thalamocortical and intracortical connections can be effective enough to shape postsynaptic activation [144–146]. Instead, activity propagation may occur via partial synchrony across subsets of neurons that change over time, such that a certain combination of neurons respond simultaneously to each event in the stimulus, but the specific combination changes from event to event. This enables both robust activity propagation, because multiple neurons respond coactively, and rich population representations, because the combinations of neurons that become coactive do so based on a shared preference for the specific stimulus event [140, 141]. Indeed, selective, sparse synchronous activation of subsets of cells is a hallmark of cortical responses during texture exploration in awake rats [41].

Spike Timing Information and Behavior

Is the information in spike timing used during behavior? In a radial distance discrimination task, precise (ms) timing of contacts within the whisking cycle was

not crucial, because uncertainty in contact time introduced by whisker azimuthal jitter had no effect on performance [20]. In a pole localization task, mice detected whether the pole fell in the target region by maintaining their whiskers approximately within the region and waiting for the object to strike the whisker [78]. This maximized the difference in number of contacts and in spike counts between positive and negative trials [102]. Consistent with use of a spike-count but not a timing code, optogenetic stimulation in layer 4 increased count and fooled animals into detecting a "phantom pole"; jittering stimulation timing within a whisk caused no appreciable effect [147].

How do these results, obtained for a task where the mouse's strategy was not based on spike timing, generalize to other situations? In texture discrimination tasks, as discussed above, sequences of ms-scale fluctuations in whisker motion differ according to texture [29, 40–42, 45], and neurons can carry texture information by sequences of spikes [41, 71]. Further data from behaving rats are required to evaluate spike timing as a candidate code for texture [43, 148]. Future work on the relevance of spike timing may test how animals solve whisker-mediated tasks that require a timing-based strategy. However, even more powerful would be the demonstration that a task potentially solvable with a non-timing scheme, such as entire-stimulus spike count, is actually solved using spike timing. This test could be accomplished, for instance, if a behavioral deficit were induced by jittering spike timing for two stimuli that evoke different spike counts.

Response Dynamics and Adaptation

Adaptation, the accommodation of response levels to ongoing or repeated stimulation, occurs across species and sensory modalities [149]. Responses evolve over time because of variation in how the sensors encounter the object and because of dynamics inherent to neuronal responses.

In one adaptation paradigm, repeated whisker stimulation decreases responses to successive deflections (reviewed in [96]), sharpening tuning properties of BC neurons, including selectivity to whisker identity [150] and direction of motion [139, 151]. This adaptation enhances discrimination between stimuli of different amplitudes or delivered at different sites, at the expense of outright detectability of the weakest stimuli [152, 153]. An enhanced ability of neuronal responses to encode different stimulus magnitudes is also found during adaptation to sinusoidal whisker stimulation, suggesting a common functional effect [154, 155]. Intriguingly, regular-spiking (putative excitatory) cortical neurons adapt more weakly to stimuli repeated at irregular intervals than at a constant rate [156], while putative inhibitory neurons do the opposite [157]. This behavior is echoed in the finding that human subjects experience an increase in the perceived intensity of a vibration when noise is introduced [157]. Thalamic adaptation to repetitive stimulation is under cortical

control, implying a rich repertoire of response dynamics depending on cerebral state [158].

In another paradigm, BC neurons modify their firing rate and sensitivity according to the ongoing statistical distribution of stimuli. Changes in the overall scale (variance or "contrast") of a stimulus distribution elicit compensatory adjustments in neuronal sensitivity (gain), thus maintaining the information conveyed about the stimulus [94, 159]. TG and VPM neurons also display adaptation and gain adjustment under changes in variance [90]. Individual neurons at each subcortical stage display variable adaptive behavior, ranging from fixed gain to full gain rescaling [90]. This diversity may enable each subcortical population to preserve representation of both relative and absolute magnitudes. Because responses to dynamic stimuli adapt over multiple timescales, adaptation allows neurons to encode components of whisker stimuli with different time courses (e.g. fast, high-frequency vibrations or slow modulations in whisking waveform) [160].

Adaptation reflects use-dependent changes in availability and strength that are inherent to biophysical mechanisms. Different forms of stimulation affect distinct biophysical mechanisms, with overlapping roles. Adaptation to repeated stimulation relies mostly on synaptic mechanisms, including short-term depression [161]. The underlying changes are complex and sensitive to specific stimulation parameters: e.g., small-amplitude stimuli sometimes elicit stronger adaptation than large-amplitude stimuli [162]. Adaptation to noise stimulus statistics likely recruits intrinsic membrane mechanisms [163, 164]. In summary, adaptation in the whisker system has the effect of refining stimulus representations in a context-dependent manner.

Coordination in Barrel Cortex Populations

The heterogeneity of functional properties across neurons raises the issue of how populations collectively represent information. Is activity coordinated or is each neuron's message independent? How many neurons must an "observer" (experimenter or downstream cell) sample to extract a robust sensory message? Is it necessary to "listen" to the "best" neurons? The answers to these questions provide constraints on the transfer of information between cortical regions. Correlations among neurons in a population condition the amount of information that can be conveyed: measuring the relationship between quantity of information versus number of neurons can provide knowledge on how the activities of different neurons are related, and on the subset of neurons that is required to communicate any given message.

In rats performing a texture discrimination task, some neurons, taken alone, nearly match the animal's performance, while others carry no readily apparent texture signal [72]. Randomly sampled clusters comprised of as few as 3–7 neurons can be linearly combined to robustly discriminate texture even in cases where no individual neuron represents the stimuli [118] (Fig. 8.4b). The robust collective sig-

nals arise from synergistic interactions between heterogeneous neurons, confirming long-standing theoretical proposals [165–168]. Population representations of sensory and motor parameters in motor cortex during a pole localization task saturate for comparable-sized groups (~2–6 neurons) [10]. Thus, population representations of parameters underlying whisker-based tasks are redundant in the sense that they are likely to allow multiple decoding schemes: for example, downstream neurons receiving input from distinct subgroups of BC neurons can each receive a robust message [118]. Moreover, population representations of task parameters remain stable even when individual neurons are plastic [10].

In sum, downstream neurons can extract texture identity through a simple, robust decoding scheme involving linear synaptic weighting [118]. The robustness of linear decoding schemes applies across cortical areas and is a candidate for a fundamental algorithm of cortical computation [169–172].

Interactions Between Emergent Activity and Tactile Responses

Neuronal populations often display structured collective activity, most prominently in the form of rhythmic oscillations [173, 174]. In cortex, oscillations are shared by a large fraction of the neurons in a region [175–185] and are synchronized across nearby neurons [186]. The relative power of different oscillation frequency ranges correlates with different network states, such as sleep, quiet wakefulness, or active attentive exploration [100, 173, 186]. The existing state when a whisker stimulus is experienced can profoundly affect responses [100, 184, 186–194].

In return, sensory input alters the state of activity [191, 195]. Ongoing stimulation entrains "spontaneous" cortical activity fluctuations [195]. This entrainment is gated by the thalamus: sensory input is relayed via the thalamus, and changes in thalamic activation modulate cortical state [106, 196] and switch between different cortical activity patterns [197]. Fluctuations in different oscillatory frequency bands can act as separate biological channels for whisker information: independent signals are provided by slow, large ("up–down" state) oscillations shared across the local network and by faster (>20 Hz) synaptic activity specific to each neuron [195]. [Note however that up–down slow oscillations are rarely found during periods of active exploration [100, 186].] Interestingly, oscillatory fluctuations can also provide an internal reference for spike timing: sensory information about a whisker stimulus is conveyed by spike timing relative to the phase of the fluctuations [195].

Conclusions and Outlook: The Neuronal Activity Underlying Whisker-Mediated Behavior

This review documents recent progress in understanding the functional principles governing how whisker-mediated tactile stimuli are translated into patterns of neuronal activity distributed across networks. We conclude by highlighting experimental paradigms that offer the opportunity to attack many remaining questions. How does the feature detection framework translate to the behaving sensory system? Can sensory neurons integrate "local" features over time to generate a "global" stimulus representation? Can such a global representation be transferred to other brain regions for storage and manipulation?

In a delayed-response pole localization task, a mouse must use generative sensing (Fig. 8.2a) to localize an object, but then delay its choice until hearing a go cue. This forced time interval between sensation and action enables the flow of activity leading from one to the other to be mapped [198]. Combining this task with optogenetic inactivation of activity in defined cortical areas has revealed that while somatosensory cortex is necessary for acquisition of sensory information, several regions of frontal cortex are involved in the conversion of the sensory input into the motor response by which the mouse indicates its choice [198].

In the localization task outlined above, cortical activity between the pole contact and the go cue could encode a memory of the recent sensation, the planning of a future action, or (more likely) some combination of the two. A recent paradigm enables dissection of the neuronal activity underlying different phases of a perceptual decision process. In this task, rats must use receptive sensing (Fig. 8.2b) to perform a tactile delayed comparison behavior [86]. By placing its whiskers on a flat plate actuated by a motor, the rat receives two stimuli, "base" and "comparison," separated by a variable inter stimulus delay (Fig. 8.5a). Each stimulus is a vibration, generated as a series of velocity values sampled from a normal distribution (Fig. 8.5b). The rat must judge which stimulus has greater velocity standard deviation (Fig. 8.5c). The temporal separations between stimuli and, later, between the second stimulus and the time of response permit analysis of the neuronal activity specifically underlying sensation, memory, decision and action selection. For instance, during the inter stimulus delay, the rat must remember the base stimulus, yet there is no information available allowing action planning until the comparison stimulus is presented. The delay thus entails a purely sensory representation.

Moreover, the stimulus is exactly the sort of "noise" used to map neuronal feature selectivity through reverse correlation methods. The design allows the investigator to examine the algorithms of whisker-mediated perception that underlie behavioral performance.

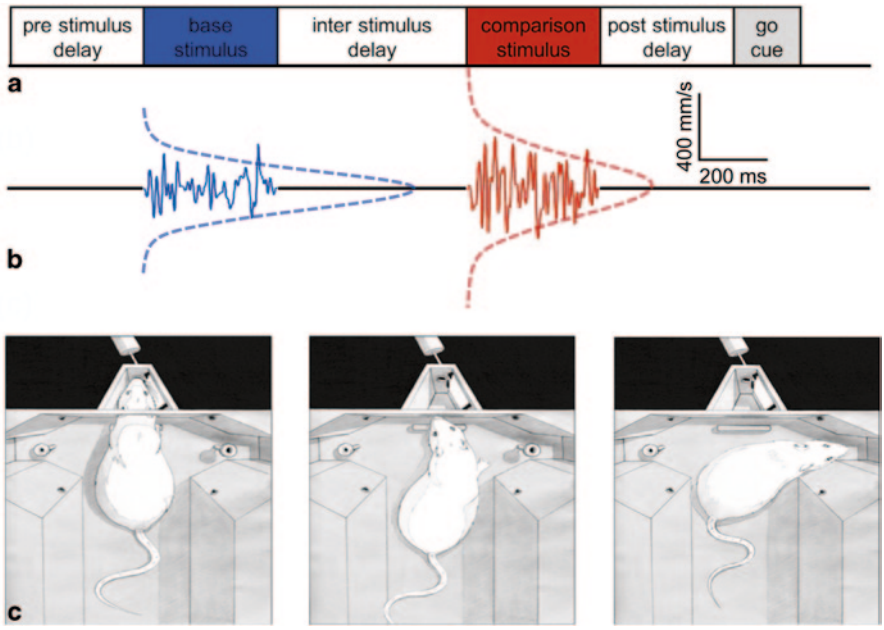

Fig. 8.5 Behavioral task designed for the study of functional principles of whisker-mediated touch perception. **a** Structure of a single trial. The rat, immobile, awaits the tactile stimuli during a pre stimulus delay. It then receives the base stimulus and the comparison stimulus, separated by the inter stimulus delay. During the post stimulus delay, the rat awaits the go cue, which signals that it may withdraw and make a choice. All time intervals and stimulus parameters are under experimenter's control and may be varied across trials. **b** Stimuli are composed of a series of velocity values where the sampling probability of a given velocity value is given by a normal distribution with mean =0 and standard deviation =σ. A sample base stimulus, of 400 ms duration, is shown by the blue trace and a comparison stimulus, also of 400 ms duration, by the red trace. The underlying normal distributions for the two stimuli are shown by the dashed lines. In this case, $\sigma_{comparison} > \sigma_{base}$. Time and velocity scales to the right. The "noisy" vibrations depicted in color are of the form suited to uncover the features that drive sensory neurons. **c** Sketches depicting one trial. Once the rat has positioned its snout in the nose poke and its whiskers on the plate connected to the motor (*left* panel), the trial begins. The rat remains immobile in this position until hearing the go cue. At that point the rat withdraws from the nose poke (middle panel) and turns to either the *left* or *right* reward spout (*right* panel), in this case to the right. The task is based upon a perceptual rule: if $\sigma_{base} > \sigma_{comparison}$, the *left* spout is rewarded; if $\sigma_{comparison} > \sigma_{base}$, the *right* spout is rewarded. (The figure is adapted from the study presented in [86])

Acknowledgements We are grateful to Stuart Ingham for help with the artwork in Fig. 8.1 and to Marco Gigante for the artwork in Fig. 8.5c. We thank Michael Bale for comments on an earlier version. Funding was from the Spanish Ministry of Economy and Competitiveness grant BFU2011-23049 (co-funded by the European Fund for Regional Development); the Valencia Regional Government grant PROMETEO/2011/086; the Human Frontier Science Program grant Neuroscience of Knowledge (RG0015/2013); the European Research Council Advanced grant CONCEPT (294498); the European Union FET grant CORONET (269459); the Italian Ministry for Universities and Research grant HANDBOT.

References

1. DiCarlo JJ, Zoccolan D, Rust NC (2012) How does the brain solve visual object recognition? Neuron 73(3):415–434
2. Diamond ME, Arabzadeh E (2013) Whisker sensory system—from receptor to decision. Prog Neurobiol 103:28–40
3. Carandini M (2012) From circuits to behavior: a bridge too far? Nat Neurosci 15(4):507–509
4. Hartmann MJ (2011) A night in the life of a rat: vibrissal mechanics and tactile exploration. Ann N Y Acad Sci 1225:110–118
5. Kleinfeld D, Deschenes M (2011) Neuronal basis for object location in the vibrissa scanning sensorimotor system. Neuron 72(3):455–468
6. Deschenes M, Moore J, Kleinfeld D (2012) Sniffing and whisking in rodents. Curr Opin Neurobiol 22(2):243–250
7. Diamond ME, von Heimendahl M, Knutsen PM, Kleinfeld D, Ahissar E (2008) 'Where' and 'what' in the whisker sensorimotor system. Nat Rev Neurosci 9(8):601–612
8. Lee S, Carvell GE, Simons DJ (2008) Motor modulation of afferent somatosensory circuits. Nat Neurosci 11(12):1430–1438
9. Matyas F, Sreenivasan V, Marbach F, Wacongne C, Barsy B, Mateo C et al (2010) Motor control by sensory cortex. Science 330(6008):1240–1243
10. Huber D, Gutnisky DA, Peron S, O'Connor DH, Wiegert JS, Tian L et al (2012) Multiple dynamic representations in the motor cortex during sensorimotor learning. Nature 484(7395):473–478
11. Petreanu L, Gutnisky DA, Huber D, Xu NL, O'Connor DH, Tian L et al (2012) Activity in motor-sensory projections reveals distributed coding in somatosensation. Nature 489(7415):299–303
12. Feldmeyer D, Brecht M, Helmchen F, Petersen CC, Poulet JF, Staiger JF et al (2013) Barrel cortex function. Prog Neurobiol 103:3–27
13. Kleinfeld D, Ahissar E, Diamond ME (2006) Active sensation: insights from the rodent vibrissa sensorimotor system. Curr Opin Neurobiol 16(4):435–444
14. Dorfl J (1982) The musculature of the mystacial vibrissae of the white mouse. J Anat 135(Pt 1):147–154
15. Dorfl J (1985) The innervation of the mystacial region of the white mouse: a topographical study. J Anat 142:173–184
16. Rice FL, Mance A, Munger BL (1986) A comparative light microscopic analysis of the sensory innervation of the mystacial pad. I. Innervation of vibrissal follicle-sinus complexes. J Comp Neurol 252(2):154–174
17. Rice FL, Kinnman E, Aldskogius H, Johansson O, Arvidsson J (1993) The innervation of the mystacial pad of the rat as revealed by PGP 9.5 immunofluorescence. J Comp Neurol 337(3):366–385
18. Ebara S, Kumamoto K, Matsuura T, Mazurkiewicz JE, Rice FL (2002) Similarities and differences in the innervation of mystacial vibrissal follicle-sinus complexes in the rat and cat: a confocal microscopic study. J Comp Neurol 449(2):103–119
19. Bagdasarian K, Szwed M, Knutsen PM, Deutsch D, Derdikman D, Pietr M et al (2013) Pre-neuronal morphological processing of object location by individual whiskers. Nat Neurosci 16(5):622–631
20. Pammer L, O'Connor DH, Hires SA, Clack NG, Huber D, Myers EW et al (2013) The mechanical variables underlying object localization along the axis of the whisker. J Neurosci 33(16):6726–6741
21. Williams CM, Kramer EM (2010) The advantages of a tapered whisker. PLoS ONE 5(1):e8806
22. Hires SA, Pammer L, Svoboda K, Golomb D (2013) Tapered whiskers are required for active tactile sensation. Elife 2:e01350

23. Voges D, Carl K, Klauer GJ, Uhlig R, Schilling C, Behn C et al (2012) Structural Characterization of the Whisker System of the Rat. Sensors J IEEE 12(2):332–339
24. Bermejo R, Houben D, Zeigler HP (1998) Optoelectronic monitoring of individual whisker movements in rats. J Neurosci Methods 83(2):89–96
25. Harvey MA, Bermejo R, Zeigler HP (2001) Discriminative whisking in the head-fixed rat: optoelectronic monitoring during tactile detection and discrimination tasks. Somatosens Mot Res 18(3):211–222
26. Knutsen PM, Derdikman D, Ahissar E (2005) Tracking whisker and head movements in unrestrained behaving rodents. J Neurophysiol 93(4):2294–2301
27. Voigts J, Sakmann B, Celikel T (2008) Unsupervised whisker tracking in unrestrained behaving animals. J Neurophysiol 100(1):504–515
28. Ritt JT, Andermann ML, Moore CI (2008) Embodied information processing: vibrissa mechanics and texture features shape micromotions in actively sensing rats. Neuron 57(4):599–613
29. Wolfe J, Hill DN, Pahlavan S, Drew PJ, Kleinfeld D, Feldman DE (2008) Texture coding in the rat whisker system: slip-stick versus differential resonance. PLoS Biol 6(8):e215
30. Perkon I, Kosir A, Itskov PM, Tasic J, Diamond ME (2011) Unsupervised quantification of whisking and head movement in freely moving rodents. J Neurophysiol 105(4):1950–1962
31. Clack NG, O'Connor DH, Huber D, Petreanu L, Hires A, Peron S et al (2012) Automated tracking of whiskers in videos of head fixed rodents. PLoS Comput Biol 8(7):e1002591
32. Mitchinson B, Martin CJ, Grant RA, Prescott TJ (2007) Feedback control in active sensing: rat exploratory whisking is modulated by environmental contact. Proc Biol Sci 274(1613):1035–1041
33. Grant RA, Mitchinson B, Fox CW, Prescott TJ (2009) Active touch sensing in the rat: anticipatory and regulatory control of whisker movements during surface exploration. J Neurophysiol 101(2):862–874
34. Birdwell JA, Solomon JH, Thajchayapong M, Taylor MA, Cheely M, Towal RB et al (2007) Biomechanical models for radial distance determination by the rat vibrissal system. J Neurophysiol 98(4):2439–2455
35. Quist BW, Hartmann MJ (2012) Mechanical signals at the base of a rat vibrissa: the effect of intrinsic vibrissa curvature and implications for tactile exploration. J Neurophysiol 107(9):2298–2312
36. Boubenec Y, Shulz DE, Debregeas G (2012) Whisker encoding of mechanical events during active tactile exploration. Front Behav Neurosci 6:74
37. Solomon JH, Hartmann MJ (2011) Radial distance determination in the rat vibrissal system and the effects of Weber's law. Philos Trans R Soc Lond B Biol Sci 366(1581):3049–3057
38. Maksimovic S, Nakatani M, Baba Y, Nelson AM, Marshall KL, Wellnitz SA et al (2014) Epidermal Merkel cells are mechanosensory cells that tune mammalian touch receptors. Nature 509(7502):617–621
39. Arabzadeh E, Zorzin E, Diamond ME (2005) Neuronal encoding of texture in the whisker sensory pathway. PLoS Biol 3(1):e17
40. Lottem E, Azouz R (2008) Dynamic translation of surface coarseness into whisker vibrations. J Neurophysiol 100(5):2852–2865
41. Jadhav SP, Wolfe J, Feldman DE (2009) Sparse temporal coding of elementary tactile features during active whisker sensation. Nat Neurosci 12(6):792–800
42. Lottem E, Azouz R (2009) Mechanisms of tactile information transmission through whisker vibrations. J Neurosci 29(37):11686–11697
43. Jadhav SP, Feldman DE (2010) Texture coding in the whisker system. Curr Opin Neurobiol 20(3):313–318
44. Morita T, Kang H, Wolfe J, Jadhav SP, Feldman DE (2011) Psychometric curve and behavioral strategies for whisker-based texture discrimination in rats. PLoS ONE 6(6):e20437
45. Zuo Y, Perkon I, Diamond ME (2011) Whisking and whisker kinematics during a texture classification task. Philos Trans R Soc Lond B Biol Sci 366(1581):3058–3069

46. Melaragno HP, Montagna W (1953) The tactile hair follicles in the mouse. Anat Rec 115(2):129–49
47. Rice FL (1993) Structure, vascularization, and innervation of the mystacial pad of the rat as revealed by the lectin Griffonia simplicifolia. J Comp Neurol 337(3):386–399
48. Hartmann MJ, Johnson NJ, Towal RB, Assad C (2003) Mechanical characteristics of rat vibrissae: resonant frequencies and damping in isolated whiskers and in the awake behaving animal. J Neurosci 23(16):6510–6519
49. Hill DN, Bermejo R, Zeigler HP, Kleinfeld D (2008) Biomechanics of the vibrissa motor plant in rat: rhythmic whisking consists of triphasic neuromuscular activity. J Neurosci 28(13):3438–3455
50. Haidarliu S, Simony E, Golomb D, Ahissar E (2011) Collagenous skeleton of the rat mystacial pad. Anat Rec 294(5):764–773
51. Simony E, Bagdasarian K, Herfst L, Brecht M, Ahissar E, Golomb D (2010) Temporal and spatial characteristics of vibrissa responses to motor commands. J Neurosci 30(26):8935–8952
52. Clarke WB, Bowsher D (1962) Terminal distribution of primary afferent trigeminal fibers in the rat. Exp Neurol 6:372–383
53. Zucker E, Welker WI (1969) Coding of somatic sensory input by vibrissae neurons in the rat's trigeminal ganglion. Brain Res 12(1):138–156
54. Mitchinson B, Arabzadeh E, Diamond ME, Prescott TJ (2008) Spike-timing in primary sensory neurons: a model of somatosensory transduction in the rat. Biol Cybern 98(3):185–194
55. Lottem E, Azouz R (2011) A unifying framework underlying mechanotransduction in the somatosensory system. J Neurosci 31(23):8520–8532
56. Gibson JM, Welker WI (1983) Quantitative studies of stimulus coding in first-order vibrissa afferents of rats. 1. Receptive field properties and threshold distributions. Somatosens Res 1(1):51–67
57. Gibson JM, Welker WI (1983) Quantitative studies of stimulus coding in first-order vibrissa afferents of rats. 2. Adaptation and coding of stimulus parameters. Somatosens Res 1(2):95–117
58. Lichtenstein SH, Carvell GE, Simons DJ (1990) Responses of rat trigeminal ganglion neurons to movements of vibrissae in different directions. Somatosens Mot Res 7(1):47–65
59. Shoykhet M, Doherty D, Simons DJ (2000) Coding of deflection velocity and amplitude by whisker primary afferent neurons: implications for higher level processing. Somatosens Mot Res 17(2):171–180
60. Szwed M, Bagdasarian K, Ahissar E (2003) Encoding of vibrissal active touch. Neuron 40(3):621–630
61. Jones LM, Depireux DA, Simons DJ, Keller A (2004) Robust temporal coding in the trigeminal system. Science 304(5679):1986–1989
62. Szwed M, Bagdasarian K, Blumenfeld B, Barak O, Derdikman D, Ahissar E (2006) Responses of trigeminal ganglion neurons to the radial distance of contact during active vibrissal touch. J Neurophysiol 95(2):791–802
63. Stuttgen MC, Kullmann S, Schwarz C (2008) Responses of rat trigeminal ganglion neurons to longitudinal whisker stimulation. J Neurophysiol 100(4):1879–1884
64. Bale MR, Petersen RS (2009) Transformation in the neural code for whisker deflection direction along the lemniscal pathway. J Neurophysiol 102(5):2771–2780
65. Leiser SC, Moxon KA (2007) Responses of trigeminal ganglion neurons during natural whisking behaviors in the awake rat. Neuron 53(1):117–133
66. Khatri V, Bermejo R, Brumberg JC, Keller A, Zeigler HP (2009) Whisking in air: encoding of kinematics by trigeminal ganglion neurons in awake rats. J Neurophysiol 101(4):1836–1846
67. Bale MR, Davies K, Freeman OJ, Ince RAA, Petersen RS (2013) Low-dimensional sensory feature representation by trigeminal primary afferents. J Neurosci 33(29):12003–12012
68. Sakurai K, Akiyama M, Cai B, Scott A, Han BX, Takatoh J et al (2013) The organization of submodality-specific touch afferent inputs in the vibrissa column. Cell Rep 5(1):87–98

69. Jones LM, Lee S, Trageser JC, Simons DJ, Keller A (2004) Precise temporal responses in whisker trigeminal neurons. J Neurophysiol 92(1):665–668
70. Carr CE, Macleod KM (2010) Microseconds matter. PLoS Biol 8(6):e1000405
71. Arabzadeh E, Panzeri S, Diamond ME (2006) Deciphering the spike train of a sensory neuron: counts and temporal patterns in the rat whisker pathway. J Neurosci 26(36):9216–9226
72. von Heimendahl M, Itskov PM, Arabzadeh E, Diamond ME (2007) Neuronal activity in rat barrel cortex underlying texture discrimination. PLoS Biol 5(11):e305
73. Prescott TJ, Diamond ME, Wing AM (2011) Active touch sensing. Philos Trans R Soc Lond B Biol Sci 366(1581):2989–2995
74. Jenks RA, Vaziri A, Boloori AR, Stanley GB (2010) Self-motion and the shaping of sensory signals. J Neurophysiol 103(4):2195–2207
75. Hutson KA, Masterton RB (1986) The sensory contribution of a single vibrissa's cortical barrel. J Neurophysiol 56(4):1196–1223
76. Carvell GE, Simons DJ (1990) Biometric analyses of vibrissal tactile discrimination in the rat. J Neurosci 10(8):2638–2648
77. Knutsen PM, Pietr M, Ahissar E (2006) Haptic object localization in the vibrissal system: behavior and performance. J Neurosci 26(33):8451–8464
78. O'Connor DH, Clack NG, Huber D, Komiyama T, Myers EW, Svoboda K (2010) Vibrissa-based object localization in head-fixed mice. J Neurosci 30(5):1947–1967
79. Yu C, Horev G, Rubin N, Derdikman D, Haidarliu S, Ahissar E (2015) Coding of object location in the vibrissal thalamocortical system. Cereb Cortex 25(3):563–577
80. Stuttgen MC, Ruter J, Schwarz C (2006) Two psychophysical channels of whisker deflection in rats align with two neuronal classes of primary afferents. J Neurosci 26(30):7933–7941
81. Stuttgen MC, Schwarz C (2008) Psychophysical and neurometric detection performance under stimulus uncertainty. Nat Neurosci 11(9):1091–1099
82. Adibi M, Arabzadeh E (2011) A comparison of neuronal and behavioral detection and discrimination performances in rat whisker system. J Neurophysiol 105(1):356–365
83. Adibi M, Diamond ME, Arabzadeh E (2012) Behavioral study of whisker-mediated vibration sensation in rats. Proc Natl Acad Sci U S A 109(3):971–976
84. Mayrhofer JM, Skreb V, von der Behrens W, Musall S, Weber B, Haiss F (2013) Novel two-alternative forced choice paradigm for bilateral vibrotactile whisker frequency discrimination in head-fixed mice and rats. J Neurophysiol 109(1):273–284
85. Miyashita T, Feldman DE (2013) Behavioral detection of passive whisker stimuli requires somatosensory cortex. Cereb Cortex 23(7):1655–1662
86. Fassihi A, Akrami A, Esmaeili V, Diamond ME (2014) Tactile perception and working memory in rats and humans. Proc Natl Acad Sci U S A 111(6):2331–2336
87. Krupa DJ, Matell MS, Brisben AJ, Oliveira LM, Nicolelis MA (2001) Behavioral properties of the trigeminal somatosensory system in rats performing whisker-dependent tactile discriminations. J Neurosci 21(15):5752–5763
88. de Boer E, Kuyper P (1968) Triggered correlation. IEEE Trans Biomed Eng 15(3):169–179
89. Sharpee TO (2013) Computational identification of receptive fields. Annu Rev Neurosci 36:103–120
90. Maravall M, Alenda A, Bale MR, Petersen RS (2013) Transformation of Adaptation and Gain Rescaling along the Whisker Sensory Pathway. PLoS One 8(12):e82418
91. Theis L, Chagas AM, Arnstein D, Schwarz C, Bethge M (2013) Beyond GLMs: A Generative Mixture Modeling Approach to Neural System Identification. PLoS Comput Biol 9(11):e1003356
92. Chagas AM, Theis L, Sengupta B, Stuttgen MC, Bethge M, Schwarz C (2013) Functional analysis of ultra high information rates conveyed by rat vibrissal primary afferents. Front Neural Circuits 7:190
93. Petersen RS, Brambilla M, Bale MR, Alenda A, Panzeri S, Montemurro MA et al (2008) Diverse and temporally precise kinetic feature selectivity in the VPm thalamic nucleus. Neuron 60(5):890–903

94. Maravall M, Petersen RS, Fairhall AL, Arabzadeh E, Diamond ME (2007) Shifts in coding properties and maintenance of information transmission during adaptation in barrel cortex. PLoS Biol 5(2):e19
95. Estebanez L, Boustani S E, Destexhe A, Shulz DE (2012) Correlated input reveals coexisting coding schemes in a sensory cortex. Nat Neurosci 15(12):1691–1699
96. Petersen RS, Panzeri S, Maravall M (2009) Neural coding and contextual influences in the whisker system. Biol Cybern 100(6):427–446
97. Jacob V, Cam J L, Ego-Stengel V, Shulz DE (2008) Emergent properties of tactile scenes selectively activate barrel cortex neurons. Neuron 60(6):1112–1125
98. Ego-Stengel V, Cam J L, Shulz DE (2012) Coding of apparent motion in the thalamic nucleus of the rat vibrissal somatosensory system. J Neurosci 32(10):3339–3351
99. Hirata A, Castro-Alamancos MA (2008) Cortical transformation of wide-field (multiwhisker) sensory responses. J Neurophysiol 100(1):358–370
100. Crochet S, Petersen CC (2006) Correlating whisker behavior with membrane potential in barrel cortex of awake mice. Nat Neurosci 9(5):608–610
101. Curtis JC, Kleinfeld D (2009) Phase-to-rate transformations encode touch in cortical neurons of a scanning sensorimotor system. Nat Neurosci 12(4):492–501
102. O'Connor DH, Peron SP, Huber D, Svoboda K (2010) Neural activity in barrel cortex underlying vibrissa-based object localization in mice. Neuron 67(6):1048–1061
103. Chen JL, Carta S, Soldado-Magraner J, Schneider BL, Helmchen F (2013) Behaviour-dependent recruitment of long-range projection neurons in somatosensory cortex. Nature 499(7458):336–340
104. de Kock CP, Bruno RM, Spors H, Sakmann B (2007) Layer- and cell-type-specific suprathreshold stimulus representation in rat primary somatosensory cortex. J Physiol 581(Pt 1):139–154
105. de Kock CP, Sakmann B (2009) Spiking in primary somatosensory cortex during natural whisking in awake head-restrained rats is cell-type specific. Proc Natl Acad Sci U S A 106(38):16446–16450
106. Barth AL, Poulet JF (2012) Experimental evidence for sparse firing in the neocortex. Trends Neurosci 35(6):345–355
107. Wolfe J, Houweling AR, Brecht M (2010) Sparse and powerful cortical spikes. Curr Opin Neurobiol 20(3):306–312
108. Ganguli S, Sompolinsky H (2012) Compressed sensing, sparsity, and dimensionality in neuronal information processing and data analysis. Annu Rev Neurosci 35:485–508
109. Harris KD, Mrsic-Flogel TD (2013) Cortical connectivity and sensory coding. Nature 503(7474):51–58
110. Quiroga RQ (2012) Concept cells: the building blocks of declarative memory functions. Nat Rev Neurosci 13(8):587–597
111. Moore CI, Nelson SB (1998) Spatio-temporal subthreshold receptive fields in the vibrissa representation of rat primary somatosensory cortex. J Neurophysiol 80(6):2882–2892
112. Zhu JJ, Connors BW (1999) Intrinsic firing patterns and whisker-evoked synaptic responses of neurons in the rat barrel cortex. J Neurophysiol 81(3):1171–1183
113. Brecht M, Sakmann B (2002) Whisker maps of neuronal subclasses of the rat ventral posterior medial thalamus, identified by whole-cell voltage recording and morphological reconstruction. J Physiol 538(Pt 2):495–515
114. Brecht M, Sakmann B (2002) Dynamic representation of whisker deflection by synaptic potentials in spiny stellate and pyramidal cells in the barrels and septa of layer 4 rat somatosensory cortex. J Physiol 543(Pt 1):49–70
115. Brecht M, Roth A, Sakmann B (2003) Dynamic receptive fields of reconstructed pyramidal cells in layers 3 and 2 of rat somatosensory barrel cortex. J Physiol 553(Pt 1):243–265
116. Yassin L, Benedetti BL, Jouhanneau JS, Wen JA, Poulet JF, Barth AL (2010) An embedded subnetwork of highly active neurons in the neocortex. Neuron 68(6):1043–1050
117. Petersen CC, Crochet S (2013) Synaptic computation and sensory processing in neocortical layer 2/3. Neuron 78(1):28–48

118. Safaai H, von Heimendahl M, Sorando JM, Diamond ME, Maravall M (2013) Coordinated population activity underlying texture discrimination in rat barrel cortex. J Neurosci 33(13):5843–5855
119. Yamashita T, Pala A, Pedrido L, Kremer Y, Welker E, Petersen CC (2013) Membrane potential dynamics of neocortical projection neurons driving target-specific signals. Neuron 80(6):1477–1490
120. Andermann ML, Moore CI (2006) A somatotopic map of vibrissa motion direction within a barrel column. Nat Neurosci 9(4):543–551
121. Kerr JN, de Kock CP, Greenberg DS, Bruno RM, Sakmann B, Helmchen F (2007) Spatial organization of neuronal population responses in layer 2/3 of rat barrel cortex. J Neurosci 27(48):13316–13328
122. Sato TR, Gray NW, Mainen ZF, Svoboda K (2007) The functional microarchitecture of the mouse barrel cortex. PLoS Biol 5(7):e189
123. Crochet S, Poulet JF, Kremer Y, Petersen CC (2011) Synaptic mechanisms underlying sparse coding of active touch. Neuron 69(6):1160–1175
124. Margolis DJ, Lutcke H, Schulz K, Haiss F, Weber B, Kugler S et al (2012) Reorganization of cortical population activity imaged throughout long-term sensory deprivation. Nat Neurosci 15(11):1539–1546
125. Elstrott J, Clancy KB, Jafri H, Akimenko I, Feldman DE (2014) Cellular mechanisms for response heterogeneity among L2/3 pyramidal cells in whisker somatosensory cortex. J Neurophysiol 112(2):233–248
126. Montemurro MA, Panzeri S, Maravall M, Alenda A, Bale MR, Brambilla M et al (2007) Role of precise spike timing in coding of dynamic vibrissa stimuli in somatosensory thalamus. J Neurophysiol 98(4):1871–1882
127. Fee MS, Mitra PP, Kleinfeld D (1997) Central versus peripheral determinants of patterned spike activity in rat vibrissa cortex during whisking. J Neurophysiol 78(2):1144–1149
128. Hill DN, Curtis JC, Moore JD, Kleinfeld D (2011) Primary motor cortex reports efferent control of vibrissa motion on multiple timescales. Neuron 72(2):344–356
129. Gentet LJ, Avermann M, Matyas F, Staiger JF, Petersen CC (2010) Membrane potential dynamics of GABAergic neurons in the barrel cortex of behaving mice. Neuron 65(3):422–435
130. Knutsen PM, Ahissar E (2009) Orthogonal coding of object location. Trends Neurosci 32(2):101–109
131. Panzeri S, Diamond ME (2010) Information carried by population spike times in the whisker sensory cortex can be decoded without knowledge of stimulus time. Front Synaptic Neurosci 2:17
132. Panzeri S, Ince RA, Diamond ME, Kayser C (2014) Reading spike timing without a clock: intrinsic decoding of spike trains. Phil Trans R Soc B 369(1637):20120467.
133. Panzeri S, Petersen RS, Schultz SR, Lebedev M, Diamond ME (2001) The role of spike timing in the coding of stimulus location in rat somatosensory cortex. Neuron 29(3):769–777
134. Petersen RS, Panzeri S, Diamond ME (2001) Population coding of stimulus location in rat somatosensory cortex. Neuron 32(3):503–514
135. Johansson RS, Birznieks I (2004) First spikes in ensembles of human tactile afferents code complex spatial fingertip events. Nat Neurosci 7(2):170–177
136. Foffani G, Tutunculer B, Moxon KA (2004) Role of spike timing in the forelimb somatosensory cortex of the rat. J Neurosci 24(33):7266–7271
137. Storchi R, Bale MR, Biella GE, Petersen RS (2012) Comparison of latency and rate coding for the direction of whisker deflection in the subcortical somatosensory pathway. J Neurophysiol 108(7):1810–1821
138. Temereanca S, Brown EN, Simons DJ (2008) Rapid changes in thalamic firing synchrony during repetitive whisker stimulation. J Neurosci 28(44):11153–11164

139. Khatri V, Bruno RM, Simons DJ (2009) Stimulus-specific and stimulus-nonspecific firing synchrony and its modulation by sensory adaptation in the whisker-to-barrel pathway. J Neurophysiol 101(5):2328–2338
140. Stanley GB, Jin J, Wang Y, Desbordes G, Wang Q, Black MJ et al (2012) Visual orientation and directional selectivity through thalamic synchrony. J Neurosci 32(26):9073–9088
141. Brette R (2012) Computing with neural synchrony. PLoS Comput Biol 8(6):e1002561
142. Rossant C, Leijon S, Magnusson AK, Brette R (2011) Sensitivity of noisy neurons to coincident inputs. J Neurosci 31(47):17193–17206
143. Bruno RM, Sakmann B (2006) Cortex is driven by weak but synchronously active thalamocortical synapses. Science 312(5780):1622–1627
144. Song S, Sjostrom PJ, Reigl M, Nelson S, Chklovskii DB (2005) Highly nonrandom features of synaptic connectivity in local cortical circuits. PLoS Biol 3(3):e68
145. Lefort S, Tomm C, Floyd Sarria JC, Petersen CC (2009) The excitatory neuronal network of the C2 barrel column in mouse primary somatosensory cortex. Neuron 61(2):301–316
146. Diaz-Quesada M, Martini FJ, Ferrati G, Bureau I, Maravall M (2014) Diverse thalamocortical short-term plasticity elicited by ongoing stimulation. J Neurosci 34(2):515–526
147. O'Connor DH, Hires SA, Guo ZV, Li N, Yu J, Sun QQ et al (2013) Neural coding during active somatosensation revealed using illusory touch. Nat Neurosci 16(7):958–965
148. Diamond ME, von Heimendahl M, Arabzadeh E (2008) Whisker-mediated texture discrimination. PLoS Biol 6(8):e220
149. Maravall M (2013) Adaptation and sensory coding. In: Quian Quiroga R, Panzeri S (eds) Principles of neural coding. Taylor & Francis/CRC Press, Boca Raton, pp 357–378
150. Katz Y, Heiss JE, Lampl I (2006) Cross-whisker adaptation of neurons in the rat barrel cortex. J Neurosci 26(51):13363–13372
151. Khatri V, Simons DJ (2007) Angularly nonspecific response suppression in rat barrel cortex. Cereb Cortex 17(3):599–609
152. Wang Q, Webber RM, Stanley GB (2010) Thalamic synchrony and the adaptive gating of information flow to cortex. Nat Neurosci 13(12):1534–1541
153. Ollerenshaw DR, Zheng HJ, Millard DC, Wang Q, Stanley GB (2014) The adaptive tradeoff between detection and discrimination in cortical representations and behavior. Neuron 81(5):1152–1164
154. Adibi M, McDonald JS, Clifford CW, Arabzadeh E (2013) Adaptation improves neural coding efficiency despite increasing correlations in variability. J Neurosci 33(5):2108–2120
155. Adibi M, Clifford CW, Arabzadeh E (2013) Informational basis of sensory adaptation: entropy and single-spike efficiency in rat barrel cortex. J Neurosci 33(37):14921–14926
156. Lak A, Arabzadeh E, Diamond ME (2008) Enhanced response of neurons in rat somatosensory cortex to stimuli containing temporal noise. Cereb Cortex 18(5):1085–1093
157. Lak A, Arabzadeh E, Harris JA, Diamond ME (2010) Correlated physiological and perceptual effects of noise in a tactile stimulus. Proc Natl Acad Sci U S A 107(17):7981–7986
158. Mease RA, Krieger P, Groh A (2014) Cortical control of adaptation and sensory relay mode in the thalamus. Proc Natl Acad Sci U S A 111(18):6798–6803
159. Garcia-Lazaro JA, Ho SS, Nair A, Schnupp JW (2007) Shifting and scaling adaptation to dynamic stimuli in somatosensory cortex. Eur J Neurosci 26(8):2359–2368
160. Lundstrom BN, Fairhall AL, Maravall M (2010) Multiple timescale encoding of slowly varying whisker stimulus envelope in cortical and thalamic neurons in vivo. J Neurosci 30(14):5071–5077
161. Chung S, Li X, Nelson SB (2002) Short-term depression at thalamocortical synapses contributes to rapid adaptation of cortical sensory responses in vivo. Neuron 34(3):437–446
162. Ganmor E, Katz Y, Lampl I (2010) Intensity-dependent adaptation of cortical and thalamic neurons is controlled by brainstem circuits of the sensory pathway. Neuron 66(2):273–286
163. Diaz-Quesada M, Maravall M (2008) Intrinsic mechanisms for adaptive gain rescaling in barrel cortex. J Neurosci 28(3):696–710

164. Mease RA, Famulare M, Gjorgjieva J, Moody WJ, Fairhall AL (2013) Emergence of adaptive computation by single neurons in the developing cortex. J Neurosci 33(30):12154–12170
165. Abbott LF, Dayan P (1999) The effect of correlated variability on the accuracy of a population code. Neural Comput 11(1):91–101
166. Sompolinsky H, Yoon H, Kang K, Shamir M (2001) Population coding in neuronal systems with correlated noise. Phys Rev E Stat Nonlin Soft Matter Phys 64(5 Pt 1):051904
167. Shamir M, Sompolinsky H (2006) Implications of neuronal diversity on population coding. Neural Comput 18(8):1951–1986
168. Chelaru MI, Dragoi V (2008) Efficient coding in heterogeneous neuronal populations. Proc Natl Acad Sci U S A 105(42):16344–16349
169. Hung CP, Kreiman G, Poggio T, DiCarlo JJ (2005) Fast readout of object identity from macaque inferior temporal cortex. Science 310(5749):863–866
170. Meyers EM, Freedman DJ, Kreiman G, Miller EK, Poggio T (2008) Dynamic population coding of category information in inferior temporal and prefrontal cortex. J Neurophysiol 100(3):1407–1419
171. Nikolic D, Hausler S, Singer W, Maass W (2009) Distributed fading memory for stimulus properties in the primary visual cortex. PLoS Biol 7(12):e1000260
172. Klampfl S, David SV, Yin P, Shamma SA, Maass W (2012) A quantitative analysis of information about past and present stimuli encoded by spikes of A1 neurons. J Neurophysiol 108(5):1366–1380
173. Buzsaki G, Draguhn A (2004) Neuronal oscillations in cortical networks. Science 304(5679):1926–1929
174. Harris KD, Thiele A (2011) Cortical state and attention. Nat Rev Neurosci 12(9):509–523
175. Zohary E, Shadlen MN, Newsome WT (1994) Correlated neuronal discharge rate and its implications for psychophysical performance. Nature 370(6485):140–143
176. Amzica F, Steriade M (1995) Short- and long-range neuronal synchronization of the slow (<1 Hz) cortical oscillation. J Neurophysiol 73(1):20–38
177. Arieli A, Shoham D, Hildesheim R, Grinvald A (1995) Coherent spatiotemporal patterns of ongoing activity revealed by real-time optical imaging coupled with single-unit recording in the cat visual cortex. J Neurophysiol 73(5):2072–2093
178. Arieli A, Sterkin A, Grinvald A, Aertsen A (1996) Dynamics of ongoing activity: explanation of the large variability in evoked cortical responses. Science 273(5283):1868–1871
179. Buracas GT, Zador AM, DeWeese MR, Albright TD (1998) Efficient discrimination of temporal patterns by motion-sensitive neurons in primate visual cortex. Neuron 20(5):959–969
180. Azouz R, Gray CM (1999) Cellular mechanisms contributing to response variability of cortical neurons in vivo. J Neurosci 19(6):2209–2223
181. Lampl I, Reichova I, Ferster D (1999) Synchronous membrane potential fluctuations in neurons of the cat visual cortex. Neuron 22(2):361–374
182. Tsodyks M, Kenet T, Grinvald A, Arieli A (1999) Linking spontaneous activity of single cortical neurons and the underlying functional architecture. Science 286(5446):1943–1946
183. Anderson J, Lampl I, Reichova I, Carandini M, Ferster D (2000) Stimulus dependence of two-state fluctuations of membrane potential in cat visual cortex. Nat Neurosci 3(6):617–621
184. Petersen CC, Hahn TT, Mehta M, Grinvald A, Sakmann B (2003) Interaction of sensory responses with spontaneous depolarization in layer 2/3 barrel cortex. Proc Natl Acad Sci U S A 100(23):13638–13643
185. Deweese MR, Zador AM (2004) Shared and private variability in the auditory cortex. J Neurophysiol 92(3):1840–1855
186. Poulet JF, Petersen CC (2008) Internal brain state regulates membrane potential synchrony in barrel cortex of behaving mice. Nature 454(7206):881–885
187. Erchova IA, Lebedev MA, Diamond ME (2002) Somatosensory cortical neuronal population activity across states of anaesthesia. Eur J Neurosci 15(4):744–752

188. Castro-Alamancos MA (2004) Absence of rapid sensory adaptation in neocortex during information processing states. Neuron 41(3):455–464
189. Sachdev RN, Ebner FF, Wilson CJ (2004) Effect of subthreshold up and down states on the whisker-evoked response in somatosensory cortex. J Neurophysiol 92(6):3511–3521
190. Haslinger R, Ulbert I, Moore CI, Brown EN, Devor A (2006) Analysis of LFP phase predicts sensory response of barrel cortex. J Neurophysiol 96(3):1658–1663
191. Hasenstaub A, Sachdev RN, McCormick DA (2007) State changes rapidly modulate cortical neuronal responsiveness. J Neurosci 27(36):9607–9622
192. Reig R, Sanchez-Vives MV (2007) Synaptic transmission and plasticity in an active cortical network. PLoS ONE 2(7):e670
193. Constantinople CM, Bruno RM (2011) Effects and mechanisms of wakefulness on local cortical networks. Neuron 69(6):1061–1068
194. Katz Y, Okun M, Lampl I (2012) Trial-to-trial correlation between thalamic sensory response and global EEG activity. Eur J Neurosci 35(6):826–837
195. Alenda A, Molano-Mazon M, Panzeri S, Maravall M (2010) Sensory input drives multiple intracellular information streams in somatosensory cortex. J Neurosci 30(32):10872–10884
196. Poulet JF, Fernandez LM, Crochet S, Petersen CC (2012) Thalamic control of cortical states. Nat Neurosci 15(3):370–372
197. MacLean JN, Watson BO, Aaron GB, Yuste R (2005) Internal dynamics determine the cortical response to thalamic stimulation. Neuron 48(5):811–823
198. Guo ZV, Li N, Huber D, Ophir E, Gutnisky D, Ting JT et al (2014) Flow of cortical activity underlying a tactile decision in mice. Neuron 81(1):179–194

Chapter 9
Location Coding by the Whisking System

Tess Baker Oram, Eldad Assa, Per Magne Knutsen and Ehud Ahissar

Abstract The rodent whisking (vibrissal) system is an active sensing system, which is well suited to the study of sensory encoding and decoding since it is sufficiently traceable at anatomical, functional and behavioral levels. Our topic herein is the process by which whisking rodents can encode and decode sensory stimuli to build complex perceptions of their external environment, using object localization as a representative case.

Keywords Object localization · Closed-loop · Active sensing · Sensory encoding · Localization behavior

Abbreviations

2DG	2-Deoxy-D-glucose
BG	Basal ganglia
BPN	Brainstem premotor nuclei
Cer	Cerebellum
FN	Facial nucleus
IO	Inferior olive
IoN	Infraorbital nerve
M1	Primary motor cortex

T.B. Oram and E. Assa contributed equally to this work.

T. B. Oram (✉) · E. Assa (✉) · E. Ahissar
Department of Neurobiology, Weizmann Institute of Science,
234 Herzl St., 7610001 Rehovot, Israel
e-mail: tess.oram@weizmann.ac.il

E. Assa (✉)
e-mail: eldad.assa@weizmann.ac.il

P. M. Knutsen
Department of Physics, University of California at San Diego,
9500 Gilman Drive, La Jolla, CA 92093-0374, USA
e-mail: pknutsen@ucsd.edu

E. Ahissar
e-mail: ehud.ahissar@weizmann.ac.il

P. Krieger, A. Groh (eds.), *Sensorimotor Integration in the Whisker System,*
DOI 10.1007/978-1-4939-2975-7_9

MCx	Motor cortex
NPLL	Neuronal implementation of a phase locked loop
PD	Phase detector
PLL	Phase locked loop
POm	Medial sector of the posterior nucleus
Pn	Pontine nucleus
PrV	Primary trigeminal nucleus
RN	Red nucleus
S1	Primary somatosensory cortex
S1L4	Layer 4 of the primary somatosensory cortex, or barrel cortex
S1L5a	Layer 5a of the primary somatosensory cortex
S1L5b	Layer 5b of the primary somatosensory cortex
S2	Secondary somatosensory cortex
S2L2/3	Layers 2/3 of the secondary somatosensory cortex
S2L4	Layer 4 of the secondary somatosensory cortex
S2L6	Layer 6 of the secondary somatosensory cortex
SC	Superior colliculus
SpVi	Interpolar trigeminal nucleus
TG	Trigeminal ganglion
TN	Trigeminal nucleus
VL	Ventrolateral thalamic nucleus
VPMdm	Dorsomedial section of the ventral posterior medial nucleus
VPMvl	Ventrolateral section of the VPM
ZI	Zona incerta

Object Localization, Whisking Systems, and Active Sensing

Rats and mice are nocturnal animals whose habitats consist of confined, dark spaces [1, 2]. In this type of environment there are low light levels and sound is greatly attenuated. Thus, these rodents cannot solely rely on either vision or audition for the sensory input required for object localization [2, 3]. In what appears to be a successful adaptation to this niche, rats and mice have developed a specialized extension of the somatosensory system in which whiskers on their snouts are used to gather sensory information from their proximal environment. This specialization is known as the whisking, or vibrissal, system. Essentially all therian mammals, except humans, possess highly sensitive whiskers [4, 5]. The murine whisking systems of rats and mice are of particular interest as these animals actively whisk to sense their environment [6].

Active sensing is a perceptual process in which the motor actions of an organism are both influenced by and affect the sensory information received by the organism. The whisking system of rats and mice has served as a prime animal model of active sensing. Sensory signals generated by mechanoreceptors in the whisker follicles provide input to the whisking system, which in turn responds by sending motor signals to the mystacial pad muscles controlling whisker movement. As sensory information acquired by the whiskers co-determines whisker movement, the whisking

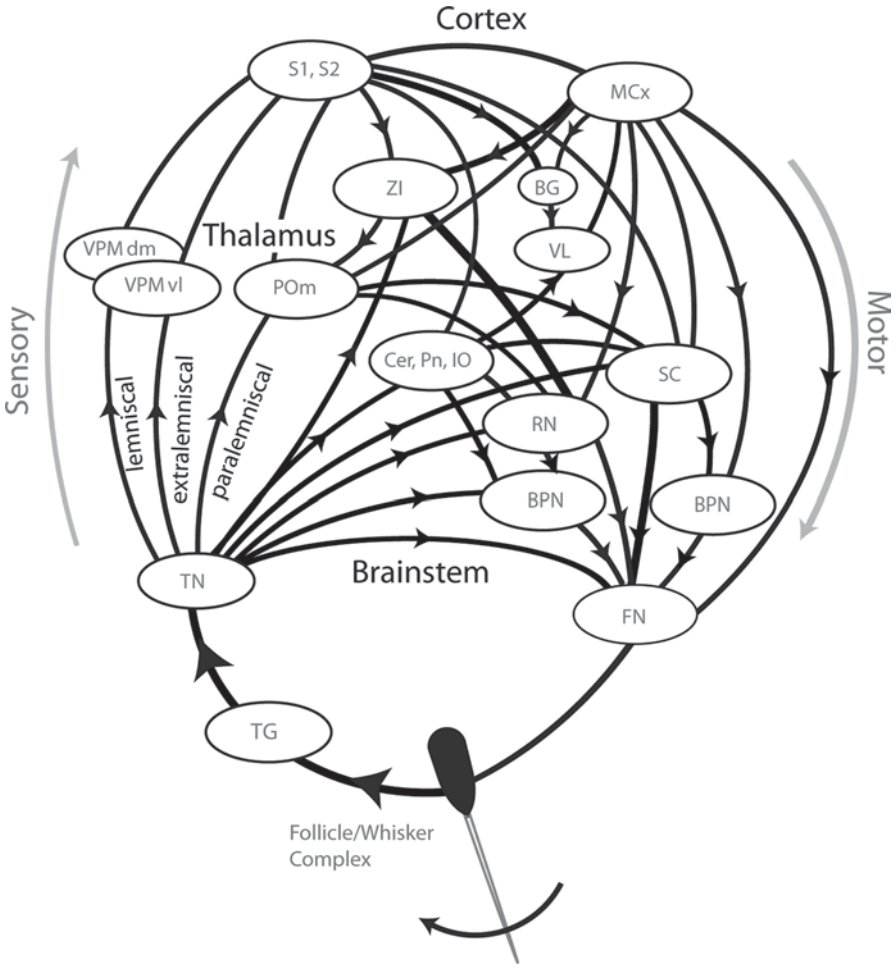

Fig. 9.1 Closed loop structure of the whisking system**.** *BG* basal ganglia, *BPN* brainstem premotor nuclei (arbitrarily divided to two oval circles), *Cer* cerebellum, *FN* facial nucleus, *IO* inferior olive, *MCx* motor cortex, *Pn* pontine nucleus, *POm* medial sector of the posterior nucleus, *RN* red nucleus, *S1* primary somatosensory cortex, *S2* secondary somatosensory cortex, *SC* superior colliculus, *TG* trigeminal ganglion, *TN* trigeminal nucleus, *VL* ventrolateral thalamic nucleus, *VPMdm* dorsomedial section of the ventral posterior medial nucleus, *VPMvl* ventrolateral section of the VPM, *ZI* zona incerta. (Reprinted with permission from [62])

system forms a "closed loop" (Fig. 9.1). Similarly, almost all mammalian sensory systems form such motor-sensory-motor closed loops.

Closed-loop control of sensation implies that brain regions cannot be divided categorically into "motor" and "sensory" stations. As all stations anatomically implicated as being part of a vibrissal system are part of a closed-loop, they are all affected by and themselves affect sensory and motor functions, albeit to different degrees. For example, the primary somatosensory cortex (S1) can play a significant role in the control of whisker motion [7] and the primary motor cortex (M1) can process somatosensory and proprioceptive signals [8–12].

In whisking animals, behaviors that reflect a goal of "minimal impingement" or "maximum contact" are examples of active-sensing strategies that require the recruitment of closed sensori-motor loops. Under normal conditions, rats employ a "minimal impingement" strategy in which they lightly contact obstacles with as many whiskers as possible [13, 14]. In contrast, rats that receive no sensory input from the whiskers, for example following deafferentation of the infraorbital nerve (IoN) which carries all of the sensory input from the whiskers to the brain, whisk without regard to the position of an object, often contacting and bending the whiskers until they pass it [15].

While sensory and motor systems are frequently considered in isolation, it is obvious that these systems have a high degree of interaction, and it is upon this interface that active sensing systems are built. Active sensing is beneficial in that sensory signals both determine and are determined by motor actions, giving these systems adaptive abilities that allow them to be more sensitive to specific sensory features. It is believed that it is this adaptive sensitivity that allows active sensing systems to complete fine perceptual tasks [16].

The Whisking System of Rats and Mice—Anatomy and Pathways

There are several anatomical features of the whisking system that facilitate its use as a model system for studying object localization. These features are particularly conducive to the examination of sensory information and motor commands; and therefore enable the study of encoding and decoding algorithms of specific behaviors, including those of object localization.

Rats and mice have about 35 whiskers (there are individual variations) arranged in 5 rows (A-E) and 7 columns (1–7) on the mystacial pad. Whiskers are moved in a characteristic oscillatory whisking motion at frequencies between 5 and 25 Hz (mice typically employ higher frequencies than rats) by sets of intrinsic and extrinsic muscles that lie in the mystacial pad [17]. Sensory signals are collected by mechanoreceptors in the whisker follicle [18] and are conveyed from the whisker follicle through the IoN to the brainstem. The cell bodies of the IoN sit in the trigeminal ganglion (TG).

At the level of the brainstem, sensory information is divided into anatomically distinct afferent pathways [19], which are likely to be functionally segregated in the follicle by virtue of mechanoreceptor specialization [18]. The whisking system contains at least six pathways that carry information from the whisker follicle to the cortex [20]. Here, we will focus on the three major pathways that are indicated in being involved in object localization. These pathways are well separated anatomically and functionally at the level of the thalamus.

The lemniscal pathway passes from the whisker follicle to the primary trigeminal nucleus (PrV) in the brainstem [21–23], then through the dorso-medial sector of the ventro-posterior-medial nucleus of the thalamus (VPMdm) and directly on to the barrels in layer 4 of the primary somatosensory cortex (S1L4, also known as the barrel cortex) and to layer 5b in S1 (S1L5b) [21, 22, 24–31]. This pathway contains topographic projections of the whiskers in the PrV ("barrelettes"), the VPMdm ("barreloids") and the S1L4 ("barrels") [25, 32–34]. These structures are somato-

topically mapped according to the whiskers' grid-like arrangement on the mystacial pad. Neurons in each barrelette, barreloid and barrel structure principally responds to a single whisker, leading to traceability of sensory signals from the whisker to the cortex within the lemniscal pathway [24, 35–39]. The extralemniscal pathway passes through the caudal part of the interpolar trigeminal nucleus (SpVi) [40], then through the ventro-lateral sector of the VPM (VPMvl) and on to the septa in S1L4 and layers 2 and 3 of the secondary somatosensory cortex (S2L2/3) [37, 40, 41]. The paralemniscal pathway passes first through the rostral part of SpVi [21–23, 42], then through the posterior complex of the thalamus (POm) to layer 5a of the somatosensory cortex (S1L5a) and layers 4 and 6 of the secondary somatosensory cortex (S2L4, S2L6) [40, 43, 44]. All three thalamic nuclei (VPMdm, VPMvl and POm) receive cortical feedback signals from layer 5 or 6 of the primary sensory cortex [45–52], from the secondary somatosensory cortex [46, 53] and from layer 6 of the primary motor cortex [54, 55].

It has been shown in electrophysiological data from anesthetized, artificially whisking rats, and 2-Deoxy-D-glucose (2DG) and c-Fos studies in behaving rats that the separation between the pathways is also preserved at the functional level; the lemniscal system carries whisking and touch signals, the extralemniscal pathway carries touch information, and the paralemniscal pathway carries information relevant to the control of whisker motion, as well as nociceptive information [37, 56–59]. According to this specialization, the extralemniscal pathway carries information that, together with the information conveyed by the paralemniscal pathway, is sufficient for recoding the location of external objects by neuronal firing rates [60–62], while the lemniscal pathway carries information that should be sufficient for object identification [62].

The motor neurons that innervate the extrinsic and intrinsic muscles are all located within the facial nucleus (FN) in the brainstem and project from the FN through the facial nerve to the mystacial pad. Thus, the FN forms a funnel through which all the motor signals to the whiskers flow. Therefore, the motor output of the whisking system can be predicted given a certain pattern of activity in the FN [63, 64]. While many other structures—including but not limited to S1, M1, the superior colliculus, the cerebellum, the basal ganglia and multiple pre-motor nuclei in the brainstem—are involved in the whisking system motor pathways, these structures will not be discussed here in depth.

Neural Encoding of Object Location by Primary Afferents

Each whisker follicle is innervated by 100–200 primary afferents that encode the vibrations, movements and deflections of a single whisker [65]. All TG afferents that originate in a whisker follicle have single-whisker receptive fields [66]. Due to sensory-motor loop dynamics, it is difficult to study the response properties of these primary afferents in awake, behaving animals. Thus, in order to characterize the primary afferents, an 'artificial whisking' paradigm was developed for use in anesthetized animals [67]. In artificial whisking, naturalistic whisking patterns are generated by electrical stimulation of motor regions in the brain or of the mo-

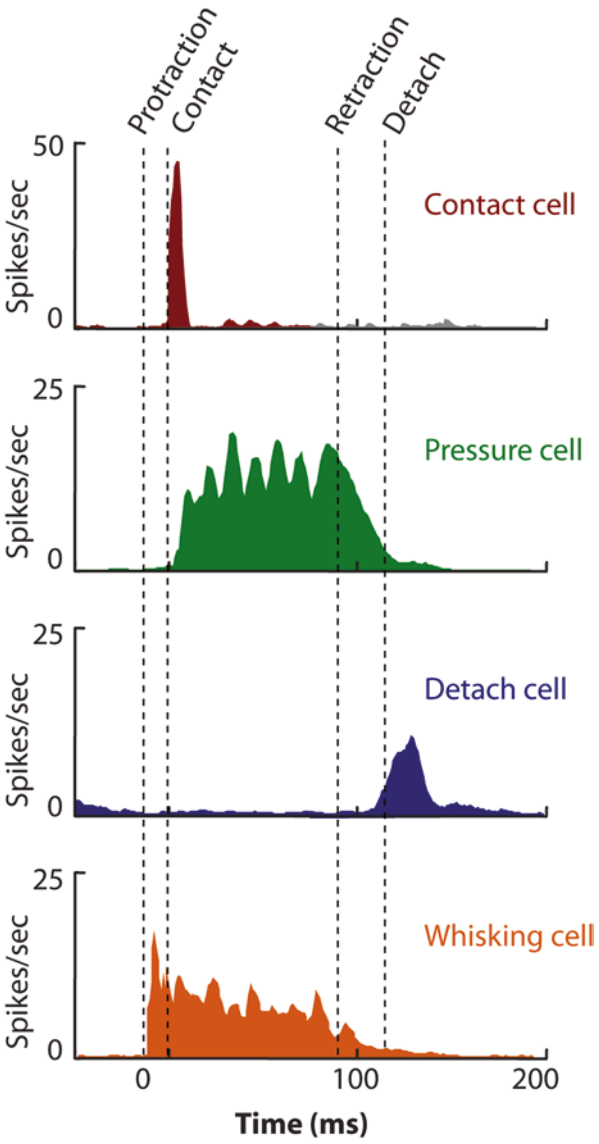

Fig. 9.2 Receptor types. Examples of the different classes of trigeminal ganglion (*TG*) cells that respond to movement and contact events. Whisking/Touch cells are not shown. (Reprinted with permission from [97])

tor nerves innervating the mystacial musculature. It is possible to record from the TG while inducing artificial whisking in order to determine how whisker afferents respond to different whisking patterns and touch events in the absence of sensorimotor feedback.

Using this protocol, it was found that the primary afferents of the TG encode information that is, in principle, sufficient to determine object location [67, 68]. On the basis of TG firing patterns during whisking, three major classes of neurons have been characterized (Fig. 9.2) [67]: Touch, Whisking and Whisking/Touch. Touch neurons respond only to touch and not to whisking in air; there are three sub-types

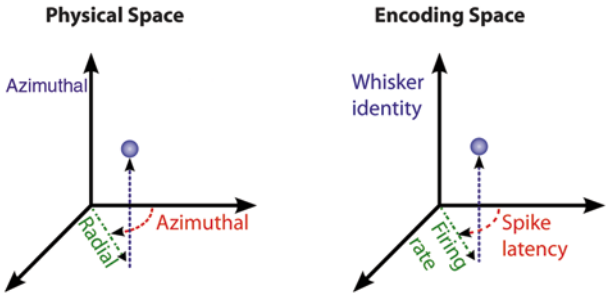

Fig. 9.3 Orthogonal coding. Proposed orthogonal encoding scheme of object location. During exploration, whisker movements are mainly along the horizontal plane. Upon contact with an object (sphere) the timing of the contact response (latency to spikes) encodes the azimuthal coordinate. The elevation (vertical coordinate) is encoded by the identity of contacting whiskers. The radial coordinate is encoded by the intensity of activation (rate and count of evoked spikes) due to bending and mechanical forces acting upon whisker shaft. These three codes for location are orthogonal and the spatial dimensions can thus be encoded independently of each other. (Reprinted with permission from [97])

of Touch cells: Contact cells respond briefly (response duration of ~12 ms) and with a short latency (~3 ms) when a whisker contacts an object, Pressure cells respond throughout whisker-object contact and Detach cells respond when the whisker detaches from the object. Upon contact, Touch cells respond with spiking rates of varying intensity that depend on the radial location of the object. Across the population of TG afferents, the rate of Touch responses drops and fewer afferents respond with increasing radial distance [68]. Whisking cells respond only to whisker movement, and not to object contact (if such contact does not affect the movement of the follicle). Additionally, a class of cells referred to as Whisking/Touch cells consists of cells that respond during whisking and increase their firing upon and during touch. If the whiskers are neither moving nor being touched, baseline firing rates of TG afferents are practically zero [67].

A Theoretical Model for Neuronal Encoding and Decoding

The following model for the encoding and decoding of object location is consistent with electrophysiological and behavioral studies. During whisking the three cylindrical coordinates of object location—azimuth, radius and elevation (all relative to the head of the animal)—are encoded by three neuronal orthogonal (independent) coding schemes: time code, rate code and labeled line code, respectively [60, 69] (Fig. 9.3). Time code is a coding scheme in which the timing of spike occurrences holds information about encoded events. Rate code is a coding scheme in which the rate at which spikes occur in a neuron encodes event related information. Finally, a labeled line code is a coding scheme in which the identity of the spiking neuron holds information. Examples of labeled line codes are those based on retinotopic, tonotopic and somatotopic anatomic organizations.

A useful feature of orthogonal coding is that individual neuronal afferents can convey information about all of the spatial coordinates of an external object simultaneously to different, specialized decoding (read-out) circuits, each tailored to decode a particular variable. The specific read-out mechanisms in the whisking system have yet to be discovered; yet, we will herein suggest several possibilities.

The transformation (decoding) of temporal contact information to spatial location requires reference signals that hold information about the whisker position or phase. These reference signals are compared with touch timing signals (such as those from Touch cells) to obtain spatial information. Re-afference signals could be generated internally (corollary discharges derived from motor commands), by proprioceptive receptors situated in muscles or by mechanoreceptors responsive to whisker motion. Re-afferent signaling of whisker motion has been observed in the TG (Whisking cells), the somatosensory thalamus [37] and the primary and secondary somatosensory cortices [70–75]; in all of these studies, a peripheral origin of signaling was indicated either by known anatomy or by specific experimental manipulations. A comparison between the Touch cells and the 'reference' Whisking signals, which would extract the azimuthal coordinate of object location, could be implemented by phase-locked loops (PLLs) or phase detectors (PDs) [67, 76, 77] (Fig. 9.4).

PLLs are widely used to decode or control temporally-modulated periodic signals in electronic circuits. The neuronal implementation of PLLs (NPLLs) includes two basic components, an intrinsic frequency-variable oscillator and a PD. The PD is used to compute the phase shift between a reference input frequency (e.g. re-afferent whisking signals) and an intrinsic frequency (e.g. local cortical oscillators). The phase shift is then used to drive the intrinsic frequency towards the reference frequency. This closed-loop mechanism ensures the gradual convergence of the intrinsic frequency to the reference input frequency, and could be used to transform the temporal contact information carried by the Contact cells into a rate code that encodes contact location; the rate of spikes at the output of the NPLL would be proportional to the phase of the whisking cycle, and thus to the location, at which the contact occurred. In order for this to happen, both Whisking and Contact cells would need to be fed into the NPLL; the periodic whisking signals would tune the frequency of intrinsic oscillators during free-air whisking and then phasic contact input would be summed with the oscillating signal, resulting in different spiking rates in the NPLL output for contacts occurring at different phases along the whisking cycle (Fig. 9.4b). While the existence of the elements required for NPLL functioning is evident in all sensory modalities [76, 78–80], whether, and in what conditions, these circuits function as NPLLs is not yet known.

NPLLs make use of neuronal phase detectors (wide-phase coincidence detectors). A recent breakthrough in the understanding of the activation mechanisms of POm neurons showed that these neurons are activated by the temporally-coincident firing of their two strongest inputs: the peripheral and the cortical [81]. This AND-like function is exactly what turns a neuron into a PD [82], thus supporting an NPLL implementation by POm-S1 loops.

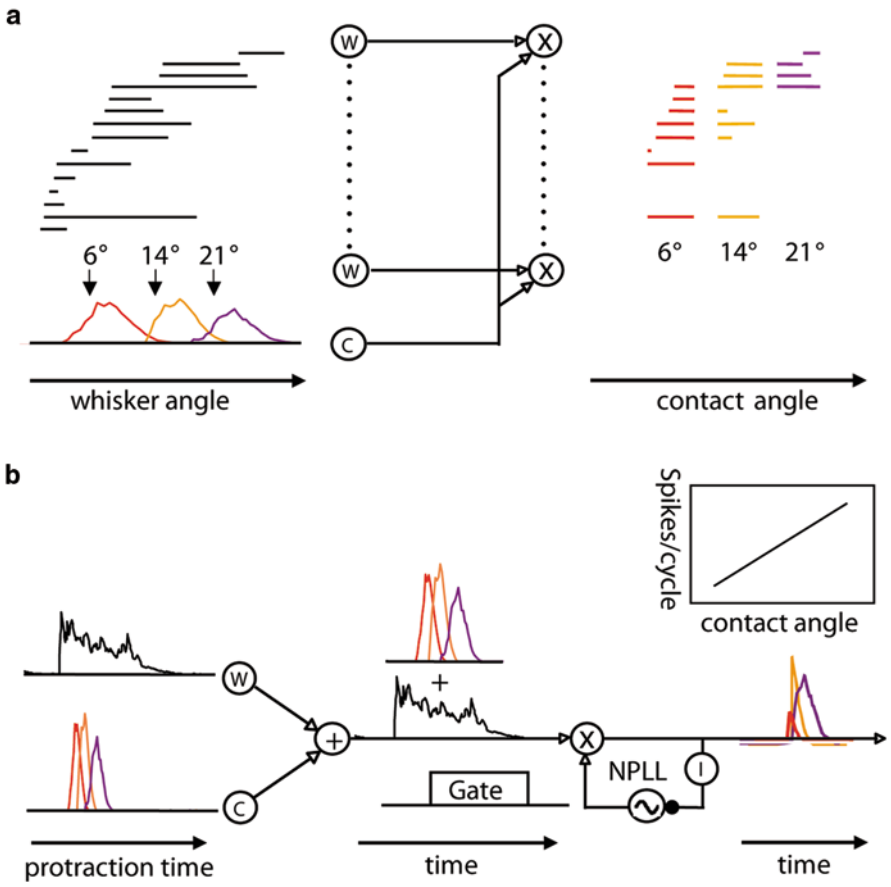

Fig. 9.4 Possible encoding-decoding schemes. **a** *Spatiotemporal scheme*. Outputs of Whisking cells (W) and a Contact cell (C) are fed separately into an array of cells that function as coincidence or phase detectors (X). Horizontal object positions are coded, from posterior to anterior (6°, 14°, and 21°, respectively). The output of the detector array provides a spatial code of horizontal object position (firing profiles). **b** *Temporal scheme*. Outputs of a population of Whisking cells (W) and a Contact cell (C) are summed and then fed into a thalamocortical neuronal implementation of a phase-locked loop (NPLL) circuit of the paralemniscal pathway. Temporal dispersion along this pathway broadens the responses. The NPLL is composed of a thalamic phase detector (X; implemented by a set of "relay" cells), cortical inhibitory neurons (I), and cortical oscillators (~). The thalamic neurons transfer only those input spikes that coincide with the cortical gating feedback ('Gate' pulse). Thus, responses to more posterior locations, which decay earlier than those to more anterior positions, will yield fewer spikes. As a result, horizontal object position is encoded by the spike count of the thalamic neurons. (Reprinted with permission from [67])

Another, somewhat simpler, potential recoding mechanism is also enabled by an array of PD neurons when each of them receives input from dedicated Whisking cells and Contact cells. A given PD neuron, in this case, will fire only if the contact

occurs within a specific range of phases around the phase represented by its input Whisking cell. Using this mechanism, the temporal contact information is recoded as a labeled line code. Recoding of the azimuthal angle via phase detectors has been observed in the cortex; responses of certain cortical neurons in layers 4 and 5 indicate a conjunction of object contact with a specific angular phase of the whisker [83].

Radial object position has been found to be primarily encoded by a population rate code [68]. The reading of a population rate code can be implemented by neural integrators, peak detectors, attractor neural networks or synfire chains [67, 84]. Encoding of vertical object location (elevation) is assumed to be determined by anatomy and a whisker-identity based labeled-line code [60, 84]. The vertical coordinate, elevation, encoded by labeled-lines, could be read out by threshold detectors—a labeled-line neuron whose firing crosses a given threshold would code for an object at its labeled elevation.

Behavioral Aspects of Object Localization

Behavioral studies of whisker-based object localization have primarily taken two directions: (1) changing the conditions under which objects are perceived by removing sub-sets of whiskers, and thus addressing the relevance of single versus multi-whisker cues; and (2) training animals to localize objects close to their perceptual limits in order to enable characterization of motor strategies [69, 85–88]. The behavioral studies reviewed here attempt to isolate the optimal behavior for localization along each spatial dimension (azimuth, radius and elevation) by holding object location constant in two dimensions and varying location only along the third dimension (Fig. 9.5).

The acuity with which rats can localize objects along the azimuthal dimension depends primarily on whisking kinematics and on the extent and conditions of prior training [69]. The identity and number of whiskers contacting objects is typically not relevant to acuity along the azimuthal dimension [69]. Two independent studies of azimuthal object localization [69, 87] agree on the following: (1) rats can be trained to accurately localize an object with a single whisker, provided they first learn the task using at least four whiskers; (2) whisker movements are required to accurately localize an object, and the power of whisking (the energy put into whisking during a task) correlates with acuity of localization (higher power leads to higher acuity); and (3) localization of an object relative to another accessible object used as a fixed reference (‘differential localization’) is more accurate than allocentric localization without a fixed reference. During localization without any reference, perceptual acuity was found to be close to the whisker spacing limit (~20°) [87]. Azimuthal acuity during a horizontal localization task that has a fixed reference is an order of magnitude better than the limit imposed by the spacing of adjacent same-row whiskers (roughly 1 and 20°, respectively), a performance level that constitutes whisk-

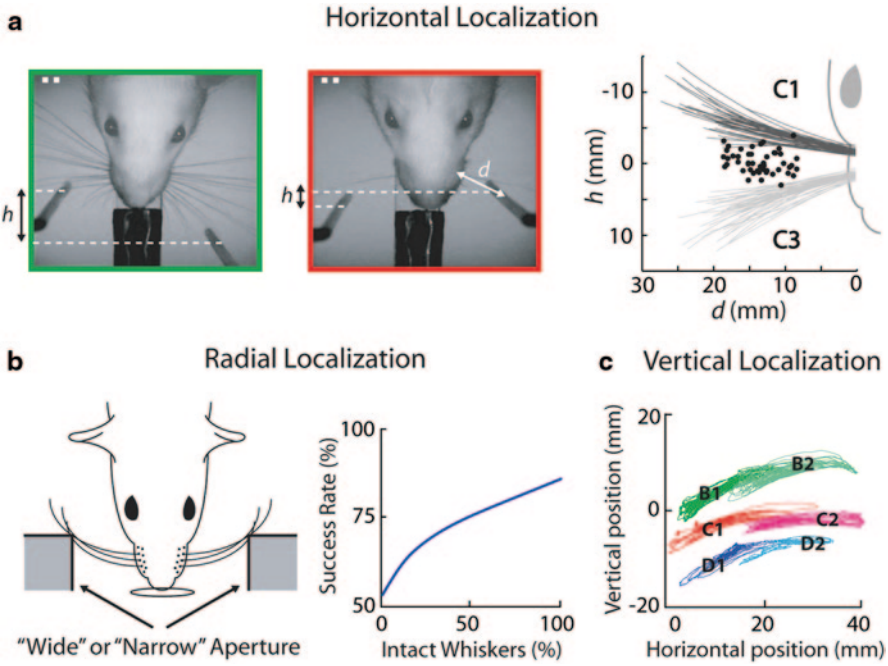

Fig. 9.5 Behavioral evidence of spatial encoding. **a** *Horizontal object localization***.** Rats can be trained to discriminate the relative horizontal offset (*h*) between two vertical poles. *Left* Rats require all or a significant subset of the whiskers to be intact to learn this localization task. *Middle* With training, rats can also learn to localize the objects accurately with a single whisker intact on each side of the snout. *Right* The performance in an experimental session can be measured by the localization threshold, which indicates the smallest difference in horizontal offset that a rat was able to discern. These performance thresholds were often smaller than the average horizontal distances between neighboring whiskers on the same row (the C2 whisker was located at $h = 0$, and the gray lines indicate the average distances of C1 and C3 whiskers from the C2 whisker in individual test trials). Black dots indicate the lowest thresholds obtained by individual rats, some as low as 0.24 mm (adapted from [69]). **b** *Radial object localization*. *Left* Rats can be trained to classify presented apertures as being either narrow or wide in the radial dimension [86]. *Right* Performance (success rate) in this radial discrimination task is positively correlated with the number of intact whiskers; performance drops as whiskers are gradually trimmed, reaching chance-performance if only a single whisker is left intact on each side of the snout. **c** *Vertical localization*. During whisking, movement primarily occurs along the horizontal plane. Here, the horizontal and vertical movements of individually tracked whiskers from B, C, and D rows were measured 20 mm from the whisker base. The results were obtained with stereo-videography and 3D reconstructions [90, 91]. (Reprinted with permission from [60])

ing hyperacuity [69]. Furthermore, it was found that only a single whisker on each side of the snout is required for accurate differential bilateral localization.

All of these findings preclude encoding of location along the azimuthal dimension by only comparing the identity of whiskers contacting the objects (i.e. a whisker-identity based labeled line code). Instead, available kinematic variables of the

whiskers, such as the relative angles and contact-times of the whiskers, may be used as primary cues for the purpose of azimuth encoding. And, indeed, a recent study has shown that azimuthal localization consists of two stages. During the first stage, the time difference between consecutive bilateral contacts is correlated with the azimuthal difference of the two objects relative to a rat's head, while in the second stage the bilateral whiskers' azimuthal difference is correlated with the azimuthal difference between the objects [89].

Behavior during localization of objects along the radial axis differs from azimuthal localization in several respects. Rhythmic whisker movements are neither required nor typically observed during radial localization [86]. Instead, the whiskers are brought in to contact with objects through head and body movements. Furthermore, performance correlates with the number (though not the identities) of intact whiskers available to the rat [86]. These observations rule out a simple labeled-line code since the identities of whiskers used in localization do not influence performance. Furthermore, the suppression of whisker motion suggests that temporal cues are not important in radial localization. Instead, the observation that whisker trimming impairs radial acuity in proportion to the number of removed whiskers, suggests that radial object location is encoded by a sensory cue that is accumulated across all whiskers.

Unlike azimuthal and radial localization, the encoding of the vertical object coordinate (elevation) is assumed to be straightforward, as whiskers primarily move within the horizontal plane (translations along the posterior-anterior axis and rotation around the follicle), and make only small vertical movements during normal, rhythmic whisking [90, 91]. Roughly, a given whisker moves within a plane confined to an elevation determined by the location of the whisker on the whisker pad. Therefore, the vertical coordinate of an object can be specified by the contacting whisker's location on the whisker pad (up to the spacing of adjacent same-column whiskers), constituting a labeled-line code.

Conclusion

The complex and delicate processes by which the nervous system builds perceptions from sensory stimuli are not yet understood. The whisking system can be used as a model system in the study of the encoding and decoding of sensory signals in perception. It has been found that by using a combination of anatomical, electrophysiological, behavioral and theoretical approaches, it is possible to form a comprehensive scheme of the way in which the vibrissal system is used in the process of object localization. Similarly, coding schemes have been proposed for texture [92–94] and shape [95, 96] perception using the whisking system. It is our hope that an understanding of the anatomical, physiological and behavioral mechanisms of these perceptions will eventually lead to a greater understanding of mammalian perceptual ability and methods for its restoration in cases of injury and disease.

References

1. Pisano RG, Storer TI (1948) Burrows and feeding of the Norway rat. J Mammal 29(4):374–383
2. Adams N, Boice R (1981) Mouse (Mus) burrows: effects of age, strain, and domestication. Learn Behav 9(1):140–144
3. Nelson ME, MacIver MA (2006) Sensory acquisition in active sensing systems. J Comp Physiol A: Neuroethol Sensory Neural Behav Physiol 192(6):573–586
4. McLean CY, Reno PL, Pollen AA, Bassan AI, Capellini TD, Guenther C et al (2011) Human-specific loss of regulatory DNA and the evolution of human-specific traits. Nature 471(7337):216–219. doi:10.1038/nature09774
5. Muchlinski MN (2010) A comparative analysis of vibrissa count and infraorbital foramen area in primates and other mammals. J Hum Evol 58(6):447–473. doi:10.1016/j.jhevol.2010.01.012
6. Mitchinson B, Grant RA, Arkley K, Rankov V, Perkon I, Prescott TJ (2011) Active vibrissal sensing in rodents and marsupials. Philos Trans R Soc Lond B Biol Sci 366(1581):3037–3048. doi:10.1098/rstb.2011.0156
7. Matyas F, Sreenivasan V, Marbach F, Wacongne C, Barsy B, Mateo C et al (2010) Motor control by sensory cortex. Science 330(6008):1240–1243. doi:330/6008/1240[pii]10.1126/science.1195797
8. Hatsopoulos NG, Xu Q, Amit Y (2007) Encoding of movement fragments in the motor cortex. J Neurosci 27(19):5105–5114. doi:27/19/5105[pii]10.1523/JNEUROSCI.3570–06.2007
9. Naito E, Matsumoto R, Hagura N, Oouchida Y, Tomimoto H, Hanakawa T (2011) Importance of precentral motor regions in human kinesthesia: a single case study. Neurocase 17(2):133–147. doi:10.1080/13554794.2010.498428
10. Nii Y, Uematsu S, Lesser RP, Gordon B (1996) Does the central sulcus divide motor and sensory functions? Cortical mapping of human hand areas as revealed by electrical stimulation through subdural grid electrodes. Neurology 46(2):360–367
11. Hatsopoulos NG, Suminski AJ (2011) Sensing with the motor cortex. Neuron 72(3):477–487. doi:10.1016/j.neuron.2011.10.020
12. Huber D, Gutnisky D, Peron S, O'Connor D, Wiegert J, Tian L et al (2012) Multiple dynamic representations in the motor cortex during sensorimotor learning. Nature 484(7395):473–478
13. Grant RA, Mitchinson B, Fox CW, Prescott TJ (2009) Active touch sensing in the rat: anticipatory and regulatory control of whisker movements during surface exploration. J Neurophysiol 101(2):862–874. doi:10.1152/jn.90783.2008
14. Mitchinson B, Martin CJ, Grant RA, Prescott TJ (1613) Feedback control in active sensing: rat exploratory whisking is modulated by environmental contact. Proc Biol Sci 2007(274):1035–1041
15. Sherman D, Oram T, Deutsch D, Gordon G, Ahissar E, Harel D (2013) Tactile Modulation of Whisking via the Brainstem Loop: statechart modeling and experimental validation. PloS ONE 8(11):e79831
16. Saig A, Gordon G, Assa E, Arieli A, Ahissar E (2012) Motor-sensory confluence in tactile perception. J Neurosci 32:14022–14032
17. Berg RW, Kleinfeld D (2003) Rhythmic whisking by rat: retraction as well as protraction of the vibrissae is under active muscular control. J Neurophysiol 89(1):104–117
18. Ebara S, Kumamoto K, Matsuura T, Mazurkiewicz JE, Rice FL (2002) Similarities and differences in the innervation of mystacial vibrissal follicle-sinus complexes in the rat and cat: a confocal microscopic study. J Comp Neurol 449(2):103–119
19. Erzurumlu RS, Murakami Y, Rijli FM (2010) Mapping the face in the somatosensory brainstem. Nat Rev Neurosci 11(4):252–263. doi:nrn2804[pii]10.1038/nrn2804
20. Bosman LW, Houweling AR, Owens CB, Tanke N, Shevchouk OT, Rahmati N et al (2011) Anatomical pathways involved in generating and sensing rhythmic whisker movements. Front Integr Neurosci 5:53. doi:10.3389/fnint.2011.00053

21. Erzurumlu RS, Killackey HP (1980) Diencephalic projections of the subnucleus interpolaris of the brainstem trigeminal complex in the rat. Neuroscience 5(11):1891–1901
22. Williams MN, Zahm DS, Jacquin MF (1994) Differential foci and synaptic organization of the principal and spinal trigeminal projections to the thalamus in the rat. Eur J Neurosci 6:429–453
23. Veinante P, Jacquin MF, Deschenes M (2000) Thalamic projections from the whisker-sensitive regions of the spinal trigeminal complex in the rat. J Comp Neurol 420(2):233–243
24. Veinante P, Deschenes M (1999) Single- and multi-whisker channels in the ascending projections from the principal trigeminal nucleus in the rat. J Neurosci 19(12):5085–5095
25. Killackey HP (1973) Anatomical evidence for cortical subdivisions based on vertically discrete thalamic projections from the ventral posterior nucleus to cortical barrels in the rat. Brain Res 51:326–331
26. Koralek KA, Jensen KF, Killackey HP (1988) Evidence for two complementary patterns of thalamic input to the rat somatosensory cortex. Brain Res 463:346–351
27. Chmielowska J, Carvell GE, Simons DJ (1989) Spatial organization of thalamocortical and corticothalamic projection systems in the rat SmI barrel cortex. J Comp Neurol 285:325–338
28. Lu SM, Lin RC (1993) Thalamic afferents of the rat barrel cortex: a light- and electron-microscopic study using Phaseolus vulgaris leucoagglutinin as an anterograde tracer. Somatosens Mot Res 10:1–16
29. Petreanu L, Mao T, Sternson SM, Svoboda K (2009) The subcellular organization of neocortical excitatory connections. Nature 457(7233):1142–1145. doi:nature07709[pii]10.1038/nature07709
30. Meyer HS, Wimmer VC, Hemberger M, Bruno RM, de Kock CP, Frick A et al (2010) Cell type-specific thalamic innervation in a column of rat vibrissal cortex. Cereb Cortex 20(10):2287–2303. doi:bhq069[pii]10.1093/cercor/bhq069
31. Constantinople CM, Bruno RM (2013) Deep cortical layers are activated directly by thalamus. Science 340(6140):1591–1594
32. Ma PM, Woolsey TA (1984) Cytoarchitectonic correlates of the vibrissae in the medullary trigeminal complex of the mouse. Brain Res 306(1–2):374–379
33. Van Der Loos H (1976) Barreloids in mouse somatosensory thalamus. Neurosci Lett 2(1):1–6
34. Woolsey TA, Van der Loos H (1970) The structural organization of layer IV in the somatosensory region (SI) of mouse cerebral cortex. The description of a cortical field composed of discrete cytoarchitectonic units. Brain Res 17(2):205–242
35. Brecht M, Sakmann B (2002) Whisker maps of neuronal subclasses of the rat ventral posterior medial thalamus, identified by whole-cell voltage recording and morphological reconstruction. J Physiol 538(Pt 2):495–515
36. Minnery BS, Simons DJ (2003) Response properties of whisker-associated trigeminothalamic neurons in rat nucleus principalis. J Neurophysiol 89(1):40–56
37. Yu C, Derdikman D, Haidarliu S, Ahissar E (2006) Parallel thalamic pathways for whisking and touch signals in the rat. PLoS Biol 4(5):e124
38. Castro-Alamancos MA (2002) Properties of primary sensory (lemniscal) synapses in the ventrobasal thalamus and the relay of high-frequency sensory inputs. J Neurophysiol 87(2):946–953
39. Deschenes M, Timofeeva E, Lavallee P (2003) The relay of high-frequency sensory signals in the Whisker-to-barreloid pathway. J Neurosci 23(17):6778–6787
40. Pierret T, Lavallee P, Deschenes M (2000) Parallel streams for the relay of vibrissal information through thalamic barreloids. J Neurosci 20(19):7455–7462
41. Haidarliu S, Yu C, Rubin N, Ahissar E (2008) Lemniscal and Extralemniscal Compartments in the VPM of the Rat. Front Neuroanat 2:4. doi:10.3389/neuro.05.004.2008
42. Peschanski M (1984) Trigeminal afferents to the diencephalon in the rat. Neuroscience 12:465–487
43. Carvell GE, Simons DJ (1987) Thalamic and corticocortical connections of the second somatic sensory area of the mouse. J Comp Neurol 265(3):409–427

44. Alloway KD, Mutic JJ, Hoffer ZS, Hoover JE (2000) Overlapping corticostriatal projections from the rodent vibrissal representations in primary and secondary somatosensory cortex. J Comp Neurol 428(4):51–67
45. Bourassa J, Pinault D, Deschenes M (1995) Corticothalamic projections from the cortical barrel field to the somatosensory thalamus in rats: a single-fibre study using biocytin as an anterograde tracer. Eur J Neurosci 7:19–30
46. Bokor H, Acsady L, Deschenes M (2008) Vibrissal responses of thalamic cells that project to the septal columns of the barrel cortex and to the second somatosensory area. J Neurosci 28(20):5169–5177
47. Deschenes M, Veinante P, Zhang ZW (1998) The organization of corticothalamic projections: reciprocity versus parity. Brain Res Rev 28(3):286–308
48. Groh A, de Kock CP, Wimmer VC, Sakmann B, Kuner T (2008) Driver or coincidence detector: modal switch of a corticothalamic giant synapse controlled by spontaneous activity and short-term depression. J Neurosci 28(39):9652–9663. doi:28/39/9652[pii]10.1523/JNEUROSCI.1554–08.2008
49. Killackey HP, Sherman SM (2003) Corticothalamic projections from the rat primary somatosensory cortex. J Neurosci 23(19):7381–7384
50. Larsen DD, Wickersham IR, Callaway EM (2007) Retrograde tracing with recombinant rabies virus reveals correlations between projection targets and dendritic architecture in layer 5 of mouse barrel cortex. Front Neural Circuits 1:5. doi:10.3389/neuro.04.005.2007
51. Hoogland PV, Welker E, Van der Loos H (1987) Organization of the projections from barrel cortex to thalamus in mice studied with Phaseolus vulgaris-leucoagglutinin and HRP. Exp Brain Res 68:73–87
52. Mease RA, Krieger P, Groh A (2014) Cortical control of adaptation and sensory relay mode in the thalamus. Proc Nat Acad Sci 111(18):6798–6803
53. Liao CC, Chen RF, Lai WS, Lin RC, Yen CT (2010) Distribution of large terminal inputs from the primary and secondary somatosensory cortices to the dorsal thalamus in the rodent. J Comp Neurol 518(13):2592–2611. doi:10.1002/cne.22354
54. Colechio EM, Alloway KD (2009) Differential topography of the bilateral cortical projections to the whisker and forepaw regions in rat motor cortex. Brain Struct Funct 213(4–5):423–439. doi:10.1007/s00429-009-0215-7
55. Cicirata F, Angaut P, Serapide MF, Papale A, Panto MR (1986) Two thalamic projection patterns to the motor cortex in the rat. Boll Soc Ital Biol Sper 62(11):1381–1387
56. Sharp FR, Evans K (1982) Regional (14 C) 2-deoxyglucose uptake during vibrissae movements evoked by rat motor cortex stimulation. J Comp Neurol 208(3):255–287. doi:10.1002/cne.902080305
57. Pouchelon G, Gambino F, Bellone C, Telley L, Vitali I, Lüscher C et al (2014) Modality-specific thalamocortical inputs instruct the identity of postsynaptic L4 neurons. Nature
58. Frangeul L, Porrero C, Garcia-Amado M, Maimone B, Maniglier M, Clascá F et al (2014) Specific activation of the paralemniscal pathway during nociception. Eur J Neurosci 39(9):1455–1464
59. Masri R, Quiton RL, Lucas JM, Murray PD, Thompson SM, Keller A (2009) Zona incerta: a role in central pain. J Neurophysiol 102(1):181–191
60. Ahissar E, Knutsen PM (2008) Object localization with whiskers. Biol Cybern 98(6):449–458
61. Derdikman D, Szwed M, Bagdasarian K, Knutsen PM, Pietr M, Yu C et al (2006) Active construction of percepts about object location. <pt>Novartis Found Symp</pt> 270:4–14 (discussion—7, 51–8)
62. Diamond ME, von Heimendahl M, Knutsen PM, Kleinfeld D, Ahissar E (2008) 'Where' and 'what' in the whisker sensorimotor system. Nat Rev Neurosci 9(8):601–612. doi:nrn2411[pii]10.1038/nrn2411
63. Hill DN, Bermejo R, Zeigler HP, Kleinfeld D (2008) Biomechanics of the vibrissa motor plant in rat: rhythmic whisking consists of triphasic neuromuscular activity. J Neurosci 28(13):3438–3455

64. Simony E, Bagdasarian K, Herfst L, Brecht M, Ahissar E, Golomb D (2010) Temporal and spatial characteristics of vibrissa responses to motor commands. J Neurosci 30(26):8935–8952. doi:30/26/8935[pii]10.1523/JNEUROSCI.0172-10.2010
65. Rice FL, Mance A, Munger BL (1986) A comparative light microscopic analysis of the sensory innervation of the mystacial pad. I. Innervation of vibrissal follicle-sinus complexes. J Comp Neurol 252:154–174
66. Shoykhet M, Shetty P, Minnery BS, Simons DJ (2003) Protracted development of responses to whisker deflection in rat trigeminal ganglion neurons. J Neurophysiol 90(3):1432–1437
67. Szwed M, Bagdasarian K, Ahissar E (2003) Encoding of vibrissal active touch. Neuron 40(3):621–630
68. Szwed M, Bagdasarian K, Blumenfeld B, Barak O, Derdikman D, Ahissar E (2006) Responses of trigeminal ganglion neurons to the radial distance of contact during active vibrissal touch. J Neurophysiol 95(2):791–802
69. Knutsen PM, Pietr M, Ahissar E (2006) Haptic object localization in the vibrissal system: behavior and performance. J Neurosci 26(33):8451–8464
70. Brecht M, Grinevich V, Jin TE, Margrie T, Osten P (2006) Cellular mechanisms of motor control in the vibrissal system. Pflugers Arch 453(3):269–281
71. Crochet S, Petersen CC (2006) Correlating whisker behavior with membrane potential in barrel cortex of awake mice. Nat Neurosci 9(5):608–610
72. Curtis JC, Kleinfeld D (2006) Seeing what the mouse sees with its vibrissae: a matter of behavioral state. Neuron 50(4):524–526
73. Derdikman D, Yu C, Haidarliu S, Bagdasarian K, Arieli A, Ahissar E (2006) Layer-specific touch-dependent facilitation and depression in the somatosensory cortex during active whisking. J Neurosci 26(37):9538–9547
74. Fee MS, Mitra PP, Kleinfeld D (1997) Central versus peripheral determinants of patterned spike activity in rat vibrissa cortex during whisking. J Neurophysiol 78(2):1144–1149
75. Yu C, Horev G, Rubin N, Derdikman D, Haidarliu S, Ahissar E (2013) Coding of object location in the vibrissal thalamocortical system. Cereb Cortex:bht241
76. Ahissar E (1998) Temporal-code to rate-code conversion by neuronal phase-locked loops. Neural Comput 10(3):597–650
77. Ahissar E, Haidarliu S, Zacksenhouse M (1997) Decoding temporally encoded sensory input by cortical oscillations and thalamic phase comparators. Proc Natl Acad Sci U S A 94:11633–11638
78. Ahissar E, Arieli A (2001) Figuring space by time. Neuron 32:185–201
79. Ahissar E, Ahissar M (2005) Processing of the temporal envelope of speech. In: Reinhard Konig R, Heil P, Budinger E, Scheich H (eds) The auditory cortex: a synthesis of human and animal research. Lawrence Erlbaum Associates, Inc., London, pp 295–313
80. Ahissar E, Arieli A (2012) Seeing via miniature eye movements: a dynamic hypothesis for vision. Front Comput Neurosci 6:89. doi:10.3389/fncom.2012.00089
81. Groh A, Bokor H, Mease RA, Plattner VM, Hangya B, Stroh A et al (2013) Convergence of cortical and sensory driver inputs on single thalamocortical cells. Cereb Cortex:bht173
82. Ahissar E, Oram T (2013) Thalamic relay or cortico-thalamic processing? Old question, new answers. Cereb Cortex:bht296
83. Curtis JC, Kleinfeld D (2009) Phase-to-rate transformations encode touch in cortical neurons of a scanning sensorimotor system. Nat Neurosci 12(4):492–501. doi:nn.2283[pii]10.1038/nn.2283
84. Knutsen PM, Ahissar E (2009) Orthogonal coding of object location. Trends Neurosci 32(2):101–109. doi:S0166-2236(08)00264-6[pii]10.1016/j.tins.2008.10.002
85. Knutsen PM, Derdikman D, Ahissar E (2005) Tracking whisker and head movements in unrestrained behaving rodents. J Neurophysiol 93(4):2294–2301
86. Krupa DJ, Matell MS, Brisben AJ, Oliveira LM, Nicolelis MA (2001) Behavioral properties of the trigeminal somatosensory system in rats performing whisker-dependent tactile discriminations. J Neurosci 21(15):5752–5763

87. Mehta SB, Whitmer D, Figueroa R, Williams BA, Kleinfeld D (2007) Active spatial perception in the vibrissa scanning sensorimotor system. PLoS Biol 5(2):e15
88. Shuler MG, Krupa DJ, Nicolelis MA (2002) Integration of bilateral whisker stimuli in rats: role of the whisker barrel cortices. Cereb Cortex 12(1):86–97
89. Horev G, Saig A, Knutsen PM, Pietr M, Yu C, Ahissar E (2011) Motor-sensory convergence in object localization: a comparative study in rats and humans. Philos Trans R Soc Lond B Biol Sci 366(1581):3070–3076. doi:366/1581/3070[pii]10.1098/rstb
90. Knutsen PM, Biess A, Ahissar E (2008) Vibrissal kinematics in 3D: tight coupling of azimuth, elevation, and torsion across different whisking modes. Neuron 59(1):35–42
91. Bermejo R, Vyas A, Zeigler HP (2002) Topography of rodent whisking I: two-dimensional monitoring of whisker movements. Somatosens Mot Res 19(4):341–346
92. Arabzadeh E, Petersen RS, Diamond ME (2003) Encoding of whisker vibration by rat barrel cortex neurons: implications for texture discrimination. J Neurosci 23(27):9146–9154
93. Arabzadeh E, Zorzin E, Diamond ME (2005) Neuronal encoding of texture in the whisker sensory pathway. PLoS Biol 3(1):e17
94. Hipp J, Arabzadeh E, Zorzin E, Conradt J, Kayser C, Diamond ME et al (2006) Texture signals in whisker vibrations. J Neurophysiol 95(3):1792–1799
95. Anjum F, Brecht M (2012) Tactile experience shapes prey-capture behavior in Etruscan shrews. Front Behav Neurosci 6:28. doi:10.3389/fnbeh.2012.00028
96. Anjum F, Turni H, Mulder PG, van der Burg J, Brecht M (2006) Tactile guidance of prey capture in Etruscan shrews. Proc Natl Acad Sci U S A 103(44):16544–16549. doi:10.1073/pnas.0605573103
97. Ahissar E, Knutsen PM (2011) Vibrissal location coding. Scholarpedia 6(10):6639

Chapter 10
The Robot Vibrissal System: Understanding Mammalian Sensorimotor Co-ordination Through Biomimetics

Tony J. Prescott, Ben Mitchinson, Nathan F. Lepora, Stuart P. Wilson, Sean R. Anderson, John Porrill, Paul Dean, Charles W. Fox, Martin J. Pearson, J. Charles Sullivan and Anthony G. Pipe

Abstract We consider the problem of sensorimotor co-ordination in mammals through the lens of vibrissal touch, and via the methodology of embodied computational neuroscience—using biomimetic robots to synthesize and investigate models of mammalian brain architecture. The chapter focuses on five major brain sub-systems and their likely role in vibrissal system function—superior colliculus, basal ganglia, somatosensory cortex, cerebellum, and hippocampus. With respect to each of these we demonstrate how embodied modelling has helped elucidate their likely function in the brain of awake behaving animals. We also demonstrate how the appropriate co-ordination of these sub-systems, with a model of brain architecture, can give rise to integrated behaviour in a life-like whiskered robot.

T. J. Prescott (✉) · J. Porrill · B. Mitchinson · S. P. Wilson · P. Dean
Department of Psychology, The University of Sheffield, Western Bank, S10 2TP Sheffield, UK
e-mail: t.j.prescott@sheffield.ac.uk

J. Porrill
e-mail: j.porrill@sheffield.ac.uk

B. Mitchinson
e-mail: b.mitchinson@sheffield.ac.uk

S. P. Wilson
e-mail: S.P.Wilson@Sheffield.ac.uk

P. Dean
e-mail: p.dean@sheffield.ac.uk

N. F. Lepora
Department of Engineering Mathematics, University of Bristol, Bristol BS8 1UB, UK
e-mail: n.lepora@bristol.ac.uk

S. R. Anderson
Automatic Control and Systems Engineering, University of Sheffield,
Mappin Street, Sheffield S1 3JD, UK
e-mail: s.anderson@sheffield.ac.uk

P. Krieger, A. Groh (eds.), *Sensorimotor Integration in the Whisker System,*
DOI 10.1007/978-1-4939-2975-7_10

Keywords Sensorimotor co-ordination · Biomimetic robot · Embodied computational neuroscience · Layered architecture

Research on active vibrissal touch has the potential to help us understand, perhaps even rethink, many of the key computations underlying sensorimotor co-ordination in the mammalian brain.

Consider, for instance, the task of visually-guided reach and grasp which is widely studied in both humans and primates. Work in humanoid robotics might decompose this task as the following steps: (i) identify a potential target in peripheral vision based on a rapid analysis of superficial salient features (colour, shape, movement); (ii) orient to and fixate on the object using foveal vision to form an internal 3-dimensional model of the object and of its key properties (shape, size, texture, and so forth); (iii) in parallel, form a second set of representations of the position and orientation of the object in space relative to those of the body, arm, and hand; (iv) match the first, "what?", model with a variety of stored "templates" in order to determine whether this particular item is, indeed, a suitable target for reaching; (iv) apply algorithms to the computed "where?" representations of the object and body, and make use of knowledge of the kinematic and dynamic properties of the arm, hand, and digits, to determine appropriate movement trajectories; (v) execute the planned movements largely ballistically but using some sensory feedback in the final approach, to locate, enclose, and lift the object in an effective way.

Now consider the capacity of an animal such as the Etruscan shrew, the smallest living terrestrial mammal—and known to be a remarkably efficient predator—to localise, identify, and entrap an agile prey insect using only its whiskers [1]. The problem is similar in many ways to that of human (or humanoid) sensory-guided reaching. The visual periphery compares to the macrovibrissae (the longer actuated facial whiskers on either side of the snout), and the visual fovea to the microvibrissae (the shorter non-moving whiskers on the upper lip and chin) and other tactile sensory surfaces around the mouth. The orienting system, as in primate vision, is likely to have the superior colliculus at its core, and will be driven by a very rapid but coarse analysis of features in the whisker signals via a midbrain loop that co-ordinates

C. W. Fox
Institute for Transport Studies, University of Leeds, 34-40 University Road,
LS2 9JT Leeds, UK
e-mail: c.w.fox@leeds.ac.uk

M. J. Pearson · J. C. Sullivan · A. G. Pipe
Bristol Robotics Laboratory, University of the West of England, T-Block, Frenchay Campus,
BS16 1QY Bristol, UK
e-mail: martin.pearson@brl.ac.uk

J. C. Sullivan
e-mail: charlie.sullivan@brl.ac.uk

A. G. Pipe
e-mail: Tony.Pipe@brl.ac.uk

movements of the whiskers, head and trunk. Further analyses of the whisker signals, from both the macro- and micro-vibrissae will involve the somatosensory cortices, and pathways through to the temporal lobes. These will likely involve the decomposition of sensory signals into components (self-motion, object properties such as shape, texture, etc.), but may also require the reintegration of decomposed features into more complete representations of the target. Alongside determination of object properties, information about the prey animal's spatial position and orientation will also have to be computed from the same set of vibrissal deflection signals. The decision of whether to make an attack will then depend on a comparison of computed features with remembered patterns corresponding to previously successful (and unsuccessful) attacks. Whilst this process will likely involve cortical systems (including hippocampus) it will ultimately involve decision-making mechanisms in basal ganglia to decide if the template fits, and, if so, whether the attack option is appropriate right now (as opposed, say, to further approach behaviour or avoidance). Planning and execution of the strike will also involve the motor cortex, and midbrain and brainstem motor systems which, together with the cerebellum, will co-ordinate precision orienting with biting, and may use additional sensory information from the vibrissae to accurately adjust the final phases of the strike.

Despite the above similarities, however, a number of features of the shrew vibrissal system might lead us to think rather differently about this problem from the way we initially conceived our example task of human visually-guided reach.

First, rather than being able to fixate and examine the target at leisure, the animal must make do with signals from a few fleeting contacts between the vibrissal tips and a small number of unknown locations on the target [2]. Further, both the sensors themselves and target are moving rapidly, the latter with unknown direction and speed. In other words, this is a task, where information about the target is relatively sparse, and where timing and dynamics are crucial. The urgency of the required response means that the preparation of attack behaviour will likely occur alongside the processing of vibrissal signals to determine object properties—so that the former can be put into effect as soon as the weight of evidence lies in its favour. In other words, this task is perhaps more similar to the challenge faced by a batter trying to hit a moving ball in fading light—the target object suddenly and rapidly appears out of nowhere, and a successful response must be executed within a critical and narrow time window.

Second, the shrew's brain is tiny [3]. Not only must its predation behaviour be accomplished with 20,000 times fewer neurons that a human might utilise for reach and grasp, we also know from the speed of the attack (which can be as little as 80 milliseconds [4]) that the shrew achieves its goal in a far smaller number of processing steps. Whatever phases are necessary for decomposition of sensory signals and their reconstruction as object representations, these will necessarily involve a small number of processing sites each made up of relatively few neurons. The construction of complex internal models, for comparison against rich templates, looks decidedly improbable in this system. More likely, key features are rapidly extracted and mapped, across a small number of synapses, into representations of their potential for action. Indeed, the step of "representing" the prey insect itself may even

be missed out entirely. This animal may encode information about objects in its tactile world only in terms of their potential as affordances [5] to guide different forms of approach, avoidance, or consummatory behaviour. Thus this is a system in which we can explore what is the minimum amount of internal transformation and representation needed in order to support complex, sensory-guided behaviour; and in which we can discover how active sensing systems [6] merge perception into action, via closed loop control [7], without the two ever being truly separate.

Overall, then, while understanding this system will not directly answer the question of how the human brain performs reach-and-grasp, the study of vibrissal-guided behaviour could help us understand many aspects of mammalian sensorimotor control and perhaps rethink a number of assumptions based on more primate-centric analyses of brain processing.

In this chapter we consider five major brain sub-systems and their likely role in vibrissal system function—superior colliculus (SC), basal ganglia (BG), primary somatosensory cortex (S1), cerebellum, and hippocampus—bearing in mind the behavioural domain of whisker-guided predation in animals such as the shrew or rat. One of these, the somatosensory cortex, is specialised for tactile processing, but shares many aspects of its computational architecture with other areas of mammalian cortex. The remaining four (basal ganglia, cerebellum, superior colliculus and hippocampus) are more "general purpose" in the sense that they appear to have some characteristic function that operates in a similar way across different sensory modalities or motor functions but that is also tuned, in some appropriate manner, to the particular requirements of processing and control for vibrissal touch. We are therefore hopeful that the insights obtained by studying the role of each of these sub-systems in the vibrissal processing of rodent-like mammals will generalise to understanding their functional capacities in other domains too. Each of these systems is the subject of a vast neuroscientific literature that we cannot even begin to summarise here. We therefore restrict our focus to providing a brief outline of the hypothesized functional role of each system in vibrissal touch and then describe how we have investigated this from an *embodied computational neuroscience* perspective [8, 9] that seeks to develop and test systems-level computational models of neural circuits embedded within the control system of biomimetic robots.

One might ask why we bother to build robot models of animals and their nervous systems? One answer, suggested the neurobiologist Valentino Braitenberg [10], is that synthesis (engineering a model of a biological system) is quite different from analysis (reverse-engineering an existing biological system); thus, in building a robot model of our target animal, that mimics sufficiently some aspects of its body, brain and behaviour, we can expect to learn a good deal about the original creature. Another answer is that a robot model should allow us to conduct experiments that will help us better understand the biological system, and moreover would be impossible (or at least much more difficult) to perform in the original animal [11, 12]. Finally, neurobiological studies have shown us that the brain nuclei and circuits that process vibrissal touch signals, and that control the positioning and movement of the whiskers, form a neural architecture that is a good model of how the mammalian brain, more generally, co-ordinates sensing with action. Thus, a further reason for

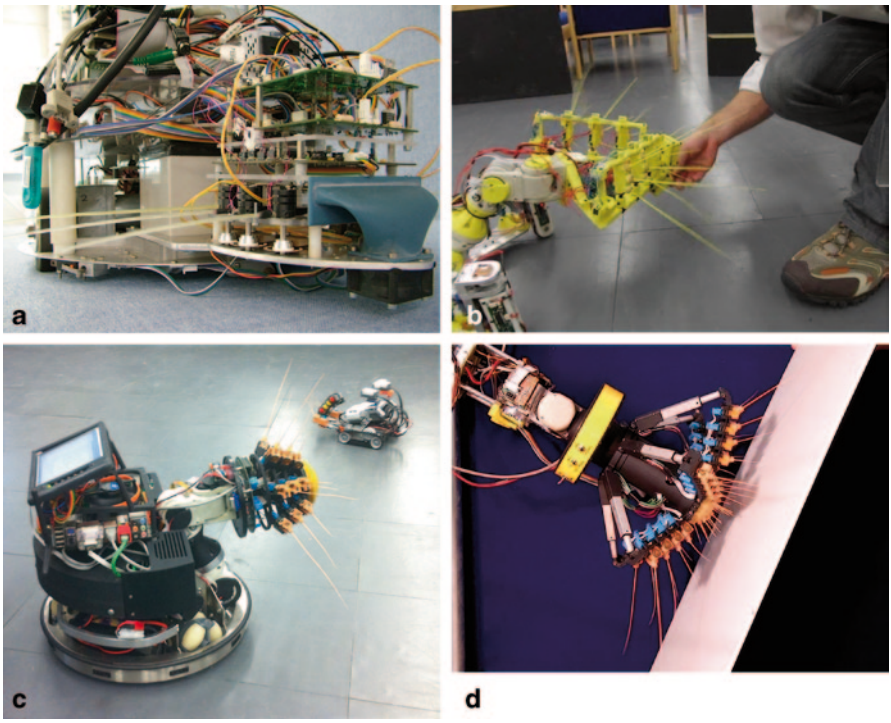

Fig. 10.1 Biomimetic whiskered robots. **a** Whiskerbot. **b** Scratchbot. **c** Shrewbot. **d** Generation 2 Biotact Sensor. Each robot has a snout configured with an array of moveable artificial whiskers. Different mechanisms have been explored for whisker actuation and for sensory transduction in the different devices. We have also gradually evolved the overall design of the whisker morphology and of the neuromimetic control architecture. The most recent model systems (Shrewbot, G2 Biotact Sensor) feature arrays of individually actuated whiskers with intrinsic transduction systems based on Hall effect sensors that can measure whisker deflection in three dimensions. For further details of the 'evolution' of our whiskered robots see [11, 105, 106]. Photos by Martin Pearson (Whiskerbot, Scratcbot, Biotact Sensor) and Tony Prescott (Shrewbot)

building biomimetic robot models is to provide improved insight into brain architecture as a whole. Indeed, by building robotic whisker systems—see examples of our whiskered robots in Figure 10.1—we consider that we are taking significant steps towards building an integrated robotic model of the mammalian brain.

A Control Architecture for Behavioural Integration in Vibrissal Touch

We begin our consideration of the sensorimotor co-ordination for vibrissal touch by addressing the overall problem of behavioural integration, or behavioural coherence, that is central to the task of building life-like systems [13]. Living, behav-

ing systems display patterns of behaviour that are integrated over space and time such that the animal controls its effector systems in a co-ordinated way, generating sequences of actions that maintain homeostatic equilibrium, satisfy drives, or meet goals. How animals achieve behavioural integration is, in general, an unsolved problem in anything other than some of the simplest invertebrates. What is clear from the perspective of behaviour is that the problem is under-constrained since similar sequences of overt behaviour can be generated by quite different underlying control architectures [14]. This implies that to understand the solution to the integration problem in any given organism is going to require investigation of mechanism in addition to observations of behaviour. In this regard, physical models—such as robots—can prove useful as a means of embodying hypotheses concerning alternative control architectures whose behavioural consequences can then be measured observationally [11]. Research with robots has repeatedly demonstrated forms of emergent behaviour [15]—the appearance of integrated behavioural sequences that are not explicitly programmed—demonstrating the value of this embodied testing for suggesting and testing candidate mechanisms.

The biological literature provides a range of different hypotheses concerning the mechanisms that can give rise to behavioural integration; here, we highlight two—behavioural and salience map competition.

The neuroethology literature suggests a decomposition of control into behavioural sub-systems that then compete to control the animal (see [16, 17] for a review). This approach has been enthusiastically adopted by researchers in behaviour-based robotics (see, e.g. [18]) as a means of generating integrated patterns of behaviour in autonomous robots that can be robust to sensory noise, or even to damage to the controller.

An alternative hypothesis emerges from the literature on spatial attention, particularly that on visual attention in primates including humans [19]. This approach suggests that actions, such as eye movements and reaches towards targets, are generated by first computing a ‘salience map’ that integrates information about the relevance (salience) to the animal of particular locations in space into a single topographic representation. Some maximisation algorithm is then used to select the most salient position in space towards which action is then directed. It is usual in this literature to distinguish between the computation of the salience map, the selection of the target within the map, and orienting actions that move the animal, or its effector systems, towards the target. In the mammalian brain these different functions may be supported by distinct (though overlapping) neural mechanisms [20].

Of course, the approaches of behavioural competition and salience map competition are not mutually exclusive and it is possible to imagine various hierarchical schemes, whereby, for instance, a behaviour is selected first and then a point in space to which the behaviour will be directed. Alternatively, the target location might be selected and then the action to be directed at it. Finally, parallel, interacting sub-systems may simultaneously converge on both a target and suitable action [21]. We recently investigated the hypothesis that a salience map model can be used to generate action sequences for a biomimetic whiskered robot snout mounted on a mobile robot platform, and compared this with an earlier control model based on

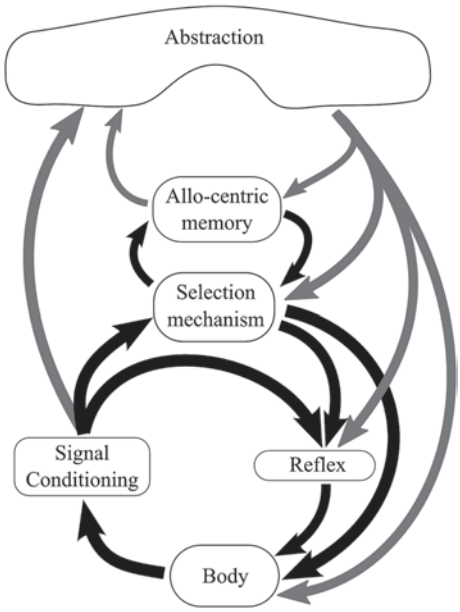

Fig. 10.2 Model of brain architecture for control of a whiskered mobile robot. The abstract components of the model can be mapped to key sub-systems in the mammalian brain (see text). Figure reproduced from Fig. 2 of [15] with permission from Springer

behaviour selection [15]. Both control systems generated life-like sequences which alternate between exploration and orienting behaviour, but in the salience map version these higher-level behavioural 'bouts' were an emergent consequence of actions determined by following a shifting focus of spatial attention (determined by a salience map) rather than resulting from the alternation of distinct behavioural primitives.

In the mammalian brain, sensorimotor loops involving the cortex, superior colliculus, basal ganglia, cerebellum and hippocampus may interact to implement a control system similar to this hypothesised salience map model. Figure 10.2 summarises the multi-level loop architecture used in our recent biomimetic robot Shrewbot, which is derived from our general understanding of the control architecture of the rat vibrissal system. We cannot represent the whole brain in our model from the outset, and there is no general agreement on the function of some of the neural centres. Since the robot must generate behaviour if we are to experiment with it, our breakdown of the control system into modules is by function, but the particular breakdown chosen is deeply inspired by our understanding of brain anatomy. This places us in a strong position to hypothesise relationships between structure and function in the neural system, and these hypotheses are a major outcome of our robot work. Here, the component 'selection mechanism', modelled on the mammalian basal ganglia and superior colliculus, is responsible for selecting and driving the majority of movements of the robot's body (neck and wheels). Below this system, motor systems implement control commands, and low-level reflex loops support some rapid responses to current conditions (for instance, whisker protraction is inhibited by contact with the environment [22]). Above this system,

we are beginning to add more cognitive components that modulate selection. The component labelled 'abstraction' [23] gleans additional information about what has been contacted by the vibrissal sensors in a manner analogous to processing centres such as the somatosensory cortex. Elsewhere, the component labelled 'allocentric memory' retains a memory of the robot's past spatial experience and thus models some of the functionality of the mammalian hippocampal system [24, 25]. 'Signal conditioning' indicates the importance of early processing of sensory signals to, for instance, distinguish components of the signal that may be due to the organism's (or robot's) own movement rather than to contact with the external world. Some neurobiological evidence, and our own modelling work, suggest an important role for the cerebellum in this regard [26, 27].

Orienting the Tactile Fovea with the Superior Colliculus

To demonstrate the capacity of this architecture for generating integrated behaviour we have focused on the problem of orienting to interesting or novel stimuli detected by the robot vibrissae. To develop our model of orienting we first assume a 'tactile fovea' [28], as the region of the snout with the highest density of microvibrissae, and focus on the key component of orienting behaviour in rodent-like mammals of bringing the fovea to a target. For instance, when faced with a task of discriminating between multiple objects, rat behaviour can be described as foveation (targeting the sensory fovea) to each discriminandum in sequence [28]. In our control architecture, then, the selection mechanism thus drives movements of the fovea with its output being the desired instantaneous velocity of the foveal position. In this model the movement of the remaining nodes of the animal/robot are unconstrained at the level of the selection mechanism and, instead, are determined at the level of the body (i.e. the motor system). Specifically, nodes such as the neck joints, and body are 'enslaved' to the fovea, and move so as to carry the fovea towards its target as smoothly and directly as possible. One could say that our robots are 'led by the nose'. This is, of course, a simplification of biological behaviour, though we have been surprised by how life-like (and practical) the resulting behaviour can be.

In primates, foveation is well studied with respect to the visual system and is known to be mediated by the Superior Colliculus (SC) [19]. In rats, stimulation of SC can evoke not only eye movements [29], but also orienting-like movements of the snout, circling, and even locomotion [30]. Recent neurobehavioural evidence also directly implicates SC as having a major role in rodent prey capture [31]. More generally, the SC appears to be a very plausible location to integrate tactile signals for spatial attention. It has the right inputs with signals arriving from the vibrissae via the trigeminal sensory complex [32], and with further inputs converging from several relevant areas of cortex including S1 [32–34]. The organization of the SC is topographic in both its sensory and motor aspects, with a sensory topography appropriate to encoding a salience map centred on the foveal region of the snout [35, 36] and motor maps suitably configured to generate orienting head movements [30].

Inspired by these facts, we have developed a model of foveal velocity vector generation that mirrors the features of SC—that is, we employ a topographic saliency map driven by sensory input and modulated by information from mid- and upper-brain, with a simple motor output transform that drives foveation to the most salient region of local space [15]. In the case of our robots, salience is excited by whisker contact and endogenous noise and suppressed by a top-down 'inhibition-of-return' signal from an allocentric memory component that lowers the salience of regions that have recently been foveated. The selection task, then, is to choose between foveation targets in nearby space.

This saliency map model of tactile attention has recently been extended to incorporate the regulation of vibrissal movement [37]. To evaluate the model we tested it within a simulated two-dimensional environment containing configurable 'obstacles', under conditions analogous to those used in behavioural experiments [38–41], and showed that it exhibits many of the modulations of whisker movement previously reported and summarised in Fig. 10.3 [37]. The model can also account for anticipatory aspects of active vibrissal control (see e.g. [38, 42]) that cannot be the outcome of purely reflexive mechanisms. Here again the SC is implicated as a key sub-system in the rodent brain. Stimulation of SC can generate modulatory (non-periodic) whisker movements [43] suggesting a role in determining the protraction amplitude of the whiskers. Accordingly, SC outputs directly target the facial nucleus which is the motor nucleus that drives the whisker musculature [44]. The receptive fields of SC neurons that are sensitive to deflection of single macrovibrissae are large and overlapping under anaesthesia [36]. Since the whiskers sweep back and forth during exploration this raises the possibility that, in the awake behaving animal, vibrissal receptive fields in SC are actually sharply tuned, but encode target locations in a head-centred spatial map (that might be contacted by moving whiskers) rather than contacts on distinct macrovibrissae *per se*.

The Role of the Cortex and Basal Ganglia in Decision-Making

Whilst the SC provides a mechanism that can control the orienting movements of the head and sensory systems, it is only one of many structures involved in identifying and *selecting* targets for foveation. Studies in primates implicate sensory processing in cortical areas [45] coupled with action selection in the basal ganglia (BG) [17, 46, 47] as critical substrates for the decision-making aspects of target selection. Our research with whiskered robots is helping us to analyse the contributions of these different neural systems to perceptual decision making in the mammalian brain.

The last two decades have seen major advances in our understanding of decision making as statistically optimal inference from noisy and ambiguous sensations using Bayesian probability theory [48]. A Bayesian approach to the task of classification involves recording the likelihoods of measurements from example sensory

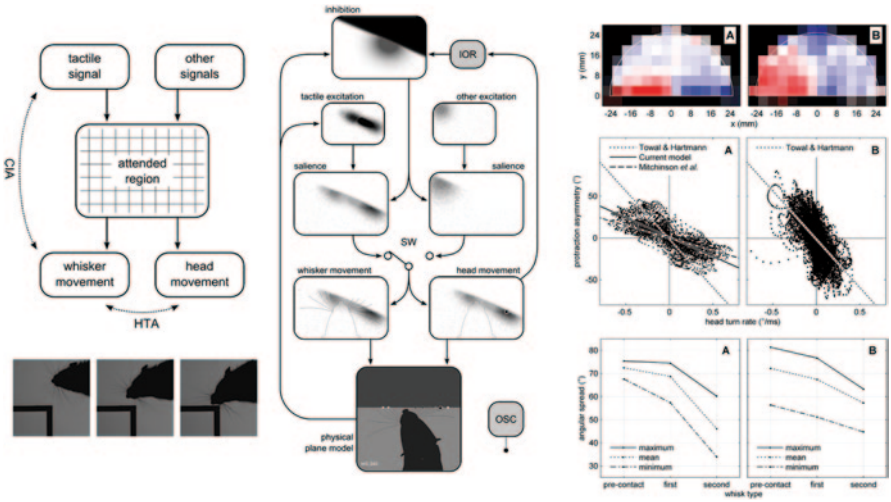

Fig. 10.3 Model of the regulation of whisking behaviour by spatial attention. *Top-left.* A mix of exogenous (*tactile*) and endogenous (*other*) influences affect the locus/region of spatial attention. This locus drives head movements and is responsible for the modulation of whisker movements from whisk to whisk. *Bottom-left.* Three frames from an overhead video of a rat executing an orient to an unexpected contact. *Centre.* The implementation used to test the model—additional components are a simple oscillator to generate periodic whisking (*OSC*), an implementation of inhibition-of-return (*IOR*) to generate sufficiently rich orienting behaviour for testing, and a physical model of whisker/environment interactions. *Right.* Comparison of results from current model **a** and recordings of rat behaviour, **b** under three analyses, from top: Contact-induced asymmetry (see, e.g. [39])—if an animal approaches a surface at an oblique angle then protraction of whiskers ipsilateral to the surface is reduced (*red color/dark shading inside boundary*), whilst protraction of whiskers on the contralateral side is increased (blue color/light shading); Head-turning asymmetry (see, e.g. [41])—as an animal turns the whiskers typically move asymmetrically as if to anticipate obstacles in the direction of the turn; Spread reduction during contact (see. e.g. [38])—whilst exploring a surface the whiskers are brought closer together with the effect of increasing the number of whisker-surface contacts. (Adapted from Figs. 2, 3, 7 and 8 of [37] which should be consulted for further explanation of the model and results)

data. Given new test data, these likelihoods can be used with Bayes' rule to calculate the posterior probability of the test data being drawn from each trained class, that is, the likelihood of the data belonging to any given category given the history of past data. Within the broader class of Bayesian classifiers the approach of *sequential analysis* [49] operates by applying Bayes' rule repeatedly to accumulating evidence for competing perceptual hypotheses, derived from time series of sensory data, until a preset threshold is reached. This method can be likened to a process that has been observed in parietal cortex when monkeys are required to make perceptual judgements about visual motion direction and where individual neurons have been recorded that noisily ramp-up their firing rates until reaching a decision threshold [50–52].

Using our whiskered robots, we have explored the possibility that sequential Bayes can provide an effective general classifier for object properties detected

using vibrissal sensors. Examining characteristics such as texture, radial distance to contact, speed of object movement and novelty, and using a range of robot platforms deploying different strategies for the control of whisker movement and position, we have shown that sequential Bayes is reliable, accurate (hit rates of >90% on several tasks), and out-performs a number of competing classification methods such as spectral templates, maximum likelihood, and multi-layer neural networks [23, 53–56]. That a classification method that matches with primate data can operate effectively with signals from artificial whiskers gives hope that a single theory of perceptual decision-making can be developed that will apply equally to primate vision and rodent vibrissal touch. The further implication of these studies is that a common memory format (log likelihoods) could be used to encode tactile memories for object properties. These models also have the potential to address questions about the nature of tactile memory in animals such as the Etruscan shrew since the ability to classify objects (for instance, as prey items that can be attached) requires efficient and compact memory traces, and the ability to make timely and appropriate decisions based on accumulating evidence.

Alongside evidence that cortex accumulates evidence for competing hypotheses, converging evidence from neurobiology and computational modelling, is showing that the BG anatomy maps onto a network implementation of an optimal statistical method for hypothesis testing that provides for timely and efficient selection of an appropriate response [57–59]. As noted above, in the sensory component of this process, evidence for the alternative interpretations of a stimulus accumulates in neuronal "evidence bins" (e.g., that a visual stimulus is moving right rather than left) and this accumulated evidence competes within the BG to elicit an action (e.g., press right lever or left lever). In the vibrissal system, the substantial projections from layer 5a of S1 cortex to the striatum—the major input structure of the BG—could provide a neural substrate for decision-making in relation to tactile object properties. We have used insights from experimental data, and from recent recordings in cortical areas during decision-making tasks (e.g. [60]), to revise and extend existing primate-based computational models of the decision-making process [54, 59] and are in the process of exploring the implications of these revisions for decision-making in embodied robotic models.

The Vibrissal Somatosensory Cortices—Feature Maps for Detecting Behavioural Affordances

Within the parietal lobes of all mammals there are localised cortical areas that are more specialised towards particular sensory modalities—such as somatosensation, vision, audition and vestibular sensing—and other areas that are more multisensory in nature. In vibrissal specialists, such as rats, mice and shrews, the somatosensory areas devoted to the region of the snout are massively expanded compared to those of most mammals. In these species, multiple somatotopic maps of the body have been identified, the principal ones being labelled primary and secondary somatosensory

cortex (S1 and S2). Whilst both of these areas have large domains devoted to the vibrissae, barrel-like aggregates of neurons ("barrels") have been identified only in S1. The size of the area of cortex devoted to the large macrovibrisae appears to reflect the high innervation levels of the whisker follicles (see also discussion of cortical area size in [61]). In the mouse, S1 cortex represents approximately 13 % of the cortical surface area in total and 69 % of the somatosensory cortex [62].

In rats and mice, S1 barrels exist for both the large and motile macrovibrissae in the posteriomedial barrel field (PMBF) and for the smaller non-actuated microvibrissae in the anterolateral barrel field (ALBF) [63], however, research has almost entirely focused on the larger barrels found in PMBF because of their ease of stimulation via the macrovibrissae. S1 and S2 are reciprocally connected with each other and also, via the corpus collosum, with their contralateral other halves [64]. S1 is also connected with a number of other cortical regions including the motor and perirhinal cortices. Other major S1 projection areas include the thalamic areas from which it receives input (VPM and POm), the reticular nucleus of the thalamus, and, of particular interest here, sub-cortical targets in the basal ganglia, pontine nuclei (cerebellum), and superior colliculus [64].

For a vibrissal-specialist like the Etruscan shrew, successful prey capture is critically dependent on accurate and rapid detection of tactile stimulus velocity. This leads to the general question of how the brain might extract movement direction and speed from patterns of vibrissal deflection. Since it was first proposed, Jeffress' place theory [65] has been a dominant model for understanding how sensory motion is encoded in the brain [66]. The idea is that coincidence detector neurons receive input from sensors after delays governed by the distance of each neuron from the corresponding signal sources. The inter-sensor time difference is then encoded by the location of neurons that are active because their connection delays exactly compensate the inter-sensor stimulation interval. The place theory therefore suggests an important role for neural geometry in computing the motion of sensory stimuli. Despite being a general theory of neural computation, most of the evidence for the place theory is provided by studies of the auditory system of auditory specialists such as the barn owl. The evidence from studies of mammalian auditory systems is inconclusive, for example, rabbit auditory cortex neurons are tuned to much longer inter-aural delays than can be accounted for by known axonal connection velocities [67], and evidence from other sensory modalities is sparse.

In order to provide a further test of the generality of the place theory, we sought to apply it to a model of tactile stimulus processing in rodent barrel cortex [68]. We asked whether model cortical neurons receiving synaptic inputs via delays governed by realistic connection geometry and plausible axonal propagation speeds would match the range of real responses to paired stimulation of adjacent whiskers. Validating this hypothesis we recreated, in simulation, the broad range of spiking patterns displayed by layer 2/3 barrel cortex neurons when adjacent whiskers are deflected through the range of inter-stimulus intervals, as measured electrophysiologically by Shimegi et al. [69]. These biological experiments have shown that, when

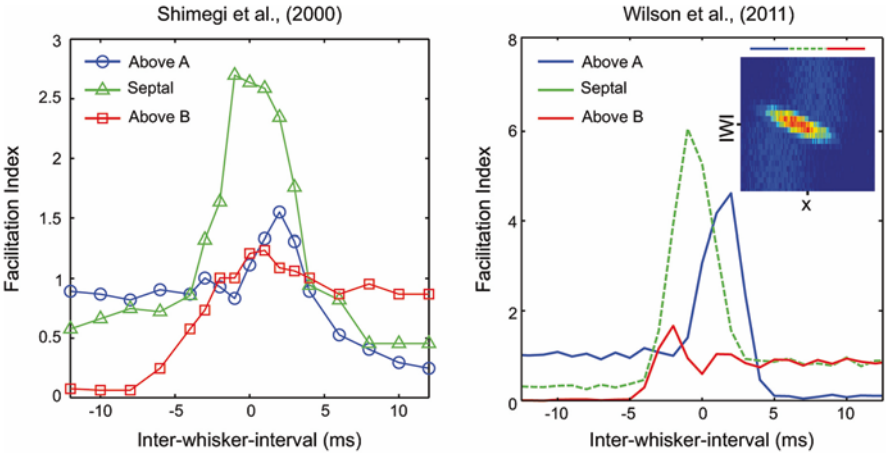

Fig. 10.4 Spatiotemporal interactions of cortical responses to paired whisker stimulations. The *left* panel shows experimental data replotted from Fig. 8e of [69] with permission from Society for Neuroscience. The *right* panel shows the behaviour of our model [68]. In both panels, the response facilitation index—computed as the ratio between the response to a paired stimulation of adjacent whiskers A and B and the linear sum of the responses to either A or B separately—is shown as a function of the time interval that separated the two whisker deflections. Figure reproduced from [68]

two adjacent whiskers are stimulated in a sequence with a few milliseconds interval, the responses of cortical neurons depends strongly on their positions (whether closer to the barrel of the first or second whisker), and are typically stronger than the sum of the responses to independent whisker deflections for a specific time interval (Fig. 10.4 left). Our modelling results (Fig. 10.4 right) showed—consistent with a place theory interpretation—that this broad range of recorded response profiles emerges naturally from the connection geometry as a function of the anatomical location of the neuron. In practical terms, the result that stimulus-evoked responses can be predicted by neuron location is important because it suggests that neural geometry needs special consideration as we construct theories of cortical processing.

Further consideration of the role of neural geometry may lead to predictions about sensory processing in species that maintain map-like representations compared with those that do not. For example, whilst individual neurons in rodent primary visual cortex respond selectively for the orientation of visual edges, they are arranged randomly in the cortex with respect to their orientation preference [70]. Presumably rodents would therefore be poor at using map-dependent mechanisms to extract stimulus velocity in the orientation domain (i.e., when extracting information about image rotation), compared to primates that have smooth topological maps for orientation preference and so might use place-coding mechanisms. In more general terms, evidence supporting the place theory from a tactile mammalian sensory system provides new insight into understanding how the brain represents

moving sensory input. Finally, in the context of the vibrissal system, and the barrel cortex, this study provided a novel account of the fusion of information at the multi-whisker level that both explained existing data, by casting it within a general and powerful framework (place theory), and made testable predictions that could be investigated experimentally.

A key feature of the mammalian sensory cortices is the presence of self-organising topological maps. Cortical maps for features of each sensory modality can be highly plastic and shaped by a combination of physical and environmental constraints [71, 72]. We recently conducted a series of experiments driving map self-organisation with activity patterns representing tactile stimulation of an array of artificial whiskers, in order to predict the organisation of object representations in the somatosensory cortex [73]. Inputs to the model were patterns of activity in simulated layer 4, encoding the spatial location and direction of whisker deflections caused by tactile stimuli that varied in shape, direction and speed. Layer 4 activity patterns were then remapped as layer 2/3 activity patterns using distance-dependent signalling delays in the layer 4 to layer 2/3 projection, to additionally encode the relative timing of whisker deflections [68]. This model represents a biologically grounded method by which to map the full spatial-temporal pattern of multi-whisker inputs to an essentially spatial representation of the stimulus across layer 2/3. Layer 2/3 activity patterns representing the range of multi-whisker stimulus patterns could thus be presented to a self-organising map model of postnatal development in layer 5, using an approach that we have shown previously to recreate known topological feature maps in layer 2/3 [74].

Our model of layer 5 map self-organisation, like our previous model for layer 2/3 map self-organisation, is based on the LISSOM (Laterally Interconnected Synergetically Self-organising Map) algorithm originally developed to capture the self-organising properties of primate visual cortex [75]. In our barrel cortex model, responses across the cortical sheet became organised into coextensive topological maps, wherein iso-feature contours for tactile stimulus shape, direction, and speed preferences intersected at right angles (see Fig. 10.5). The model therefore makes the critical prediction that orthogonal tactile feature spaces are represented in the somatosensory cortex by orthogonal feature maps (and hence by orthogonal spatial codes). A series of controlled simulation experiments suggested further that (i) speed and shape selective neurons align to regions of low selectivity in and between direction pinwheels, (ii) direction, shape, and speed maps are acquired in developmental sequence, (iii) stimulus direction is resolved by afferent projections to layer 5, whereas shape and speed are resolved by subsequent recurrent interactions in layer 5. These findings constitute specific, testable predictions about the development of functional maps and object representations in somatosensory cortex, i.e., that maps for the tactile motion direction implied by multi-whisker deflection sequences emerge earlier and more robustly than lower-order feature maps representing e.g., stimulus shape and speed. These modelling predictions were validated in experiments that connected self-organising networks to an artificial sensor array stimulated by a table-top positioning robot [73].

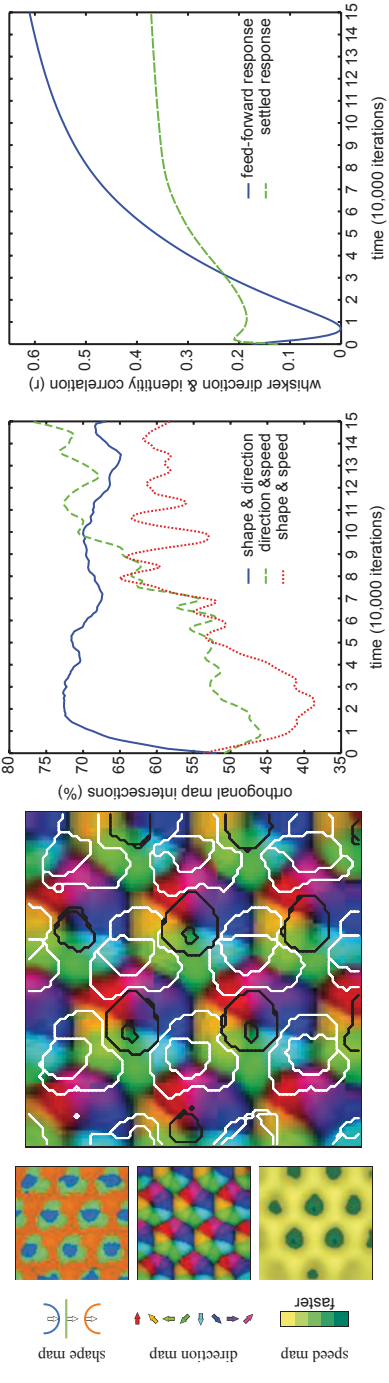

Fig. 10.5 The emergence of orthogonal coding for tactile stimuli of different shapes (concavity/convexity), directions, and speeds, in a self-organising model of map development in the barrel cortex. See [73] for further details

The Cerebellum Viewed as an Adaptive Filter and Forward Model

In experiments with the Scratchbot robot platform we occasionally observed that the robot would orient (foveate) as if to a target when no object is in fact present. On further investigation it appeared that on these occasions the sensory signal generated by active whisking is wrongly interpreted as contact with a target. This empirical observation in our biomimetic robot contrasts with the lack of reports of such 'phantom' orienting in normal rats. On the other hand, it has been shown that in rats sensory signals *are* generated by whisking movements. Specifically, a study by Leiser and Moxon reported that trigeminal ganglion cells of the rat fired during active whisking in air with no object contacts but were silent when the whiskers were at rest [76]. The implication of this result is that whisker sensory signals may include self-generated artefacts during whisking. The fact that the robot does show phantom orienting and rats appear not to suggests that, unlike the robot, rats can discriminate between the component of a sensory signal that originates from an external source and the component that is self-generated by its own whisking movements. We can ask the question: how is this discrimination achieved? This leads us to suggest that the rat may actively cancel self-generated sensory signals—what we might call 'self-induced' or 'self-generated' noise.

Interestingly, noise cancellation in biological systems has a well-investigated precedent—interference cancellation in passive electro-sensing in electric fish (for review see Bell et al. [77]). Of particular interest here is the evidence that suggests a cerebellar-like structure performs the function of noise cancellation in these animals [77, 78]. Additionally, this cerebellar-like structure is thought to act analogously to an adaptive filter [79, 80], linking biological noise cancellation to both the signal processing literature [81] as well as the adaptive filter model of the cerebellum [82]. In humans, a similar capacity to predict or cancel self-induced sensory signals is indicated by our inability to entertain ourselves by self-tickling (as opposed to being tickled by someone else). In this case, functional MRI data [83] also indicates a role for the cerebellum in predicting sensory signals due to self-movement thereby making them seem less amusing!

The above considerations led us to the hypothesis that rats may use their cerebellum to generate a signal which cancels the effects of self-generated whisking noise on incoming sensory signals from the whiskers (see [26, 84] for a review of the wider literature on the role of the cerebellum in sensory noise cancellation). Our first step in investigating this hypothesis was to determine whether our proposed mechanism would work *in principle*, by using it to achieve noise cancellation in a whisking robot [26]. The step had two goals, first to solve the practical problem of noise cancellation in the robot, and secondly to provide a theoretical basis for studying noise cancellation in whisking animals. Our approach was to use inspiration from the signal processing literature to form a prototype hypothesis of a whisking noise cancellation scheme.

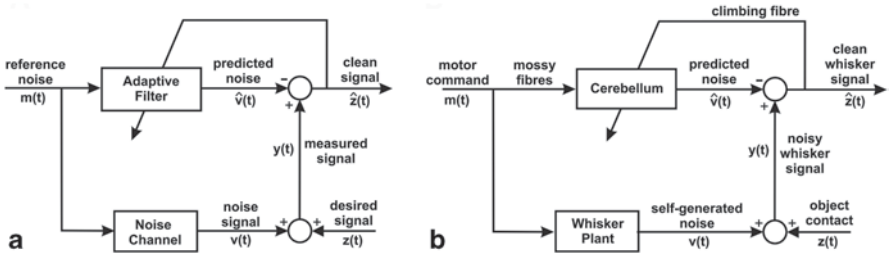

Fig. 10.6 Noise cancellation schemes. **a** A generic adaptive noise cancellation scheme, see for instance Widrow and Stearns [81], **b** A proposed biological whisking noise cancellation scheme. See [26] for further details

The subject of noise cancellation has been studied in the signal processing literature since the 1960s (for early references see Widrow et al. [81]). Much of the formative work was conducted by Bernard Widrow and was linked as an application problem to the least-mean-squares (LMS) adaptive filtering algorithm. The generic noise cancellation scheme is illustrated in Fig. 10.6, for detailed explanation see [26]. The weights of the adaptive filter in the noise cancellation scheme (Fig. 10.6a) are adjusted by removing the correlations in the clean signal from the reference noise, implemented via the LMS rule. In the context of whisking, the self-generated noise is thought to be caused by the movement of the whisker, either by inertia of the whisker base in the follicle or the whisker musculature pressing and activating the mechanoreceptors [76]. Ultimately, this activation is caused by the motor command to the whisker plant. Hence, we regard the motor command (either high- or low-level) as the reference noise, which is correlated with the noise signal but uncorrelated with signals related to object contacts. In our proposed whisking noise cancellation scheme (illustrated in Fig. 10.6b) the cerebellum learns to predict self-generated noise from the motor commands that cause the whisker movements. Hence, the cerebellum learns an internal forward model of the whisker dynamics that transform motor commands into sensory signals.

Adaptive Filter Model of the Cerebellum In the above whisking noise cancellation scheme we use the adaptive-filter to computationally model the cerebellum, as originally proposed by Fujita [82]. The mapping of this scheme onto the cerebellar microcircuit is illustrated in Fig. 10.7. We have previously investigated the computational properties of this model for adaptive motor control [85–88], and others have proposed that it could be used in principle to learn forward models (see [84] for review). However, our vibrissal noise study was, to our knowledge, the first instance of the adaptive-filter model of the cerebellum being applied to learning a specific forward model (i.e. of whisker dynamics) for the purposes of noise cancellation.

To develop and validate our proposed whisking noise cancellation scheme we recorded experimental data from Scratchbot during ‘free’ whisking (i.e. with no object contacts). Note that free-whisking is an ideal scenario to test the noise cancellation scheme because during free whisking the whisker sensory signal should be zero.

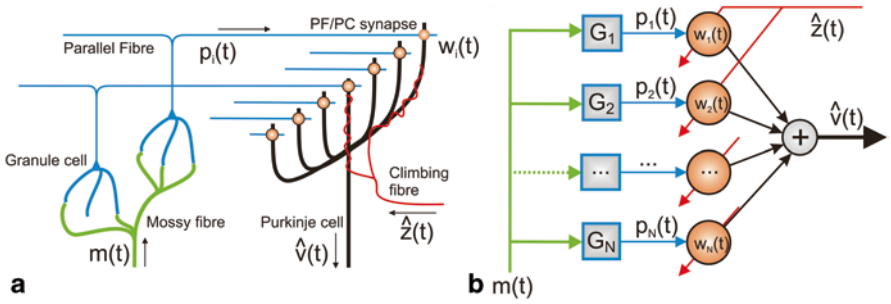

Fig. 10.7 Schematic diagram of the organization of the cerebellar microcircuit and its interpretation as an adaptive linear filter. **a** Simplified architecture of cerebellar cortex, **b** Adaptive filter model of the cerebellum. (Adapted from Fig. 1a, b of [84] with permission from Nature Publishing Group)

Hence, whilst the whisker dynamics are unknown and therefore the optimal cerebellar filter is also unknown, the output of the cancellation scheme is known: it should be zero. Therefore it is straight-forward to evaluate the performance of the noise cancellation scheme during free-whisking. Figure 10.8 shows example results of the application of the cerebellar noise cancellation algorithm to free-whisking data.

In a further extension of our sensory noise cancellation model [27] we have shown that the addition of sensory information from the whiskers allows the adaptive filter to learn a more complex internal model that performs more robustly than a forward model based on efference copy signals alone, particularly when the whisking-induced interference has a periodic structure. More generally, our analysis of the whisking noise cancellation scheme reveals that the functional role of the cerebellum may be to learn a forward model of the whisker/follicle dynamics. This links to separate speculation over the functional role of the cerebellum in motor control and sensory processing, where it has been suggested that the cerebellum can learn a variety of forward and inverse models in control and state estimation tasks, see for instance [89, 90]. Our development of the whisking noise cancellation scheme from a theoretical basis has led to a number of experimental predictions relating to the functionality of different components of the cerebellar micro-circuit: (i) that the mossy fibres transmit a copy of motor command, (ii) that the Purkinje cell output is an estimate of the self-induced noise signal, (iii) that the climbing fibre teaching signal is an estimate of the 'clean' whisker sensory signal, and (iv) that the superior colliculus is the target of the cerebellar output and acts to compare predicted and actual sensory signals [27].

Cerebellar/Collicular Algorithms for Orienting and Predictive Pursuit Cerebellar circuits are likely to be important for fast predictive control of ballistic movements needed for tasks such as prey tracking and capture since cerebellar damage is known to impair predictive aspects of motor behaviour [91]. An important role might lie in the calibration of sensory maps used to generate fast orienting movements. We have hypothesised [92] that the known extensive cerebellar-collicular connectivity (see

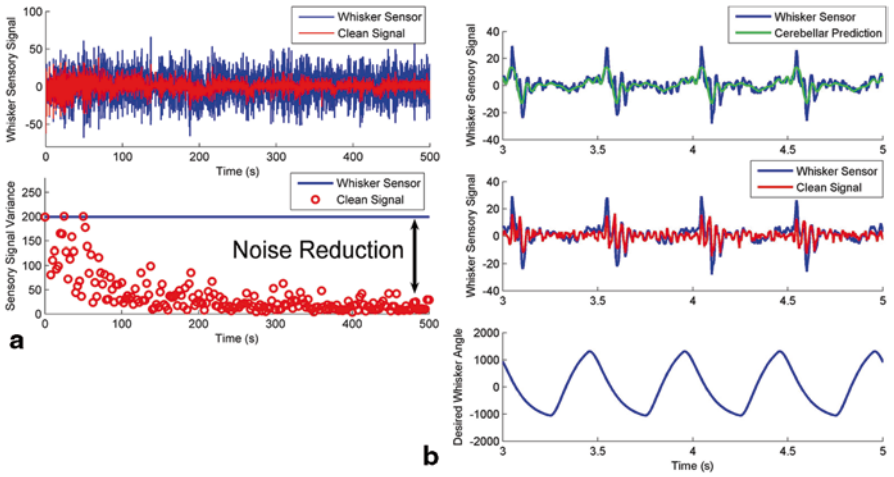

Fig. 10.8 Results from applying the noise cancellation algorithm to the free-whisking sensory signal. **a** Low frequency linear noise cancellation in the range 0–5 Hz. **b** High frequency nonlinear noise cancellation (up to 100 Hz). See [26] for further details

[27, 93]), together with the adaptive filter cerebellar architecture described above, could play a role in calibrating predictive topographic maps in the colliculus. We are currently investigating how this model can be employed in a predictive architecture in which features appear in the salience map at their predicted rather than their current positions.

The cerebellum may also calibrate sensory information that provides input to the predictive system. For example, as described above, we have developed a cortical algorithm for estimating contact timing for a target moving through the robotic whisker array illustrated in Fig. 10.9 left [73]. Figure 10.9 (centre) shows target velocities recovered from these timings, whilst incorporating a cerebellar learning element produced a more accurate calibration as shown in Fig. 10.9 (right).

Tactile Self-Localisation and Mapping in the Hippocampus

The lifestyle of any small mammal, even one as tiny as the Etruscan shrew, requires the capacity to know where you are at all times with respect to key locations such as the nest, important feeding sites, and significant danger zones. Indeed, as we have seen above, simply to explore space efficiently using vibrissal touch requires some long-term memory of locations you have visited in the recent past, and the capacity to update an estimate of your own position as you move around. In the mammalian brain the hippocampal system is known to be important in building and maintaining representations of the environment (the ‘place cell’ system [25]) and in maintaining estimates of changes in position determined through path integration (the ‘grid cell’

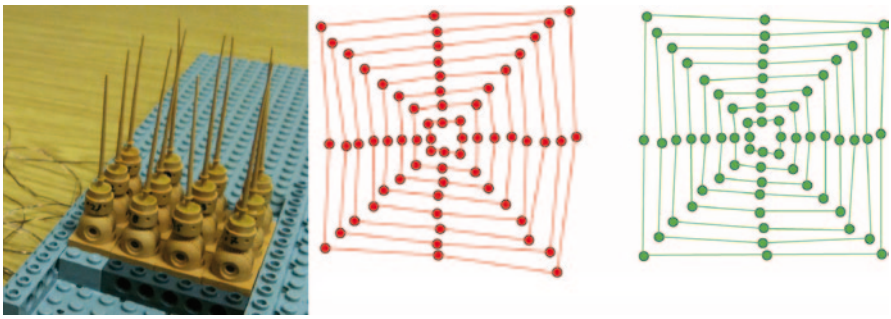

Fig. 10.9 Cortical algorithm for contact timing. **a** A planar target is moved through a robotic whisker array on an xy-plotter through eight speeds and eight directions to generate a set of multi-whisker deflection patterns, **b** plot of target velocities recovered from the relative timing of whisker responses, as computed using a cortical velocity-encoding algorithm based on [73]; plotted against the x and y components of the stimulus motion velocity, the distortion of the cortical estimates compared to a regular grid of true velocities is clear, **c** estimation of the motion velocities are improved by cerebellar correction after randomised representation of the data set

system [94]). Recent data also demonstrates that the hippocampus also encodes tactile information that describe the environmental context obtained through vibrissal touch [95].

The principal input structures of the hippocampus are the superficial layers of Entorhinal Cortex (EC). EC projects to Dentate Gyrus (DG) which is believed to increase the sparcity of the encoding generated by the EC. Both EC and DG project to CA3, which also receives strong recurrent connections that are disabled [96] by septal acetylcholine (ACh). CA3 and EC project to CA1, which in turn projects to the deep layers of Entorhinal cortex, there is also a back-projection from CA3 to DG [97]. Although the classical view of hippocampus is as a single loop, there is also a second loop—EC and CA1 project to Subiculum (Sub), which projects to the midbrain Septum (Sep) via fornix. Septal ACh and GABA fibres then project back to all parts of hippocampus. Figure 10.10 summarises many of these connections.

There have been two broad schools of hippocampal modelling one based on acquiring spatial sequences, and the other on the notion of auto-associative memory including pattern reconstruction based on partial or noisy input (see [98] for review). However, the objectives of both auto-associative and spatial sequence memories can be combined by a general Bayesian filter with noisy observations, which infers the (hidden) state of the world. Such a filter that maintains just a single estimate of the current state-of-the-world (e.g. of location in a spatial map) is known as a 'unitary particle filter'. We have developed a model of a spatial learning in the rodent hippocampus [98], viewed as a unitary particle filter, by mapping key structures in the hippocampal system onto the components of a Temporal Restricted Boltzmann Machine—a probabilistic algorithm for learning sequence data developed by researchers in machine learning (see, e.g. [99]). The algorithm approximates Bayesian filtering to infer both auto-associative de-noised percepts and temporal sequences, that is, it can clean-up and fill-out incoming sensory patterns and can use these to

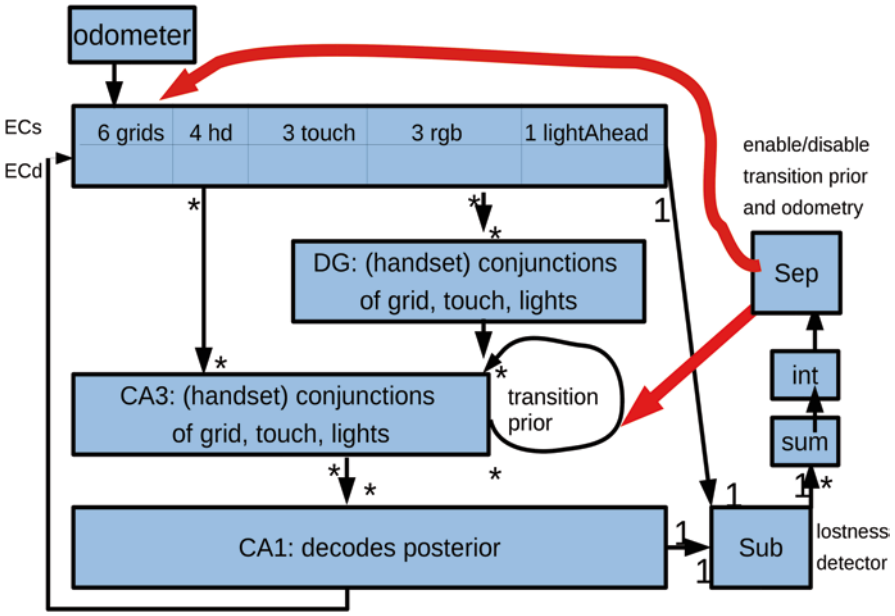

Fig. 10.10 Model of spatial memory in the hippocampal system viewed as a particle filter. Structures are labelled with UML notation indicating many-to-many fully connected links (*→ *), one-to-one links (*1* → *1*) and many-to-one links (*→ *1*). Thick lines are ACh projections, thin lines are glutamate. The model implements a spatial memory system for location based on multisensory signals from tactile, visual, and path integration signals. See text for abbreviations showing the proposed mapping to regions of the rodent hippocampal system. Reproduced from Fig. 1 of [98] with permission from IEEE

recall or forecast sequences of places visited during navigation. The mapping to the hippocampal system (see Fig. 10.10) proposes a novel role for the subiculum, and for ACh from the septum, in detecting when the animal has become lost (by detecting a mismatch between predicted and actual sensory signals). A follow-up paper [100] extended this model to include online learning of connections to and from the simulated hippocampal CA3 region.

Building on our computational models of hippocampus, we have developed tactile Self-Localisation and Mapping (tSLAM) for whiskered mobile robot platforms. tSLAM provides a robot with a means of mapping and navigating a novel environment by touch information alone, something which has never previously been developed in robotics. A critical step, was the development of a hierarchical Bayesian 'blackboard' architecture [101] to investigate how to fuse information from multiple local tactile feature reports to recognise objects in the world. This work also involved developing techniques for online head-centric spatial localisation of whisker contacts, and their subsequent world-centric transformation. To achieve tSLAM we have developed a particle-filter based mapping and localisation algorithm, taking odometry (path integration) and tactile information from the robot in real-time. This information is then integrated into an occupancy grid map, and a current position estimate.

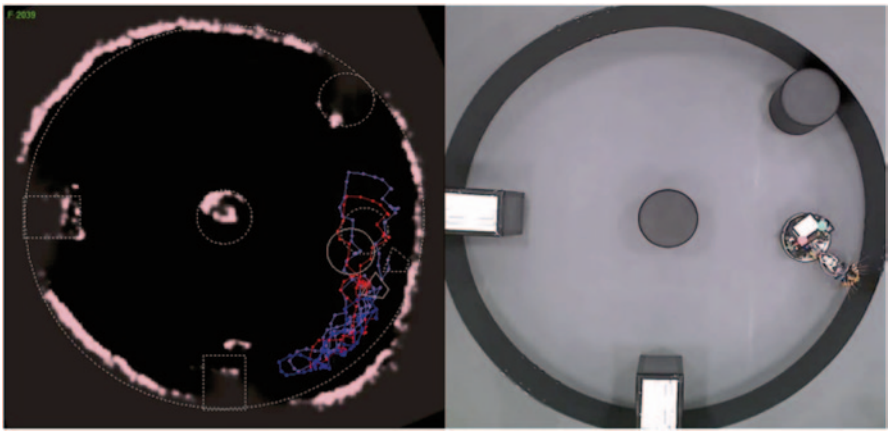

Fig. 10.11 Tactile Self-localisation and Mapping (tSLAM) in the Shrewbot whiskered robot platform. Screen shot taken from a combined video of overhead camera view (*right*) with an appropriately scaled and rotated 2d occupancy grid representation of the arena in a typical particle after approximately 1 h of whisker based tactile exploration (*left*). Figure reproduced from multimedia supplement to [102] with permission from IEEE

The tSLAM system has now been piloted on two whiskered robot systems—Crunchbot, a modified Roomba vacuum-cleaner robot with a small array of static whiskers [101], and Shrewbot a robot with multiple actively controlled whiskers and a 3 degrees-of-freedom neck (see Fig. 10.1 and [102]). In the case of the Shrewbot platform, odometry derived from the robot base and neck were passed at regular intervals (in phase with the whisking) to a population of particles each maintaining an estimate of head pose and location within a 2-dimensional occupancy grid. The importance of each particle was calculated by fusing the likelihood that each whisker in the array is at the estimated location in the map based on tactile information sampled throughout the previous whisk. The screen shot shown in Fig. 10.11 shows a one hour experimental run of Shrewbot in a 3 m diameter arena. The pink regions representing areas of the map that have a high probability of occupancy, the dashed white line representing ground truths taken from the over head video camera. The dashed white representation of Shrewbot is its ground truth location, whilst the solid representation is the current best estimate of pose and location taken from the particle with highest importance (cloud visible as red dots near the head).

We have also used the Shrewbot platform to model the active touch based hunting behaviour of the Etruscan Shrew [103]. A study of vibrissal-guided predation of insects by the shrew [2] identified three distinct phases of hunting behaviour: search, contact and attack. The search phase was reproduced on Shrewbot using the tactile attention based model of action selection described above, whereby the locus of attention drives the orienting behaviour of the robot between subsequent whisks. Upon making contact, an internal geometric model of two classes of object was compared to the sparse 3-dimensional tactile information derived from the whisker array. The two classes of object were vertical "walls" and the dome shaped covering of a mobile robot referred to as "preybot" (see Fig. 10.12). Shrewbot's re-

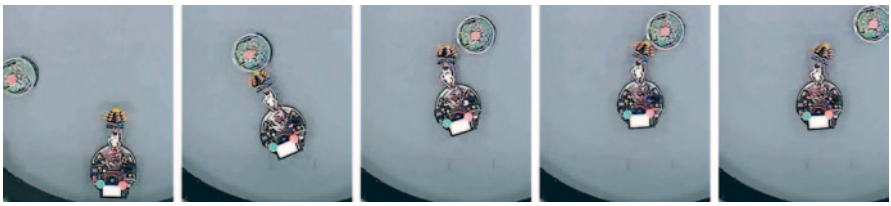

Fig. 10.12 Tactile identification and tracking of a target in a whiskered robot. Snapshots taken with an overhead camera of Shrewbot approaching the "preybot" during hunting behaviour. The images indicate: *search* (*frame 1*), *contact* (*frame 2 and 3*), *attack* (*frame 4*) and a return to *search* (*frame 5*). Figure reproduced from Fig. 3 of [103] with permission from Elsevier

flexive whisker control strategies [104] caused an increase in the whisking set angle similar to that reported in [2] as well as an increase in the number and frequency of whiskers making controlled contacts with the object. This information was collated into a "prey belief" metric that influenced the decision to either attack the object (preybot) or to ignore it (walls). In parallel to the attack decision process, the centre of mass of the preybot was also estimated. To accommodate the relatively sparse information from whisker contacts, some of the known characteristics of the preybot were used to better infer its location and orientation and hence its affordances as a potential "prey" object. The velocity of the preybot was derived from this information and thence a prediction of where a particular point on that robot (in this case the tail) should be in the near future. This location in space was then set as the target for an attack.

Conclusion

In this chapter we have briefly summarised an extensive programme of work aimed at describing and simulating, in biomimetic (robotic) models, the control architecture for sensorimotor co-ordination in the vibrissal touch system of small mammals. We have shown how the evolution of our robot models has progressively captured more-and-more of the important features of the biological target system including morphology, sensory transduction, motor control, and internal processing. Focusing initially on the problem of orienting to vibrissal contacts we have shown that models of the superior colliculus and basal ganglia can be combined to generate sequences of exploratory and orienting movements that allow the robot to explore an environment, and orient to unexpected contacts, in a life-like way. Our robot experiments also revealed a need to pre-process sensory signals in order to distinguish real physical contacts from 'ghost' contact signals induced by the whisking movements of the artificial vibrissae. This led to a novel hypothesis about the role of the cerebellum in vibrissal processing and the demonstration that adaptive filter algorithms modelled on cerebellar microcircuitry can be effective in predicting/cancelling self-induced sensory noise. The task of developing integrated sequences of movements in whiskered robots also revealed the need for spatial memory systems

that could effectively encode and remember the location of object contacts and allow the robot/animal to maintain a good estimate of its position in space. To make these systems more effective in identifying, and responding appropriately, to tactile environmental affordances, we are also developing models of cortical systems (particularly of primary somatosensory cortex), and have shown that model basal ganglia circuits can make timely decisions between alternatives based on cortical encodings of vibrissal touch signals. Whilst we have yet to realise the full architecture shown in Fig. 10.2 in a single robot, our latest robotic models show a capacity for integrated behaviour that has surprised and impressed exhibition and conference audiences into thinking that they are observing something like a 'robot animal'. From the perspective of understanding brain architecture, we also consider that we have made important steps towards understanding and demystifying the neural-basis for sensorimotor co-ordination in mammalian brains including our own.

Acknowledgement The authors would like to acknowledge the support of the European Union FP7 BIOTACT Project 'Biomimetic Technology for Vibrissal Active Touch' (ICT-215910) and the Weizmann Institute of Science project "Development of motor-sensory strategies for vibrissal active touch". We would also like to thank various collaborators whose experimental and theoretical research has inspired our biomimetic models including Mathew Diamond, Michael Brecht, Ehud Ahissar, David Golomb, Mitra Hartmann, Chris Yeo, Peter Redgrave and Kevin Gurney.

References

1. Brecht M, Naumann R, Anjum F, Wolfe J, Munz M, Mende C et al (2011) The neurobiology of Etruscan shrew active touch. Philos Trans R Soc Lond B Biol Sci 366(1581):3026–3036
2. Munz M, Brecht M, Wolfe J (2010) Active touch during shrew prey capture. Front Behav Neurosci 5:12
3. Roth-Alpermann C, Anjum F, Naumann R, Brecht M (2010) Cortical organization in the Etruscan shrew (Suncus etruscus). J Neurophysiol 104(5):2389–2406
4. Anjum F, Turni H, Mulder PG, van der Burg J, Brecht M (2006) Tactile guidance of prey capture in Etruscan shrews. Proc Natl Acad Sci U S A 103(44):16544–16549
5. Gibson JJ (1979) The ecological approach to visual perception. Houghton Mifflin, Boston
6. Prescott TJ, Diamond ME, Wing AM (2011) Active touch sensing. Philos Trans R Soc Lond B Biol Sci 366(1581):2989–2995
7. Ahissar E, Kleinfeld D (2003) Closed-loop neuronal computations: focus on vibrissa somatosensation in rat. Cereb Cortex 13(1):53–62
8. Prescott TJ, Gonzalez FM, Humphries MD, Gurney K, Redgrave P (2006) A robot model of the basal ganglia: behaviour and intrinsic processing. Neural Networks 19(1):31–61
9. Prescott, TJ, Ayers J, Grasso FW, Verschure P. F. M. J (In press) Embodied Models and Neurorobotics. In: Arbib MA, Bonaiuto JJ (eds) From Neuron to Cognition via Computational Neuroscience. MIT Press, MA, Cambridge
10. Braitenberg V (1986) Vehicles: experiments in synthetic psychology. MIT Press, Cambridge
11. Mitchinson B, Pearson M, Pipe T, Prescott TJ (2011) Biomimetic robots as scientific models: a view from the whisker tip. In: Krichmar J (ed) Neuromorphic and brain-based robots. MIT Press, Boston
12. Rosenblueth A, Wiener N (1945) The role of models in science. Philos Sci 12(4):316–321
13. Prescott TJ (2007) Forced moves or good tricks in design space? Landmarks in the evolution of neural mechanisms for action selection. Adapt Behav 15(1):9–31

14. Hallam JCT, Malcolm CA (1994) Behaviour—perception, action, and intelligence—the view from situated robotics. Philos Trans R Soc Lond Ser A 349(1689):29–42
15. Mitchinson B, Pearson MJ, Pipe AG, Prescott TJ (2012) The emergence of action sequences from spatial attention: insight from mammal-like robots. Living machines: biomimetic and biohybrid systems. Barcelona, Spain
16. Prescott TJ, Redgrave P, Gurney KN (1999) Layered control architectures in robots and vertebrates. Adapt Behav 7(1):99–127
17. Redgrave P, Prescott TJ, Gurney KN (1999) The basal ganglia: a vertebrate solution to the selection problem? Neuroscience 89:1009–1023
18. Brooks RA (1991) New approaches to robotics. Science 253:1227–1232
19. Gandhi NJ, Katnani HA (2011) Motor functions of the superior colliculus. Annu Rev Neurosci 34:205–231
20. Posner MI (1980) Orienting of attention. Q J Exp Psychol 32:3–25
21. Cisek P (2007) Cortical mechanisms of action selection: the affordance competition hypothesis. Phil Trans Roy Soc B 362(1485):1585–1599
22. Pearson MJ, Mitchinson B, Welsby J, Pipe T, Prescott TJ (2010) SCRATCHbot: Active tactile sensing in a whiskered mobile robot. In: Meyer J-A, Guillot A (eds) The 11th international conference on simulation of adaptive behavior. Paris, Springer
23. Sullivan JC, Mitchinson B, Pearson MJ, Evans M, Lepora NF, Fox CW et al (2012) Tactile discrimination using active whisker sensors. IEEE Sens J 12(2):350–362
24. Fox CW, Evans M, Pearson M, Prescott TJ (2012a) Tactile SLAM with a biomimetic whiskered robot. IEEE International Conference on Robotics and Automation (ICRA)
25. O'Keefe JA, Nadel L (1978) The hippocampus as a cognitive map. London, Oxford University Press
26. Anderson SR, Pearson MJ, Pipe A, Prescott T, Dean P, Porrill J (2010) Adaptive cancelation of self-generated sensory signals in a whisking robot. Robotics. IEEE Trans 26(6):1065–1076
27. Anderson SR, Porrill J, Prescott TJ, Dean P (2012) An internal model architecture for novelty detection: Implications for cerebellar and collicular roles in sensory processing. PLoS One 7(9):e44560
28. Brecht M, Preilowski B, Merzenich MM (1997) Functional architecture of the mystacial vibrissae. Behav Brain Res 84(1–2):81–97
29. McHaffie JG, Stein BE (1982) Eye movements evoked by electrical stimulation in the superior colliculus of rats and hamsters. Brain Res 247:243–253
30. Sahibzada N, Dean P, Redgrave P (1986) Movements resembling orientation or avoidance elicited by electrical stimulation of the superior colliculus in rats. J Neurosci 6(3):723–733
31. Favaro PD, Gouvea TS, de Oliveira SR, Vautrelle N, Redgrave P, Comoli E (2011) The influence of vibrissal somatosensory processing in rat superior colliculus on prey capture. Neuroscience 176:318–327
32. Cohen JD, Hirata A, Castro-Alamancos MA (2008) Vibrissa sensation in superior colliculus: wide-field sensitivity and state-dependent cortical feedback. J Neurosci 28(44):11205–11220
33. Hemelt ME, Keller A (2007) Superior sensation: superior colliculus participation in rat vibrissa system. BMC Neurosci 8:12
34. Miyashita E, Hamada Y (1996) The 'functional connection' of neurones in relation to behavioural states in rats. Neuroreport 7(14):2407–2411
35. Benedetti F (1991) The postnatal emergence of a functional somatosensory representation in the superior colliculus of the mouse. Dev Brain Res 60(1):51–57
36. Drager UC, Hubel DH (1976) Topography of visual and somatosensory projections to mouse superior colliculus. J Neurophysiol 39(1):91–101
37. Mitchinson B, Prescott TJ (2013) Whisker movements reveal spatial attention: a unified computational model of active sensing control in the rat. PLoS Comput Biol 9(9):e1003236
38. Grant RA, Mitchinson B, Fox C, Prescott TJ (2009) Active touch sensing in the rat: anticipatory and regulatory control of whisker movements during surface exploration. J Neurophysiol 101(2):862–74

39. Mitchinson B, Martin CJ, Grant RA, Prescott TJ (2007) Feedback control in active sensing: rat exploratory whisking is modulated by environmental contact. Proc Biol Sci 1613(274):1035–1041
40. Mitchinson B, Grant RA, Arkley K, Rankov V, Perkon I, Prescott TJ (2011) Active vibrissal sensing in rodents and marsupials. Philos Trans R Soc Lond B Biol Sci 366(1581):3037–3048
41. Towal RB, Hartmann MJ (2006) Right-left asymmetries in the whisking behavior of rats anticipate head movements. J Neurosci 26(34):8838–8846
42. Arkley K, Grant RA, Mitchinson B, Prescott TJ (2014) Strategy change in vibrissal active sensing during rat locomotion. Curr Biol 24(13):1507–1512
43. Hemelt ME, Keller A (2008) Superior colliculus control of vibrissa movements. J Neurophysiol 100(3):1245-1254
44. Miyashita E, Mori S (1995) The superior colliculus relays signals descending from the vibrissal motor cortex to the facial nerve nucleus in the rat. Neurosci Lett 195(1):69–71
45. Gold JI, Shadlen MN (2001) Neural computations that underlie decisions about sensory stimuli. Trends Cogn Sci 5(1):10–16
46. Chambers J, Humphries M, Gurney KN, Prescott TJ (2011) Mechanisms of choice in the primate brain: a quick look at positive feedback. In: Seth A, Bryson JJ, Prescott TJ (eds) Modelling natural action selection. Cambridge University Press, Cambridge, pp 390–418
47. Hikosaka O, Takikawa Y, Kawagoe R (2000) Role of the basal ganglia in the control of purposive saccadic eye movements. Physiol Rev 80(3):953–978
48. Knill DC, Pouget A (2004) The Bayesian brain: the role of uncertainty in neural coding and computation. Trends Neurosci 27(12):712–719
49. Wald A (1947) Sequential analysis. Wiley, New York
50. Bogacz R, Brown E, Moehlis J, Holmes P, Cohen JD (2006) The physics of optimal decision making: a formal analysis of models of performance in two-alternative forced-choice tasks. Psychol Rev 113(4):700–765
51. Gold JI, Shadlen MN (2007) The neural basis of decision making. Annu Rev Neurosci 30:535–574
52. Platt ML, Glimcher PW (1999) Neural correlates of decision variables in parietal cortex. Nature 400(6741):233–238
53. Lepora N, Pearson MJ, Mitchinson B, Evans M, Fox CW, Pipe T et al (eds) (2010) Naive Bayes novelty detection for a moving robot with whiskers. IEEE International Conference on Robotics and Biomimetics (ROBIO) Tainjin, December 14–18
54. Lepora N, Fox CW, Evans MH, Diamond ME, Gurney K, Prescott TJ (2012) Optimal decision-making in mammals: insights from a robot study of rodent texture discrimination. J R Soc Interface 9(72):1517–1528
55. Lepora NF, Evans M, Fox CW, Diamond ME, Gurney K, Prescott TJ (eds) (2010) Naive Bayes texture classification applied to whisker data from a moving robot. Neural Networks (IJCNN), The 2010 International Joint Conference on, 2010 18–23
56. Lepora NF, Sullivan JC, Mitchinson B, Pearson M, Gurney K, Prescott TJ (eds) (2012) Brain-inspired Bayesian perception for biomimetic robot touch. Robotics and Automation (ICRA), 2012 IEEE International Conference on, 2012 14–18
57. Bogacz R, Gurney K (2007) The basal ganglia and cortex implement optimal decision making between alternative actions. Neural Comput 19(2):442–477
58. Gurney K, Prescott TJ, Wickens JR, Redgrave P (2004) Computational models of the basal ganglia: from robots to membranes. Trends Neurosci 27(8):453–459
59. Lepora N, Gurney K (2012) The basal ganglia optimize decision making over general perceptual hypotheses. Neural Comput 24(11):2924–2945
60. Diamond ME, von Heimendahl M, Arabzadeh E (2008) Whisker-mediated texture discrimination. PLoS Biol 6(8):e220
61. Catania KC, Catania EH (2015) Comparative studies of somatosensory systems and active sensing. In: Krieger P, Groh A (eds) Sensorimotor integration in the whisker system. Springer, New York This Volume

62. Lee L-J, Erzurumlu RS (2005) Altered parcellation of neocortical somatosensory maps in N-methyl-D-aspartate receptor-deficient mice. J Comp Neurol 485:57–63
63. Woolsey TA, Welker C, Schwartz RH (1975) Comparative anatomical studies of the SmL face cortex with special reference to the occurrence of "barrels" in layer IV. J Comp Neurol 164(1):79–94
64. Keller A (1995) Synaptic organization of the barrel cortex. In: Jones EG, Diamond IT (eds) Cerebral cortex volume II: the barrel cortex of rodents. Plenum, New York
65. Jeffress LA (1948) A place theory of sound localization. J Comp Physiol Psychol 41(1):35–39
66. Joris PX, Smith PH, Yin TC (1998) Coincidence detection in the auditory system: 50 years after Jeffress. Neuron 21(6):1235–1238
67. Fitzpatrick DC, Kuwada S, Batra R (2000) Neural sensitivity to interaural time differences: beyond the Jeffress model. J Neurosci 20(4):1605–1615
68. Wilson SP, Bednar JA, Prescott TJ, Mitchinson B (2011) Neural computation via neural geometry: a place code for inter-whisker timing in the barrel cortex? PLoS Comput Biol 7(10):e1002188
69. Shimegi S, Akasaki T, Ichikawa T, Sato H (2000) Physiological and anatomical organization of multiwhisker response interactions in the barrel cortex of rats. J Neurosci 20(16):6241–6248
70. Ohki K, Chung S, Ch'ng YH, Kara P, Reid RC (2005) Functional imaging with cellular resolution reveals precise micro-architecture in visual cortex. Nature 433(7026):597–603
71. Feldman DE, Brecht M (2005) Map plasticity in somatosensory cortex. Science 310(5749):810–815
72. Fox K, Wong RO (2005) A comparison of experience-dependent plasticity in the visual and somatosensory systems. Neuron 48(3):465–477
73. Wilson SP (2011) Figuring time by space: representing sensory motion in Cortical Maps [PhD]. Sheffield
74. Wilson SP, Law JS, Mitchinson B, Prescott TJ, Bednar JA (2010) Modeling the emergence of whisker direction maps in rat barrel cortex. PLoS One 5(1):e8778
75. Miikkulainen R, Bednar JA, Choe Y, Sirosh J (2005) Computational maps in the visual cortex. Springer, Berlin
76. Leiser SC, Moxon KA (2007) Responses of trigeminal ganglion neurons during natural whisking behaviors in the awake rat. Neuron 53(1):117–133
77. Bell CC, Han V, Sawtell NB (2008) Cerebellum-like structures and their implications for cerebellar function. Annu Rev Neurosci 31:1–24
78. von der Emde G, Bell CC (1996) Nucleus preeminentialis of mormyrid fish, a center for recurrent electrosensory feedback. I. Electrosensory and corollary discharge responses. J Neurophysiol 76(3):1581–1596
79. Montgomery JC, Bodznick D (1994) An adaptive filter that cancels self-induced noise in the electrosensory and lateral line mechanosensory systems of fish. Neurosci Lett 174(2):145–148
80. Sawtell NB, Williams A (2008) Transformations of electrosensory encoding associated with an adaptive filter. J Neurosci 28(7):1598–1612
81. Widrow B, Stearns SD (1985) Adaptive signal processing. Prentice-Hall, Englewood Cliffs
82. Fujita M (1982) Adaptive filter model of the cerebellum. Biol Cybern 45(3):195–206
83. Blakemore S-J, Wolpert DM, Frith CD (1998) Central cancellation of self-produced tickle sensation. Nat Neurosci 1(7):635–640
84. Dean P, Porrill J, Ekerot CF, Jorntell H (2010) The cerebellar microcircuit as an adaptive filter: experimental and computational evidence. Nat Rev Neurosci 11(1):30–43
85. Dean P, Porrill J, Stone JV (2002) Decorrelation control by the cerebellum achieves oculomotor plant compensation in simulated vestibulo-ocular reflex. Proc Biol Sci 269(1503):1895–1904
86. Dean P, Porrill J (2008) Adaptive-filter models of the cerebellum: computational analysis. Cerebellum 7(4):567–571

87. Porrill J, Dean P, Stone JV (2004) Recurrent cerebellar architecture solves the motor-error problem. Proc Biol Sci 271(1541):789–796
88. Porrill J, Dean P (2007) Recurrent cerebellar loops simplify adaptive control of redundant and nonlinear motor systems. Neural Comput 19(1):170–193
89. Dean P, Porrill J (2014) Decorrelation learning in the cerebellum: computational analysis and experimental questions. Prog Brain Res 210:157–192
90. Wolpert DM, Miall RC, Kawato M (1998) Internal models in the cerebellum. Trends Cogn Sci 2(9):338–347
91. Bastian AJ (2006) Learning to predict the future: the cerebellum adapts feedforward movement control. Curr Opin Neurobiol 16(6):645–649
92. Porrill J, Anderson S, Dean P (2010) Can cerebellar input calibrate collicular topographic maps? BMC Neurosci 11(Suppl 1):120
93. Teune TM, van der Burg J, van der Moer J, Voogd J, Ruigrok TJ (2000) Topography of cerebellar nuclear projections to the brain stem in the rat. Prog Brain Res 124:141–172
94. Moser EI, Kropff E, Moser MB (2008) Place cells, grid cells, and the brain's spatial representation system. Annu Rev Neurosci 31:69–89
95. Itskov PM, Vinnik E, Diamond ME (2011) Hippocampal representation of touch-guided behavior in rats: persistent and independent traces of stimulus and reward location. PLoS One 6(1):e16462
96. Hasselmo ME, Schnell E, Barkai E (1995) Dynamics of learning and recall at excitatory recurrent synapses and cholinergic modulation in rat hippocampal region CA3. J Neurosci 15(7 Pt 2):5249–5262
97. Scharfman HE (2007) The CA3 "backprojection" to the dentate gyrus. Prog Brain Res 163:627–637
98. Fox CW, Prescott TJ (2010a) The hippocampus as a unitary coherent particle filter. International Joint Conference on Neural Networks (IJCNN). Barcelona
99. Taylor GW, Hinton GE, Roweis ST (2007) Modeling human motion using binary latent variables Advances in neural information processing systems (NIPS). 19. p 1345
100. Fox CW, Prescott TJ (2010b) Learning in the unitary coherent hippocampus. 20th International Conference on Artificial Neural Networks (ICANN). ThessalonIka
101. Fox CW, Evans MH, Pearson MJ, Prescott TJ (2012b) Towards hierarchical blackboard mapping on a whiskered robot. Robot Auton Syst 60(11):1356–1366
102. Pearson M, Fox C, Sullivan JCP, T. J, Pipe AG, Mitchinson B (eds) (2013) Simultaneous localisation and mapping on a multi-degree of freedom biomimetic whiskered robot. IEEE International Conference on Robotics and Automation (ICRA). Karlsruhe
103. Mitchinson B, Pearson MJ, Pipe AG, Prescott TJ (2014) Biomimetic tactile target acquisition, tracking and capture. Robot Auton Syst 62(3):366–375
104. Pearson MJ, Mitchinson B, Sullivan JC, Pipe AG, Prescott TJ (2011) Biomimetic vibrissal sensing for robots. Philos Trans R Soc Lond B Biol Sci 366(1581):3085–3096
105. Mitchinson B, Sullivan JC, Pearson MJ, Pipe AG, Prescott TJ (eds) (2013) Perception of simple stimuli using sparse data from a tactile whisker array. Biomimetic abd biohybrid systems. Springer, London
106. Prescott TJ, Pearson MJ, Mitchinson B, Sullivan JCW, Pipe AG (2009) Whisking with robots: From rat vibrissae to biomimetic technology for active touch. IEEE Robot Autom Mag 16(3):42–50

Part IV
Development of the Whisker System

Chapter 11
Impact of Monoaminergic Neuromodulators on the Development of Sensorimotor Circuits

Dirk Schubert, Nael Nadif Kasri, Tansu Celikel and Judith Homberg

Abstract State dependent changes in sensorimotor control are critical for interactions with the environment and are modulated by three principal monoaminergic neuromodulators: serotonin, dopamine and norepinephrine (noradrenaline). The neuromodulatory neurotransmitter release starts during embryonic development and transiently exerts neurotrophic actions that cease after the first 2–3 postnatal weeks in rodents. Particularly during these early postnatal weeks neuronal projections along sensorimotor circuits are most sensitive to experience-dependent development. This implies that early changes in neuromodulatory action will have long-lasting consequences, contributing to the normal range of individual differences in sensorimotor integration up to neurodevelopmental disorders like autism spectrum disorders. To delineate these neurodevelopmental processes we review herein (1) the basics of the three principal neuromodulators, (2) the organization of neuromodulatory innervation of sensorimotor circuits, (3) how targeted manipulation of neuromodulation during development affect the anatomical and functional organization of sensorimotor circuits and their behavioral correlates, and (4) how alterations in the anatomical and functional organization of these circuits contribute to sensorimotor deficits in adulthood, for example in brain disorders. Finally

D. Schubert (✉)
Cognitive Neuroscience, Donders Institute for Brain, Cognition and Behaviour, Radboud University Medical Center, Nijmegen, The Netherlands
e-mail: d.schubert@donders.ru.nl

N. Nadif Kasri · J. Homberg
Donders Institute for Brain, Cognition and Behaviour,
Radboud University Medical Centre, Nijmegen, The Netherlands
e-mail: n.nadif@donders.ru.nl

T. Celikel
Neurophysiology, Donders Institute for Brain, Cognition, and Behaviour,
Radboud University Nijmegen, The Netherlands
e-mail: t.celikel@donders.ru.nl

J. Homberg
e-mail: Judith.Homberg@radboudumc.nl

P. Krieger, A. Groh (eds.), *Sensorimotor Integration in the Whisker System,*
DOI 10.1007/978-1-4939-2975-7_11

(5) we discuss the evidence for a developmental switch for neuromodulator neurotransmitter action in sensorimotor integration, and propose that neuromodulatory influences during early postnatal development is critical for sensorimotor function in adulthood.

Keywords Sensorimotor · Serotonin · Dopamine · Noradrenaline · Norepinephrine · Neurodevelopment · Brain disorders

Abbreviations

5-HT	Serotonin
AC	Adenylate cyclase
AMPA α	Amino-3-hydroxy-5-methyl-4-isoxazolepropionic acid
COMT catechol	O-methyl transferase
DA	Dopamine
DAT	Dopamine transporter
DRN	Dorsal raphe nucleus
E	Embryonic day
EPSC	Excitatory Postsynaptic Current
IP3	inositol trisphosphate
KO	Knockout
LC	Locus Coeruleus
M1	Primary motor cortex
MAO	Monoamine oxidase
Mo7	Facial motor nuclei
MRN	Median raphe nucleus
NE	Norepinephrine = noradrenaline
NET	Noradrenaline transporter
P	Postnatal day
Pr5	Principal trigeminal nucleus
PLC	Phospholipase C
PIP2	Phosphatidyl inositol bisphosphate
PMBSF	Posteromedial barrel subfield
S1	Primary somatosensory cortex
SERT	Serotonin Transporter
Tph	Tryptophan hydroxylase
VL	ventrolateral nucleus of the thalamus
VMAT	Vesicular monoamine transporter
VPM	Ventroposteromedial nucleus of the thalamus
VTA	Ventral Tegmental Area

Monoaminergic Modulation of Sensorimotor Control

In the wild, most rodents are nocturnal and often navigate underground tunnels using their whiskers and sense of smell as the primary sensory organs [1–4]. Rats and mice, for example, use their whiskers to identify tactile targets of interest [5–8], discriminate surface features [9–12] and guide their locomotion [13, 14].

Rats and mice move their whiskers back-and-forth to scan the tactile space surrounding their snout. Frequency and amplitude of whisker motion depend on the mode of exploration. In the absence of an object within their tactile space, actively whisking animals protract and retract their whiskers with low frequency and large amplitude [8]. Upon contact with a target, whisking amplitude is reduced while frequency is increased [15]. The adaptive nature of sensory exploration by whisker touch is controlled by multiple sensorimotor closed-loop [16–21] whose development is shaped by neuromodulatory neurotransmitters during early postnatal brain development. In particular monoamines, such as dopamine, noradrenaline and serotonin got more and more into focus of interest as they, by acting on various sets of specific receptors, not only modulate activity in the mature sensorimotor system but also during the early ontogeny of the brain. The impact of monoamines on the development and shaping of networks of the sensorimotor system depends on the ontogeny of neurotransmitter release sites as well as the availability (expression level) and functional state of the different types of monoamine receptors. Both, monoaminergic innervation as well as monoaminergic receptor expression is undergoing changes and modulation during brain development. Abnormalities in the temporal or spatial pattern of the development of monoaminergic systems have been found to lead to distorted sensorimotor function and sensory perception.

In this chapter, after providing a general overview of the structure and function of the dopaminergic, serotonergic and norepinephrinergic system, we will highlight the anatomical organization and development of monoaminergic innervation of the rodent sensorimotor system. In the final sections we will illustrate how manipulation or dysfunction of monoaminergic modulation can alter the function of the sensorimotor system and how this can be relevant for neurological disorders in human such as depression, attention deficit disorders and Parkinson's disease.

Principal Monoaminergic Neuromodulators in the Mammalian Brain

Dopamine

Dopamine (DA) is one of the three monoaminergic neuromodulators, classified as a catecholamine, regulating specific behavioral components. DA-releasing neurons disperse into three major pathways according to their anatomical location and function [22]. The nigrostriatal pathway consists of dopaminergic neurons that project from the substantia nigra into different parts of the striatum. These neurons are

important for motor control. The mesolimbic pathway includes neurons that project from the ventral tegmental area (VTA) to the nucleus accumbens, the amygdala and hippocampus. These brain areas are responsible for memory formation, motivation and emotional responses, and are able to arouse reward and desire. The third pathway is called the mesocortical pathway. It contains neurons, which also originate in the VTA but terminate in various areas of the neocortex, ranging from prefrontal to occipital cortical areas.

Five distinct DA receptors are known to be present in the mammalian brain, all encoded by a gene family which has emerged from gene duplications followed by selection of the duplicated genes [23]. DA receptors are divided into two main families: the dopamine D1-like receptors and the dopamine D2-like receptors. The dopamine D1-like receptor family consists of the D1 and D5 receptors and both stimulate adenylate cyclase (AC) through the Gs-protein that intracellularly coupled to these receptors. D2, D3, and 4 represent the D2-like receptors which inhibit AC through Gi. Dopamine synthesis is mediated in a two-step process by the enzymes tyrosine hydroxylase and aromatic L-amino acid decarboxylase. In neurons, DA is packaged after synthesis into vesicles by VMAT (vesicular monoamine transporter). DA breakdown is mediated by two pathways. The first one involves reuptake via the DA transporter (DAT), then enzymatic breakdown by monoamine oxidase (MAOA and MAOB). In the prefrontal cortex, which is extensively innervated by the dopaminergic axons, however, there are very few DAT proteins, and DA is inactivated instead by reuptake via the norepinephrine transporter (NET), presumably in neighboring norepinephrine neurons, followed by enzymatic breakdown by catechol-O-methyl transferase (COMT). Hence, drugs and genetic factors targeting these receptors or enzymes will alter dopaminergic neurotransmission and affect the development and function of the sensorimotor system.

Norepinephrine (Noradrenaline)

Norepinephrine (NE), also known as noradrenaline, is the other catecholamine. NE is synthesized from DA by DA β-hydroxylase [24]. It is released from the adrenal medulla into the blood as a hormone, and is also a neurotransmitter in the central nervous system and sympathetic nervous system, where it is released from noradrenergic neurons in the locus coeruleus (LC). Like DA, NE is stored in synaptic vesicles and released into the synaptic cleft upon an action potential, whereby it can bind to both presynaptic and postsynaptic adrenergic receptors. These are classified as α and β adrenergic receptors, and for each of these metabotropic G-protein coupled receptors subtypes have been identified. α Receptors have the subtypes α1 and α2, which are linked to inhibitory G-proteins, and β Receptors have the subtypes β1, β2 and β3, which are linked to Gs proteins. NE is taken up by the noradrenaline transporter (NET) and presynaptically degraded by COMT and MAO. As a stress hormone, norepinephrine affects parts of the brain, such as the amygdala, where attention and responses are controlled [25]. NE also mediates sensory and nociceptive responses, through the sensory cortices [26], and therefore environmental, pharmacological or genetic manipulation is expected to alter sensory perception.

Serotonin

Serotonin (5-HT) is a monoaminergic neurotransmitter, which is synthesized in the raphe nuclei. The raphe nuclei are clustered in the brainstem. Serotonergic neurons, particularly those located in the dorsal and median raphe nuclei, project to widespread brain regions, and thereby serotonin is implicated in many different central processes, including the regulation of emotion (amygdala), cognitive functions (prefrontal cortex), sleep, sexual and eating behavior (hypothamalus), learning and memory (hippocampus), as well as sensory perception (sensory cortices).

5-HT is derived from the essential amino acid L-tryptophan, and its synthesis is mediated by the enzymes tryptophan-hydroxylase (TPH), and 5-hydroxy-tryptophan-decarboxylase. Like other neurotransmitters, 5-HT is transported into the vesicles near the presynaptic membrane of neurons by VMAT. Upon fusion of the vesicle with the cell membrane, 5-HT is released into the synaptic cleft, where it can diffuse and bind to receptors. There are 15 genes encoding 5-HT receptors in mammalian brains: *HTR1A*, *HTR1B*, *HTR1D*, *HTR1E*, *HTR1F*, *HTR2A*, *HTR2B*, *HTR2C*, *HTR3A*, *HTR3B*, *HTR4*, *HTR5A*, *HTR5B*, *HTR*6 and *HTR*7. All of them code for G-protein coupled receptors, except for the 5-HT3A and 5-HT3B receptors, which are ligand-gated ion channel receptors [27, 28]. The presynaptic 5-HT1B receptor can be found in rodents and autoregulates 5-HT release, while in humans the 5-HT1D receptor fulfils this purpose [28]. The presynaptic 5-HT1A receptor is located in the raphe nuclei and regulates the firing of serotonergic raphe neurons that project to widespread regions in the brain, as well as to the spinal cord. The 5-HT1A and 5-HT1B/D receptors, as all other 5-HT receptors, are also found postsynaptically, and mediate a myriad of signaling pathways. Serotonin signaling is terminated through the presynaptically located 5-HT transporter (SERT). The SERT is integrated in the presynaptic cellular membrane and imports 5-HT from outside the cell into the cytosol [29]. Degradation of 5-HT is mediated by monoamine oxidase A (MAOA). Particularly the existence of 15 5-HT receptors render the 5-HT system as the most complex monoaminergic system, and offers multiple targets for modulation of sensory systems.

Anatomy of the Neuromodulatory Systems: A Sensorimotor-Centric View

If one focuses on the whisker related systems, the rodent sensorimotor system encompasses two major systems: (i) the topologically precisely organized somatosensory system, in which of ascending fiber connections link the sensory periphery (whiskers) via specific nuclei in the brain stem and thalamus to the whisker related primary somatosensory cortex (S1; barrel cortex) and (ii) the whisker related motor system in which the primary motor cortex (M1) controls whisker movement by the pathways via motor related nuclei of the thalamus and the brain stem. On the cortical level S1 and M1 show extensive bidirectional intracortical connections,

which is important for the somatosensory system to work as an active sensory system. Even though there are more brainstem, midbrain and cortical regions involved in the whisker sensorimotor system of rodents, in this chapter we will focus on selected core regions, i.e. for the somatosensory ascending pathway the principal trigeminal nucleus (Pr5) in the brainstem, the ventroposteromedial (VPM) nucleus and on the cortical level S1, and for the descending motor system on the cortical level M1, the ventrolateral nucleus (VL) in the thalamus and the facial motor nuclei Mo7 in the brainstem.

For the development of the sensorimotor system and the correct topological patterning of the somatosensory system in particular, the first two postnatal weeks are critical. During this phase monoaminergic neuromodulators play not only an important role in modulating the neural activity within and between the networks of S1 and M1, but also in ensuring proper organization of local and global structural connectivity and therefore in cortical maturation [30, 31].

How monoamines affect the structural organization and neural activity during development depends on the temporal and spatial profile of innervating monoaminergic fibers, of the expression of specific monoaminergic transporters systems and the expressions of the various monoaminergic receptors [32]. Eventually, for all three monoaminergic systems discussed in this chapter the modulation of the various parts sensorimotor system is achieved by projections that arise from a surprisingly small number of monoaminergic neurons, each of which located in specialized nuclei in the brain [33, 34].

To understand the neuromodulatory impact on the development and activity of the sensorimotor system it is necessary to understand the different temporal and spatial profiles of axon innervation and regional, layer and cell type specific receptor expression of the DA, NE and 5-HT systems in the sensorimotor system during development.

Sensorimotor-Centric View of the Dopaminergic System

Dopaminergic Innervation of the Sensorimotor System

The neocortex is extensively innervated by DA axons originating mainly from the ventral tegmental area (VTA) [35–37]. Even though the “classical” and most dense dopaminergic innervation is found in the prefrontal and anterior cingulate cortex [38, 39], dopaminergic projections originating from neurons in the VTA also target, less densely, both sensorimotor related cortical areas M1 and the medial part of S1 [35] (Fig. 11.1). In S1, anatomical studies imply a pattern of thin dopaminergic axon bundles that indicate a columnar innervation pattern. Furthermore, the cortical innervation is not uniform across layers but layer specific: approximately 90 % of the dopaminergic fibers in M1 and S1 innervate the deep cortical layer VIb [40, 41] (Fig. 11.1).

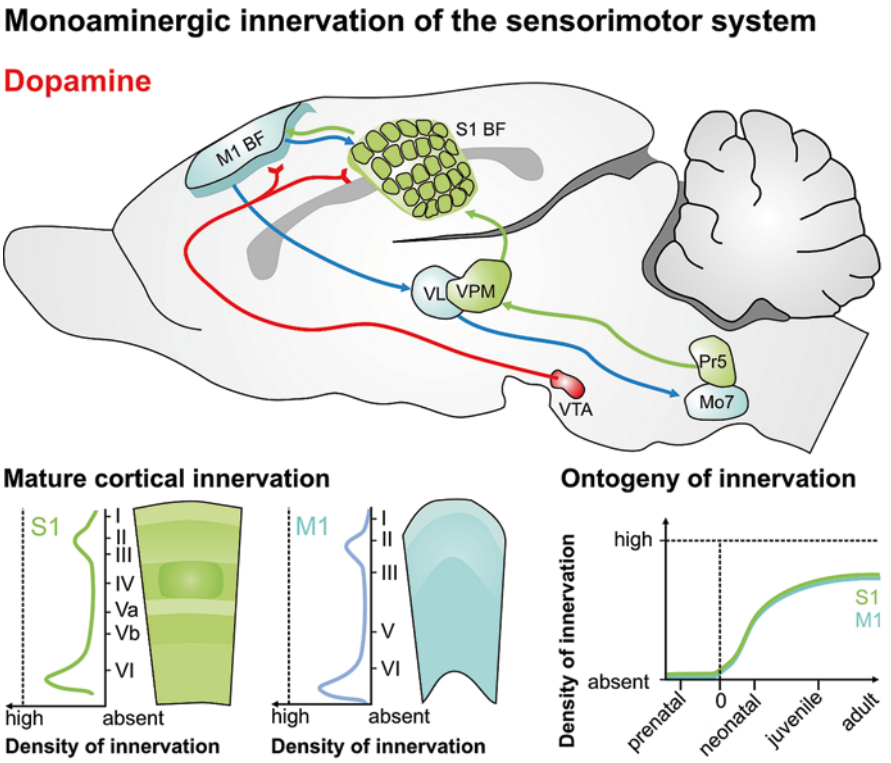

Fig. 11.1 Dopaminergic innervation of the rodent sensorimotor system. Upper panel: Simplified overview of major afferent and efferent pathways and structures of the sensorimotor system and the main origins and projections of the dopaminergic system (*red*) targeting the sensorimotor system. The afferent projections and main processing structures of the lemniscal somatosensory pathway within the central nervous system are given in green, the efferent motor related projections in blue. Lower left panels: relative layer specific density of dopaminergic innervation of the primary somatosensory (*S1, green*) and primary motor cortex (*M1, blue*) in the mature rodent brain. The dark shaded area in layer *IV* of the *S1* represents a barrel structure. Lower right panel: Ontogeny of dopaminergic innervation of the *S1* (*green*) and *M1* (*blue*), representing changes in the relative density of innervation between prenatal and adult state. *Pr5* principal trigeminal nucleus in the brainstem; *VPM* ventroposteromedial nucleus of the thalamus; *S1 BF* barrel field of the primary somatosensory cortex; *M1 BF* barrel field associated primary motor cortex, *VL* ventrolateral nucleus of the thalamus; *Mo7* facial motor nuclei of the brainstem; *VTA* ventral tegmental area

Dopaminergic fibers in the deeper layers of S1 and M1 belong to a particular class of mesocortical dopaminergic projections (Class 1 afferents; [42]), which differ from the dopaminergic projections targeting other cortical areas and which there target superficial cortical layers (Class 2 afferents). Dopaminergic class 1 afferents (i) originate from neurons in the VTA, (ii) develop largely prenatally, reaching the targeted cortical areas at around birth [43], (iii) give rise to few collaterals and (iii) possess a high dopamine content. After reaching the cortex, from the early developmental stage on, the general innervation pattern already resembles that of

the mature cortex with the intracortical axon collaterals progressively increasing in density (Fig. 11.1). The preferential intracortical targets of synapses formed by the dopaminergic axons are excitatory pyramidal cells in layer VI [44].

In the rodent sensorimotor system the direct dopaminergic innervation seems to be focused on the cortical areas only. In rats the somatosensory related VPM and motor system related VL in the thalamus lack dopaminergic innervation of motor and somatosensory related thalamic nuclei [45] (Fig. 11.1), whereas in primates they are sparsely innervated.

Besides the direct monosynaptic dopaminergic innervation, one also has to consider an indirect dopaminergic modulation of the sensorimotor system, especially of M1. Activity in M1 is known to be modulated via basal ganglia - cortex circuits [46]. Dopaminergic projections originating from neurons in the substantia nigra are targeting and thus influencing the activity in the basal ganglia and therefore enabling indirect dopaminergic modulation of M1 activity.

Dopamine Receptor Expression in the Sensorimotor System

As described in section "Sensorimotor-centric view of the dopaminergic system" DA acts through two distinct, biochemically and pharmacologically defined G protein coupled receptor families [47]: D1-like (D1 and D5) and D2-like receptors (D2, D3, D4). Along the sensorimotor axis D1, D2 and D3 receptors are of particular relevance.

In the rodent brain D1 receptors are the most abundant receptors. While they show relatively low expression in thalamic nuclei [48] and the brainstem [49], in the cortex they are typically expressed in the entire cortical column except in LIV, showing peak expression in layers V and VI [48, 50–52]. In the sensorimotor system D1 receptors show an almost identical expression density in S1 and M1 [53, 54].

D2 receptor expression shows a widespread ubiquity in the brain, however with relatively lower expression densities then D1 receptors [49, 55]. In brainstem and thalamus the D2 expression level is generally low. However, in the S1 and M1 cortex D2 receptors are more prominently expressed and display a layer specific pattern. The D2 receptors are almost exclusively expressed in corticostriatal and corticocortical neurons of layer V, with generally higher expression levels in rostral than caudal cortical areas [51, 55, 56]. Taken together, while in the cortex D1 receptors are more widely expressed across cortical layers, D2 receptors expression shows strong similarities with the cortical innervation pattern of the dopaminergic axons [55].

Considering a modulating role of the dopaminergic system in the development of the sensorimotor system, D3 receptor expressions show remarkable properties, as they show a transient expression in the somatosensory cortex. Unlike D1 receptors, D3 receptors are expressed almost exclusively in layer IV of S1, showing a pattern, which corresponds to the layer IV barrels [57]. D3 receptor expression, which becomes detectable at around postnatal day P4-5, reaches a peak in expression at P14 and then declines again. This temporal expression profile of D3 receptors is very

different from those of other dopamine receptors of the D1 or D2 subfamilies. The similarity of the spatial and temporal profile of D3 receptor expression with the critical phase for barrel formation in S1 indicates a potential role in cortical maturation also for dopamine.

Sensorimotor-Centric View of the Norepinephrinergic System

Norepinephrinergic Innervation of the Sensorimotor System

The largest density of norepinephrinergic (NE) neurons within the mammalian brain is located in the LC of pons. From three subparts of this region all cortical and subcortical parts of the sensorimotor system receive partially extensive noradrenergic innervation [58–60] (Fig. 11.2). The noradrenergic neurons of the dorsoventral extent of the LC give rise to ipsilateral projections into both sensorimotor associated cortical areas M1 and S1 [34, 59, 61]. The ventral subdivision of LC contains neurons that project, again mainly ispilaterally, into the VPM and VL in the thalamus [34, 59]. In the brainstem, somatosensory nucleus Pr5, and the facial motor nucleus Mo7 both receive divergent ipsi- and contralateral projections from a small number of noradrenergic neurons in the ventral margin of the LC (Fig. 11.2). The widespread innervation of the sensorimotor regions implies the potential relevance of NE modulatory role in vibrissal sensorimotor integration [34, 59].

The noradrenergic neurons of the LC begin to differentiate at E10 to E13 [62, 63] and by E17 the axonal projections of these neurons start to innervate the cortex [60, 64] (Fig. 11.2). This early anatomical presence of noradrenergic projections enables this monoaminergic system to not only modulate ongoing network activity but also to influence neurodevelopment, including development of neurons in the cortex and even that of other monoaminergic systems, such as the serotonergic system [65, 66]. After reaching the cortex in the vicinity of the cortical plate [67], noradrenergic axons gradually innervate all cortical layers during the following weeks. In the mature brain the intracortical distribution of the noradrenergic innervation of M1 and S1 is nearly identical: the number of noradrenergic terminals is about twice as high in cortical layer I than in layers II/III and then progressively decreases towards the deep layer VI [41, 60, 64, 68] (Fig. 11.2). Since dopaminergic terminals in the sensorimotor cortical areas mainly occupy the deep layer VIb, the two types of monoamine innervations could be considered as displaying some complementarity. The functional implications of this monoaminergic innervation pattern for cortical development and modulation of cortical activity still needs to be investigated.

Norepinephrine Receptor Expression in the Sensorimotor System

Noradrenergic innervation of the cortex and other brain regions is important in regulating excitability of individual cells, synaptic transmission and network function. The corresponding receptors, α1-, α2- and β1-adrenoceptors, are widely distributed

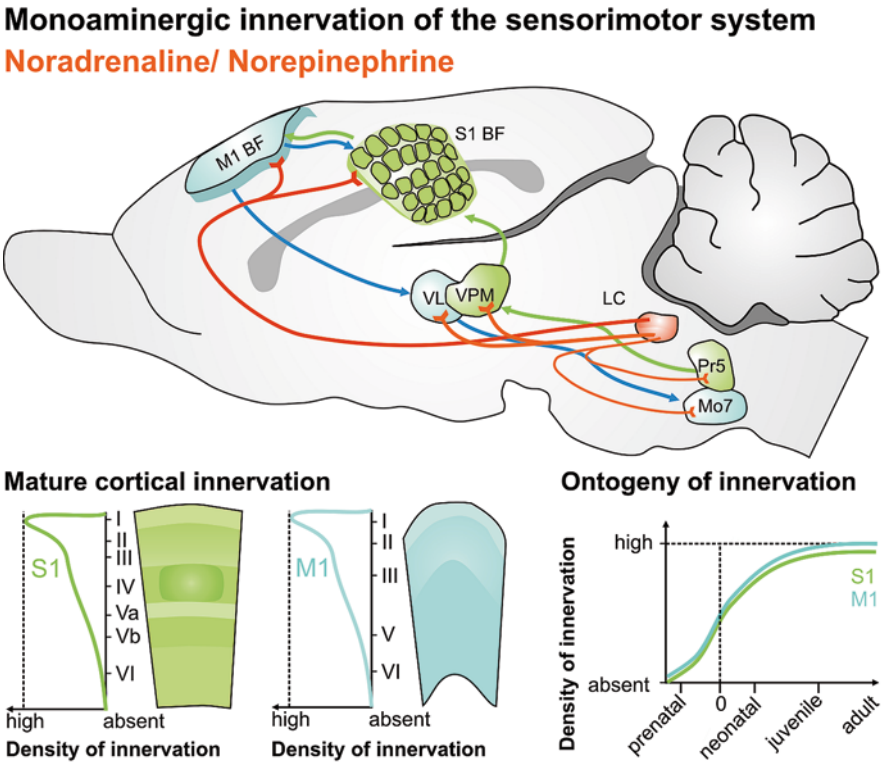

Fig. 11.2 Noradrenergic innervation of the rodent sensorimotor system. Upper panel: Simplified overview of major afferent and efferent pathways and structures of the sensorimotor system and the main origins and projections of the adrenergic system (*orange*) targeting the sensorimotor system. The afferent projections and main processing structures of the lemniscal somatosensory pathway within the central nervous system are given in green, the efferent motor related projections in blue. Lower left panels: relative layer specific density of noradrenergic innervation of the primary somatosensory (*S1, green*) and primary motor cortex (*M1, blue*) in the mature rodent brain. The dark shaded area in layer IV of the *S1* represents a barrel structure. Lower right panel: Ontogeny of noradrenergic innervation of the *S1* (*green*) and *M1* (*blue*), representing changes in the relative density of innervation between prenatal and adult state. *Pr5* principal trigeminal nucleus in the brainstem; *VPM* ventroposteromedial nucleus of the thalamus; *S1 BF* barrel field of the primary somatosensory cortex; *M1 BF* barrel field associated primary motor cortex, *VL* ventrolateral nucleus of the thalamus; *Mo7* facial motor nuclei of the brainstem; *LC* Locus coeruleus

in the brain. The effects of adrenoceptors are heterogeneous [69] and can be pre- as well as postsynaptic. Generally α2-adrenoceptors have been found to alter synaptic transmission [69], and activation of α1- and β-adrenoceptors depolarizes pyramidal neurons [70, 71] and alters action potential firing behavior [69, 70, 72].

The expression of α1 and α2-adrenoceptors shows regional specificity with partially very dense expressions. In the cortical areas M1 and S1, as well as in the motor related nucleus of the brain stem α1A, α1B, α2A and α2C- adrenoceptors are being expressed [73]. In the cortical areas α1 A-adrenergic receptor mRNA expressed

highest in the superficial layers II/III, moderate in the deeper layers V/VI and weakest in layer IV of S1, whereas α1B-adrenergic receptor expression is spatially more limited to the deeper layers V and VI. α2A receptors are expressed in all layers, but in the adult strongest in superficial layers I-III and deep layer VI [74]. In the thalamic VPM and VL nuclei α1A and α2A receptors are weakly or not expressed at all. Unlike for the cortex and Mo7, α2B adrenoceptors display strong expression in the thalamus [73, 75–77]. The most restricted set of adrenoceptors is found in the Pr5 of the brainstem, where only α2-adrenoceptors are expressed prominently [73]. Of the three types of β-adrenoceptor, in terms of expression level only the β1-adrenoceptors seem to be of direct relevance for the sensorimotor system. In contrast to the regional specificity of α- adrenoceptors expression, β1-adrenoceptors are widely distributed over all sensorimotor system related brain regions at a relatively low expression level [78–80]. β1-adrenoceptors show no distinct regional specificity, but layer specificity in adult M1 and S1 cortex, where the receptor expression is most abundant in layers II/III [80].

Similar to the expression patterns, the ontogeny of the different adrenoceptors is heterogeneous and depends on both receptor type and brain region. In rats distinct expression of α1-adrenoceptors in general starts at around birth [81, 82] and increases until expression reaches a peak after the 3rd postnatal week [83]. Subsequently, α1-adrenoceptor expression is reduced to moderate levels, which is typical for the adult brain. α2-adrenoceptors mRNA expression shows more sequential timelines of expression: whereas α2A-adrenoceptors are expressed prenatally in many brain regions, α2B and α2C-adrenoceptors are expressed only after birth [77, 84, 85]. α2A-adrenoceptors are strongly expressed until P1 in sensorimotor related brainstem and thalamic nuclei [84] as well as in the cortex. Subsequently there is generally a reduction in mRNA expression, with the exception of the brainstem nuclei: after early postnatal reduction, expression is up-regulated again until it reaches a transient peak at around P7-P14 [84]. There also are several other brain regions which transiently express α2-adrenergic receptor mRNA, which is suggestive of specific roles of these receptors in brain development [74]. In contrast to α2A- adrenoceptors, α2 C adrenoceptors appear in the early postnatal phase and α2B after the first postnatal week [74, 77, 85]. Similar to this, β1-adrenoceptor expression show a more postnatal development [86]. The receptor density increases sharply between postnatal days 10 and 21 and subsequently declines again after 6 weeks of age [87].

Sensorimotor-Centric View of the Serotonergic System

Serotonergic Innervation of the Sensorimotor System

The cerebral cortex is extensively innervated by serotonergic axons originating from a relatively small number of neurons located mainly in the median raphe nuclei (MRN) and the mesencephalic dorsal raphe nuclei (DRN) [88–90]. The DRN is of particular relevance for the sensorimotor system. DRN neurons give rise to the dense serotonergic projections into the motor and somatosensory areas [91, 92].

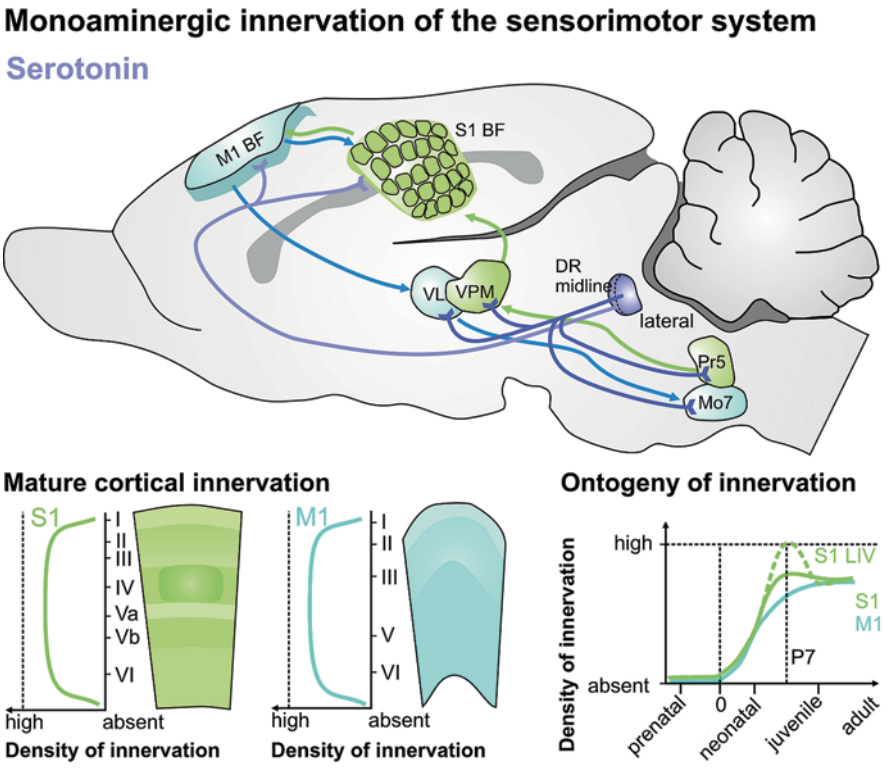

Fig. 11.3 Serotonergic innervation of the rodent sensorimotor system. Upper panel: Simplified overview of major afferent and efferent pathways and structures of the sensorimotor system and the main origins and projections of the serotonergic system (*dark blue*) targeting the sensorimotor system. The afferent projections and main processing structures of the lemniscal somatosensory pathway within the central nervous system are given in green, the efferent motor related projections in blue. Lower left panels: Relative layer specific density of serotonergic innervation of the primary somatosensory (*S1, green*) and primary motor cortex (*M1, blue*) in the mature rodent brain. The dark shaded area in layer IV of the *S1* represents a barrel structure. Lower right panel: Ontogeny of serotonergic innervation of the *S1* (*green*) and *M1* (*blue*), representing changes in the relative density of innervation between prenatal and adult state. *Pr5* principal trigeminal nucleus in the brainstem; *VPM* ventroposteromedial nucleus of the thalamus; *S1 BF* barrel field of the primary somatosensory cortex; *M1 BF* barrel field associated primary motor cortex, *VL* ventrolateral nucleus of the thalamus; *Mo7* facial motor nuclei of the brainstem; *DR* dorsal raphe nucleus

In the mature brain projections from DRN neurons are region, layer and target cell specific [93] and depend on the subdivisions of the DRN in which they are located [94, 96].

Serotonergic neurons in the midline subdivision of the DRN densely project *ipsilaterally* into both S1 and M1 [94] (Fig. 11.3) whereas neurons of the lateral wing of the DRN were found to innervate Pr5 in the brainstem and VPM as well as VL in the thalamus. Furthermore, serotonergic axon collaterals of the lateral wing of the DRN target mainly *contralaterally* the facial motor nuclei (Mo7) in the brainstem [94].

The divergence of the axonal projections of DRN neurons implies subdivision specific functional roles of 5-HT modulation [33, 95]: The projections of DRN neurons of the lateral wing into the sensorimotor brainstem nuclei suggest a role of 5-HT in modulating the integration of somatosensory and motor functions at the medullary and thalamic level. The projections of DRN neurons in the midline division of the DRN suggest a modulating role in signal processing and signal propagation within and across the cortical sensorimotor networks.

Whereas the different subdivision specific projections in the mature brain imply different modulatory functions of 5-HT in the sensorimotor system, the ontogeny of the serotonergic system indicates that 5-HT also plays a role during brain development and maturation. In the mature brain the distribution of serotonergic fibers in the cortex is relatively uniform across the different layers [96] (Fig. 11.3), however during brain development the innervation pattern and number of collaterals undergo partially transient, partially progressive changes.

In rodents, at around embryonic day (E) 11–15, serotonergic neurons start to be generated in the raphe nuclei [31, 62, 96], and they subsequently grow projections into the various brain regions. Similar to the noradrenergic system, when reaching the cortex, serotonergic axons enter in the vicinity of the cortical plate [96]. From there, during corticogenesis, serotonergic axon collaterals grow into all layers of the developing cortex following the inside-out sequence. Consequently, the serotonergic innervation parallels the development of intracortical neural connectivity [97]. After birth, the density of serotonergic axon arborisation in the cortex and number of synapse onto cortical neurons increases continuously, until by the end of the 3 rd week the distribution pattern of innervation becomes characteristic for the mature cortex (Fig. 11.3). Whereas during development in M1 the distribution pattern of serotonergic axons remains relatively uniform across the different layers, S1 displays a transient, layer specific 5-HT hyperinnervation [97–99] (Fig. 11.3). In the early stages of postnatal development of rats the serotonergic axons form dense clusters in S1 layer IV, which correspond to the barrel structures. After reaching a peak at around P7, by the end of the second postnatal week the density of the serotonergic axons gets distinctively reduced, while throughout the cerebral cortex the progressive increase in density of the serotonergic innervation becomes more and more apparent. This transient region and layer specific hyperinnervation by serotonergic neurons of the DRN, which coincides with the critical period of cortical network formation in S1, already indicates that within the sensorimotor system 5-HT is of particular importance for the development and maturation of the somatosensory system.

Serotonin Receptor Expression in the Sensorimotor System

The 5-HT receptor family consists of at least 15 receptor subtypes [100]. However, of particular interest for the sensorimotor system are postsynaptic 5-HT1A, 5-HT1B, 5-HT2A and 5-HT3 receptors.

5-HT1A receptors can be found as auto- and heteroreceptors. As autoreceptors they are typically expressed on cell bodies of DRN, where they mediate a reduction in the firing rate [101–104] associated with a reduction of 5-HT release.

As heteroreceptors they can induce presynaptic inhibition in intracortical glutamatergic terminals [105, 106] and modulate neuronal firing by increasing potassium conductance [107, 108]. Heteroreceptors are expressed in pyramidal neurons and interneurons mainly of the deeper layers V to VI of S1 and M1 [109–114]. In the sensorimotor related brainstem nuclei and the thalamus only low expression levels have been reported [109, 112]. Similar to 5-HT1A receptors, also 5-HT1B receptors can act as both auto- and heteroreceptors. Autoreceptors can mediate a 5-HT inhibition of 5-HT release in various territories of 5-HT innervation [101, 104, 115]. As heteroreceptors, they induce presynaptic inhibition of neurotransmitter release, including acetylcholine [116, 117], glutamate [118], and GABA [119]. Both, autoreceptors as well as heteroreceptors in the adult brain are mainly expressed at axon preterminals [103]. In the mature rat sensorimotor system 5-HT1B heteroreceptors are expressed with moderate density in the deeper layers IV to VI of S1 and M1 whereas at this age these heteroreceptors are almost absent within sensorimotor related nuclei of the thalamus and the brain stem [112]. However, in young rats (P8) 5HT1A heteroreceptors are also densely expressed in layer IV of S1. These receptors are not expressed in cortical neurons but on the terminals of thalamocortical axons originating from neurons in the VPM [120, 121]. The ontogeny of this particular transient expression is described in detail below.

5HT1 receptors in general start to be expressed in S1 and M1 after the first postnatal week and reach mature expression density after 3 weeks [122]. However, on layer specific level the changes are more complex: in both cortical areas in the 1st postnatal week 5-HT1 receptors are almost uniformly expressed across the cortical layers. Subsequently, the relative expression density in the middle layers (layer IV in S1, lower layer III in M1) decreases whereas the relative expression in layer V increases, creating a more bi-laminar distribution pattern with the prevalence of layer V expression typical for the adult cortex [122]. The reduction of general 5-HT1 expression density in S1 layer IV might be explained with a dramatic change in 5-HT1B receptor expression: 5-HT1B receptors are transiently expressed by thalamocortical projection most densely into S1 layer IV. However the expression of these 5-HT1B heteroreceptors disappears after the second week of life [120, 121, 123, 124].

In respect to the transient expression profile of 5-HT1B in S1 one also has to consider the transient co-expression of the 5-HT specific transporter (SERT; [120, 125, 126]). The level of extracellular 5-HT is tightly controlled by SERT activity. At mid-gestation (E11 in mice) expression of the SERT gene begins in the 5-HT neurons of the raphe nuclei, but expression soon transiently extends to non-serotonergic neurons, including the principal projection neurons of the VPM most extensively targeting S1 layer IV. The SERT expression in glutamatergic VPM axon terminals ends rapidly during the 2nd post-natal week, coinciding with the changes in 5-HT1B receptor expression and with the critical phase of maturation of S1 [27, 83, 127]. The timing of this transient co-expression of SERT and 5-HT1B receptor indicates the important role of 5-HT level regulation and 5-HT2B receptor activation

on glutamate release at thalamocortical synapses in layer IV of the developing S1 [120, 125–128].

Activation of 5-HT2A receptors has been shown to induce depolarization and a reduced potassium conductance [129, 130]. In juvenile and adult S1 and M1 these receptors are expressed most prominently in individual deeper layer cortical pyramidal and interneurons [111, 112, 114, 131–133] and, more widespread but less densely, in cells of S1 layer IV [111]. The morphology of the neurons that express 5-HT2 receptors indicates a prevalence of non-pyramidal GABAergic cells [111, 134, 135]. Compared to the cortical areas, expression in sensorimotor related thalamic and brainstem nuclei is generally absent or at best weak only [111–113, 136, 137]. 5-HT2A expression in the sensorimotor related cortical areas of rats starts in the early postnatal phase at around P0–7. In the second postnatal week the density of receptor expression generally increases until it develops a transient hyperexpression at around P14-20 [138]. Thereafter, as for the expression of other types of 5-HT receptor, 5-HT2A receptor density drops until after 1 month one finds the mature expression pattern and density, which is sparse in the adult sensorimotor cortex areas [111, 113, 135, 138].

Ligand gated 5-HT3 ion-channels are particularly important for neuromodulation along the sensorimotor circuits [100]. In S1 and M1 they are expressed on subpopulations of cortical GABAergic interneurons, mainly in superficial layers I- III but also in deeper layer V [139]. In these interneurons they are thought to induce fast excitation [107, 140] by which they can mediate inhibition of pyramidal neuron activity. Furthermore, 5-HT3 receptors are very densely expressed in both the somatosensory and motor related brainstem nucleus Sp5 and Mo7 [140–144]. In the thalamus 5-HT3 receptor expression is, if detectable at all, generally very low [145, 146].

Information about the ontogeny of 5-HT3 receptor expression is relatively sparse, but the temporal profile of mRNA expression in various brain regions indicates that 5-HT3 is an early manifestation of the serotonergic phenotype [147, 148]. Transcripts of mRNA are detectable in the subventricular zone as early as at E14.5. From this zone, neurons migrate to the cortical plate, where the respective mRNA transcripts are detectable at E16.5. At birth, mRNA is present in the superficial cortical layers. The early developmental onset and spatiotemporal profile of 5-HT3 receptor transcription supports the notion that 5-HT3 might play a role in proliferation, differentiation and migration of neurons in the central nervous system [148].

Sensorimotor Circuit (Mal)Formations After Targeted Manipulation of Neuromodulation During Development—the Case for Serotonin

Studies on the neuroanatomical consequences of early-life perturbations of monoaminergic systems have been primarily concentrated on 5-HT which allows a comprehensive overview about the link between the development and function of the rodent serotonergic system and the sensorimotor system.

Anatomical Changes in Sensorimotor Pathways and Local Networks

The 5-HT is the first monoaminergic system to develop in the brain. At mid-gestation (E11 in mice) expression of the SERT gene begins in the 5-HT neurons of the raphe nuclei, but expression soon extends to non-serotonergic neurons, including the principal projection neurons of the sensory systems (thalamus, retina, somatosensory cortex), the corticolimbic pathways (hippocampus (E14–E15), and the prefrontal/cingulate cortex (P0). SERT expression in non-serotonergic neurons ends rapidly during the second post-natal week, coinciding with the maturation of the barrel cortex [149]. This strongly suggests that 5-HT has a modulatory role in the development of the barrel cortex. The serotonergic innervation of the barrel cortex is provided by the DRN, as electrical stimulation of area enhanced the responsiveness of barrel cortex neurons to principal whisker deflection [150]. Further evidence for a modulatory role of 5-HT is provided by the finding that neonatal depletion of 5-HT with selective neurotoxins cause a delay in the formation of the barrel field [151], and isocaloric malnutrition (decreasing serotonin levels by 50 %) delayed the development of barrels with two days [152]. A delay in the formation of the barrel cortex is also seen when 5-HT levels are increased during the first postnatal week, either through knockout (KO) of SERT (decreased removal of 5-HT from the synaptic cleft) or MAOA (decreased 5-HT breakdown). Both types of KO in mice lead to a lack of barrels due to disrupted clustering and segregation of the thalamocortical fibers [153–156]. In SERT KO rats, however, barrels are smaller in size but are clearly visible [157]. When glucose utilization was measured in the barrel cortex, SERT KO mice showed a decrease in glucose utilization in the barrel cortex, as measured by 2-deoxy[14 C]glucose uptake during unilateral whisker stimulation in awake mice. Hence, also in SERT KO mice the barrels are not completely lost as the anatomical studies suggested. This effect in SERT KO mice was restored by lowering 5-HT levels using the selective tryptophan hydroxylase inhibitor p-chlorophenylalanine at P0 and P1 [158]. Furthermore, it was shown using [14 C]-iodoantipyrine mapping that fear conditioning, a process during which the animals learn an association between environmental stimuli and foot shocks, reduced regional blood flow in the somatosensory cortex in SERT KO mice. This is also indicative for reduced somatosensory function in mice characterized by high developmental 5-HT levels [159].

Whereas MAOA is not selective for 5-HT reuptake, and increases 5-HT, DA and NE levels, it was found that pharmacological inhibition of 5-HT synthesis, but not catecholamine synthesis, restored the normal barrel patterns in MAOA knockout mice [160]. Furthermore, double KO of MAOA and VMAT2 (the transporter responsible for the packaging of neurotransmitter in vesicles), resulted in a selective increase in 5-HT levels but profoundly reduced DA and NE levels. In addition, the MAOA/Vmat2 double KO was associated with a failure of thalamocortical axons and granular neurons to form barrels, like in single MAOA knockout mice [161]. Chen and coworkers [162] were able to rescue the barrel less phenotypes using forebrain-specific MAOA transgenic mice. These animals carried the human MAOA

transgene, and exhibited lower levels of 5-HT, NE and DA in the forebrain compared to MAOA KO mice. Another study employed clorgyline, a MAOA inhibitor also increasing 5-HT levels. Clorgyline treatment from P0 to P7 disrupted the formation of barrels of mice. Most severe effects were obtained during treatment at P0 to P4, suggesting this period as most sensitive to the developmental effects of 5-HT [163]. In line, Kesterson and coworkers [164] showed that clorgyline treatment from P0 to P6 delayed the organization of the thalamocortical afferents. In another study employing clorgyline treatment at P0 to P6 it was found that the percentage of posteromedial barrel subfield (PMBSF) in the barrel cortex was significantly increased compared to control treatment in a dose dependent manner, and as a result barrels were completely fused [165]. This fusion of barrels matches well with the barrel pattern observed in SERT KO rats [157]. MAOA KO not only affects barrel cortex formation, but also cortico-cortical innervation, as was elucidated by visualization of zinc-containing axon terminals, which are known to originate from the somatosensory cortex. In MAOA KO mice the zinc staining did not reveal signs of barrel compartmentalization. Yet, the laminar pattern of zinc staining in the somatosensory cortex matured faster in MAOA KO (P8) than in wild-type (P12) rats [166].

5-HT exerts its neurotrophic actions through 5-HT receptors and their downstream signaling pathways. Almost all 5-HT receptors have been, in one way or another, implicated in the developmental functions of 5-HT, which include control of proliferation, migration, cell death, and synaptogenesis [27]. For instance, the growth of thalamocortical neurons is under the control of the serotonin receptor 1B (5HT1B; [156] and SERT [167], which are both transiently expressed in the somatosensory (barrel) during early postnatal life [168]). Activation of the 5HT1B receptor leads to a depression of the presynaptic release of glutamate, which on its turn leads to a decrease in the synchronization of the coordination of axon and dendrite development (see also section III-ii). The 5-HT1B receptor does so by modulating cAMP production. Downstream protein kinase A (PKA)-mediated signals are involved in the response of axons to attractive guidance factors, such as netrins [169], or to repellent molecules, such as ephrins [170]. In primary cultures of thalamocortical neurons it was found that 5-HT increased neurite outgrowth, and that these effects were mimicked by a 5-HT1B receptor agonist [171]. Furthermore, single axon reconstructions of the thalamocortical neurons revealed that the 5-HT1B receptor influenced the production and retraction of collateral axon branches on thalamic axons [167]. In nutritionally restricted rats with delayed development of thalamocortical fibers SERT immunoreactivity was decreased, and 5-HT1B receptor availability increased [172]. The effect of MAOA and SERT may also be mediated via the 5-HT1B receptor, since simultaneous MAOA and 5-HT1B receptor, as well as SERT and 5-HT1B receptor, knockout rescued the barrelless phenotype as observed in the single MAOA and 5-HT1B knockout mice [156, 167]. Because 5-HT1B binding in the barrel cortex is evident between P4 and P16, it may be that 5-HT1B receptors regulate peripherally-induced activity of thalamocortical axons [168].

Besides the involvement of the 5-HT1B receptors, the 5-HT3 receptor, an ion channel, may be involved in the development of thalamocortical fibers as well. It has been shown that in utero increases in 5-HT through SSRI (selective serotonin

reuptake inhibitor) treatment decreased the dendritic complexity of cortical layer 2/3 neurons, an effect that could be prevented by 5-HT3 receptor antagonism and 5-HT3 knockout in mice [173]. 5-HT3 receptors are located at Cajal-Retzius neurons in cortical layer 1 and there can trigger the release of the glycoprotein reelin, which mediates the outgrowth of neurons. Finally, 5-HT may exert its effects trough the BDNF (brain-derived neurotrophic factor) system, since double MAOA and TrkB (BDNF receptor) KO mice exhibited more severe barrel cortex phenotypes than single MAOA knockout mice [174].

Sensory Information Encoding During (or in the Absence of) Monoaminergic Neuromodulation

Besides that 5-HT influences the neuroanatomy of the barrel cortex, the monoamine also affects the physiological properties of the barrel cortex. It has been shown that in thalamocortical slices of P5-P9 mice 5-HT reduces monosynaptic EPSCs evoked by low frequency internal capsule stimulation and relieves the short-term depression of EPSCs evoked by high-frequency stimulation. Furthermore, 5-HT was found to reduce the presynaptic release of glutamate, based on the observation that 5-HT similarly reduced the AMPA-kainate and NMDA components and the paired pulse depression of thalamocortical EPSCs. These effects were mediated by the 5-HT1B receptor, because these effects of 5-HT could be mimicked by a 5-HT1B agonist. Furthermore, 5-HT had no effect in 5-HT1B KO mice. These data show that in the developing barrel cortex the 5-HT1B exerts activity-dependent regulation of thalamocortical EPSCs [123]. The role of 5-HT in the functioning of the barrel cortex has been further examined using visual deprivation, which is based on the concept that adaption to sensory deprivation in one modality (e.g., visual cortex) increases plasticity and retuning neuronal circuits in other remaining modalities. It was found that visual deprivation led to increases in extracellular 5-HT levels in the barrel cortex. Thereby, 5-HT facilitated the delivery of the AMPA receptor subunit GluA1 into layer 4−2/3 synapses. This resulted in synaptic strengthening and a sharpening of the functional whisker-barrel map; the relative response of surrounding whiskers to the response evoked by stimulation of the principal whiskers was lower in rats exposed to visual deprivation than in control rats.

Behavioral Consequences of Arrested Sensorimotor Circuit Development

At the behavioral level SERT KO mice show decreased whisker function, as measured in the gap-crossing task. In this task the animals have to cross a gap between two platforms, and use their whiskers to sense the platform across the gap [159]. SERT KO mice and rats also show exploratory changes in the open field and reduced social interactions, including decreased play and aggression [175–177],

which may be related to reduced whisker function as well. MAOA KO mice also show altered exploratory behavior, and this could be rescued by controlling 5-HT levels during early postnatal life [156]. Since MAOA KO leads to a barrelless phenotype, this finding implies that there is a direct relationship between exploratory behavior, whisker function and neuroanatomical features of the barrel cortex.

Outlook: Role of Sensorimotor Circuit Deficits in Brain Disorders

Serotonin

Monoaminergic changes during early life development do not only experimentally reveal the mechanisms of cortical development, but can also lead to symptoms of brain disorders. SSRIs are among the most frequently prescribed drugs for the treatment of depression and anxiety-related disorders. SERT inhibition by SSRIs leads to an accumulation of 5-HT in the extracellular space. Because SSRIs have proven to be safe in adults, SSRIs are the drugs of choice for treating depressed pregnant and postpartum women [178]. Yet, as most SSRIs reach the fetus via the placenta [179] and are detectable in breast milk and breast-fed infants [180], a significant number of unborn and newborn children are exposed to SSRIs during critical phases of neurodevelopment. Amongst others, perinatal administration of SSRIs is associated with blunted somatosensory responses in children [181], which may point towards functional changes in the somatosensory cortex. Furthermore, it has been demonstrated that prenatal exposure to SSRIs leads a decrease in head circumference of unborns [182]—which is possibly indicative for decreased development - and autism-like symptoms in children, particularly in those that were exposed to SSRIs during the first trimester of pregnancy [183]. Since autism is associated with distortions in sensory information processing [184], prenatal SSRI exposure in humans may affect the development of the somatosensory cortex.

Rodent studies revealed more detailed effects of prenatal SSRI exposure on development of the somatosensory cortex. For instance, chronic paroxetine treatment in rat pups at P0 to P8 resulted in partial disruption of the organization of thalamocortical fibers in barrel fields [185]. Furthermore, Lee [186] showed that SSRI treatment at P0 to P6 in rats lead to sensorimotor learning deficits in the gap-crossing test. This was associated with thinned out terminal clusters of TCAs in layer IV barrels and altered dendritic organization of the spiny stellate neurons, the dominant population of excitatory neurons in the barrels. Strikingly, these behavioral and structural alterations may resemble those seen in SERT KO rats [127]. Furthermore, prenatal SSRI exposure and SERT KO are both associated with decreased social interactions [177, 187–190], which thus link to the finding in humans that prenatal SSRI exposure leads to autism-related symptoms [183]. In other words, there is emerging evidence that both prenatal or early postnatal SSRI treatment (in ro-

dents corresponding to the last trimester of pregnancy) lead to neurodevelopmental changes that point towards autism-like behavioral outcomes [191]. Since autism is characterized by hyperserotoneamia [192], increased 5-HT immunoreactive axons [193] and alterations in SERT binding [194], and animal models of autism show changes in the outgrowth of serotonergic neurons as well as alterations in SERT function [195], it is tempting to speculate that early life increases in 5-HT levels sets up the development of the somatosensory cortices and other brain circuits that are manifested as autism-like symptoms. However, more research is needed to evaluate whether the effects of prenatal SSRI exposure, SERT KO and autism on development of the somatosensory cortex are similar. For instance, whereas SERT KO rodents model the human SERT polymorphism (5-HTTLPR; [196]), evidence for an association between the 5-HTTLPR and autism is weak [197]. Furthermore, desensitization of the 5-HT1A receptor is found in SERT KO rodents [198], but not in mice treated with SSRIs as neonates [199], whereas the 5-HT1A receptor is hypersensitive in the SERT Ala56 mutant mouse model for autism [195]. To what extent there are similarities between SERT KO and prenatal SSRI exposure in rats regarding barrel cortex function and structure is currently under investigation.

Dopamine

Parkinson's disease (PD) is a neurodegenerative disorder that is characterized by asymmetric onset of resting tremor, rigidity, and bradykinesia in the limbs followed by postural instability. Other clinical manifestations, include sensory symptoms (eg, pain and tingling), hyposmia, sleep alterations, depression and anxiety, and abnormal executive, working memory-related functions [200]. The hallmark of PD pathology is the loss of the dopaminergic neurons in the SN and their terminals in the striatum, which results in striatal dopamine deficiency [201]. It has been estimated that classical PD symptoms appear when 80 % of striatal dopamine and 50 % of the nigra compacta cells have been lost. Since sensorimotor dysfunction is considered to mark the initial stages of PD, reduced dopamine input to cortical and subcortical brain structures, particularly those in the sensorimotor network, has been proposed as one of the hallmarks of Parkinson's disease (PD). Of interest therefore is the recent observation that PD patients show structural and functional deficits in sensorimotor connections. Specifically, using diffusion-weighted magnetic resonance imaging and resting-state functional MRI, cortical-subcortical connections of the sensorimotor cortex with the putamen and thalamus were found to be reduced compared with associative and limbic connections to these regions [202]. These observations strengthen the general idea that reduced dopamine contribute to sensorimotor dysfunction in PD patients.

Attention-deficit/hyperactivity disorder (ADHD) is another neurodevelopmental disorder that is common in children and is characterized by developmentally inappropriate, persistent and impairing levels of inattention, impulsiveness and hyperactivity. The most prominent theory for ADHD's neurological mechanism is the DA hypothesis. It is based on the malfunctioning or decreased functioning of the

D4 and D2 receptors and DAT, causing abnormally low levels of DA in the brain [203]. Current treatments are geared towards increasing DA levels by means of psychostimulants, which exerts short-term therapeutic effects. Beside hypereactivity and inattention, ADHD is also associated with sensorimotor deficits and altered neural processing of somatosensory stimuli, including impaired discrimination of light touch and temperature, weakened intensity processing and atypical pain processing [204–206]. Of interest, a recent study showed increased thickness in the primary somatosensory cortex (SI) in adults but not in adolescents of ADHD patients, suggesting that sensorimotor brain regions are altered in ADHD [207]. Whether the structural changes in the sensory cortex are directly related to the impaired motor and somatosensory function in these individuals and whether they are caused by altered dopamine levels during development has further to be investigated.

References

1. Brecht M, Preilowski B, Merzenich MM (1997) Functional architecture of the mystacial vibrissae. Behav Brain Res 84:81–97
2. Deschenes M, Moore J, Kleinfeld D (2012) Sniffing and whisking in rodents. Curr Opin Neurobiol 22:243–250
3. Hartmann MJ (2011) A night in the life of a rat: vibrissal mechanics and tactile exploration. Ann N Y Acad Sci 1225:110–118
4. Polley DB, Kvasnak E, Frostig RD (2004) Naturalistic experience transforms sensory maps in the adult cortex of caged animals. Nature 429:67–71
5. Mehta SB, Whitmer D, Figueroa R, Williams BA, Kleinfeld D (2007) Active spatial perception in the vibrissa scanning sensorimotor system. PLoS Biol 5:e15
6. O'Connor DH, Peron SP, Huber D, Svoboda K (2010) Neural activity in barrel cortex underlying vibrissa-based object localization in mice. Neuron 67:1048–1061
7. Shuler MG, Krupa DJ, Nicolelis MA (2001) Bilateral integration of whisker information in the primary somatosensory cortex of rats. J Neurosci 21:5251–5261
8. Voigts J, Sakmann B, Celikel T (2008) Unsupervised whisker tracking in unrestrained behaving animals. J Neurophysiol 100:504–515
9. Adibi M, Diamond ME, Arabzadeh E (2012) Behavioral study of whisker-mediated vibration sensation in rats. Proc Natl Acad Sci U S A 109:971–976
10. Maricich SM, Morrison KM, Mathes EL, Brewer BM (2012) Rodents rely on merkel cells for texture discrimination tasks. J Neurosci 32:3296–3300
11. Ritt JT, Andermann ML, Moore CI (2008) Embodied information processing: vibrissa mechanics and texture features shape micromotions in actively sensing rats. Neuron 57:599–613
12. Wu HP, Ioffe JC, Iverson MM, Boon JM, Dyck RH (2013) Novel, whisker-dependent texture discrimination task for mice. Behav Brain Res 237:238–242
13. Berg RW, Whitmer D, Kleinfeld D (2006) Exploratory whisking by rat is not phase locked to the hippocampal theta rhythm. J Neurosci 26:6518–6522
14. Kleinfeld D, Deschenes M (2011) Neuronal basis for object location in the vibrissa scanning sensorimotor system. Neuron 72:455–468
15. Carvell GE, Simons DJ (1990) Biometric analyses of vibrissal tactile discrimination in the rat. J Neurosci 10:2638–2648
16. Ganguly K, Kleinfeld D (2004) Goal-directed whisking increases phase-locking between vibrissa movement and electrical activity in primary sensory cortex in rat. Proc Natl Acad Sci U S A 101:12348–12353
17. Hattox AM, Priest CA, Keller A (2002) Functional circuitry involved in the regulation of whisker movements. J Comp Neurol 442:266–276

18. Hemelt ME, Keller A (2008) Superior colliculus control of vibrissa movements. J Neurophysiol 100:1245–1254
19. Kleinfeld D, Berg RW, O'Connor SM (1999) Anatomical loops and their electrical dynamics in relation to whisking by rat. Somatosens Mot Res 16:69–88
20. Mitchinson B, Martin CJ, Grant RA, Prescott TJ (2007) Feedback control in active sensing: rat exploratory whisking is modulated by environmental contact. Proc Biol Sci 274:1035–1041
21. Sachdev RN, Berg RW, Champney G, Kleinfeld D, Ebner FF (2003) Unilateral vibrissa contact: changes in amplitude but not timing of rhythmic whisking. Somatosens Mot Res 20:163–169
22. Wolf ME, Roth RH (1987) Dopamine neurons projecting to the medial prefrontal cortex possess release-modulating autoreceptors. Neuropharmacology 26:1053–1059
23. Callier S, Snapyan M, Crom S L, Prou D, Vincent JD, Vernier P (2003) Evolution and cell biology of dopamine receptors in vertebrates. Biol Cell 95:489–502
24. Molinoff PB, Nelson DL, Orcutt JC (1974) Dopamine-beta-hydroxylase and the regulation of the noradrenergic neuron. Adv Biochem Psychopharmacol 12:95–104
25. Joels M, Fernandez G, Roozendaal B (2011) Stress and emotional memory: a matter of timing. Trends Cogn Sci 15:280–288
26. Dharmshaktu P, Tayal V, Kalra BS (2012) Efficacy of antidepressants as analgesics: a review. J Clin Pharmacol 52:6–17
27. Gaspar P, Cases O, Maroteaux L (2003) The developmental role of serotonin: news from mouse molecular genetics. Nat Rev Neurosci 4:1002–1012
28. Kriegebaum C, Gutknecht L, Schmitt A, Lesch KP, Reif A (2010) Serotonin now: part 1. Neurobiology and developmental genetics. Fortschr Neurol Psychiatr 78:319–331
29. Tavoulari S, Forrest LR, Rudnick G (2009) Fluoxetine (Prozac) binding to serotonin transporter is modulated by chloride and conformational changes. J Neurosci 29:9635–9643
30. Lauder JM (1993) Neurotransmitters as growth regulatory signals: role of receptors and second messengers. Trends Neurosci 16:233–240
31. Wallace JA, Lauder JM (1983) Development of the serotonergic system in the rat embryo: an immunocytochemical study. Brain Res Bull 10:459–479
32. Parnavelas JG, Papadopoulos GC (1989) The monoaminergic innervation of the cerebral cortex is not diffuse and nonspecific. Trends Neurosci 12:315–319
33. Kirifides ML, Simpson KL, Lin RC, Waterhouse BD (2001) Topographic organization and neurochemical identity of dorsal raphe neurons that project to the trigeminal somatosensory pathway in the rat. J Comp Neurol 435:325–340
34. Simpson KL, Altman DW, Wang L, Kirifides ML, Lin RC, Waterhouse BD (1997) Lateralization and functional organization of the locus coeruleus projection to the trigeminal somatosensory pathway in rat. J Comp Neurol 385:135–147
35. Berger B, Verney C, Alvarez C, Vigny A, Helle KB (1985) New dopaminergic terminal fields in the motor, visual (area 18b) and retrosplenial cortex in the young and adult rat. Immunocytochemical and catecholamine histochemical analyses. Neuroscience 15:983–998
36. Papadopoulos GC, Parnavelas JG (1991) Monoamine systems in the cerebral cortex: evidence for anatomical specificity. Prog Neurobiol 36:195–200
37. Smythies J (2005) Section II. The dopamine system. Int Rev Neurobiol 64:123–172
38. Berger B, Thierry AM, Tassin JP, Moyne MA (1976) Dopaminergic innervation of the rat prefrontal cortex: a fluorescence histochemical study. Brain Res 106:133–145
39. Lindvall O, Bjorklund A, Moore RY, Stenevi U (1974) Mesencephalic dopamine neurons projecting to neocortex. Brain Res 81:325–331
40. Descarries L, Lemay B, Doucet G, Berger B (1987) Regional and laminar density of the dopamine innervation in adult rat cerebral cortex. Neuroscience 21:807–824
41. Doucet G, Descarries L, Audet MA, Garcia S, Berger B (1988) Radioautographic method for quantifying regional monoamine innervations in the rat brain. Application to the cerebral cortex. Brain Res 441:233–259
42. Berger B, Gaspar P, Verney C (1991) Dopaminergic innervation of the cerebral cortex: unexpected differences between rodents and primates. Trends Neurosci 14:21–27

43. Verney C, Grzanna R, Farkas E (1982) Distribution of dopamine-beta-hydroxylase-like immunoreactive fibers in the rat cerebellar cortex during ontogeny. Dev Neurosci 5:369–374
44. Seguela P, Watkins KC, Descarries L (1988) Ultrastructural features of dopamine axon terminals in the anteromedial and the suprarhinal cortex of adult rat. Brain Res 442:11–22
45. Garcia-Cabezas MA, Martinez-Sanchez P, Sanchez-Gonzalez MA, Garzon M, Cavada C (2009) Dopamine innervation in the thalamus: monkey versus rat. Cereb Cortex 19:424–434
46. Alexander GE, DeLong MR, Strick PL (1986) Parallel organization of functionally segregated circuits linking basal ganglia and cortex. Annu Rev Neurosci 9:357–381
47. Civelli O, Bunzow JR, Grandy DK (1993) Molecular diversity of the dopamine receptors. Annu Rev Pharmacol Toxicol 33:281–307
48. Savasta M, Dubois A, Scatton B (1986) Autoradiographic localization of D1 dopamine receptors in the rat brain with [3H]SCH 23390. Brain Res 375:291–301
49. Boyson SJ, McGonigle P, Molinoff PB (1986) Quantitative autoradiographic localization of the D1 and D2 subtypes of dopamine receptors in rat brain. J Neurosci 6:3177–3188
50. Ariano MA, Sibley DR (1994) Dopamine receptor distribution in the rat CNS: elucidation using anti-peptide antisera directed against D1A and D3 subtypes. Brain Res 649:95–110
51. Gaspar P, Bloch B, Le Moine C (1995) D1 and D2 receptor gene expression in the rat frontal cortex: cellular localization in different classes of efferent neurons. Eur J Neurosci 7:1050–1063
52. Wachtel SR, Hu XT, Galloway MP, White FJ (1989) D1 dopamine receptor stimulation enables the postsynaptic, but not autoreceptor, effects of D2 dopamine agonists in nigrostriatal and mesoaccumbens dopamine systems. Synapse 4:327–346
53. Lidow MS, Goldman-Rakic PS, Gallager DW, Geschwind DH, Rakic P (1989a) Distribution of major neurotransmitter receptors in the motor and somatosensory cortex of the rhesus monkey. Neuroscience 32:609–627
54. Lidow MS, Goldman-Rakic PS, Rakic P, Innis RB (1989b) Dopamine D2 receptors in the cerebral cortex: distribution and pharmacological characterization with [3H]raclopride. Proc Natl Acad Sci U S A 86:6412–6416
55. Ariano MA, Fisher RS, Smyk-Randall E, Sibley DR, Levine MS (1993) D2 dopamine receptor distribution in the rodent CNS using anti-peptide antisera. Brain Res 609:71–80
56. van der Weide J, Camps M, Horn AS, Palacios JM (1987) Autoradiographic localization of dopamine D2 receptors in the rat brain using the new agonist [3H]N-0437. Neurosci Lett 83:259–263
57. Gurevich EV, Joyce JN (2000) Dopamine D(3) receptor is selectively and transiently expressed in the developing whisker barrel cortex of the rat. J Comp Neurol 420:35–51
58. Berridge CW, Waterhouse BD (2003) The locus coeruleus-noradrenergic system: modulation of behavioral state and state-dependent cognitive processes. Brain Res Brain Res Rev 42:33–84
59. Lee SB, Beak SK, Park SH, Waterhouse BD, Lee HS (2009) Collateral projection from the locus coeruleus to whisker-related sensory and motor brain regions of the rat. J Comp Neurol 514:387–402
60. Levitt P, Moore RY (1978) Noradrenaline neuron innervation of the neocortex in the rat. Brain Res 139:219–231
61. Room P, Postema F, Korf J (1981) Divergent axon collaterals of rat locus coeruleus neurons: demonstration by a fluorescent double labeling technique. Brain Res 221:219–230
62. Lauder JM, Bloom FE (1974) Ontogeny of monoamine neurons in the locus coeruleus, raphe nuclei and substantia nigra of the rat. I. Cell differentiation. J Comp Neurol 155:469–481
63. Specht LA, Pickel VM, Joh TH, Reis DJ (1981) Light-microscopic immunocytochemical localization of tyrosine hydroxylase in prenatal rat brain. I. early ontogeny. J Comp Neurol 199:233–253
64. Levitt P, Moore RY (1979) Development of the noradrenergic innervation of neocortex. Brain Res 162:243–259
65. Blue ME, Molliver ME (1987) 6-Hydroxydopamine induces serotonergic axon sprouting in cerebral cortex of newborn rat. Brain Res 429:255–269

66. Naqui SZ, Harris BS, Thomaidou D, Parnavelas JG (1999) The noradrenergic system influences the fate of cajal-retzius cells in the developing cerebral cortex. Brain Res Dev Brain Res 113:75–82
67. Latsari M, Dori I, Antonopoulos J, Chiotelli M, Dinopoulos A (2002) Noradrenergic innervation of the developing and mature visual and motor cortex of the rat brain: a light and electron microscopic immunocytochemical analysis. J Comp Neurol 445:145–158
68. Agster KL, Mejias-Aponte CA, Clark BD, Waterhouse BD (2013) Evidence for a regional specificity in the density and distribution of noradrenergic varicosities in rat cortex. J Comp Neurol 521:2195–2207
69. Dodt HU, Pawelzik H, Zieglgansberger W (1991) Actions of noradrenaline on neocortical neurons in vitro. Brain Res 545:307–311
70. Foehring RC, Schwindt PC, Crill WE (1989) Norepinephrine selectively reduces slow Ca2+- and Na+-mediated K + currents in cat neocortical neurons. J Neurophysiol 61:245–256
71. Madison DV, Nicoll RA (1986) Actions of noradrenaline recorded intracellularly in rat hippocampal CA1 pyramidal neurones, in vitro. J Physiol 372:221–244
72. Lorenzon NM, Foehring RC (1993) The ontogeny of repetitive firing and its modulation by norepinephrine in rat neocortical neurons. Brain Res Dev Brain Res 73:213–223
73. Day HE, Campeau S, Watson SJ Jr, Akil H (1997) Distribution of alpha 1a-, alpha 1b- and alpha 1d-adrenergic receptor mRNA in the rat brain and spinal cord. J Chem Neuroanat 13:115–139
74. Happe HK, Coulter CL, Gerety ME, Sanders JD, O'Rourke M, Bylund DB, Murrin LC (2004) Alpha-2 adrenergic receptor development in rat CNS: an autoradiographic study. Neuroscience 123:167–178
75. McCune SK, Voigt MM, Hill JM (1993) Expression of multiple alpha adrenergic receptor subtype messenger RNAs in the adult rat brain. Neuroscience 57:143–151
76. Scheinin M, Lomasney JW, Hayden-Hixson DM, Schambra UB, Caron MG, Lefkowitz RJ, Fremeau RT Jr (1994) Distribution of alpha 2-adrenergic receptor subtype gene expression in rat brain. Brain Res Mol Brain Res 21:133–149
77. Winzer-Serhan UH, Leslie FM (1997) Alpha2B adrenoceptor mRNA expression during rat brain development. Brain Res Dev Brain Res 100:90–100
78. Cash R, Raisman R, Lanfumey L, Ploska A, Agid Y (1986) Cellular localization of adrenergic receptors in rat and human brain. Brain Res 370:127–135
79. Nicholas AP, Pieribone V, Hokfelt T (1993) Distributions of mRNAs for alpha-2 adrenergic receptor subtypes in rat brain: an in situ hybridization study. J Comp Neurol 328:575–594
80. Palacios J, Kuhar MJ (1982) Beta adrenergic receptor localization in rat brain by light microscopic autoradiography. Neurochem Int 4:473–490
81. Johansson B, Georgiev V, Fredholm BB (1997) Distribution and postnatal ontogeny of adenosine A2A receptors in rat brain: comparison with dopamine receptors. Neuroscience 80:1187–1207
82. Jones LS, Gauger LL, Davis JN, Slotkin TA, Bartolome JV (1985) Postnatal development of brain alpha1-adrenergic receptors: In vitro autoradiography with [125i]HEAT in normal rats and rats treated with alpha-difluoromethylornithine, a specific, irreversible inhibitor of ornithine decarboxylase. Neuroscience 15:1195–1202
83. Morris MJ, Dausse JP, Devynck MA, Meyer P (1980) Ontogeny of alpha 1 and alpha 2-adrenoceptors in rat brain. Brain Res 190:268–271
84. Winzer-Serhan UH, Raymon HK, Broide RS, Chen Y, Leslie FM (1997a) Expression of alpha 2 adrenoceptors during rat brain development–I. Alpha 2 A messenger RNA expression. Neuroscience 76:241–260
85. Winzer-Serhan UH, Raymon HK, Broide RS, Chen Y, Leslie FM (1997b) Expression of alpha 2 adrenoceptors during rat brain development–II. Alpha 2 C messenger RNA expression and [3H]rauwolscine binding. Neuroscience 76:261–272
86. Duman RS, Saito N, Tallman JF (1989) Development of beta-adrenergic receptor and G protein messenger RNA in rat brain. Brain Res Mol Brain Res 5:289–296

87. Pittman RN, Minneman KP, Molinoff PB (1980) Ontogeny of beta 1- and beta 2-adrenergic receptors in rat cerebellum and cerebral cortex. Brain Res 188:357–368
88. Moore RY, Halaris AE, Jones BE (1978) Serotonin neurons of the midbrain raphe: ascending projections. J Comp Neurol 180:417–438
89. Steinbusch HW, Nieuwenhuys R, Verhofstad AA, van der KD (1981) The nucleus raphe dorsalis of the rat and its projection upon the caudatoputamen. A combined cytoarchitectonic, immunohistochemical and retrograde transport study. J Physiol (Paris) 77:157–174
90. Steinbusch HW, Nieuwenhuys R (1981) Localization of serotonin-like immunoreactivity in the central nervous system and pituitary of the rat, with special references to the innervation of the hypothalamus. Adv Exp Med Biol 133:7–35
91. Azmitia EC, Segal M (1978) An autoradiographic analysis of the differential ascending projections of the dorsal and median raphe nuclei in the rat. J Comp Neurol 179:641–667
92. Waterhouse BD, Mihailoff GA, Baack JC, Woodward DJ (1986) Topographical distribution of dorsal and median raphe neurons projecting to motor, sensorimotor, and visual cortical areas in the rat. J Comp Neurol 249:460–481
93. Morrison JH, Foote SL, Bloom FE (1984). Regional, laminar developmental, and functional characteristics of noradrenaline and serotonin innervation patterns in monkey cortex. In: Descarries L, Reader TA, Jasper HH (eds) Monoamine innervation of cerebral cortex , Alan R. Liss, New York, pp 61–75
94. Lee SB, Lee HS, Waterhouse BD (2008) The collateral projection from the dorsal raphe nucleus to whisker-related, trigeminal sensory and facial motor systems in the rat. Brain Res 1214:11–22
95. Imai H, Steindler DA, Kitai ST (1986) The organization of divergent axonal projections from the midbrain raphe nuclei in the rat. J Comp Neurol 243:363–380
96. Lidov HG, Grzanna R, Molliver ME (1980) The serotonin innervation of the cerebral cortex in the rat–an immunohistochemical analysis. Neuroscience 5:207–227
97. Dori I, Dinopoulos A, Blue ME, Parnavelas JG (1996) Regional differences in the ontogeny of the serotonergic projection to the cerebral cortex. Exp Neurol 138:1–14
98. D'Amato RJ, Blue ME, Largent BL, Lynch DR, Ledbetter DJ, Molliver ME, Snyder SH (1987) Ontogeny of the serotonergic projection to rat neocortex: transient expression of a dense innervation to primary sensory areas. Proc Natl Acad Sci U S A 84:4322–4326
99. Fujimiya M, Kimura H, Maeda T (1986) Postnatal development of serotonin nerve fibers in the somatosensory cortex of mice studied by immunohistochemistry. J Comp Neurol 246:191–201
100. Hoyer D, Clarke DE, Fozard JR, Hartig PR, Martin GR, Mylecharane EJ, Saxena PR, Humphrey PPA (1994) International union of pharmacology classification of receptors for 5-hydroxytryptamine (serotonin). Pharmacol Rev 46:157–203
101. Davidson C, Stamford JA (1995) The effect of paroxetine on 5-Ht efflux in the rat dorsal raphe nucleus is potentiated by both 5-Ht1A and 5-Ht1B/D receptor antagonists. Neurosci Lett 188:41–44
102. Dong JM, deMontigny C, Blier P (1997) Effect of acute and repeated versus sustained administration of the 5-HT1A receptor agonist ipsapirone: electrophysiological studies in the rat hippocampus and dorsal raphe. Naunyn Schmiedebergs Arch Pharmacol 356:303–311
103. Riad N, Garcia S, Watkins KC, Jodoin N, Doucet E, Langlois X, Mestikawy S E, Hamon M, Descarries L (2000) Somatodendritic localization of 5-HT1A and preterminal axonal localization of 5-HT1B serotonin receptors in adult rat brain. J Comp Neurol 417:181–194
104. Sprouse JS, Aghajanian GK (1987) Electrophysiological responses of serotoninergic dorsal raphe neurons to 5-Ht1A and 5-Ht1B agonists. Synapse 1:3–9
105. Murakoshi T, Song SY, Konishi S, Tanabe T (2001) Multiple G-protein-coupled receptors mediate presynaptic inhibition at single excitatory synapses in the rat visual cortex. Neurosci Lett 309:117–120
106. Schmitz D, Gloveli T, Empson RM, Heinemann U (1999) Potent depression of stimulus evoked field potential responses in the medial entorhinal cortex by serotonin. Br J Pharmacol 128:248–254

107. Foehring RC, van Brederode JF, Kinney GA, Spain WJ (2002) Serotonergic modulation of supragranular neurons in rat sensorimotor cortex. J Neurosci 22:8238–8250
108. Schmitz D, Gloveli T, Empson RM, Draguhn A, Heinemann U (1998) Serotonin reduces synaptic excitation in the superficial medial entorhinal cortex of the rat via a presynaptic mechanism. J Physiol 508:119–129
109. Chalmers DT, Watson SJ (1991) Comparative anatomical distribution of 5-Ht1A receptor messenger-Rna and 5-Ht1A binding in rat-brain—a combined insitu hybridization invitro receptor autoradiographic study. Brain Res 561:51–60
110. Kia HK, Miquel MC, Brisorgueil MJ, Daval G, Riad M, ElMestikawy S, Hamon M, Verge D (1996) Immunocytochemical localization of serotonin(1 A) receptors in the rat central nervous system. J Comp Neurol 365:289–305
111. Morilak DA, Garlow SJ, Ciaranello RD (1993) Immunocytochemical localization and description of neurons expressing serotonin(2) Receptors in the rat-brain. Neuroscience 54:701–717
112. Pazos A, Palacios JM (1985) Quantitative autoradiographic mapping of serotonin receptors in the rat-brain.1. serotonin-1 receptors. Brain Res 346:205–230
113. Pompeiano M, Palacios JM, Mengod G (1992) Distribution and cellular-localization of messenger-Rna coding for 5-Ht1A receptor in the rat-brain—correlation with receptor-binding. J Neurosci 12:440–453
114. Zhou FM, Hablitz JJ (1999) Activation of serotonin receptors modulates synaptic transmission in rat cerebral cortex. J Neurophysiol 82:2989–2999
115. Hjorth S, Sharp T (1991) Effect of the 5-Ht1A receptor agonist 8-Oh-Dpat on the release of 5-Ht in dorsal and median raphe-innervated rat-brain regions as measured by invivo microdialysis. Life Sci 48:1779–1786
116. Bolanos-Jimenez F, dC M, Fillion G (1994) Effect of chronic antidepressant treatment on 5-HT1B presynaptic heteroreceptors inhibiting acetylcholine release. Neuropharmacology 33:77–81
117. Maura G, Roccatagliata E, Raiteri M (1986) Serotonin autoreceptor in rat hippocampus—pharmacological characterization as a subtype of the 5-Ht1 receptor. Naunyn Schmiedebergs Arch Pharmacol 334:323–326
118. Raiteri M, Maura G, Bonanno G, Pittaluga A (1986) Differential pharmacology and function of two 5-HT1 receptors modulating transmitter release in rat cerebellum. J Pharmacol Exp Ther 237:644–648
119. Johnson SW, Mercuri NB, North RA (1992) 5-Hydroxytryptamine(1B) receptors block the gaba(B) synaptic potential in rat dopamine neurons. J Neurosci 12:2000–2006
120. Bennett-Clarke CA, Leslie MJ, Chiaia NL, Rhoades RW (1993) Serotonin 1B receptors in the developing somatosensory and visual cortices are located on thalamocortical axons. Proc Natl Acad Sci U S A 90:153–157
121. Leslie MJ, Bennettclarke CA, Rhoades RW (1992) Serotonin-1B receptors form a transient vibrissa-related pattern in the primary somatosensory cortex of the developing rat. Dev Brain Res 69:143–148
122. Zilles K, Schleicher A, Glaser T, Traber J, Rath M (1985) The ontogenetic development of serotonin (5-Ht1) receptors in various cortical regions of the rat-brain. Anat Embryol 172:255–264
123. Laurent A, Goaillard JM, Cases O, Lebrand C, Gaspar P, Ropert N (2002) Activity-dependent presynaptic effect of serotonin 1B receptors on the somatosensory thalamocortical transmission in neonatal mice. J Neurosci 22:886–900
124. Rhoades RW, Bennett-Clarke CA, Shi MY, Mooney RD (1994) Effects of 5-HT on thalamocortical synaptic transmission in the developing rat. J Neurophysiol 72:2438–2450
125. Lebrand C, Cases O, Adelbrecht C, Doye A, Alvarez C, ElMestikawy S, Seif I, Gaspar P (1996) Transient uptake and storage of serotonin in developing thalamic neurons. Neuron 17:823–835

126. Hansson SR, Mezey E, Hoffman BJ (1998) Serotonin transporter messenger RNA in the developing rat brain: Early expression in serotonergic neurons and transient expression in non-serotonergic neurons. Neuroscience 83:1185–1201
127. Homberg JR, Schubert D, Gaspar P (2010) New perspectives on the neurodevelopmental effects of SSRIs. Trends Pharmacol Sci 31:60–65
128. van Kleef ES, Gaspar P, Bonnin A (2012) Insights into the complex influence of 5-HT signaling on thalamocortical axonal system development. Eur J Neurosci 35:1563–1572
129. Araneda R, Andrade R (1991) 5-hydroxytryptamine2 and 5-hydroxytryptamine1a receptors mediate opposing responses on membrane excitability in rat-association cortex. Neuroscience 40:399–412
130. Tanaka E, North RA (1993) actions of 5-hydroxytryptamine on neurons of the rat cingulate cortex. J Neurophysiol 69:1749–1757
131. Hamada S, Senzaki K, Hamaguchi-Hamada K, Tabuchi K, Yamamoto H, Yamamoto T, Yoshikawa S, Okano H, Okado N (1998) Localization of 5-HT2A receptor in rat cerebral cortex and olfactory system revealed by immunohistochemistry using two antibodies raised in rabbit and chicken. Mol Brain Res 54:199–211
132. Preece MA, Dalley JW, Theobald DE, Robbins TW, Reynolds GP (2004) Region specific changes in forebrain 5-hydroxytryptamine1A and 5-hydroxytryptamine2A receptors in isolation-reared rats: an in vitro autoradiography study. Neuroscience 123:725–732
133. Willins DL, Deutch AY, Roth BL (1997) Serotonin 5-HT2A receptors are expressed on pyramidal cells and interneurons in the rat cortex. Synapse 27:79–82
134. Francis PT, Pangalos MN, Pearson RCA, Middlemiss DN, Stratmann GC, Bowen DM (1992) 5-hydroxytryptamine-1 A but not 5-hydroxytryptamine-2 receptors are enriched on neocortical pyramidal neurons destroyed by intrastriatal volkensin. J Pharmacol Exp Ther 261:1273–1281
135. Morilak DA, Somogyi P, Lujanmiras R, Ciaranello RD (1994) Neurons expressing 5-ht2 receptors in the rat-brain—neurochemical identification of cell-types by immunocytochemistry. Neuropsychopharmacology 11:157–166
136. Blue ME, Yagaloff KA, Mamounas LA, Hartig PR, Molliver ME (1988) Correspondence between 5-HT2 receptors and serotonergic axons in rat neocortex. Brain Res 453:315–328
137. Wright DE, Seroogy KB, Lundgren KH, Davis BM, Jennes L (1995) Comparative localization of serotonin, (1 A), (1 C) and (2) receptor subtype messenger-rnas in rat-brain. J Comp Neurol 351:357–373
138. Morilak DA, Ciaranello RD (1993) ontogeny of 5-hydroxytryptamine(2) receptor immunoreactivity in the developing rat-brain. Neuroscience 55:869–880
139. Morales M, Battenberg E, de Lecea L, Bloom FE (1996a) The type 3 serotonin receptor is expressed in a subpopulation of GABAergic neurons in the rat neocortex and hippocampus. Brain Res 731:199–202
140. Tecott LH, Maricq AV, Julius D (1993) Nervous-system distribution of the serotonin 5-Ht3 receptor messenger-Rna. Proc Natl Acad Sci USA 90:1430–1434
141. Gehlert DR, Gackenheimer SL, Wong DT, Robertson DW (1991) Localization of 5-HT3 receptors in the rat brain using [3H]LY278584. Brain Res 553:149–154
142. Laporte AM, Koscielniak T, Ponchant M, Verge D, Hamon M, Gozlan H (1992) Quantitative autoradiographic mapping of 5-HT3 receptors in the rat CNS using [125I]iodo-zacopride and [3H]zacopride as radioligands. Synapse 10:271–281
143. Morales M, Battenberg E, Bloom FE (1998) Distribution of neurons expressing immunoreactivity for the 5HT3 receptor subtype in the rat brain and spinal cord. J Comp Neurol 402:385–401
144. Waeber C, Dixon K, Hoyer D, Palacios JM (1988) Localisation by autoradiography of neuronal 5-HT3 receptors in the mouse CNS. Eur J Pharmacol 151:351–352
145. Kilpatrick GJ, Jones BJ, Tyers MB (1987) Identification and distribution of 5-HT3 receptors in rat brain using radioligand binding. Nature 330:746–748

146. Morales M, Battenberg E, de Lecea L, Sanna PP, Bloom FE (1996b) Cellular and subcellular immunolocalization of the type 3 serotonin receptor in the rat central nervous system. Brain Res Mol Brain Res 36:251–260
147. Miquel MC, Emerit MB, Gingrich JA, Nosjean A, Hamon M, El Mestikawy S (1995) Developmental changes in the differential expression of two serotonin 5-HT3 receptor splice variants in the rat. J Neurochem 65:475–483
148. Tecott L, Shtrom S, Julius D (1995) Expression of a serotonin-gated ion channel in embryonic neural and nonneural tissues. Mol Cell Neurosci 6:43–55
149. Nonkes LJ, Tomson K, Maertin A, Dederen J, Maes JH, Homberg J (2010) Orbitofrontal cortex and amygdalar over-activity is associated with an inability to use the value of expected outcomes to guide behaviour in serotonin transporter knockout rats. Neurobiol Learn Mem 94:65–72
150. Sheikhkanloui-Milan H, Sheibani V, Afarinesh M, Esmaeili-Mahani S, Shamsizadeh A, Sepehri G (2010) Effects of electrical stimulation of dorsal raphe nucleus on neuronal response properties of barrel cortex layer IV neurons following long-term sensory deprivation. Neurosci Bull 26:388–394
151. Blue ME, Erzurumlu RS, Jhaveri S (1991) A comparison of pattern formation by thalamocortical and serotonergic afferents in the rat barrel field cortex. Cereb Cortex 1:380–389
152. Gutierrez-Ospina G, Manjarrez-Gutierrez G, Gonzalez C, Lopez S, Herrera R, Medina A I, Hernandez R (2002) Neither increased nor decreased availability of cortical serotonin (5HT) disturbs barrel field formation in isocaloric undernourished rat pups. Int J Dev Neurosci 20:497–501
153. Cases O, Vitalis T, Seif I, De Maeyer E, Sotelo C, Gaspar P (1996) Lack of barrels in the somatosensory cortex of monoamine oxidase A-deficient mice: role of a serotonin excess during the critical period. Neuron 16:297–307
154. Persico AM, Mengual E, Moessner R, Hall SF, Revay RS, Sora I, Arellano J, DeFelipe J, Gimenez-Amaya JM, Conciatori M, Marino R, Baldi A, Cabib S, Pascucci T, Uhl GR, Murphy DL, Lesch KP, Keller F, Hall SF (2001) Barrel pattern formation requires serotonin uptake by thalamocortical afferents, and not vesicular monoamine release. J Neurosci 21:6862–6873
155. Persico AM, Baldi A, Dell'Acqua ML, Moessner R, Murphy DL, Lesch KP, Keller F (2003) Reduced programmed cell death in brains of serotonin transporter knockout mice. Neuroreport 14:341–344
156. Salichon N, Gaspar P, Upton AL, Picaud S, Hanoun N, Hamon M, De Maeyer E, Murphy DL, Mossner R, Lesch KP, Hen R, Seif I (2001) Excessive activation of serotonin (5-HT) 1B receptors disrupts the formation of sensory maps in monoamine oxidase a and 5-ht transporter knock-out mice. J Neurosci 21:884–896
157. Miceli S, Negwer M, van Eijs F, Kalkhoven C, van L, I, Homberg J, Schubert D (2013) High serotonin levels during brain development alter the structural input-output connectivity of neural networks in the rat somatosensory layer IV. Front Cell Neurosci 7:88
158. Esaki T, Cook M, Shimoji K, Murphy DL, Sokoloff L, Holmes A (2005) Developmental disruption of serotonin transporter function impairs cerebral responses to whisker stimulation in mice. Proc Natl Acad Sci U S A 102:5582–5587
159. Pang RD, Wang Z, Klosinski LP, Guo Y, Herman DH, Celikel T, Dong HW, Holschneider DP (2011) Mapping functional brain activation using [14C]-iodoantipyrine in male serotonin transporter knockout mice. PLoS One 6:e23869
160. Cases O, Seif I, Grimsby J, Gaspar P, Chen K, Pournin S, Muller U, Aguet M, Babinet C, Shih JC (1995) Aggressive behavior and altered amounts of brain serotonin and norepinephrine in mice lacking MAOA. Science 268:1763–1766
161. Alvarez C, Vitalis T, Fon EA, Hanoun N, Hamon M, Seif I, Edwards R, Gaspar P, Cases O (2002) Effects of genetic depletion of monoamines on somatosensory cortical development. Neuroscience 115:753–764
162. Chen K, Cases O, Rebrin I, Wu W, Gallaher TK, Seif I, Shih JC (2007) Forebrain-specific expression of monoamine oxidase A reduces neurotransmitter levels, restores the brain

structure, and rescues aggressive behavior in monoamine oxidase A-deficient mice. J Biol Chem 282:115–123
163. Vitalis T, Cases O, Callebert J, Launay JM, Price DJ, Seif I, Gaspar P (1998) Effects of monoamine oxidase A inhibition on barrel formation in the mouse somatosensory cortex: determination of a sensitive developmental period. J Comp Neurol 393:169–184
164. Kesterson KL, Lane RD, Rhoades RW (2002) Effects of elevated serotonin levels on patterns of GAP-43 expression during barrel development in rat somatosensory cortex. Brain Res Dev Brain Res 139:167–174
165. Lane RD, Chiaia NL, Kesterson KL, Rhoades RW, Mooney RD (2006) Boundary-limited serotonergic influences on pattern organization in rat sensory cortex. Neurosci Lett 395:165–169
166. Brown CE, Seif I, De Maeyer E, Dyck RH (2003) Altered zincergic innervation of the developing primary somatosensory cortex in monoamine oxidase-A knockout mice. Brain Res Dev Brain Res 142:19–29
167. Rebsam A, Seif I, Gaspar P (2002) Refinement of thalamocortical arbors and emergence of barrel domains in the primary somatosensory cortex: a study of normal and monoamine oxidase a knock-out mice. J Neurosci 22:8541–8552
168. Mansour-Robaey S, Mechawar N, Radja F, Beaulieu C, Descarries L (1998) Quantified distribution of serotonin transporter and receptors during the postnatal development of the rat barrel field cortex. Brain Res Dev Brain Res 107:159–163
169. Bonnin A, Torii M, Wang L, Rakic P, Levitt P (2007) Serotonin modulates the response of embryonic thalamocortical axons to netrin-1. Nat Neurosci 10:588–597
170. Nicol X, Muzerelle A, Rio JP, Metin C, Gaspar P (2006) Requirement of adenylate cyclase 1 for the ephrin-A5-dependent retraction of exuberant retinal axons. J Neurosci 26:862–872
171. Lotto B, Upton L, Price DJ, Gaspar P (1999) Serotonin receptor activation enhances neurite outgrowth of thalamic neurones in rodents. Neurosci Lett 269:87–90
172. Medina-Aguirre I, Gutierrez-Ospina G, Hernandez-Rodriguez J, Boyzo A, Manjarrez-Gutierrez G (2008) Development of 5-HT(1B), SERT and thalamo-cortical afferents in early nutrionally restricted rats: an emerging explanation for delayed barrel formation. Int J Dev Neurosci 26:225–231
173. Smit-Rigter LA, Noorlander CW, von Oerthel L, Chameau P, Smidt MP, van Hooft JA (2012) Prenatal fluoxetine exposure induces life-long serotonin 5-HT(3) receptor-dependent cortical abnormalities and anxiety-like behaviour. Neuropharmacology 62:865–870
174. Vitalis T, Cases O, Gillies K, Hanoun N, Hamon M, Seif I, Gaspar P, Kind P, Price DJ (2002) Interactions between TrkB signaling and serotonin excess in the developing murine somatosensory cortex: a role in tangential and radial organization of thalamocortical axons. J Neurosci 22:4987–5000
175. Homberg JR, Schiepers OJ, Schoffelmeer AN, Cuppen E, Vanderschuren LJ (2007b) Acute and constitutive increases in central serotonin levels reduce social play behaviour in periadolescent rats. Psychopharmacology 195:175–182
176. Homberg JR, Pattij T, Janssen MC, Ronken E, De Boer SF, Schoffelmeer AN, Cuppen E (2007a) Serotonin transporter deficiency in rats improves inhibitory control but not behavioural flexibility. Eur J Neurosci 26:2066–2073
177. Page DT, Kuti OJ, Prestia C, Sur M (2009) Haploinsufficiency for Pten and Serotonin transporter cooperatively influences brain size and social behavior. Proc Natl Acad Sci U S A 106:1989–1994
178. Nonacs R, Cohen LS (2003) Assessment and treatment of depression during pregnancy: an update. Psychiatr Clin North Am 26:547–562
179. Rampono J, Proud S, Hackett LP, Kristensen JH, Ilett KF (2004) A pilot study of newer antidepressant concentrations in cord and maternal serum and possible effects in the neonate. Int J Neuropsychopharmacolog 7:329–334
180. Kristensen JH, Ilett KF, Hackett LP, Yapp P, Paech M, Begg EJ (1999) Distribution and excretion of fluoxetine and norfluoxetine in human milk. Br J Clin Pharmacol 48:521–527

181. Oberlander TF, Grunau RE, Fitzgerald C, Papsdorf M, Rurak D, Riggs W (2005) Pain reactivity in 2-month-old infants after prenatal and postnatal serotonin reuptake inhibitor medication exposure. Pediatrics 115:411–425
182. Marroun H E, Jaddoe VW, Hudziak JJ, Roza SJ, Steegers EA, Hofman A, Verhulst FC, White TJ, Stricker BH, Tiemeier H (2012) Maternal use of selective serotonin reuptake inhibitors, fetal growth, and risk of adverse birth outcomes. Arch Gen Psychiatry 69:706–714
183. Croen LA, Grether JK, Yoshida CK, Odouli R, Hendrick V (2011) Antidepressant use during pregnancy and childhood autism spectrum disorders. Arch Gen Psychiatry 68:1104–1112
184. Russo N, Foxe JJ, Brandwein AB, Altschuler T, Gomes H, Molholm S (2010) Multisensory processing in children with autism: high-density electrical mapping of auditory-somatosensory integration. Autism Res 3:253–267
185. Xu Y, Sari Y, Zhou FC (2004) Selective serotonin reuptake inhibitor disrupts organization of thalamocortical somatosensory barrels during development. Brain Res Dev Brain Res 150:151–161
186. Lee LJ (2009) Neonatal fluoxetine exposure affects the neuronal structure in the somatosensory cortex and somatosensory-related behaviors in adolescent rats. Neurotox Res 15:212–223
187. Kalueff AV, Olivier JDA, Nonkes LJP, Homberg JR (2009) Conserved role for the serotonin transporter gene in rat and mouse neurobehavioral endophenotypes. Neurosci Biobehav Rev 34:373–386
188. Moy SS, Nadler JJ, Young NB, Nonneman RJ, Grossman AW, Murphy DL, D'Ercole AJ, Crawley JN, Magnuson TR, Lauder JM (2009) Social approach in genetically engineered mouse lines relevant to autism. Genes Brain Behav 8:129–142
189. Olivier JD, Valles A, van Heesch F, Afrasiab-Middelman A, Roelofs JJ, Jonkers M, Peeters EJ, Korte-Bouws GA, Dederen JP, Kiliaan AJ, Martens GJ, Schubert D, Homberg JR (2011) Fluoxetine administration to pregnant rats increases anxiety-related behavior in the offspring. 217:419–432
190. Rodriguez-Porcel F, Green D, Khatri N, Harris SS, May WL, Lin RC, Paul IA (2011) Neonatal exposure of rats to antidepressants affects behavioral reactions to novelty and social interactions in a manner analogous to autistic spectrum disorders. Anat Rec (Hoboken) 294:1726–1735
191. Kinast K, Peeters D, Kolk SM, Schubert D, Homberg JR (2013) Genetic and pharmacological manipulations of the serotonergic system in early life: neurodevelopmental underpinnings of autism-related behavior. Front Cell Neurosci 7:72
192. Anderson GM, Horne WC, Chatterjee D, Cohen DJ (1990) The hyperserotonemia of autism. Ann N Y Acad Sci 600:331–340
193. Azmitia EC, Singh JS, Whitaker-Azmitia PM (2011) Increased serotonin axons (immunoreactive to 5-HT transporter) in postmortem brains from young autism donors. Neuropharmacology 60:1347–1354
194. Makkonen I, Riikonen R, Kokki H, Airaksinen MM, Kuikka JT (2008) Serotonin and dopamine transporter binding in children with autism determined by SPECT. Dev Med Child Neurol 50:593–597
195. Veenstra-VanderWeele J, Muller CL, Iwamoto H, Sauer JE, Owens WA, Shah CR, Cohen J, Mannangatti P, Jessen T, Thompson BJ, Ye R, Kerr TM, Carneiro AM, Crawley JN, Sanders-Bush E, McMahon DG, Ramamoorthy S, Daws LC, Sutcliffe JS, Blakely RD (2012) Autism gene variant causes hyperserotonemia, serotonin receptor hypersensitivity, social impairment and repetitive behavior. Proc Natl Acad Sci U S A 109:5469–5474
196. Caspi A, Hariri AR, Holmes A, Uher R, Moffitt TE (2010) Genetic sensitivity to the environment: the case of the serotonin transporter gene and its implications for studying complex diseases and traits. Am J Psychiatry 167:509–527
197. Huang CH, Santangelo SL (2008) Autism and serotonin transporter gene polymorphisms: a systematic review and meta-analysis. Am J Med Genet B Neuropsychiatr Genet 147B:903–913

198. Kalueff AV, Olivier JD, Nonkes LJ, Homberg JR (2010) Conserved role for the serotonin transporter gene in rat and mouse neurobehavioral endophenotypes. Neurosci Biobehav Rev 34:373–386
199. Popa D, Lena C, Alexandre C, Adrien J (2008) Lasting syndrome of depression produced by reduction in serotonin uptake during postnatal development: evidence from sleep, stress, and behavior. J Neurosci 28:3546–3554
200. Thenganatt MA, Jankovic J (2014) Parkinson disease subtypes. JAMA Neurol 71:499–504
201. Rodriguez-Oroz MC, Jahanshahi M, Krack P, Litvan I, Macias R, Bezard E, Obeso JA (2009) Initial clinical manifestations of parkinson's disease: features and pathophysiological mechanisms. Lancet Neurol 8:1128–1139
202. Sharman M, Valabregue R, Perlbarg V, Marrakchi-Kacem L, Vidailhet M, Benali H, Brice A, Lehericy S (2013) Parkinson's disease patients show reduced cortical-subcortical sensorimotor connectivity. Mov Disord 28:447–454
203. Shaw P, Gornick M, Lerch J, Addington A, Seal J, Greenstein D, Sharp W, Evans A, Giedd JN, Castellanos FX, Rapoport JL (2007) Polymorphisms of the dopamine D4 receptor, clinical outcome, and cortical structure in attention-deficit/hyperactivity disorder. Arch Gen Psychiatry 64:921–931
204. Parush S, Sohmer H, Steinberg A, Kaitz M (1997) Somatosensory functioning in children with attention deficit hyperactivity disorder. Dev Med Child Neurol 39:464–468
205. Scherder EJ, Rommelse NN, Broring T, Faraone SV, Sergeant JA (2008) Somatosensory functioning and experienced pain in ADHD-families: a pilot study. Eur J Paediatr Neurol 12:461–469
206. Yochman A, Ornoy A, Parush S (2006) Perceptuomotor functioning in preschool children with symptoms of attention deficit hyperactivity disorder. Percept Mot Skills 102:175–186
207. Duerden EG, Tannock R, Dockstader C (2012) Altered cortical morphology in sensorimotor processing regions in adolescents and adults with attention-deficit/hyperactivity disorder. Brain Res 1445:82–91

Index

P. Krieger, A. Groh (eds.), *Sensorimotor Integration in the Whisker System*,
DOI 10.1007/978-1-4939-2975-7